

The Study of Soil-Reinforcement Interaction by Means of Large Scale
Laboratory Tests.

by

Ennio Marques Palmeira

A Thesis Submitted for the
Degree of Doctor of Philosophy at
the University of Oxford

Magdalen College

Trinity Term, 1987

The Study of Soil-Reinforcement Interaction by Means of Large Scale Laboratory Tests.

A Thesis Submitted for the Degree of Doctor of Philosophy.

Ennio Marques Palmeira
Magdalen College, University of Oxford.
Trinity Term, 1987.

Abstract:

This thesis presents the results of an investigation into soil-reinforcement interaction by means of direct shear and pull-out tests. Scale and other factors affecting test results were studied; for this purpose an apparatus able to contain a 1 cu.m sample of sand was designed by the author in order to perform large scale tests. Plastic and metal sheet and grid reinforcements were used in conjunction with Leighton Buzzard sand.

Direct Shear tests on unreinforced sand samples showed that soil strength parameters were not affected by the test scale, although the post peak behaviour and the shear band thickness at the centre of the sample were significantly affected by the scale of the test. The presence of a reinforcement layer inclined to the central plane of the box had a marked effect on the strength and behaviour of the sample. The reinforcement increased the vertical stress and inhibited the shear strain development in the central region of the sample. The behaviour of the reinforced sample was found to depend on the type and form of the reinforcement as well as its mechanical properties.

Pull-out test results can be severely affected by boundary conditions, in particular by the friction on the front wall of the box. The results obtained in the series of tests showed that interference between grid bearing members is the main factor conditioning the pull-out resistance of a grid reinforcement. The intensity of such interference was quantified on the basis of results obtained in tests using single isolated bearing members and grids with different geometric characteristics. An expression for the bond coefficient between soil and grid, taking into account the degree of interference, was suggested. It was also observed that the maximum bearing pressure exhibited by a bearing member depends on the ratio of the member diameter to the mean particle size.

<u>Index</u>	page
<u>Abstract</u>	
<u>Acknowledgements</u>	A.1
<u>Introduction</u>	I.1
<u>Chapter 1: Soil Reinforcement Technique</u>	1.0
1.1 - Introduction;	1.1
1.2 - The Soil-Reinforcement Technique;	1.1
1.3 - Factors Affecting the Behaviour of Reinforced Soil	1.3
1.3.1 - Influence of Fill Material;	1.4
1.3.2 - Influence of Reinforcement Characteristics;	1.4
1.3.3 - Interaction Between Soil and Reinforcement;	1.6
1.4 - Measurement of Soil-Reinforcement Interaction;	1.7
1.5 - Conclusions.	1.18
<u>Part I - Direct Shear Tests:</u>	2.0
<u>Chapter 2: Direct Shear Apparatus</u>	2.0
2.1 - Introduction;	2.1
2.2 - Factors Controlling the Design of the Large Shear Box;	2.1
2.3 - Mechanical Characteristics and Instrumentation	2.3
2.3.1 - Large Shear Box;	2.3

2.3.2 - Medium Size Shear Box;	2.12
2.3.3 - Standard Casagrande Shear Box or Small Shear Box;	2.15
 <u>Chapter 3: Soil and Reinforcement Characteristics</u>	 3.0
3.1 - Introduction;	3.1
3.2 - Soil Characteristics;	3.1
3.3 - Reinforcement Characteristics;	3.2
 <u>Chapter 4: Sample Preparation and Test Procedure</u>	 4.0
4.1 - Introduction;	4.1
4.2 - Large Direct Shear Box;	4.1
4.2.1 - Sample Preparation;	4.1
4.2.2 - Test Procedure;	4.6
4.2.3 - Post-Test Procedure;	4.9
4.3 - Medium Size Shear Box and Casagrande Shear Box;	4.10
4.3.1 - Sample Preparation;	4.10
4.3.2 - Test Procedure;	4.11
4.3.3 - Post-Test Procedure;	4.11
4.4 - Repeatability of Test Results.	4.12
 <u>Chapter 5: Direct Shear Tests on Unreinforced Sand</u>	 5.0
5.1 - Introduction;	5.1
5.2 - Some Considerations on the Direct Shear Test;	5.1
5.2.1 - Soil Friction Angle in a Direct Shear Test;	5.1
5.2.2 - Flow Rules;	5.7

5.2.3 - Influence of Boundary Conditions in Direct Shear Tests;	5.9
5.3 - Large Scale Direct Shear Tests on Unreinforced Sand;	5.12
5.3.1 - Scale Effect;	5.12
5.3.2 - Stress and Strain Distributions in the Large Shear Box;	5.18
5.4 - Conclusions;	5.26
 <u>Chapter 6: Large Direct Shear Tests on Reinforced Sand</u>	 6.0
6.1 - Introduction;	6.1
6.2 - Test Results in the Large Shear Box;	6.1
6.3 - Strain and Stress Distribution in Reinforced Sand Samples;	6.8
6.3.1 - Strain Distribution;	6.8
6.3.2 - Stress Distribution;	6.11
6.4 - Forces in the Reinforcement;	6.17
6.5 - Conclusions.	6.27
 <u>Part II - Pull-out Tests</u>	
 <u>Chapter 7: Pull-out Test Apparatus</u>	 7.0
7.1 - Introduction;	7.1
7.2 - Description of Equipments and Instrumentation;	7.1
7.2.1 - Medium Size Pull-out Box;	7.1
7.2.2 - Large Pull-out Box.	7.2

<u>Chapter 8: Soils and Reinforcements Used in Pull-out Tests</u>	8.0
8.1 - Introduction;	8.1
8.2 - Soils Used in the Pull-out Tests;	8.1
8.3 - Reinforcement Characteristics.	8.2
 <u>Chapter 9: Sample Preparation and Test Procedure in Pull-out Tests</u>	 9.0
9.1 - Introduction;	9.1
9.2 - Tests with the Large Pull-out Box;	9.1
9.3 - Tests with the Medium Size Pull-out Box;	9.2
9.4 - Post-Test Procedure.	9.2
 <u>Chapter 10: Pull-out Test Results</u>	 10.0
10.1 - Introduction;	10.1
10.2 - Effects of Boundary Conditions on Pull-out Test Results;	10.1
10.2.1 - Influence of the Top Boundary;	10.1
10.2.2 - Influence of the Roughness of the Front Wall;	10.2
10.3 - Influence of Soil Particle Size to Member Diameter Ratio;	10.5
10.4 - Interference Between Grid Bearing Members in Pull-out Tests;	10.9
10.5 - Comparisons Between Performances of Different Reinforcements Under Pull-out Solicitation;	10.20
10.6 - Stress, Strain and Displacement Distributions in Pull-out Tests;	10.25
10.6.1 - Stresses on The Front Wall of the Large Pull-out Box;	10.25
10.6.2 - Strains and Displacements in the Sand Mass in Pull- out Tests in the Large Pull-out Box;	10.32

10.6.3 - Strain and Force Distribution in the Reinforcement Layer;	10.35
10.7 - Interference Between 2 Layers of Reinforcement Under Pull-out Condition;	10.41
10.8 - Conclusions.	10.43

<u>Chapter 11: Summary, Main Conclusions and Suggestion for Future Work.</u>	11.0
--	------

References

List of Symbols

List of Figures

Appendices

- A1: Additional Data on Instrumentation of the Large Direct Shear and Pull-out Boxes.
- A2: Software for the Large Direct Shear and Pull-out Boxes.
- A3: Additional Data on Reinforcement Materials.
- A4: Summary of Test Results.

Acknowledgements:

It has been for me a great pleasure and honour to be a research student of such an active and qualified research group as the Oxford University Soil Mechanics group. In the following lines I will try to express my sincere gratitude for the help I received from members of this group and of the Department of Engineering Science as a whole.

Dr. George W.E. Milligan, my supervisor, was extremely patient and always willing to help and assist me in all my needs. I thank him sincerely for the suggestions and understanding supervision of this work.

Prof. C.P. Wroth put his vast and most valuable library at my disposal. His sharp perception for events of scientific significance and challenging criticisms were a constant source of inspiration.

Dr. R.A. Jewell lent me several of his personal publications and assisted me with suggestions throughout this work.

Dr. G.T. Houlsby and Dra. Gilliane Sills were always very kind in lending me their personal publications that were of much value for the development of this research.

Mr. R. Earl and Mr. C. Donnelly helped me in assembling the equipment and in the manufacturing of more complex parts of it. Mr. Earl was specially helpful with his suggestions during the phase of the design of the large direct shear and pull-out boxes.

Mr. Ken Howson and his staff were always ready to assist and instruct me on the manufacturing of parts for the equipments.

Mr. R. Stone and Mr. S. Oldham gave me important advice on the design and strain gauge installation of the total pressure cells.

The following colleagues were always willing to exchange valuable information of mutual interest for our researches: Mr. K. Evans, Mr. R.J. Fannin, Mr. P.E.L. de Santa Maria and Mr. C.I.Teh.

I am indebted to Mr. N. Knight who patiently reviewed the English of my manuscripts.

I thank the following Brazilian friends and their respective families, most of whom I was lucky to know in Oxford, that shared with me their joyful moments and alleviated my homesickness: Cesar and Kate Cardoso, Gilberto and Leticia Correa, Aura Ferreira, Bendix and Ana Lima, Paulo and Silma Santa Maria and Alvaro and Amira Tronconni.

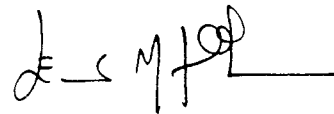
During this period in Oxford I have been financially supported by CAPES, a body of the Brazilian Education Ministry, and I would like to thank Mrs. C.A. Colonelli and the CAPES staff for their kind attention. The Oxford University Department of Engineering Science and the Science and Engineering Research Council provided the funds for the construction of the equipments used in the present research.

Many of my former lecturers have encouraged me in the pursuit of knowledge as a geotechnical engineering and researcher and I would like to thank them sincerely and mention, in particular, the names of Dr.

M.S.S. Almeida, Prof. F.E. Barata, Prof. W.A. Lacerda, Prof. J.A. Ramalho Ortigao and Prof. M.L.G. Werneck. Professor Ramalho Ortigao and his family kindly welcomed me in his home during my first days in England.

I must also express my eternal gratitude to my parents, Fernanda and Eloy, and my grand-parents, Antonio and Celeste, because without their help and support I would not have come this far.

Last, but by no means least, I am eternally indebted to my wife, Deusa Palmeira, who with limitless patience offered me her help and support throughout this work, sacrificing her ideals for the sake of mine and bearing my occasional bad temper moods for faults that were not hers. I sincerely hope that I will prove worthy of her dedication.

A handwritten signature in black ink, appearing to read 'Ennio Marques Palmeira', with a stylized flourish at the end.

Ennio Marques Palmeira.

"In research the horizon recedes as we advance, and is no nearer at sixty than it was at twenty. As the power of endurance weakens with age, the urgency of the pursuit grows more intense....And research is always incomplete."

Mark Pattinson (1813 - 1884).

To Deusa.

Introduction:

During the last decade there has been a considerable increase in the use of reinforced soil structures as a solution for civil engineering problems. Traditional solutions have lost ground, or have been improved, in order to cope with the savings in cost and reduction in construction time provided by the solution using reinforced soil. Research associated with this area has also flourished over the last decade, as a result of the increase in demand for such structures. Nevertheless, research has not been able to keep pace with the advance of construction techniques and challenges in design. As a consequence, designs of reinforced soil structures, in most cases, have been based on conservative assumptions or on the observations of the performance of real structures as guidelines for design procedures. This way of solving problems (know how, not knowing why), although practical, is not the most economical and, besides, is contradictory to the scientific approach (knowing how because one knows why).

It is the aim of the present thesis to investigate some fundamental factors directly affecting the behaviour of reinforced soil. Soil-reinforcement interaction is investigated by making use of large laboratory equipment specially designed by the author for the present work. Tests with small apparatus were also performed in order to investigate the influence of factors like scale on test results.

The main concern of the present work was to study the influence of the presence of inclusions such as geotextiles, geogrids, metal sheet and strips on the behaviour of the reinforced soil matrix. Other forms of

soil reinforcement are out of the context of this work, although some conclusions reached may be applied on a wider basis.

The structure of the work is divided into four main sections. It starts with a literature review on soil reinforcement techniques with special attention to the interaction between soil and reinforcement and how it has been measured. The experimental part that follows is concentrated in two main sections related to direct shear and pull-out tests. Each one starts with a description of the apparatus and experimental technique used for this research, followed by the test results, discussions and conclusions. The work ends with a presentation of the main conclusions and suggestions for future work.

As in much research, the present work provides some answers and raises additional questions. It is the opinion of the author that the need for correct answers is what gives life to research activity and it is his hope that the answers obtained in the present work will be useful to progress in understanding reinforced soil behaviour.

Chapter 1: Soil Reinforcement Technique

Chapter 1: Soil Reinforcement Technique

1.1 - Introduction:

In this chapter a literature review is made of work done by other researchers on the subject of soil reinforcement by means of inclusions.

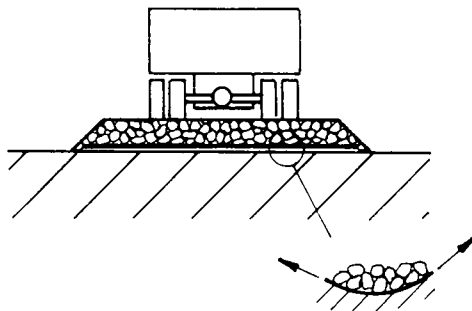
1.2 - The Soil Reinforcement Technique:

To reinforce a soil by means of an inclusion consists of placing the inclusion in regions of the soil matrix where its presence will cause a favourable redistribution of stresses and strains. The inclusion causes an increase in strength of the composite material and a decrease in its compressibility. Higher loads can be applied to the reinforced soil structure than in the case for an unreinforced one. In figure 1.1 some typical examples of reinforced soil structures are presented, with the mechanisms provided by the reinforcement to improve the performance of the structure. Other forms of soil reinforcement or improvement are available such as soil nailing, deep compaction, pile driving, etc. However, the study of these techniques does not fall within the scope of the present work.

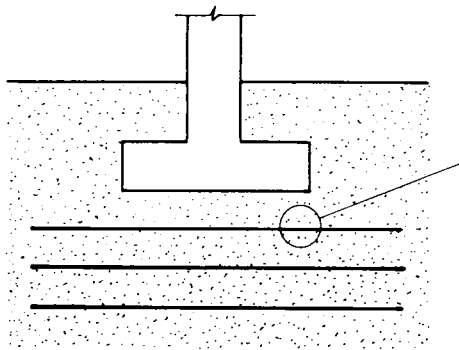
Because soils have very little tensile resistance, the use of reinforcement in regions of tensile strains is highly attractive. Not only the region where the reinforcement is placed is important, but also the orientation of the reinforcing element. Placing the reinforcement in regions of tensile strains and, in particular, on orientations coinciding with the direction of principal tensile strains, will cause the reinforcement to inhibit the development of tensile stresses in that

region of the soil and also increase the shearing characteristics of the

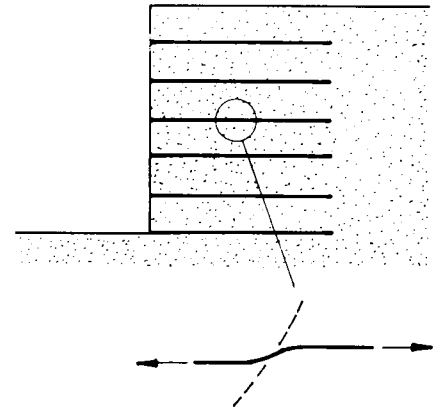
unpaved roads



foundations



retaining walls



embankments

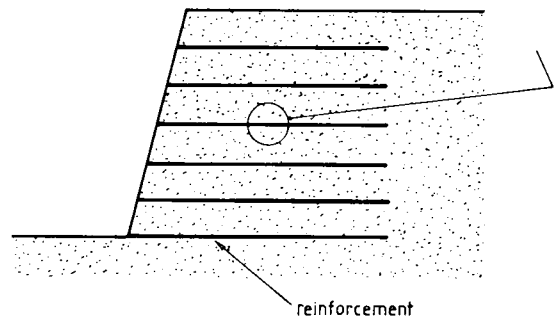


Figure 1.1 - Typical Examples of Soil Reinforcement Application

material (McGown et al - 1978, Jewell - 1980). The orientation of the tensile principal strain will be dependent on geometry, construction technique and type of load imposed on the structure. In the case of gravitational load in retaining walls or embankments, the direction of minor principal strains (tensile) coincides approximately with the horizontal (Milligan & Bransby - 1976, Sims and Jones - 1979). In fact, for embankments, that only happens in regions beyond the embankment crest. For regions in the embankment slope the orientation of minor principal strain is a function of the construction technique (McGown, 1981). In a reinforced unpaved road the presence of the reinforcement, as a frictional layer between fill and foundation, restrains the lateral

movement of the fill material as the foundation is deformed, with the additional settlement reducing effect caused by the vertical component of the load in the reinforcement (see fig. 1.1).

In effect, soil reinforcement is not a new technique at all. In ancient times man used to reinforce structures by means of reed matting, and the Ziggurat of Agar Quf, in Mesopotamia (1400 BC), is a major example of this. The technique was revived by Henri Vidal in the 60s on a commercial basis, using metal strips as reinforcing material. The strong and fast advance of the plastic industry over the last two decades has put forward this material as a major competitor to steel. Fears related to corrosion of steel reinforcement have also added to the increasing attention directed to plastic reinforcement.

1.3 - Factors Affecting the Behaviour of Reinforced Soil:

For the good performance of a reinforced soil structure three factors are of utmost importance:

- a. Nature and mechanical characteristics of the soil;
- b. Nature and mechanical characteristics of the reinforcement;
- c. Interaction between soil and reinforcement and how this affects the response of each material.

In fact, the factors above are linked together and the discrimination of a component due to each one exclusively is not easy. Nevertheless, some individual characteristics can be distinguished as follows.

1.3.1 - Influence of Fill Material:

Granular material has been the standard requirement for fill material in reinforced soil structures. This requirement comes from the obvious fact that highly frictional materials will develop a higher bond with reinforcement than poor materials. Recommendations on percentage of fines in the fill material can be found in Schlosser and Elias (1978) and Brown & Rochester (1979). Aggressive fill material should be avoided (Brown & Rochester, 1979). Despite these recommendations some successful trials with non-recommended fill materials can be found in the literature. Murray & Boden (1979) used silty clayey sand as a fill material for a reinforced wall and concluded that, despite construction difficulties and pore pressure development, cost savings could be achieved in comparison with the utilization of granular material imported over substantial distances. Blivet & Gestin (1979) have found high friction coefficients between phosphogypse and geotextile. Ramalho-Ortigao & Palmeira (1982) reported fill material savings in a reinforced access road on soft ground where poor quality fill material was used. Recent research work using pulverised fuel ash and chalk as fill materials have been carried out at Strathclyde University and at the Transport and Road Research Laboratory, respectively.

1.3.2 - Influence of Reinforcement Characteristics:

At the present time the most common types of reinforcements are made of steel or plastic. Related to steel reinforcement, the main concern is corrosion. This is not only a function of steel properties but also of environmental characteristics. The usual, but not economical solution, is to increase the thickness of the reinforcement, as a safety measure

against corrosion. Galvanising, plastic coating or the utilization of stainless steel or aluminium strips can also be employed, but also with increasing cost of the structure.

Plastic reinforcement is of a more complex nature, where time and temperature dependency may play an important role in its behaviour. The continuous industrial development has provided a large variety of high tensile strength and stiff reinforcement materials. The remaining uncertainties regarding plastic reinforcement are its durability and long term behaviour (creep). Durability will depend on the reinforcement material and environmental characteristics. Some data on degradation resistance of some synthetic fibres are presented in Ingold (1982). Creep behaviour depends on type of reinforcement, stress level and temperature. Studies by McGown et al (1984) have shown that since the factors affecting the time dependent behaviour of a reinforcement are identified and quantified, safe designs incorporating creep allowances can be achieved. Figure 1.2 presents the results of creep studies performed by McGown et al (1984) for a polymer reinforcement. Figure 1.2a permits the identification of a tendency to failure caused by creep. Figure 1.2b allows for the determination of the load in the reinforcement as a function of the strain and elapsed time. Results of this kind should be provided as a rule and not an exception in manufacturers' catalogues.

Direct shear tests on reinforced sand in a medium size shear box, with the reinforcement inclined to the shear plane, have shown that reinforcement longitudinal stiffness is an important parameter, although bending stiffness seems to show negligible effect on test results (Jewell, 1980). Palmeira (1984) reached the same conclusions regarding longitudinal stiffness using numerical analysis to model pull-out tests.

Form of reinforcement is very important since it influences markedly the failure mechanism developed and the degree of bond between soil and reinforcement. This and other reinforcement characteristics strongly related to bond are discussed next.

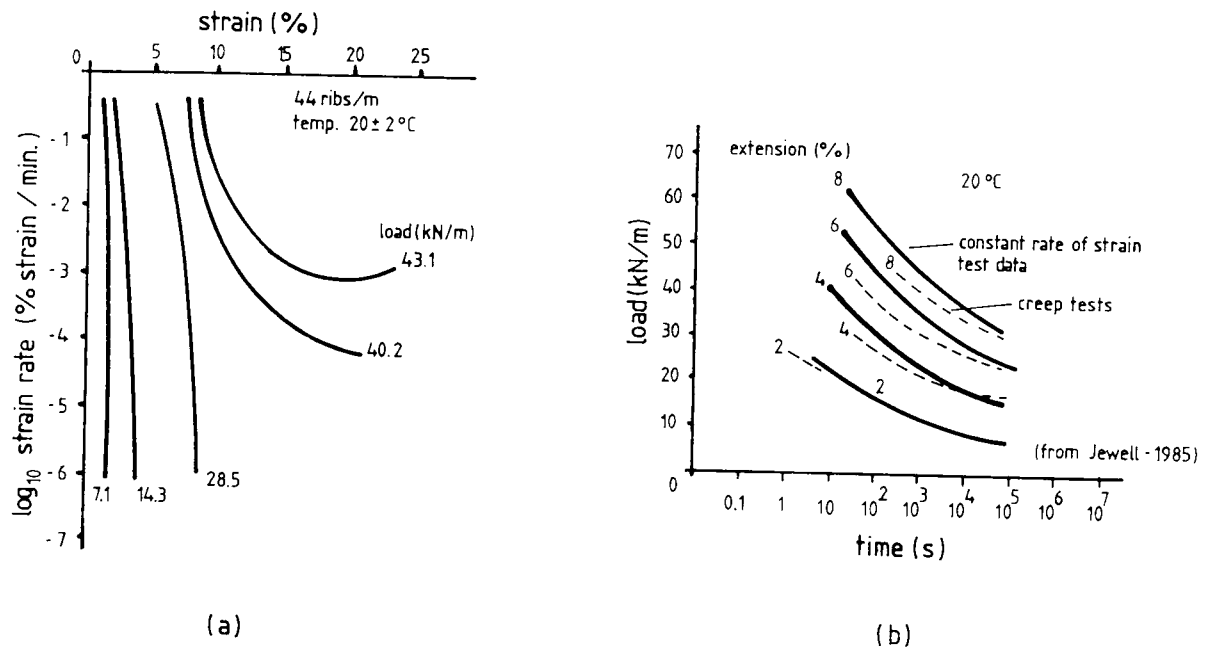


Figure 1.2 – Long Term Behaviour of Polymer Reinforcement (After McGown, 1984).

1.3.3 – Interaction Between Soil and Reinforcement:

Bond between soil and reinforcement is of major importance to reinforced soil structures design. It depends on soil type, reinforcement type and how they interact with each other. The degree of interaction between soil and reinforcement as well as the failure mechanism developed is a function of the reinforcement form. In Table 1.1 some typical reinforcements are shown with the main mechanisms involved between them and the surrounding soil.

Geotextiles and plain metal strips generate bond with soil by a frictional mechanism. In grids, depending on the geometry, the bearing mechanism may prevail due to the interaction between grid bearing members and surrounding soil (Tab. 1.1). Dyer (1985), using photoelasticity, has clarified and identified different mechanisms of interaction between soil and reinforcement. Of great importance is then the identification of the right mechanism and the choice of a convenient and accurate way of measuring the magnitude of bond stresses between soil and reinforcement. The measurement of soil reinforcement interaction is discussed in the following sections.

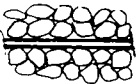
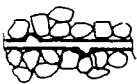

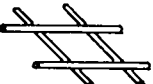
reinforcement type	mechanism	
	frictional	bearing
plain metal strip		
ribbed metal strip		
geotextile		
geogrid		

Table 1.1 - Common Types of Reinforcement.

1.4 - Measurement of Soil-Reinforcement Interaction:

Accurate testing conditions must be chosen to measure bond stresses between soil and reinforcement. Although some studies using triaxial

tests can be found in the literature, testing procedures under plane strain conditions are preferred because this is the most common case in real reinforced soil structures. In Table 1.2 some of the testing procedures that have been used to study soil-reinforcement interaction are presented. The most common testing methods are direct shear and pull-out tests. Boundary conditions may change from study to study using these tests. Nevertheless, boundaries seem to vary more among pull-out tests than direct shear and they also appear to influence pull-out test results more than direct shear tests.

Despite some differences in equipment or boundary conditions, McGown et al (1978), Jewell (1980) and Dyer (1985) reached similar fundamental conclusions, as follows:

- a. The most effective way of placing the reinforcement is in the regions of tensile strains, in particular, coinciding with the direction of minor principal (tensile) strain. In regions of compressive strains the reinforcement may not affect or may decrease the strength of the reinforced soil;
- b. Reinforcement longitudinal stiffness is a very important variable for the response of reinforced soil samples. The composite material can present a brittle or ductile behaviour, depending on the stiffness of the inclusion. The behaviour of the reinforcement as a stiff or extensible material may also be conditioned by the stress level;
- c. Reinforcement bending stiffness is not of major importance in the behaviour of reinforced sand samples undergoing direct shear;

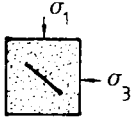





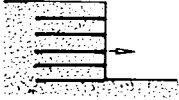
testing procedure	author
plane strain unit cell 	McGown et al (1978)
direct shear 	Jewell (1980), Dyer (1985)
	Delmas et al (1979), Dyer (1985), Degoutte & Mathieu (1986), Elias (1979), Koivumäki (1983), Miyamori et al (1986), Palmeira (1981), Perrier et al (1986), Sarsby & Marshal (1983), Shen et al (1979)
pull-out 	Chang et al (1977), Dyer (1985), Gardner & Morgado (1984), Ingold & Templeman (1979), Jewell (1980), Shen et al (1979)
	Blivet & Gestin (1979), Delmas et al (1979), Rowe et al (1985)
	Schlosser & Elias (1978)
	Terre Armee / Schlosser & Elias (1978)

Table 1.2 – Some Plane Strain Testing Configurations for the Study of Soil-Reinforcement Interaction.

d. The form and degree of roughness of the reinforcement is of utmost importance for the load transfer between soil and reinforcement and for the overall strength of reinforced samples. Dyer (1985) has emphasised the fact that the main mechanism of interaction between a grid reinforcement and the surrounding soil is due to bearing.

In figure 1.3 possible internal failure mechanisms in a retaining wall structure are presented as an example. If failure along surface 1-2 occurs, the mechanism involved in region A is of sliding of soil on the plane of reinforcement. If failure along surface 3-4 prevails, soil and reinforcement, as a composite material, is sheared. In the case of failure along the length 5-6, because of insufficient anchorage, sliding of the reinforcement inside the soil matrix takes place. Based on this example, the choice of direct shear tests and pull-out tests to represent each specific situation seems sensible.

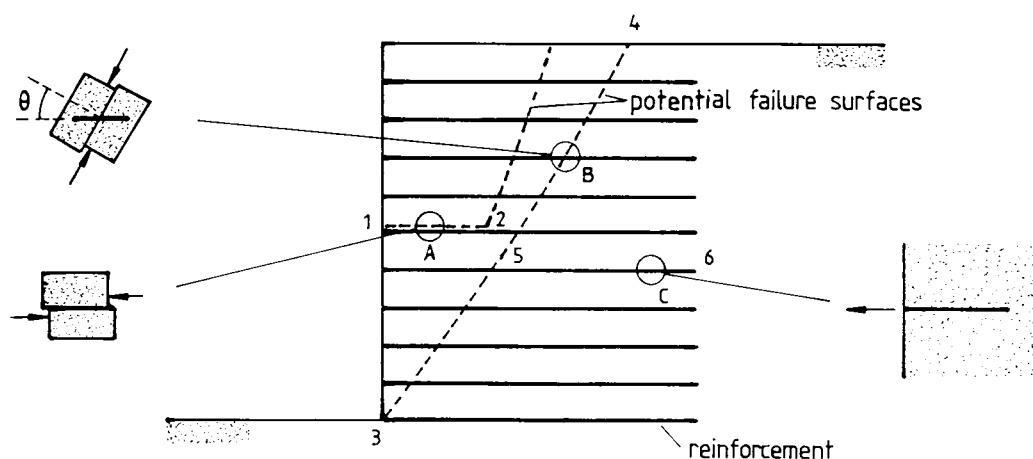


Figure 1.3 - Failure Mechanisms in a Reinforced Soil Retaining Wall.

A good guess for the orientation of a planar failure surface in fig. 1.3, based on earth pressure theories would result in a angle of $\pi/4 +$

$\phi/2$ with the horizontal measured from the bottom corner of the wall, ϕ being the soil friction angle. For most granular backfills, this expression would lead to orientations between 60° and 70° for the failure plane. As a result, values between 20° to 30° are obtained for the angle formed by the normal to the failure plane and the reinforcement direction (θ in fig. 1.3) at the intersection between failure plane and reinforcement plane (region B in fig. 1.3). In fact, in direct shear tests with the reinforcement inclined to the shear plane, values of $\theta \approx 30^\circ$ have been found to be the most efficient orientation for the reinforcement (Jewell - 1980, Gray & Al-Refeai - 1986) which is also the direction where coincidence between reinforcement orientation and direction of minor principal strain occurs in a direct shear box when testing dense sand.

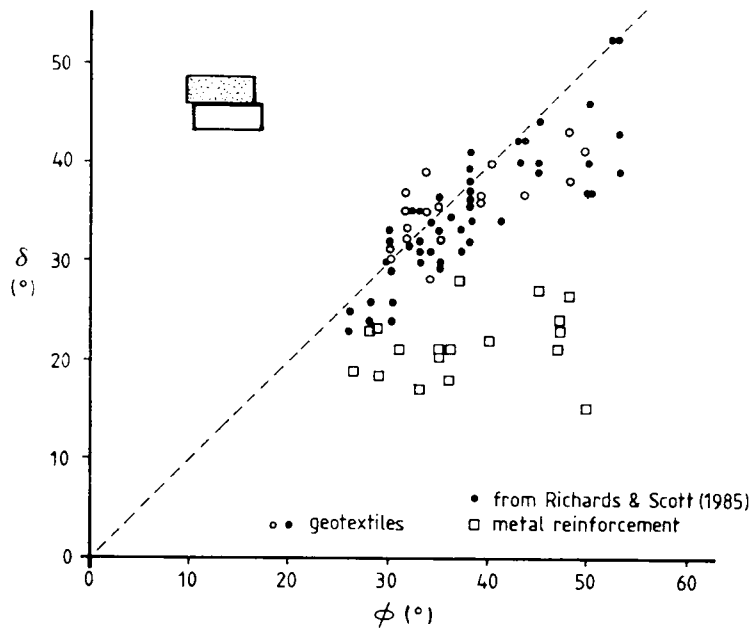
In the case of direct sliding of soil on reinforcement, Sarsby & Marshal (1983) have shown that a polymer grid reinforcement (Netlon SR2) can develop an interface friction angle equal to the soil friction angle. Jewell et al (1984) proposed an equation to obtain a friction coefficient between soil and reinforcement in direct sliding as a function of the soil strength parameters, reinforcement form and geometry. For a potential failure surface intersecting the reinforcement layer, Jewell (1980) has demonstrated that a limit equilibrium analysis may be successfully used to obtain reinforcement forces in a direct shear box.

The freedom of choice of boundary conditions for pull-out tests seems to be either an advantage or a limitation of the test. An advantage in the sense that simple boundary conditions can be chosen to eliminate some obstacles to the interpretation of results and a limitation because, if some precautions are not taken, the result of the test may be affected

by the boundaries as will be seen later in this work. Angles of friction between soil and reinforcement obtained in pull-out tests greater than the friction angle of the soil alone have been reported in the literature (Schlosser & Elias, 1978). This has been attributed to boundary conditions or soil dilatancy.

The usual criterion to check the reliability of a test result is that the interface angle of friction between soil and a plain sheet of reinforcement cannot be greater than the angle of friction for the soil alone. A collection of data on direct shear and pull-out test results is presented in figures 1.4a and b. Most of the data in fig. 1.4a was originally collected by Richards & Scott (1985) with some additions made by the author. Reinforcements presenting bearing-like mechanisms were avoided in order to have a common basis for comparison. Reinforcement types are various geotextiles and plain metal sheets. It can be seen that, independently from boundaries and test arrangements, two marked patterns of results arise in fig. 1.4a:

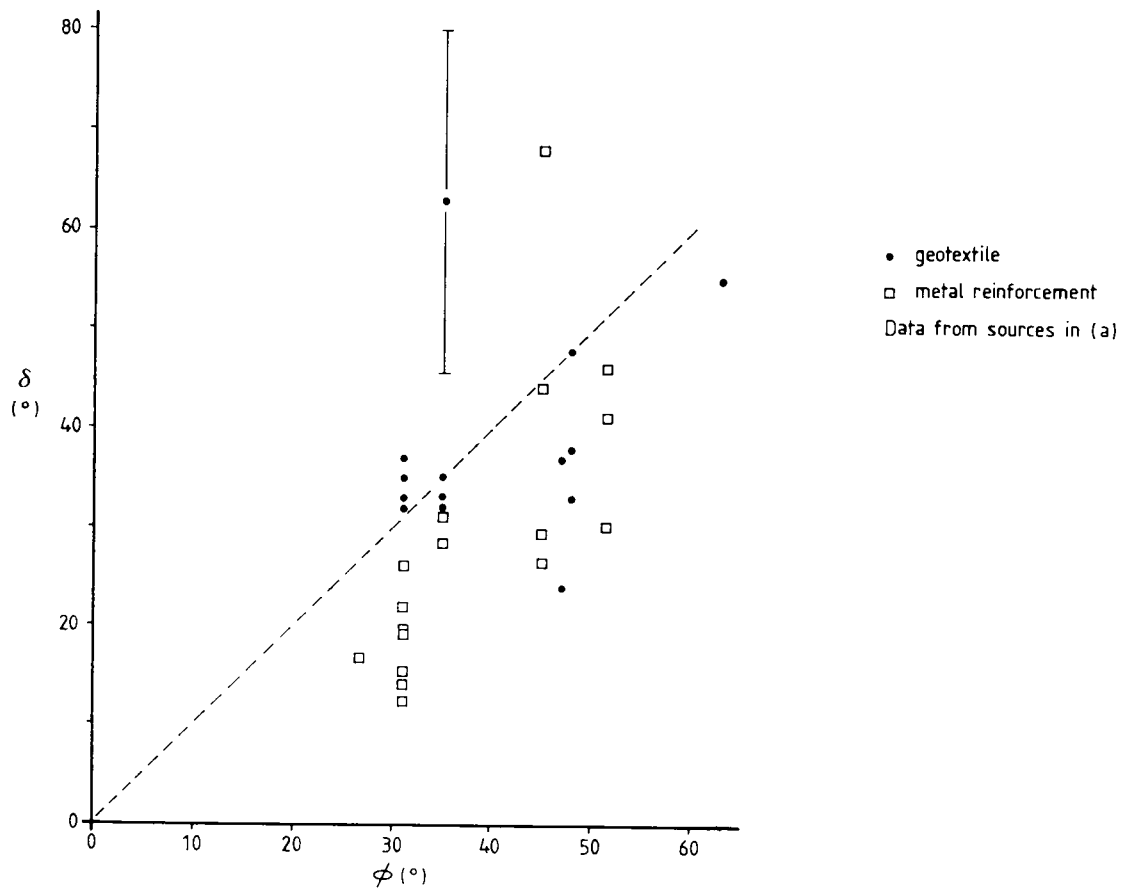
1. Most of the interface friction angle values (δ) are smaller than the soil friction angle (ϕ). Values of δ greater than ϕ may be expected to be due to boundary or scale problems or to inaccurate measurement of the soil friction angle. Also, most of the values of interface friction angles for geotextiles are within the limits $0.75\phi < \delta < \phi$;
2. Plain metal reinforcement, besides showing a larger scattering of results, presents smaller values of interface friction angle ($0.3\phi < \delta < 0.7\phi$).



Data collected from:

- Al-Hussaini & Perry (1978)
- Bolton et al (1978)
- Chang et al (1977)
- Dash (1978)
- Degoutte & Mathieu (1986)
- Delmas et al (1979)
- Dyer (1985)
- Guilloux et al (1979)
- Ingold & Templeman (1979)
- Koivumäki (1983)
- Miyamori et al (1986)
- Palmeira (1981)
- Perrier et al (1986)
- Richards & Scott (1985)
- Rowe & Fisher (1985)
- Schlosser & Elias (1978)
- Shen et al (1979)

(a) Interface Direct Shear Test Results



(b) Pull-out Test Results

Figure 1.4 – Direct Shear and Pull-out Test Results Collected from Literature.

Figure 1.4b shows the data collected from the literature regarding pull-out tests. Tests results from real reinforced walls were avoided because of the difficulty of controlling factors that may affect test results, such as: influence of construction procedure, more difficult control of soil properties, tests being performed in a reinforced (composite) soil, and boundary effects. Schlosser & Elias (1978) have presented a large number of field pull-out test results performed by the Reinforced Earth Company. Test results from reinforcements presenting bearing-like mechanisms were again avoided. It can be observed that the bulk of the test results, in fact, presents interface friction angles smaller than soil friction angles. The same reasons given in the previous paragraph for values of δ slightly above ϕ may be applied. Nevertheless, some results are well above the value of the soil friction angle. Some reasons may be found in the following explanations:

1. Boundary Conditions: influence of factors like friction on the front wall of the pull-out box and depth to length of reinforcement ratio are usually ignored. As will be shown later in this work, these factors can severely affect the test results;
2. Stress Level: it is not common to find reference to the stress level at which the friction angle of the soil was obtained. Comparisons between soil friction angles and interface friction angles, obtained at different stress levels, appears to be common. The assumption of constant soil friction angle, independent of the stress level, is not correct. In figure 1.5 the dependency of the friction angle on the stress level for

sands is shown (Bolton, 1986). In this figure the difference between maximum friction angle is plotted against mean stress level for several sands at some relative density index (I_D) values. This shows the dependency of the friction angle on stress level. Some soil friction angles have been also obtained from test conditions different from plane strain, which is usually the case in pull-out tests. Figure 1.5 shows that the friction angle obtained for a sand is dependent on whether a plane strain or an axisymmetric condition is imposed to the sample. In real reinforced soil walls the vertical stress near the wall can be greater than the stress due to the weight of the soil alone (Smith & Wroth - 1978, Juran et al - 1979). Smith & Wroth (1978) have reported pressures at the base of reinforced earth wall models, near the corner of the wall, up to 2.5 times greater than the pressure due to the weight of soil;

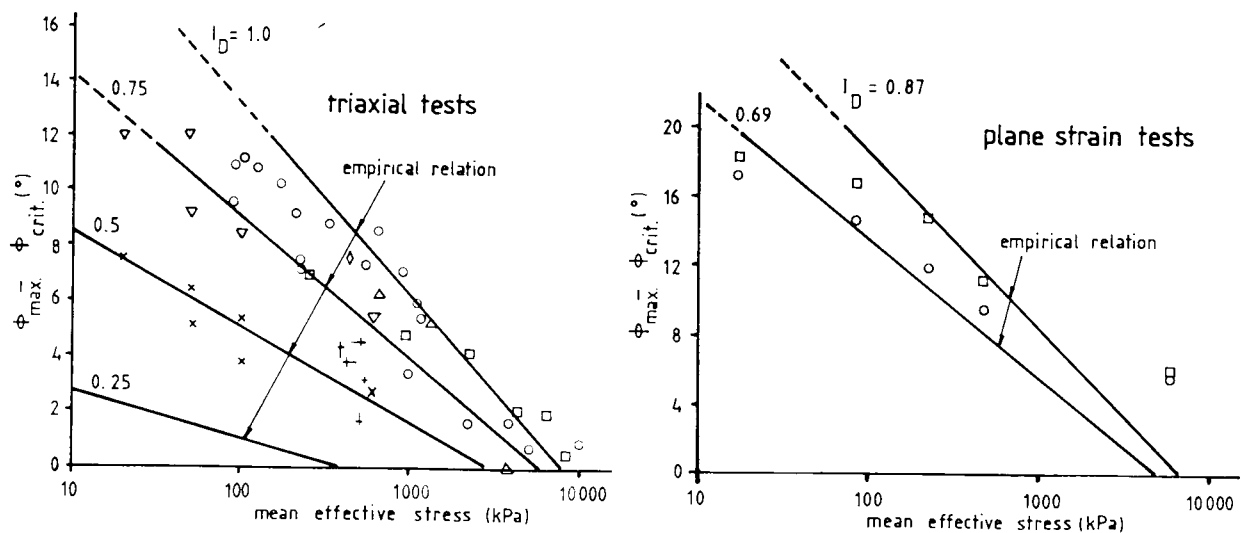


Figure 1.5 – Friction Angle Dependence on Stress Level (After Bolton, 1986)

3. Scale: may impose additional difficulties in interpreting results. The influence of factors such as the relation between soil particle size and container volume, side friction and low stress levels must be quantified and taken into account. Kerisel (1972) has shown the influence of scale on the magnitude of results obtained from models;
4. Mechanism of Interaction: bearing-like mechanisms presented by ribbed strips or grids are usually quantified in terms of bond strength using the same approach as for flat reinforcements. This may lead to "friction angles" between soil and reinforcement greater than the soil friction angle. However, as will be shown later in this work, this seems not to be the appropriate way of approaching grid or ribbed strip behaviour. A grid buried in soil should be seen as a succession of anchor members providing bearing resistance and interfering with each other. It is fundamental, for this sort of reinforcement, that the bearing mechanism is understood to be accurately quantified. Three dimensional effects involved in the case of pull-out tests of strips should also be pointed out.

Of course the simple comparison between a test result and the soil friction angle is not a guarantee of accuracy for the result or reliability in the test procedure. Nevertheless, it provides an upper limit for judgement of values obtained from tests.

Figure 1.6 shows the histogram plot for test results presented in figures 1.4 a and b. Figure 1.6a emphasises the higher adherence between soil and geotextiles compared with plain steel reinforcement. Figure 1.6b

is not as accurate as fig. 1.6a, in the sense that there are fewer pull-out test results published in the literature than direct shear test results. Nonetheless, the same trend is observed in the case of pull-out tests. A larger spreading of results is a measure of the effect of different boundary conditions but, for geotextiles, the mean value of δ/ϕ from pull-out tests compares very well with the value obtained from direct shear tests.

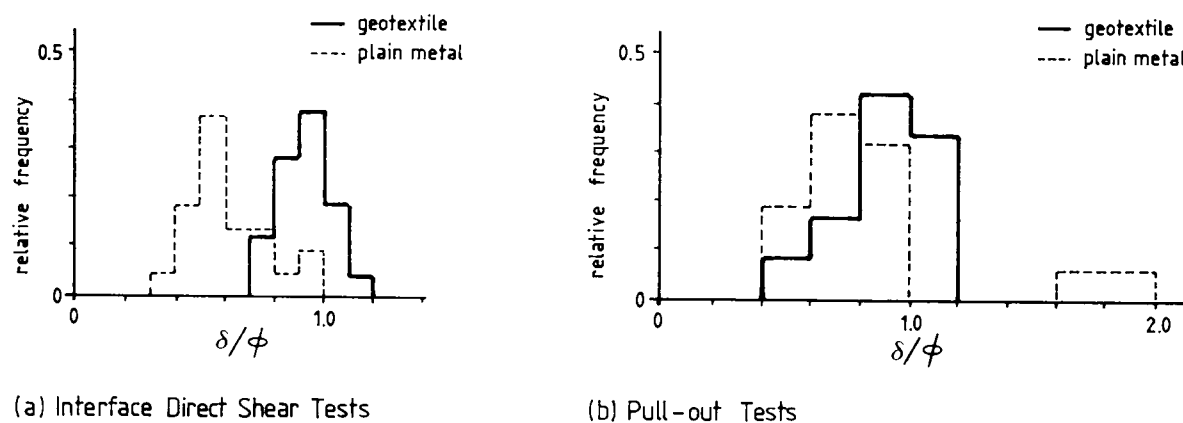


Figure 1.6 - Histogram of Direct Shear and Pull-out Test Results.

Pull-out tests are extremely useful to the study of interference between bearing members of a grid reinforcement. Boundary conditions can be chosen that make the interpretation of the test results easier than in direct shear tests with the reinforcement inclined to the central plane. Although some pioneer methods of predicting pull-out resistance are available (Jewell et al, 1984), the mechanisms involved in the pull-out behaviour of a grid are not completely understood; such understanding is needed to obtain an accurate prediction of pull-out resistance, as suggested by Dyer (1985).

1.5 - Conclusions:

The presence of an inclusion can favourably affect the behaviour of the soil-reinforcement composite. When the orientation of the reinforcement coincides with the orientation of minor principal strain, the efficiency of the reinforcement reaches a maximum. The degree of soil reinforcement is a function of soil type and characteristics, reinforcement form and properties and the mechanism of interaction between soil and reinforcement. Fears of corrosion in steel and relative cost have been the major reasons for the increasing utilization of polymer reinforcement. Nevertheless, due attention must be paid when using plastic reinforcement to long term behaviour and durability.

Direct shear interface tests and pull-out tests have shown clearly that, in general terms, geotextile reinforcement provides a higher bond strength with surrounding soil than plain metal strips. The presence of ribs on strips or the use of grid reinforcement can increase the bond between soil and reinforcement, due to the bearing mechanism developed by such reinforcements. However, this mechanism of interaction between soil and reinforcement is yet to be perfectly understood and accurately quantified.

Direct shear and pull-out tests are sensible means of studying soil reinforcement interaction. Pull-out tests seem more susceptible to influences such as boundary conditions and scale effects. Field pull-out tests may overestimate interface friction coefficients between soil and reinforcement due to factors difficult to control or quantify. So, large scale and carefully controlled pull-out tests and direct shear tests are recommended for the study of soil-reinforcement interaction.

The present work aims to achieve a better understanding of the mechanisms of interaction between soil and reinforcement, in particular with respect to grid reinforcement. Factors influencing direct shear and pull-out test results ,such as scale and boundary conditions, are also to be investigated. In the next chapter a large direct shear apparatus, designed by the author for the present work, is described. Test procedure and a discussion of the general behaviour of the equipment are also presented.

Part I - Direct Shear Tests

Chapter 2: Direct Shear Apparatus

Chapter 2 - Direct Shear Apparatus:

2.1 - Introduction:

In this chapter the details of all equipment used in this work are presented. Emphasis is laid on the description of the large shear box. Instrumentation used to monitor the tests in each box is also described. Additional information is provided in Appendices A1 and A2.

2.2 - Factors Controlling the Design of the Large Shear Box:

As discussed in the previous chapter, direct shear and pull-out tests are sensible test procedures for studying interaction between soil and reinforcement. However, the design of a proper apparatus was needed in order to avoid or minimise the adverse effects on test results presented earlier. The size of the equipment was a conditioning factor because of the following:

1. In a large volume of soil the reinforcement can be placed away from the boundaries to minimise interference with them;
2. The larger the apparatus, the closer one is to the conditions presented in a real reinforced structure;
3. Large soil samples allow for the utilization of instruments buried in the soil mass (eg, pressure cells) without serious consequences to the test results and on a more attractive economical and practical basis, since the instruments can be

large enough to minimise the complexities and increase in cost of manufacturing small ones;

4. Last, but by no means least, the use of a large apparatus allows for the testing of real reinforcement materials. So, neither reinforcement nor soil need to be modelled.

On the other hand, the use of a large equipment brings some adverse consequences such as:

1. Cost of equipment is higher;
2. Size of the equipment may impose limits on loads or pressures applied to the sample because of difficulty in providing reaction to those forces;
3. Heavier loads have to be handled, which limits the versatility of the equipment and claims more time for sample preparation;
4. For practical and economical reasons, stress levels in a large apparatus are usually low and because of that the soil weight is not negligible. This implies that the sample cannot be considered symmetric, at least as far as stresses are concerned, since the vertical stress increases with depth.

The adverse effects presented above cannot, however, match the benefits brought by a large apparatus. The pace of testing may be delayed but the quality of results is certainly improved. In the present work two

additional shear boxes were also used on a complementary basis. The first one is a medium size box originally designed by Jewell (1980) and on which some modifications were made. The second is a standard Casagrande shear box. These boxes can provide benefits that the large one lacks such as versatility in changing boundary conditions, for example. So, three scales of testing were used to bring maximum benefit from what each one could offer.

The observation of the results of the photoelastic study of the direct shear and pull-out tests carried out by Dyer (1985) led to the decision of installing pressure cells on the side wall of the large shear box. The location of these cells were conditioned by the results obtained in Dyer's work. Stiffer pressure cells were placed in regions of higher horizontal stress.

2.3 - Mechanical Characteristics and Instrumentation:

2.3.1 - Large Shear Box:

The large shear box basically is an enlarged version of the standard Casagrande shear Box. It consists of a 1.10 x 1.10 x 1.10 m box split in the middle in order to allow relative movement between the two halves. The internal volume of the box is 1 m^3 . The shear load is applied by an hydraulic jack (600 kN) activated by an electric pump (69 Mpa). The normal pressure is provided by a rubber bag filled with water and connected to the hydraulic system. Figure 2.1 presents schematically how the apparatus, as a whole, works. Figure 2.2 shows the equipment in more detail whereas figure 2.3 shows a general view of the box during a test.

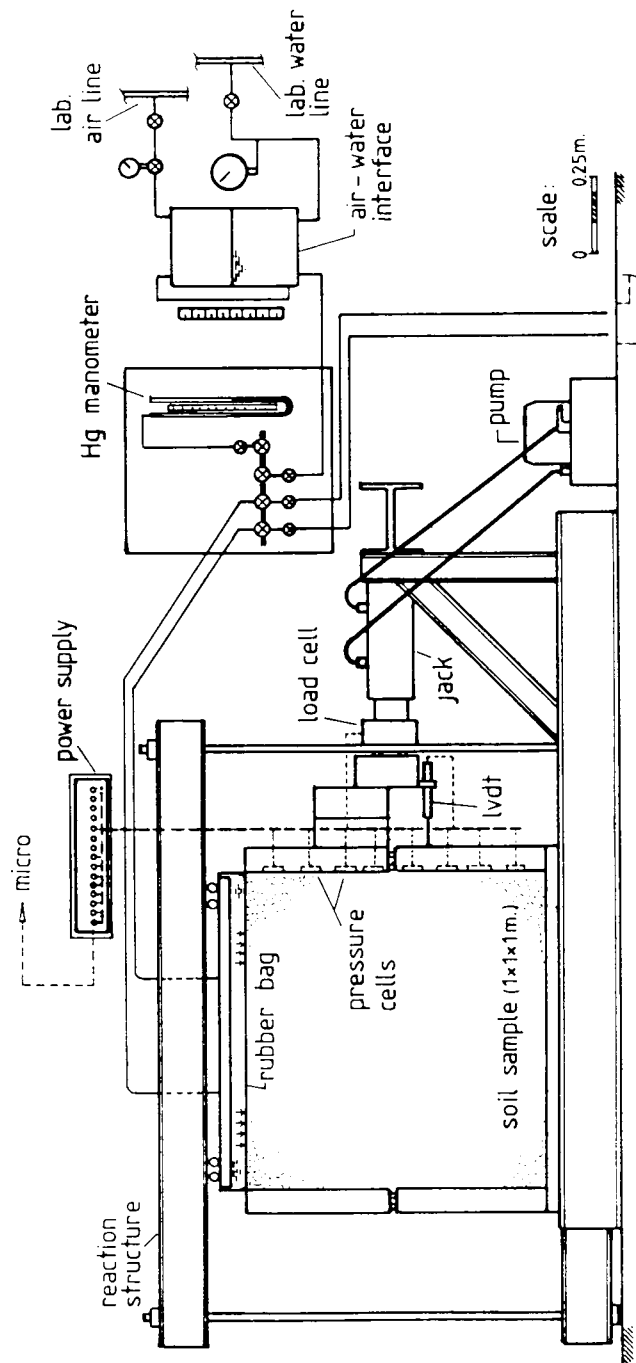
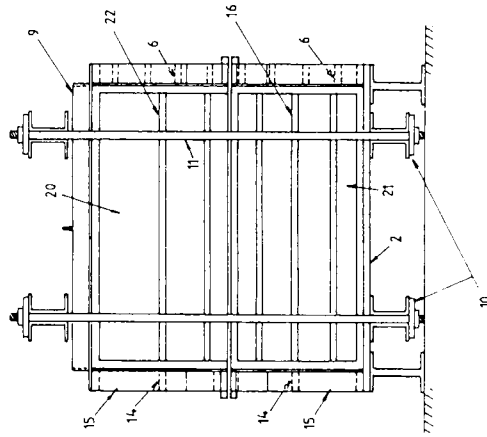
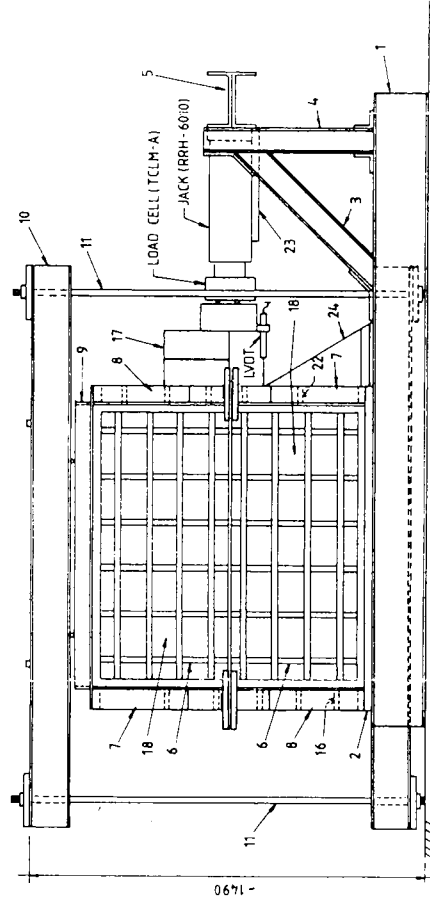


Figure 2.1 – Schematic View of the Large Shear Box.

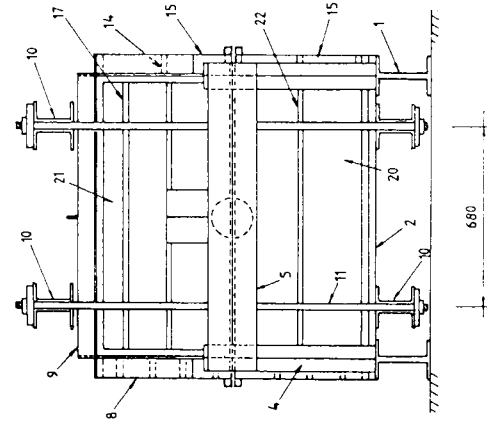
LEFT SIDE VIEW



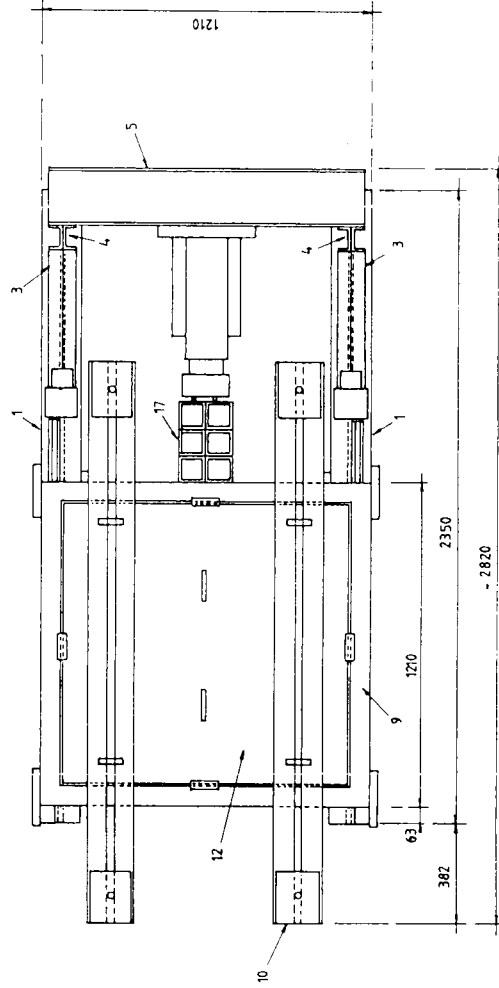
ELEVATION



RIGHT SIDE VIEW



PLAN



NOTE

1. ALL DIMENSIONS IN MILLIMETERS.

ISSUE	DATE	MODIFICATION	MATERIALS FINISH	TOLERANCES	DEPARTMENT OF ENGINEERING SCIENCE OXFORD UNIVERSITY
			SCALE 1/200	TRD.	CHK'D.

Fig.2.2 - Detailed Views of the Large Shear Box
(After Palmeira, 1984).



Figure 2.3 - The Large Shear Box During a Test.

The decision to have a flexible boundary on top was taken based on the fact that the pressure distribution is uniform and known at any stage of the test. With a rigid fixed plate on top of the sample, as in Jewell's original box (Jewell, 1980) non uniform stress distributions may occur on top of the sample, in particular in reinforced tests. Dyer's results (Dyer, 1985) have shown that, even if the top plate is allowed to move, interference between reinforcement and top plate happens during the test. Arthur et al (1977a) have shown that direct shear tests with flexible top boundary lead to peak friction angles very close to the values obtained by other plane strain devices. Use of the rubber bag filled with water has also the practical advantage of avoiding the more

complex and costly design involving a jack on top of the box to apply the vertical load.

The reaction against the vertical load on the sample is provided by four reaction beams resting on rollers on top and bottom of the box, as shown in figs. 2.1 to 2.3. The bottom beams are connected to the top ones by means of four 25mm dia. bars. The rollers (19mm dia.) between the reaction frame and the box and the ball bearings (13.5 mm) separating the two halves minimise friction in the system. Rollers were also used between the top half of the box and the load cell fixed to the jack. The box lid consists of a 25mm thick mild steel plate to which the rubber bag is clamped.

A 25mm thick perspex wall in one of the sides of the box allowed for the use of markers at the boundary of the soil sample. These markers are made of flattened 11.5mm diameter drawing pins. The spike at the back of the pin (8mm long) helps to provide anchorage and to make the marker move following the trend of the surrounding soil. During the test, photographs could be taken in order to assess displacements and strains in the soil and in the reinforcement (if an extensible one). It was also possible to inspect the soil mass in order to identify and measure shear band thickness.

To keep a constant vertical pressure during the test, an air-water interface was used (fig. 2.1). A control valve automatically compensates the variation of pressure by allowing air out of the container or inputting air to it from the laboratory compressed air line. The container has an external hose which permits one to measure water level changes that are related to volume variations of the rubber bag on top of

the soil sample. By calibration, the change in water level in the container can be related to volume variations of the sample during the test.

The maximum normal pressure that can be applied to the sample is, in fact, limited by the maximum shear load expected during the test. The box structure and reaction frame were designed to stand safely a maximum shear load of 140 kN. The top and bottom reaction beams and rods can safely resist the load due to a pressure of 150 kPa in the top rubber bag.

The box is equipped with several devices to measure changes of displacement, stresses and loads. The shear load applied to the sample is measured by a 200 kN load cell TCLM 20A fixed to the jack ram. The relative displacement between top and lower halves of the box is obtained by a 150mm stroke RDP-LVDT fixed on the top half of the box with the end of the stick resting on the bottom half. The normal pressure applied to the sample is measured by a mercury manometer close to the box and levelled to the position of the rubber bag. The pressure can also be checked by a Budenberg (160 kPa) pressure gauge connected to the air-water interface container.

Total pressure at the boundaries of the sample and inside the soil mass were measured by means of 11 strain gauged pressure cells designed by the author. Two types of pressure cells were employed. The first type is schematically shown in figure 2.4a and 8 of them were set into the internal sides of the box (fig. 2.1) to record pressure distribution at that boundary. The other 3 pressure cells are of the type shown in figure 2.4b and were used inside the soil mass. Both types of pressure cell were

designed following the recommendations presented in Weiler & Kulhawy (1982) regarding cell geometry, soil-cell stiffness ratio, arching effect, etc. The pressure cells were calibrated buried in the soil used in the experiments. In figure 2.5 a general view of the cells is presented. A constant voltage 15 channels power supply was designed and built by the author to feed all the electronic instruments in the box.

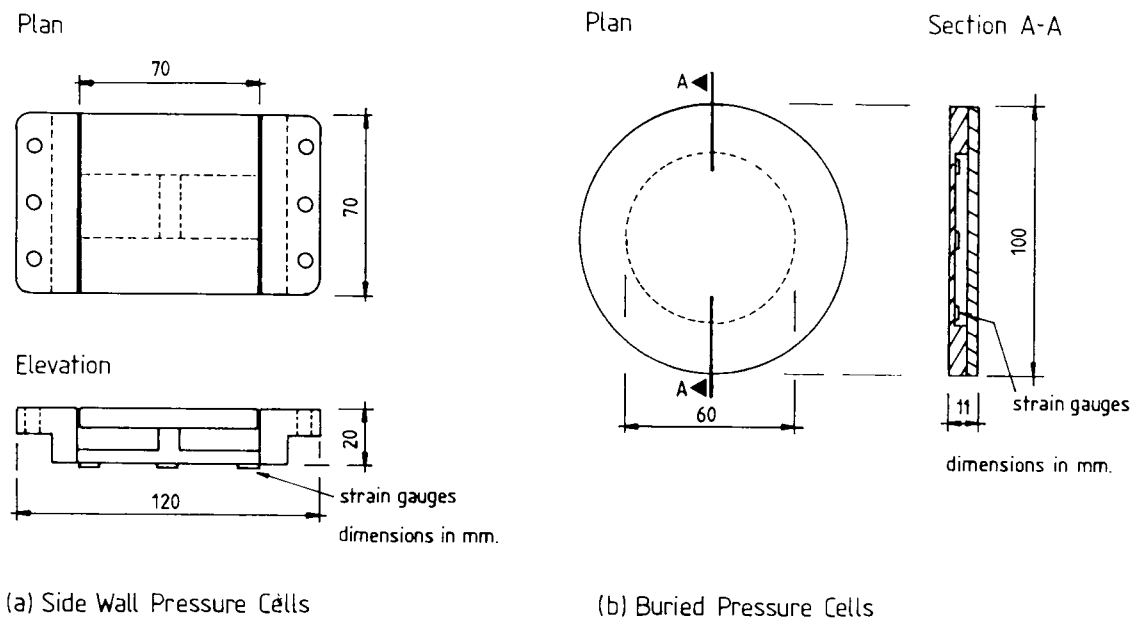


Figure 2.4 - Total Pressure Cells Used in The Large Shear Box.

During testing the instrumentation readings were scanned at equal intervals of shear displacement using a computerised system consisting of a 380Z micro-computer, Schlumberger Solartron 7060 voltmeter and a Schlumberger 7010 Minate interface. Because the voltmeter is precise to a microvolt and the test speed was low (0.5mm/min.) in comparison to the scanning speed, the voltmeter could be used in its maximum precision with no need to amplify the output signals from the instruments.

A Basic program (BS.BAS) was written to log the data from the instrumentation during the test. The program plots on the micro-computer screen: shear force value, shear displacement, time elapsed and test speed throughout the test. The test speed is adjusted by a dump valve in the electric pump. The jack cylinder and pump were overdesigned by recommendation from the manufacturer (Enarpac) in order to make it easier to have constant speed testing conditions, which would otherwise require more expensive devices. This proved to be very successful since only ≈ 6 adjustments of testing speed, based on the reading on the screen, were usually needed during the entire test (≈ 2 hours). At the end of the test, the program calculates the results in terms of displacements, pressures and forces and stores them on a floppy disk.

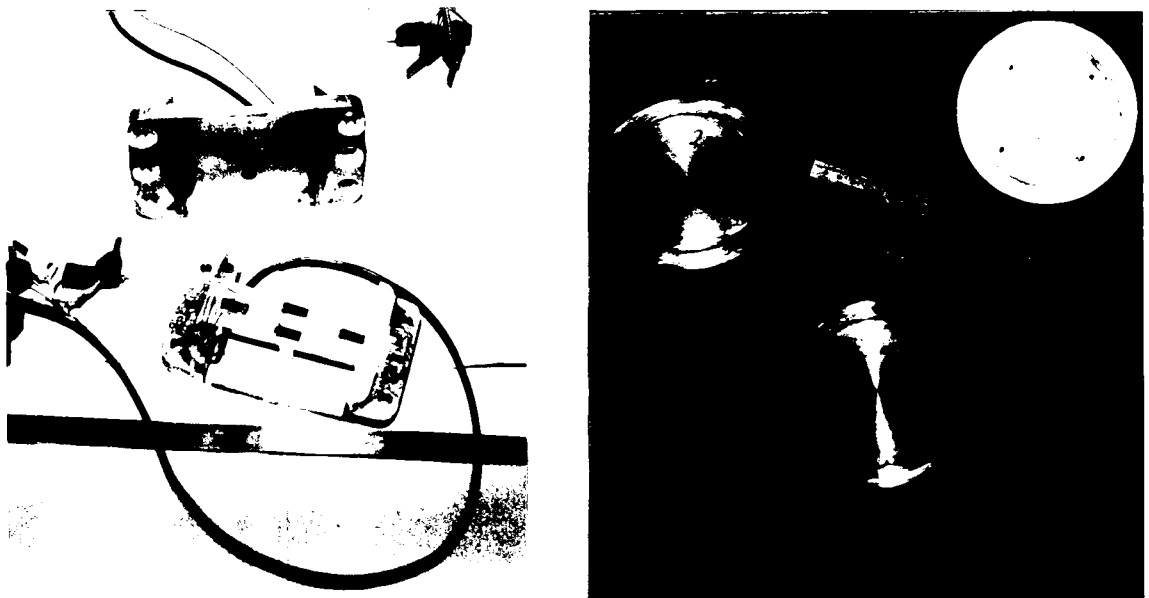


Figure 2.5 - General View of the Total Pressure Cells.

Measurement of marker movements were possible by the use of a perspex wall on one of the sides of the box. Marker positions were related to reference markers positioned on the outside face of the

perspex wall. Figure 2.6 shows schematically the photographic technique employed. An Olympus OM1n camera installed with a 135mm Vivitar lens and loaded with a 400 ASA slide film was used for the tests. The camera was firmly held on a stand bolted to the wall of the laboratory in front of the perspex face. After the film had been developed, the movement of markers could be traced by projecting the film by means of a photographic enlarger Varicon Devere 203 onto a digitising pad (Bitpad). The position of the markers could then be spotted by a cursor and recorded by the micro-computer. The markers' coordinates were related to axes on the digitising pad. Known magnitudes of distance between reference markers in the real box could be compared to the same distance projected on the digitising pad in order to obtain a scale factor.

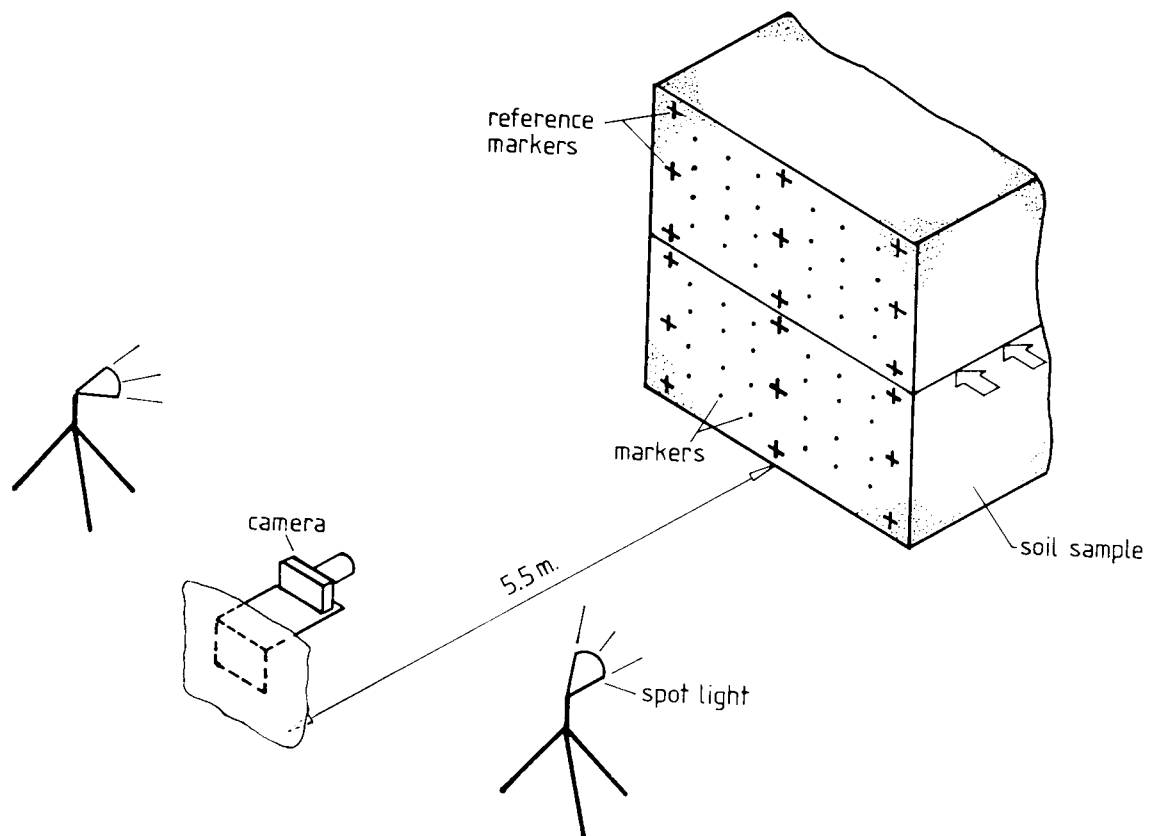


Figure 2.6 - Photographic Technique to Monitor Marker Movements

A rather large Fortran program (BIT.FOR) was written by the author to calculate displacements and strains from the marker movements. The markers are assumed to be at the corners of soil elements that can be triangular or rectangular, as far as the program is concerned. Strain relations like the ones found in Poulos & Davis (1974) are used to calculate strains in different directions. The program can take into account not only horizontal relative movement between the two halves of the box but also vertical movement of the top half of the box, which is very important for traditional direct shear box tests. The program output furnishes, for each element, horizontal and vertical strains, principal strain values and orientation, volumetric strain, shear strain, zero extension line orientation and also mean vertical displacement on the top of the soil sample. Other Fortran programs were written mainly to plot results of calculations.

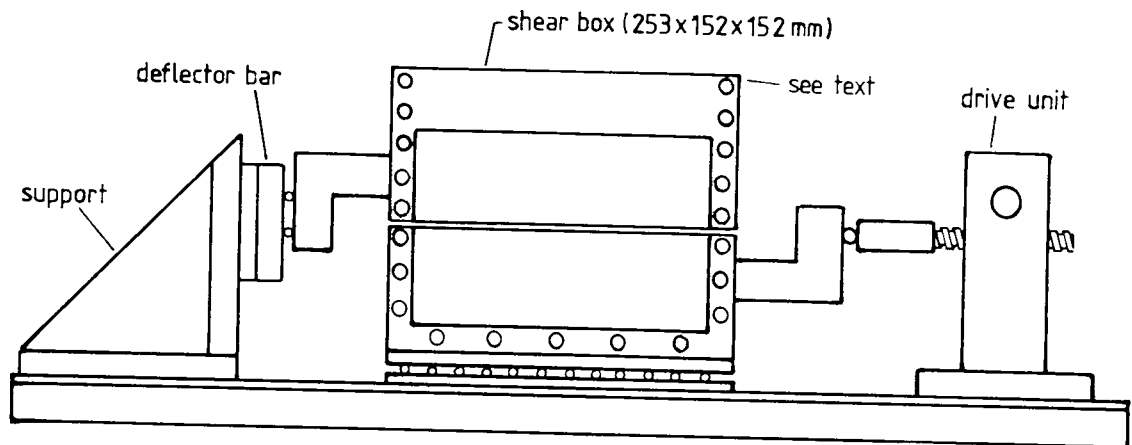
Additional data on instrumentation used in the large box can be found in Appendix A1 and in Palmeira (1987). A list of computational programs to process and plot test results is presented in Appendix A2.

2.3.2 - Medium Size Shear Box:

This shear box works in a similar way to the large shear box. It was designed by Jewell (1980) and suffered some small modifications to allow for the utilization of photoelastic technique by Dyer (1985). It consists of a 253 x 152 x 152mm box with perspex side walls to allow the observation of soil behaviour and marker movements. The apparatus is schematically shown in figure 2.7.

In Jewell's original design the vertical load is applied by a rigid rough top plate fixed to the top of the upper half of the box. In the

SIDE ELEVATION



PLAN VIEW

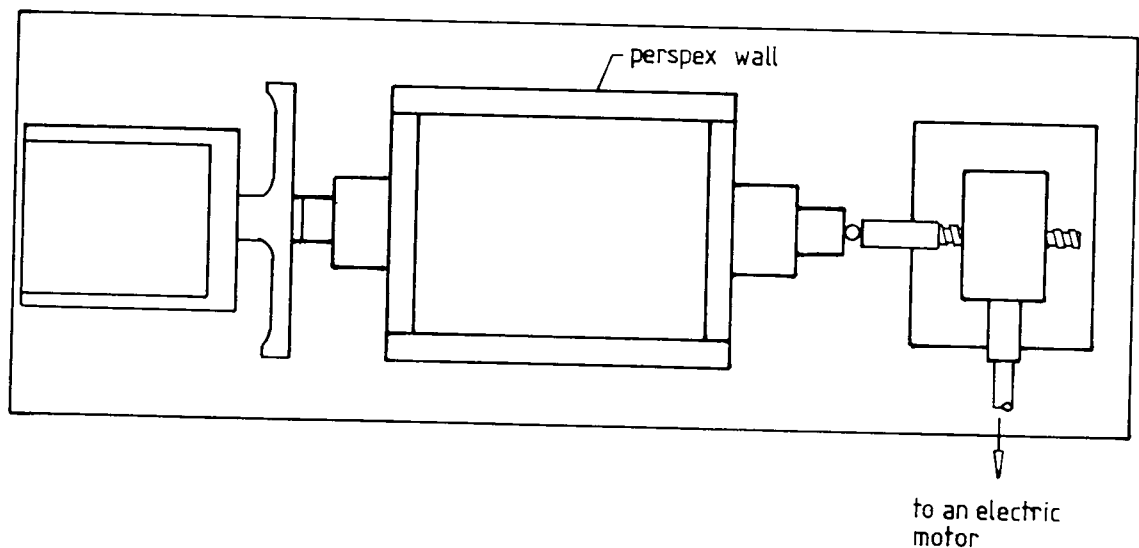


Figure 2.7 - Medium Size Shear Box (After Jewell, 1980).

present work alterations were made to allow the utilization of a freely rotating top plate or a flexible boundary, as in the large shear box. The shear load is applied by a motor which pushes the bottom half of the box at a constant rate of displacement while the top half reacts against a calibrated deflector bar. The bottom half moves on ball bearings to minimise friction although, if any occurs, it is not included in the shear force measured, anyway. Reaction against normal pressure is provided by a hanger with weights.

Shear displacements and vertical displacements on the top boundary were obtained by 0.01mm sensitivity dial gauges. The shear load is calculated as a function of the deflection at the middle of the deflector bar. This deflection was measured with a 0.002mm sensitivity dial gauge. The shear load was then obtained by multiplying the bar deflection by its calibration constant ($K=1.667 \text{ kN/mm}$).

The transparent side walls permit the observation of marker movements. The technique employed was the same as in the large box, described in the previous item. The markers in this case were flat head countersunk screws (5.3mm head dia. and 13.3mm long). The photographic camera was placed at a distance of 1m away from the box, resting on a tripod.

More details of this equipment may be found in Jewell (1980).

2.33 - Standard Casagrande Shear Box or Small Shear Box:

This direct shear box has been extensively described in basic soil mechanics books and publications; a summary description only is therefore given here. It allows testing of 60 x 60 x 31mm soil samples. The normal pressure is applied by a rigid rough top plate and a hanger and weights. The shear load is provided by a motor which pushes the bottom half of the box at a constant rate of displacement. The top half reacts against a proving ring.

Vertical displacement at the top boundary and shear displacements were measured by dial gauges (0.01mm sensitivity). Shear loads were measured by a calibrated proving ring equipped with a 0.002mm sensitivity dial gauge. The normal pressure is known as a function of the weights put on the hanger plus the weight of hanger and rigid top plate.

Chapter 3: Soil and Reinforcement Characteristics

Chapter 3: Soil and Reinforcement Characteristics

3.1 - Introduction:

This chapter presents the main characteristics of the soil and reinforcement materials used in the direct shear tests. Additional information can also be found in Appendix A3.

3.2 - Soil Characteristics:

The soil used in direct shear tests was dry Leighton Buzzard Sand 14/25. This is a very uniform sand (Coefficient of Uniformity $CU = 1.3$) with angular grain shape ($G_s = 2.66$) and particle diameters varying between 0.6 and 1.18mm ($D_{50} = 0.8\text{mm}$). Maximum and minimum void ratios are 0.49 and 0.79, respectively. The sand sample was prepared in order to obtain a dense state ($e = 0.53 \pm 0.005$) with a Relative Density Index equal to 87%.

The choice of the soil was based on the following reasons:

1. Reinforced soil structures are built mainly with coarse granular backfill materials;
2. The behaviour of uniform sands is easier to understand than non-uniformly graded soils or soils with large values of CU because the different shapes and particle sizes bring more complicated interparticle mechanisms;
3. Leighton Buzzard sand 14/25 has been a standard sand used in research. As a consequence, its behaviour is very well documented

by high quality experimental data reported by Cole (1967), Stroud (1971), Jewell (1980) and others.

Figure 3.1 presents an enlarged photographic view of Leighton Buzzard sand 14/25.

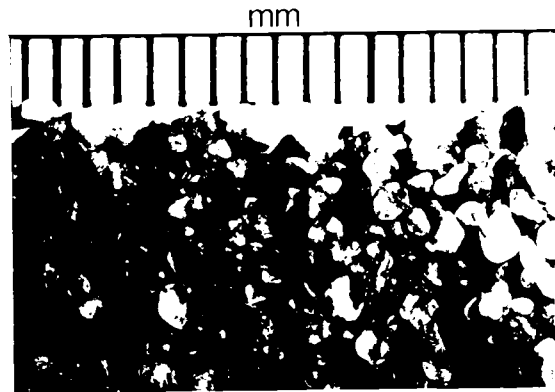
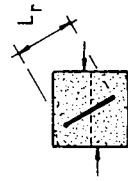
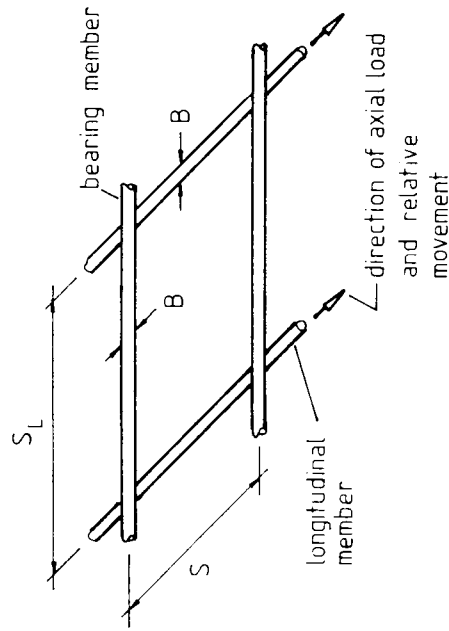


Figure 3.1 - Photographic View of Leighton Buzzard Sand 14/25.

3.3 - Reinforcement Characteristics:

Real or potentially real reinforcing materials were chosen to give a range of properties and interaction mechanisms with the surrounding soil. The study concentrated on the behaviour of grids, although two woven geotextiles, a "perfectly rough" sheet and a smooth metal strip (interface friction angle of 16° with dense Leighton Buzzard sand 14/25) were also used in the tests. A rather large variety of grid geometries were tested since this is one of the parameters affecting grid performance. The importance of each parameter can then be investigated by varying reinforcement characteristics and interaction mechanisms.

Table 3.1 shows the nomenclature of grid member adopted throughout this work. Bearing members are defined as members which interact with the



L_r - reinforcement length

W_r - reinforcement width

α_s - fraction of grid surface area which is solid

α_B - fraction of member area available for bearing

E_L - equivalent longitudinal stiffness

K - bending stiffness (EI/W_r)

D_{50} - mean particle diameter of Leighton Buzzard sand 14/25

Notes:

1. Not all reinforcements were used in both direct shear and pull-out tests.
2. See appendix 4 for data on L_r and W_r .

REINFORCEMENT CODE	RAW MATERIAL	B (mm)	S (mm)	S_L (mm)	α_s (%)	α_B (%)	S/B	B/ D_{50}	E_L^* (kN/mm ϵ)	K (Nmm)
grid 1	g.s. +	1.63	12.5	12.5	20.4	100	7.7	2.0	6844	1137
grid 2	g.s.	1.63	19.1	19.1	14.5		11.7	2.0	4479	744
grid 3	g.s.	1.63	12.5	25.4	16.2		7.7	2.0	3368	559
grid 4	m.s. +	4.78	76.2	76.2	11.1		15.9	6.0	49455	70623
grid 5	m.s.	3.15	50.8	50.8	11.0		16.1	3.9	32216	19979
grid 6	m.s.	3.15	200.0	82.0	5.1		63.5	3.9	19958	12377
grid 7	g.s.	1.00	25.4	25.4	7.3		25.4	1.3	1268	79
grid 8	m.s.	4.78	152.4	76.2	8.6		31.9	6.0	49455	70623
grid 9	g.s.	1.00	12.5	25.4	10.6		12.5	1.3	1268	79
netlon tensar SR1 ^x	polymer	4.4	53.2	10.2	380	74	12.1	5.5	440 ⁺	—
netlon tensar SR2 ^x	polymer	4.4	111.0	22.2	46.0	72	25.2	5.5	550 ⁺	—
geolon 70	polyester	0.62 [*]	—	—	100	—	—	—	550	—
stabilenka 400	polyester	1.26 [*]	—	—	100	—	—	—	4000	—
rough sheet	aluminium	0.8 [*]	—	—	100	—	—	—	56000	2987
plain metal strip	aluminium	1.68 [*]	—	—	100	—	—	—	11760	3951

+ - secant modulus at 10 % deformation (taken from McGown - 1983)

x - see appendix A3

+ - g.s. - galvanised steel

m.s. - mild steel

* - thickness

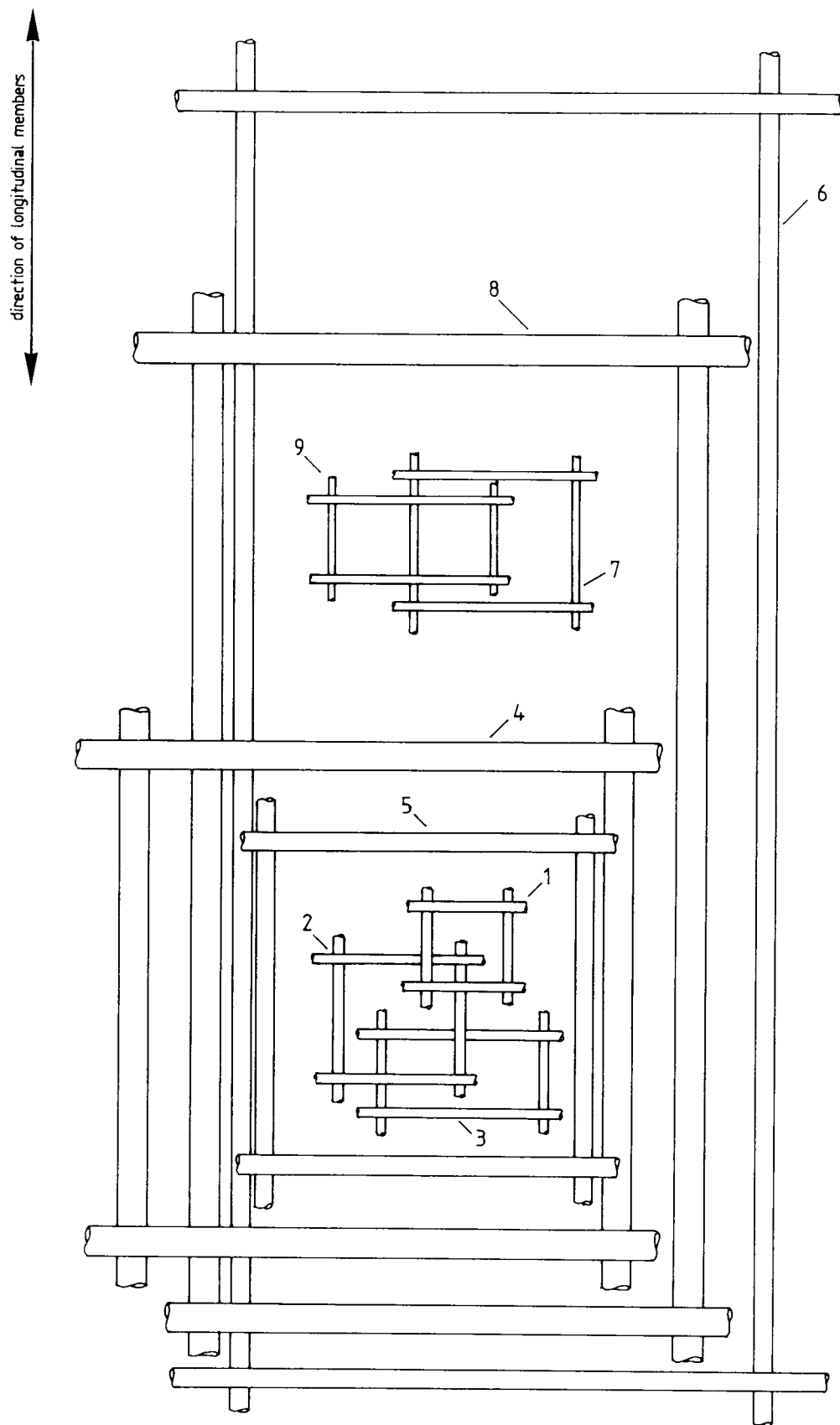
* - specific tensile strain

Table 3.1 - Characteristics of the Reinforcements Used in the Present Work

surrounding soil by bearing mechanism. Longitudinal members are the ones which coincide with the direction of axial load and relative movement between grid and soil. For the specimens used in the tests total length and width are denoted by L_r and W_r , respectively. Also in Tab. 3.1 the geometric characteristics of reinforcement are presented. The Equivalent Longitudinal Stiffness for a grid is defined as the modulus of a plain sheet of the same material and with the same total cross-section area of the grid. Reinforcement Bending Stiffness is defined as the product between the raw material Young's modulus (E) and the total second moment of area (I) per unit width of reinforcement. For geotextiles and polymer grids it was considered to be nil. In figures 3.2 to 3.4 and in Appendix A3 more details on the reinforcements used are given.

The different geometries of metal grids (see fig. 3.2 and Tab. 3.1) try to encompass the practical values of ratios between bearing member diameter to bearing member spacing and, to a smaller extent, the relation between grid aperture size to soil particle size. The two woven geotextiles are commercially available materials and have different stiffness and surface roughness (see fig. 3.3). Interface direct shear tests, which are presented later, have shown a mean interface friction angle slightly higher for the Stabilenka geotextile. The Netlon grids SR1 and SR2 are uniaxial geogrids manufactured from co-polymer grade high density polyethylene (see fig. 3.3). One should note that the longitudinal stiffness of these polymeric grids compares closely with the value for Geolon 70 geotextile.

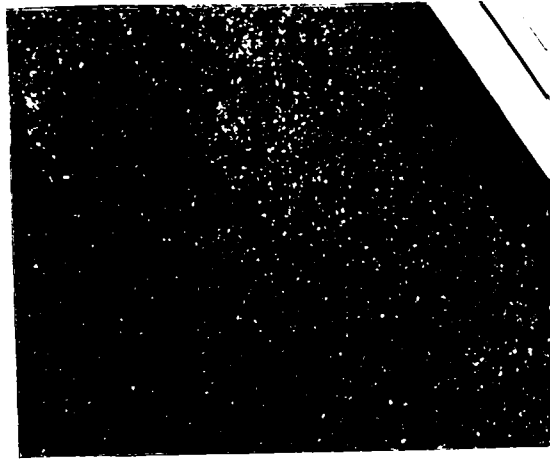
The "perfectly rough" sheet (fig. 3.3) consists of an aluminium sheet with Leighton Buzzard sand glued to both sides. This reinforcement was prepared by first roughening the original metal surface and then



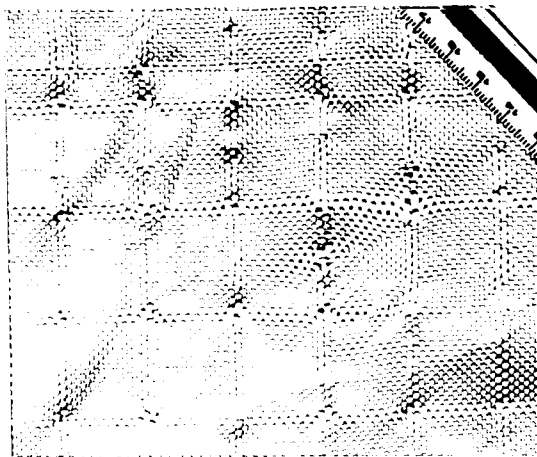
Scale: 1/1

Dimensions are given in Tab. 3.1

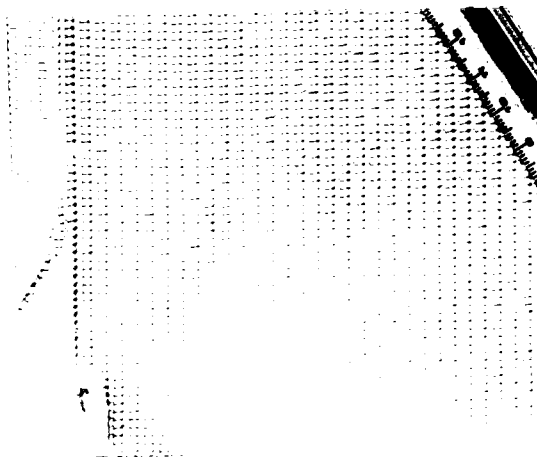
Figure 3.2 - Geometry of the Metal Grids Used in the Present Work.



Rough Sheet

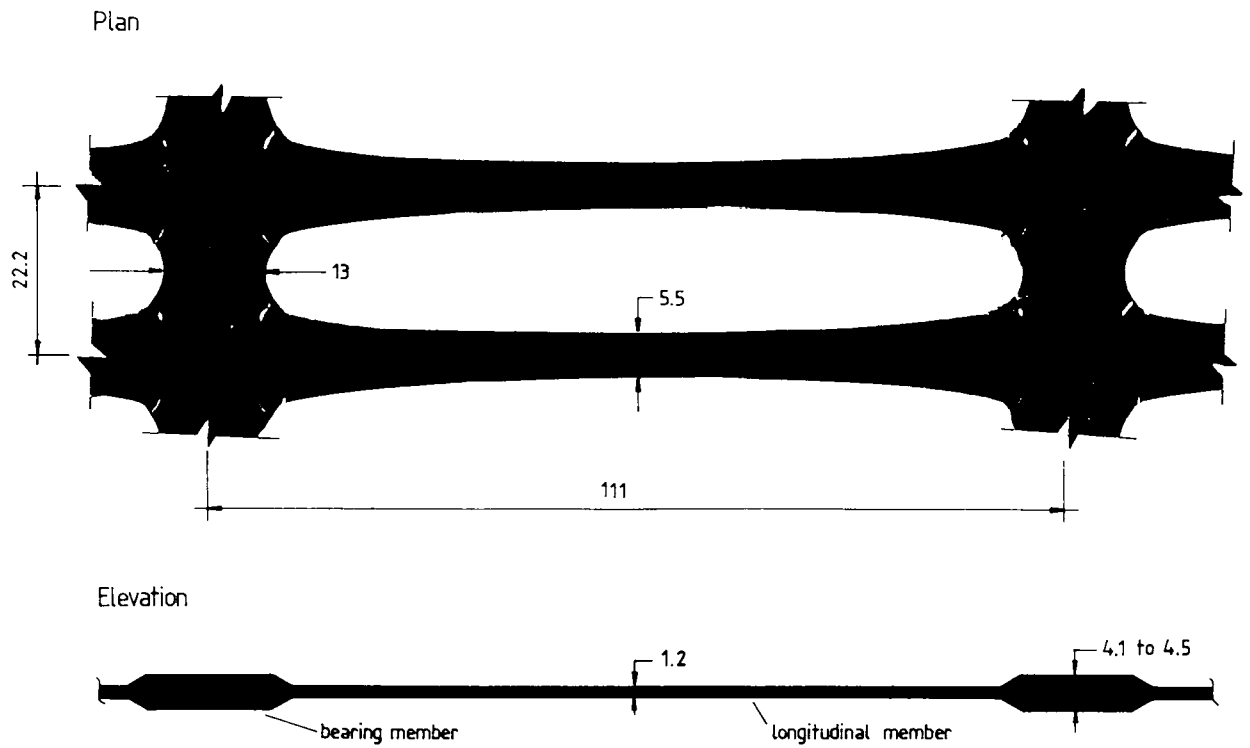


Geolon 70

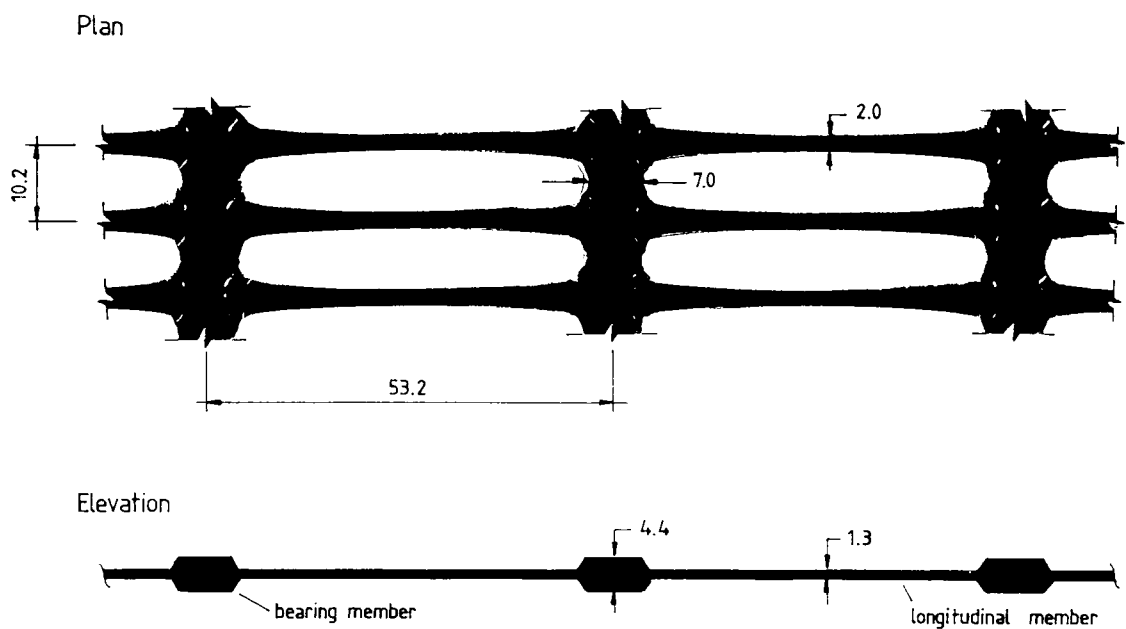


Stabilenka 400

Figure 3.3 – Photographic View of the Frictional Reinforcements Used in the Present Work.



Netlon Tensar SR2



Netlon Tensar SR1

Notes:

1. All dimensions in mm.;
2. Scale = 1/1.

Figure 3.4 - Geometry of the Polymer Grids Used in the Present Work.

applying Araldite to the surface and spreading sand evenly on it. Before and after the reinforced test with this material the state of the surface was checked and no deterioration was observed in either case. The result of the test with this reinforcement can be considered as a reference value for comparison between performances of purely frictional materials.

Chapter 4: Sample Preparation and Test Procedure

Chapter 4: Sample Preparation and Test Procedure

4.1 - Introduction:

This chapter deals with the description of sample preparation in each of the direct shear devices used. The procedure to be followed during the test and after it are also presented. Description is more detailed with regard to the large direct shear box. References are given where additional information on the other apparatus can be obtained.

4.2 - Large Direct Shear Box:

4.2.1 - Sample Preparation:

Before the hopper that was used to prepare the sample was placed on top of the box, the internal side walls of the box were lubricated in order to minimise the friction force on the plates that transfer the shear load to the sample. The original painted metal surface already provided a smooth surface. On top of that a double layer of polythene, grease (Castor grease) and oil was placed as schematically shown in figure 4.1a. First the grease was spread evenly on the face of the wall. The first polythene layer was then laid using a painting roll to expel any trapped air bubbles. After that, the oil was spread on the polythene surface already installed and the second layer was similarly positioned.

Despite the measures presented above, perfectly frictionless surfaces are impossible to achieve. Therefore, interface direct shear tests were conducted using the standard Casagrande shear box to assess the friction coefficient between dense Leighton Buzzard sand 14/25 and

the lubricating arrangement used on the side walls. The sand sample was prepared in the top half of the box with the same density used for the tests in the large shear box. In the bottom half, a metal block replicating the conditions on the lubricated internal side walls was used. The variation of the peak interface friction angle with the vertical pressure obtained in these tests is presented in figure 4.1b. A markedly non-linear behaviour can be observed. Because the stress distribution on the sides of the box was measured, the shear stress due to friction could be then estimated. The procedure adopted in the present work was to add the friction force on the side to the vertical force due to the pressure at the top bag plus the weight of soil, to obtain the total vertical pressure at the central plane (σ'_y). This caused an increase of approximately 8% in the vertical pressure originally intended (σ_y).

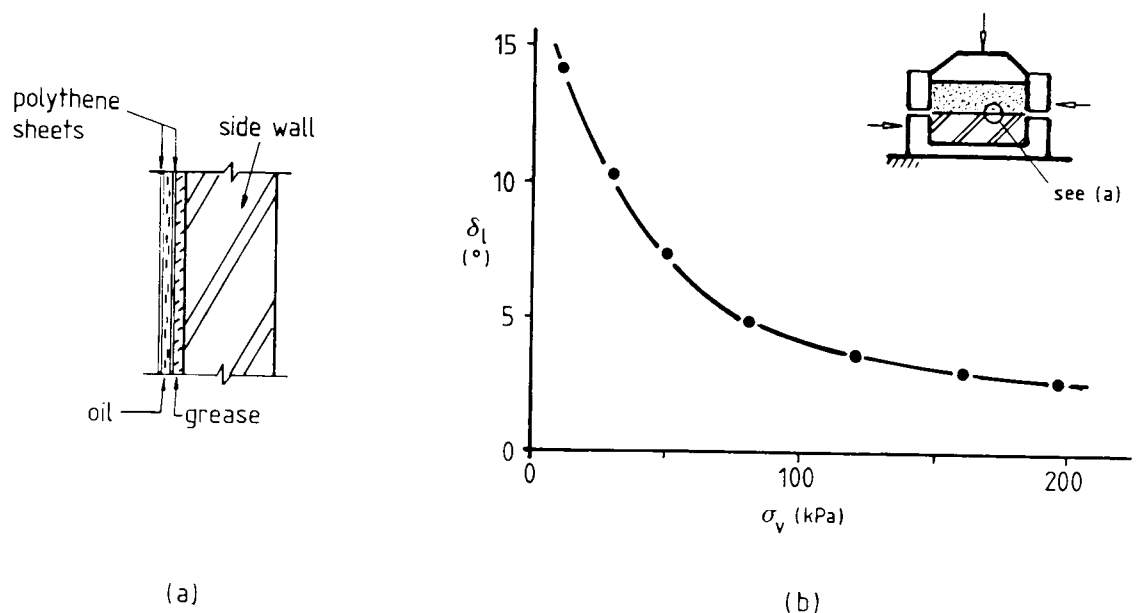


Figure 4.1 - Friction on the Sides of the Large Shear Box.

The sample was prepared using a hopper covering the whole area of the box with a minimum height of 620mm above the final sand sample surface. This follows the recommendation by Cole (1967) on the preparation of dense and uniform samples of sand. In figure 4.2 the sample preparation is schematically presented. During sample preparation the two halves of the box were bolted together to avoid movements of the top half. The hopper consists of a metal box (1050x1050x250mm) open on top and with two 2.38mm thick plates at the bottom perforated with holes 6.35mm dia. on a 11.3mm triangular pitch. One of the perforated plates is fixed to the hopper structure whereas the other is free to move. By pushing the free plate one can make the holes to overlap by about 3.0mm, just enough for the sand grains to pass. The sides of the hopper are closed with layers of polythene (as well as the top during pouring) in order to control dust.

Because of the markers on the sample boundaries and on the reinforcement layer, the sand mass could not be poured at once. Instead, it had to be pluviated in layers of thickness approximately equal to the vertical spacing between the lines of markers. So, the total volume of sand (1m^3) was divided in 14 dust bins ($\approx 0.1\text{m}^3$) and one bin at a time was put into the hopper. To do so, each bin had to be placed on a specially designed cage which was then lifted using a manual hoist. After the sand was poured from the bin into the hopper, it was uniformly spread concentrating a slightly bigger height of sand on the internal side walls in order to compensate for the border effects during pouring. The free perforated sheet was then moved causing the sand to be pluviated into the box.

After each sand bin had been poured, the dust inside the box was removed using a small vacuum cleaner. The line of markers was then

positioned, with each marker having its face lubricated with grease to minimise friction with the perspex wall. The procedure used to install markers on the reinforcement depended on the type of reinforcement. For polymer grid reinforcements, the marker had its pin driven into the bearing member of the grid with Araldite filling any gap between the back face of the marker and the grid member. For geotextiles and metal grids the technique is not accurate enough for strain measurements. In these cases, the marker was simply glued to the surface of the geotextile or to the bearing member of the metal grid using Araldite. The aim in such operation was only to obtain the deformed shape of the reinforcement during the test.

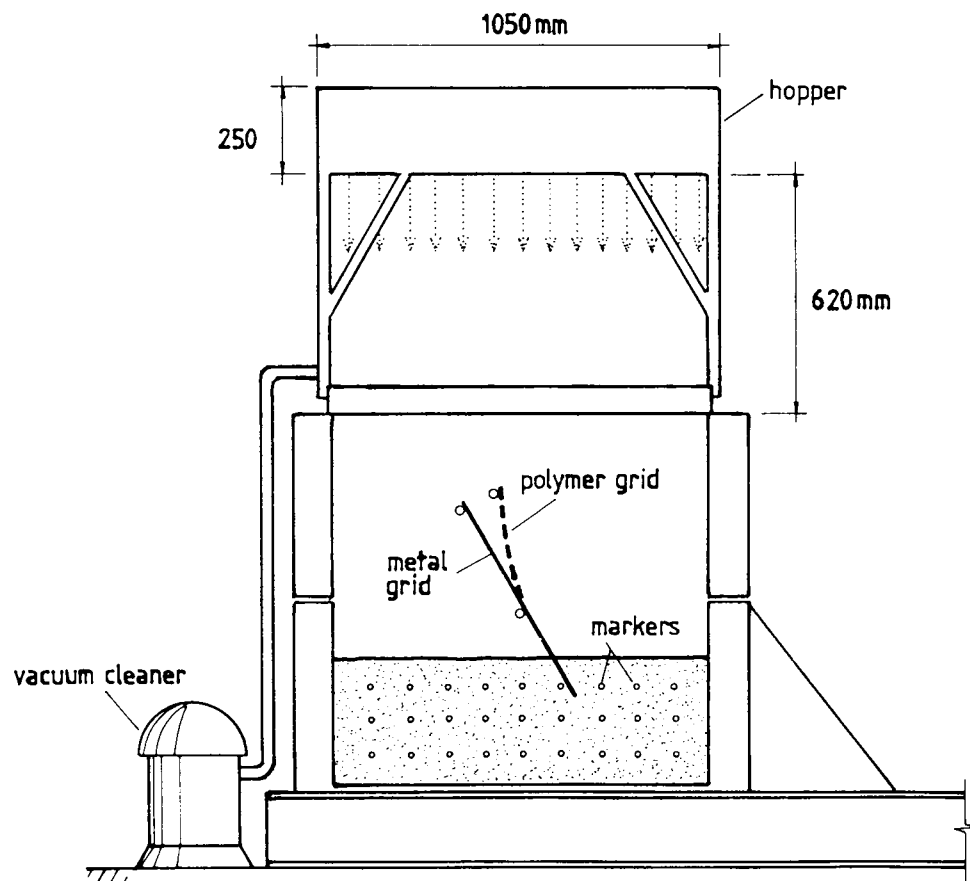


Figure 4.2 – Sample Preparation in the Large Shear Box.

A sample was prepared with the specific intention of density measurement and repeatability checks at different points inside the box. Thin walled containers with known volume were used to accomplish this. The sand was pluviated with the containers resting on top of the sand surface at different points and elevations inside the box. Three measurements at the middle plane of the box, two at the bottom and two at the top led to a mean void ratio of 0.53 ± 0.005 . The variation of density with depth was within the scattering of the results, no tendency being noticed towards higher densities at the bottom. The value of the void ratio obtained compares very well with values obtained in smaller apparatus (Stroud - 1971, Jewell - 1980). At this state the Relative Density Index is 87%.

The preparation of reinforced samples required the reinforcement to be held in position during pouring. When the sand surface reached the level of the reinforcement transverse bars (see fig. 4.2) were installed to hold the reinforcement layer in place. Usually two of those bars were needed for metal grids and three for polymer grids. The reinforcement was fixed to those bars by means of adhesive tape. When the sand reached the level of the bar it was removed.

In the case of inclined polymeric grids, the reinforcement was always slightly bent in its upper length (see fig. 4.2) in order to minimise sample disturbance since, for those grids, the fraction of grid surface area which is solid is higher.

In the case of geotextile it was noticed that it was impossible to prepare a good quality sample with the reinforcement inclined due to sample disturbance. Tests with geotextile were limited to those with the

reinforcement in a vertical plane, where the effect on sample preparation was a minimum.

The procedure described above was followed until the sand level reached the top of the box. Then, the sand surface was levelled by carefully removing any excess of sand using a meter rule. The hopper was removed and the lid with the top bag was put in place, the reaction beams assembled and the two halves of the box unbolted. The testing phase could then start.

It usually took one complete day of work to prepare a sample in the large shear box.

4.2.2 - Test Procedure:

After the sample preparation had been finished and the reaction frame structure assembled, the standard procedure was:

1. To position the photographic equipment (camera and spot lights). Aperture size and exposure time were decided as a function of the light conditions at the time. Care must be taken when positioning the spot lights in order to minimise shades caused by the metal frame holding the perspex wall, since it can be difficult to see the markers on the side of the box. Shots were taken at approximately the following shear displacements: 0 (after vertical pressure had been applied), 2.5, 5.0, 10.0, 15.0, 20.0, 27.5, 35.0, 45.0 and 54.0mm. Shots were also taken at peak load shear displacement or for any other event of interest occurring

during the test, such as failure of the reinforcement material for instance;

2. Before the vertical pressure was applied to the sample, the trolley with the micro-computer was brought close to the box. All the instrument cables were connected to the interface board. The logging program (BS.BAS) was loaded and run. The first step followed by the program is to present, on the screen, the continuous scanning of all instrument readings at that time. This allows one to check whether all instruments are behaving properly and to take the necessary measures if any faulty instrument is detected. The program displays on the screen instructions on how to proceed to continue the logging of the test data;
3. The vertical pressure was applied to the sample by slowly filling the rubber bag on top of the sample with water, using the pressure system shown in figure 2.1. A minimum volume of water of about 60 litres inside the bag was required in order to avoid it being completely compressed against the lid due to dilation of the sand mass. In preliminary tests it was observed that when closure of the bag occurred, a sudden increase in shear load was observed because of the increase in vertical stress, which is not controlled by the rubber bag any more, under these circumstances. During the filling of the bag the water pressure could be checked by the mercury manometer (fig. 2.1) until the final pressure value was reached. For most of the tests where comparisons between different reinforcements were made, a constant vertical pressure of 21.5 kPa was applied on top of the sample. This value plus the pressure due to the weight of the soil ($\gamma \approx 17 \text{ kN/m}^3$) gave a vertical pressure on the horizontal plane, in the middle of the box of approximately 30 kPa. Tests at different vertical

pressures were also performed to investigate stress level influence on sample response. But, again, the weight of the sand had to be considered in the definition of the pressure to be applied on top, as explained above;

4. After the nominal vertical pressure was applied to the sample, all instrument readings were scanned by the computerised system and the first shot with the photographic camera fired to obtain the initial position of the markers. The instructions presented at the screen monitor were followed to the next stage of the test;
5. The electric pump was switched on and the shear load application started by increasing the oil pressure in the jack using the dump valve in the pump, until the constant test speed was reached (this value is plotted on the screen throughout the test for control purposes). During the test the oil pressure in the jack was manually adjusted using the dump valve to keep a constant value of test speed of 0.5 mm/min.;
6. The logging program reads all the channels at increments of 1.5mm relative displacement between top and bottom halves of the box. The test data logging is stopped by instructions given to the computer via the keyboard;
7. After the test was finished, the jack ram movement was reversed until its original position before the test was achieved. The electric pump was switched off, the valves connecting the rubber bag to the pressure system closed and the pressure released. The drain valves to the bag were opened in order to permit the flow of water by gravity. The top reaction beams were removed and, when most of the water volume inside the bag was released, the top lid was also removed, exposing the sand surface.

The complete testing phase usually took about 3 hours.

4.2.3 - Post-test Procedure:

After the test was completely finished the box had to be emptied and prepared for the next test. To empty the box, a 4800W vacuum cleaner was used to suck the sand into its container. A trap door under the vacuum cleaner container allows the sand to be transferred to the plastic sand bins. In figure 4.3 the emptying technique is schematically shown. Each full sand bin was pushed to the corner of the room to allow space for the work to continue.

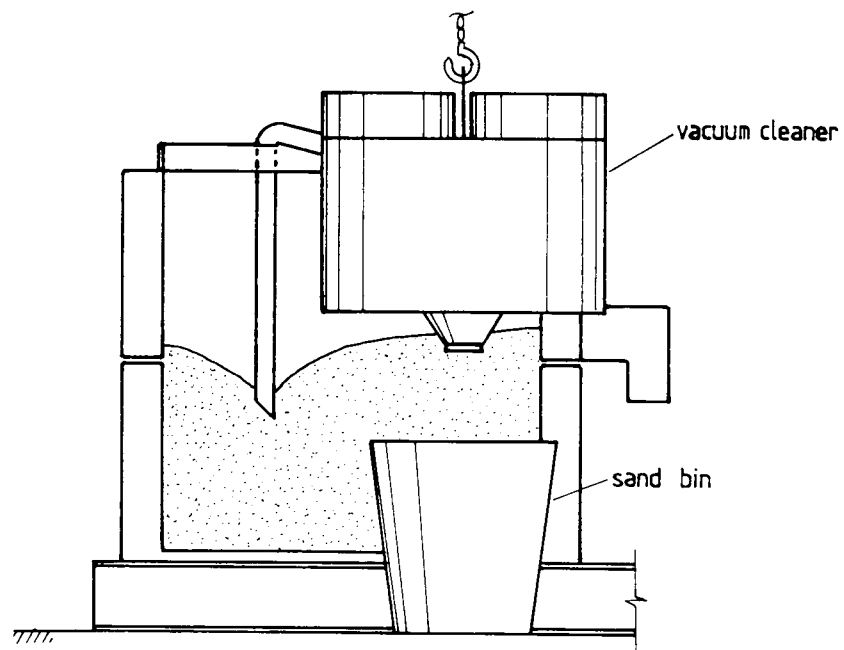


Figure 4.3 - Emptying Procedure in the Large Shear Box.

As the sand level was being lowered inside the box, the markers at the boundary were removed. After all markers had been removed they were left immersed in Genklene solution for one day for cleaning purposes.

When the box was completely empty the internal faces were cleaned. The perspex wall was cleaned using Genklene solution. The polythene sheets, grease and oil on the lubricated side walls were removed and replaced by a new set after each test. Following this operation, the hopper could be placed on top of the box again and a new sample preparation phase started.

To empty the box and reassemble it for the next sample preparation usually took 3.5 hours, under the conditions at that time.

4.3 - Medium Size Shear Box and Casagrande Shear Box:

4.3.1 - Sample Preparation:

The sample preparation in these boxes was accomplished making use of a single hose hopper kept at a constant height of 500mm above the sand surface. The hose was moved uniformly from side to side of the box during pouring. The rate of sand flow used was 107 g/min. which led to a dense sand sample with void ratio equal to 0.52 ± 0.005 .

In reinforced sand tests (medium size box only) the reinforcement was held in place by the use of strings following the procedure presented by Dyer (1985).

During sample preparation the two halves of the boxes were bolted together to prevent relative movement and consequent sample disturbance.

When the sand sample reached its final height the top lid and flexible bag (when present) were placed. The hanger of weights and dial gauges were installed and the testing phase started.

4.3.2 - Test Procedure:

After the vertical pressure had been applied and dial gauges positioned, the standard procedure was as follows:

1. All dial gauges were set to zero. Consolidation settlements due vertical pressure application were observed to be negligible;
2. The motor was switched on at maximum speed (≈ 2.0 mm/min.) until the loading axle touched the box. This could be noticed by the beginning of movement of the needle in the dial gauge for the deflector bar (or proving ring in the Casagrande shear box). The test was then stopped. The dial gauge for shear displacement was reset. The standard test speed (0.5mm/min) was set in the gear box and the test re-started;
3. Readings were taken each 0.25mm displacement until peak stress ratio was achieved and beyond. At later stages in the test the interval between readings was increased to 0.5 and 1.0mm;
4. When the test was finished the motor was switched off and reversed and the loading frame and top boundary removed.

4.3.3 - Post-test Procedures:

The emptying and reassembling of both boxes involve much simpler and quicker operation than for the large shear box. Basically, it consists of pouring the sand back from the box to the sand bin, cleaning the internal

faces of the box and changing the lubricating elements (when present). It usually took half an hour to accomplish this.

4.4 - Repeatability of Test Results:

This item presents data on the repeatability of test results obtained in the direct shear apparatus. At this stage no considerations are made of the influence of the reinforcement on the strength of the reinforced sand. The aim is just to provide a basis of reference for repeatability of test results. Emphasis is given to the behaviour of the large shear box since the other apparatus have proven to give very repeatable results on other occasions (see Jewell - 1980 on the repeatability of the medium size shear box).

Figure 4.4a presents the results for shear stress to normal stress ratio against shear displacement for four direct shear tests in the large shear box. This set of results comprises:

1. Two unreinforced test results;
2. Two reinforced sand test results using grid 4 inclined 30° to the vertical direction;
3. Two reinforced sand test results using grids 1 and 3 (same spacing between bearing members and same member diameter) in the vertical direction;

All these tests were performed under 30 kPa vertical pressure. The repeatability shown is very encouraging.

In figure 4.4b a comparison between normalised increments of horizontal stresses at the boundary for repeated tests is presented.

These results are also very repeatable, although not as closely as the previous ones.

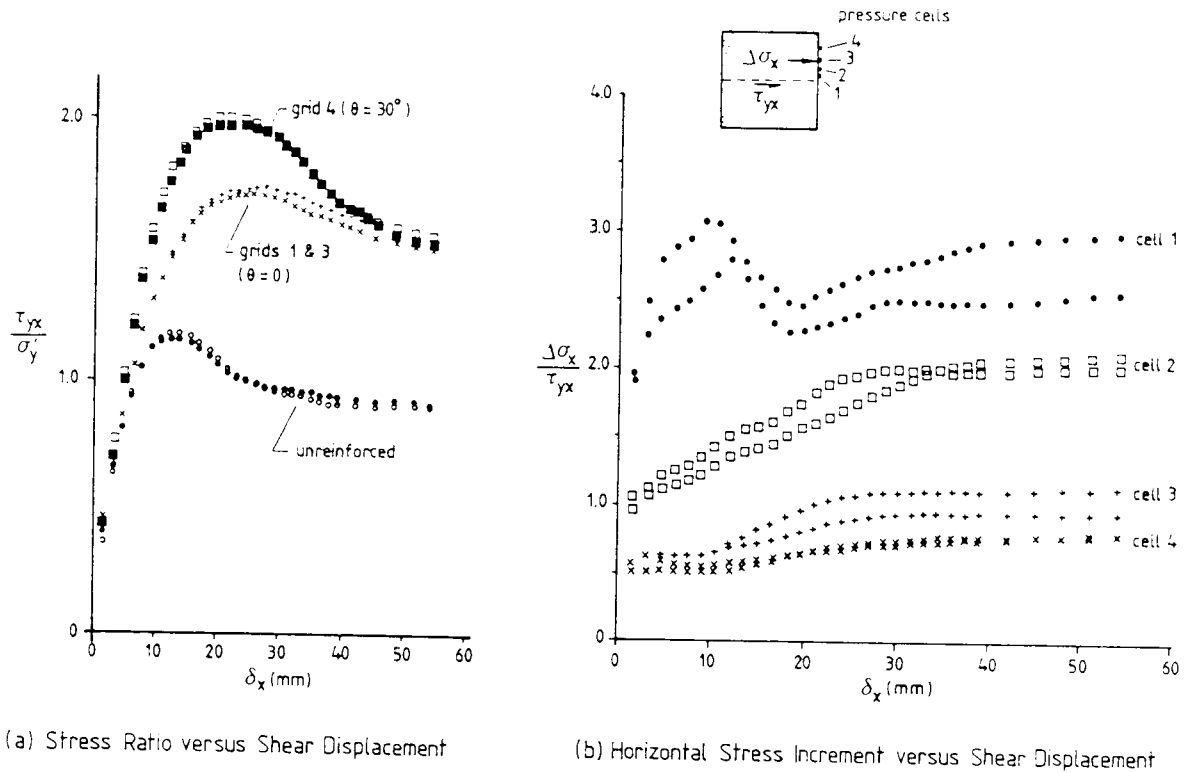


Figure 4.4 – Repeatability of Test Results in the Large Shear Box.

The photographic technique used to measure displacements of markers revealed an accuracy of 0.3mm. This was obtained by digitising four times the same slide and checking the values obtained for markers movements. In this case the accuracy is not only a function of the technique itself but, particularly, a function of the accuracy of the digitising equipment available and the scale of the test. The accuracy on strain measurement was observed to be 1.2% which is acceptable for the magnitude of strains observed in direct shear tests, as will be shown later.

Regarding displacements and strains obtained from markers at the boundary, there is always the inevitable question whether or not what is being measured can be extrapolated to the inner regions of the sand mass. Kerisel (1972) cites a series of small scale tests at low stress levels with sand where influence of friction on the sides proved to be negligible to strain measurements. In the large shear box, after any test was finished, it could be observed that the sand surface lifted evenly due to dilation, no constraints being noticed due to the side walls. A check on the accuracy of displacements obtained at the boundary in the large shear box can be done by comparing the mean vertical displacement on top of the sample using the volume variation at the top bag and the data obtained from the top line of markers. This comparison is shown in figure 4.5 where very good agreement can be observed, confirming the

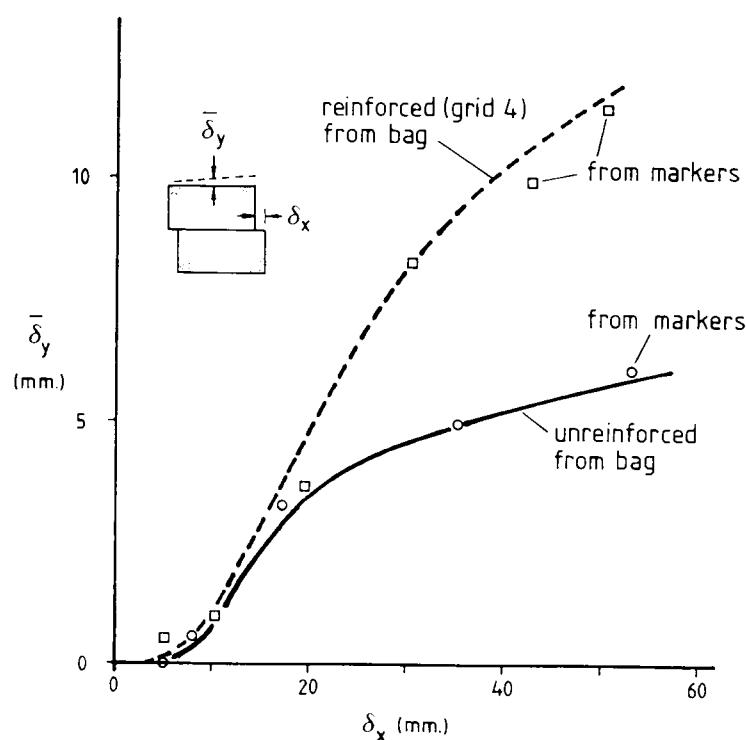


Figure 4.5 - Comparison Between Mean Vertical Displacements at the Top of the Large Shear Box.

comments by Kerisel (1972) mentioned above. As far as the load versus displacement behaviour is concerned the same applies, since in figure 4.4a one of the unreinforced tests was performed with all the internal walls lubricated with the arrangement presented in figure 4.1 and it shows no difference of behaviour. This is not unusual, since the horizontal pressure on the smooth lateral plates parallel to the direction of shear is certainly much smaller than on the plates that transfer the shear load to the sample.

Chapter 5: Direct Shear Tests on Unreinforced Sand

Chapter 5: Direct Shear Tests on Unreinforced Sand

5.1 - Introduction:

This chapter presents the results of direct shear tests on unreinforced sand. The influence of boundary conditions and scale were investigated and are also presented.

5.2 - Some Considerations on the Direct Shear Test:

5.2.1 - Soil Friction Angle in a Direct Shear Test:

In a direct shear test, after the application of the vertical load, horizontal loads are applied to the top and bottom half of the box. As a consequence of this and of the boundary conditions, a failure mechanism is induced along a narrow horizontal region in the middle of the sample. In a soil element in that region, the horizontal stress increases from its initial K_0 value, the vertical stress is constant and shear stresses develop on the horizontal and vertical faces of the element until failure is reached; this is usually assumed to occur when a drastic change in the curve relating shear stress to shear displacement of the box is observed. Under these loading conditions there is rotation of the principal stresses in the soil element in the central region of the box.

The standard approach adopted to interpret results from the test is summarised in figure 5.1a. The stress path on a horizontal plane in the soil element in the central region of the box is represented by the vector AB. The Mohr circle of stresses at failure is tangent to the failure envelope at B. The friction angle is then defined as:

$$\phi_{ds} = \tan^{-1} \left(\frac{\tau_{yx}}{\sigma_y} \right) \quad [5.1]$$

where:

ϕ_{ds} - friction angle in a direct shear test or mobilised friction angle on the central plane of the box;

τ_{yx} , σ_y - shear and vertical stresses on the central plane.

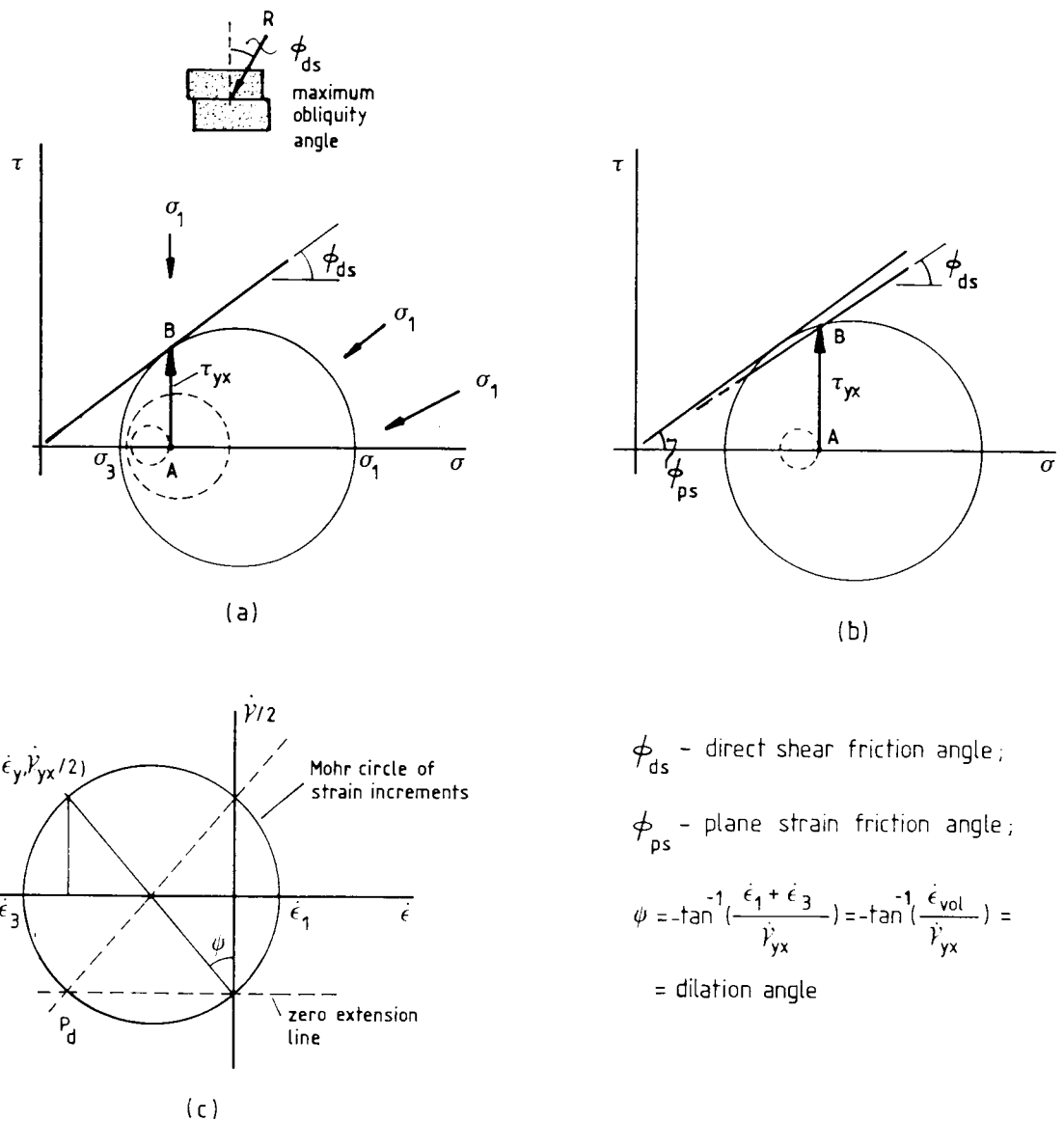


Figure 5.1 - Definition of Parameters in Direct Shear Tests.

The approach described above is known as the Maximum Obliquity Criterion and it is similar to the approach used for the study of the sliding of a block on a rough surface.

Experimental observation of strains developed in samples undergoing simple shear or direct shear, in conjunction with a hypothesis from the Theory of Plasticity for isotropic materials led to another approach to the problem, which is shown in figure 5.1b. In this figure, the Mohr circle of stresses at failure is tangent to the failure envelope at a point other than B, making an angle to the horizontal equal to the plane strain friction angle of the soil (ϕ_{ps}). Obviously, this angle is different from the one obtained by the maximum obliquity criteria. Also from that figure one can observe that the value of ϕ_{ps} will only be determined from a direct shear test if other variables of the test are known, for example, the orientation of principal stresses at failure.

Several authors have reported the horizontal region in the middle of a shear box as being a region of zero extension (Jewell - 1980, Scarpelli & Wood - 1982, Dyer - 1985). If that is so, the Mohr circle of strain increments at failure is similar to the one presented in figure 5.1c. In this figure the following important variable is defined for a soil:

$$\tan\psi = \frac{\dot{\epsilon}_1 + \dot{\epsilon}_3}{\dot{\gamma}_{yx}} = \frac{\dot{\epsilon}_v}{\dot{\gamma}_{yx}} \quad [5.2]$$

where:

ψ - soil dilation angle;

$\dot{\epsilon}_1, \dot{\epsilon}_3$ - principal strain increments;

- $\dot{\gamma}_{yx}$ - shear strain increment;
 $\dot{\epsilon}_v$ - volumetric strain increment;

If the soil is assumed to be a perfectly plastic isotropic material, the directions of principal stresses and principal strains increments coincide (coaxiality). This means that the Mohr circle of stresses and strain increments are geometrically similar. Then, the following relations are valid:

$$\begin{aligned} \sin \phi_{ps} &= t/s & \tan \phi_{ds} &= \tau_{yx}/\sigma_y \\ \tau_{yx} &= t \cdot \cos \psi & \sigma_y &= s - t \cdot \sin \psi \end{aligned} \quad [5.3]$$

$$\text{where : } t = (\sigma_1 - \sigma_3)/2 \quad \text{and} \quad s = (\sigma_1 + \sigma_3)/2$$

which leads to:

$$\sin \phi_{ps} = \frac{\tan \phi_{ds}}{\cos \psi + \sin \psi \tan \phi_{ds}} \quad [5.4]$$

Figure 5.2 presents the variation of ϕ_{ps} with ϕ_{ds} for different values of ψ , obtained from expression 5.4. For dilation angles between 0 and 30° the greater the dilation angle the closer the values of ϕ_{ps} and ϕ_{ds} . In fact, figure 5.2 or the differentiation of expression 5.4 with respect to ψ shows that a minimum value of $\phi_{ps} = \phi_{ds}$ is obtained when ψ is equal to ϕ_{ds} . Therefore, from expression 5.4, ϕ_{ps} is always greater or equal to ϕ_{ds} and the difference between the two may reach significant values.

It is usually argued that ϕ_{ds} would be equal or close to the plane strain friction angle. This would imply non-coincidence of principal axes or perhaps small deviations between them. This problem can only be solved by carrying out experiments where directions of stresses and strain increments are measured. However, experimental evidence presented in the literature has been conflicting. In Table 5.1 conclusions obtained by authors who investigated this subject are set out. In some cases, for the same type of equipment, coaxiality is observed by one and not by the other. Dyer (1985) reports coaxiality occurring in a direct shear test apparatus but the accuracy of strain measurements was poor and a simple statistical analysis of the deviations measured shows that a mean deviation of 5 degrees occurred, with a 95% level of confidence.

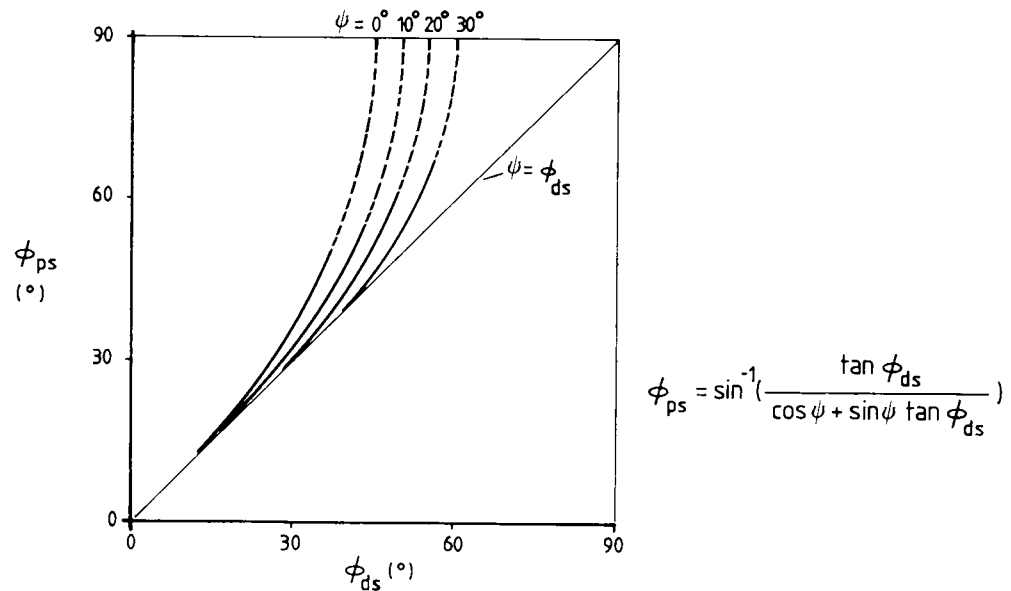


Figure 5.2 – Theoretical Relation Between ϕ_{ps} and ϕ_{ds} Based on Coaxiality Between Stress and Strain Increments Direction.

Arthur et al (1977b) give a compromise explanation to the problem by assuming that coaxiality may or may not occur depending on the constraints imposed on the deforming soil element. Wong & Arthur (1985)

and Matsuoka et al (1986) reported significant deviations of principal directions when severe rotation of principal axes of stress were imposed on the sample under plane strain test conditions.

In a real soil structure, such as an embankment or a slope, higher friction angles would be available if coaxiality between stresses and strain increments occurred. However, the possibility of progressive failure in such cases would cause a reduction in the friction angle to be used in stability analysis to a value (not necessarily above ϕ_{ds}) yet to be accurately quantified (Milligan, 1986).






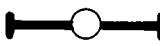

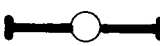
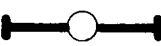
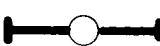




Author	Test	Coaxiality	Non Coaxiality	Comments
Allersma (1982)	simple shear			
Arthur et al (1977a)	flexible boundary apparatus			
Basset (1967)	simple shear			some deviations
Cole (1967)	simple shear			some deviations
De Josselin De Jong (1958,59,71)	non standard			
Drescher (1976)	double shear			
Drescher & De Josselin De Jong (1972)	non standard			
Dyer (1985)	direct shear			poor accuracy on strain measurements
Matsuoka et al (1986)	simple shear			coaxiality at large strains
Oda & Konishi (1974)	simple shear			
Spencer (1964)	non standard			
Stroud (1971)	simple shear			
Symes et al (1982)	hollow cylinder			

Table 5.1 - Works in the Literature Where the Orientation of Principal Axes of Stress and Strain Increments Were Measured.

Another important point in expression 5.4 is that it can overestimate ϕ_{ps} if ψ is underestimated. This can happen if one takes as the soil dilation angle, the slope of the curve relating mean vertical displacement on top of the sample versus shear displacement. It has already been reported by Scarpelli & Wood (1982), and confirmed by the present work, that values of ψ obtained under such conditions can be about 5° smaller than the correct value obtained by expression 5.2 if measurements are made in the central region of the box.

The reasons outlined above have undermined the use of the coaxiality concept in direct shear tests. Besides, the maximum obliquity criteria gives values of friction angles in direct shear tests close to the ones obtained by other plane strain devices, particularly when a flexible boundary is used at the top of the sample. Arthur et al (1977a) reported 1° difference between the friction angle (ϕ_{ds}) for Leighton Buzzard sand obtained from direct shear tests and other plane strain devices. This difference rises to 8° when coaxiality is assumed. Wernick (1978) also reported very close results obtained by direct shear and biaxial tests in the same sand.

5.2.2 - Flow Rules:

Flow rules relate strains and stresses during the plastic flow of a material. The best known, and extensively confirmed by experimental data, is due to Rowe (1962) and presented below:

$$\frac{\sigma_1 \dot{\epsilon}_1}{\sigma_3 \dot{\epsilon}_3} = -\tan^2(\pi/4 + \phi_f/2) \quad [5.5]$$

where:

- $\varepsilon_1, \varepsilon_3$ - principal strains increments;
- σ_1, σ_3 - principal stresses;
- $\dot{\varepsilon}_v$ - volumetric strain increment
- ϕ_f - equivalent friction angle ($\phi_\mu < \phi_f < \phi_{cv}$);
- ϕ_μ, ϕ_{cv} - interparticle friction angle and constant volume friction friction angle.

Note that expression 5.5 is valid even with non-coincidence of principal directions, as demonstrated by De Josselin de Jong (1976), confirmed by an empirical relation in Bolton (1986) and also observed by Matsuoka et al (1986).

Another flow rule arises when the balance of energy in a direct shear test is calculated. Based on the energy correction proposed by Taylor (1948) it can be derived that the increment of energy per unit volume in a soil element in the central region of the shear box, after an increment of shear strain, is given by:

$$\dot{E} = \sigma_y \dot{\varepsilon}_y + \sigma_x \dot{\varepsilon}_x + \tau_{yx} \dot{\gamma}_{yx} \quad \text{or}$$

$$\frac{\dot{E}}{\sigma_y \dot{\gamma}_{yx}} = \frac{\tau_{yx}}{\sigma_y} + \frac{\dot{\varepsilon}_y}{\dot{\gamma}_{yx}} = C \quad (\dot{\varepsilon}_x = 0) \quad [5.6]$$

where:

- $\dot{\varepsilon}_x, \dot{\varepsilon}_y$ and $\dot{\gamma}_{yx}$ - strain increments;
- σ_x, σ_y and τ_{yx} - stresses on the soil element faces;

Wroth (1958) found that this expression is valid for an assembly of steel balls in simple shear. Stroud (1971) obtained for Leighton Buzzard sand $14/25$ $C = \sin \phi_{cv} = 0.575$ and Jewell (1980) observed a value of C of 0.62 in direct shear tests with the medium size shear box. So, expression 5.6 provides a powerful and simple flow rule for soil elements tested under simple shear conditions. Its applicability can also be extended to direct shear tests, since it has been observed experimentally and by numerical analysis, that the soil in the central region of a shear box behaves in a similar way as in a simple shear test (Jewell - 1980, Potts et al - 1987). Good agreement between the results coming from these two flow rules has been found by Stroud (1971) and Jewell & Wroth (1987).

5.2.3 - Influence of Boundary Conditions in Direct Shear Tests:

The medium size shear box was used to investigate the influence of boundary conditions on test results. The top boundary is the one which may differ from one to another apparatus. Tests with dense Leighton Buzzard sand 14/25 under a vertical pressure of 30 kPa were performed to assess the influence of the top boundary. The following cases were investigated:

1. Rigid rough top plate fixed to the upper half of the box (original Jewell's shear box);
2. Rigid rough top plate free to move;
3. Flexible rubber bag filled with water on top.

Figure 5.3a shows the result of these tests in terms of stress ratio versus shear displacement. Figure 5.3b shows the variation of mean vertical displacement of the top of the box versus shear displacement.

The peak stress ratio increased with the use of the flexible boundary in comparison with the other two conditions. Cases 1 or 2 above gave approximately the same peak stress ratio but the post peak stress ratio drops more severely in case 1 than in the others, which may be caused by the greater restriction on sample rotation inside this box. Regarding the variation of vertical displacement of the top boundary, cases 2 and 3 compare very closely, whereas case 1 indicates a slightly greater slope. It is worth mentioning that ϕ_{ds} for the flexible boundary tests was about 2° greater than the value obtained with other boundary conditions. It was also noticed that for the geometry of the medium size box, no difference was observed in unreinforced tests when a free rough plate or a smooth top plate was used.

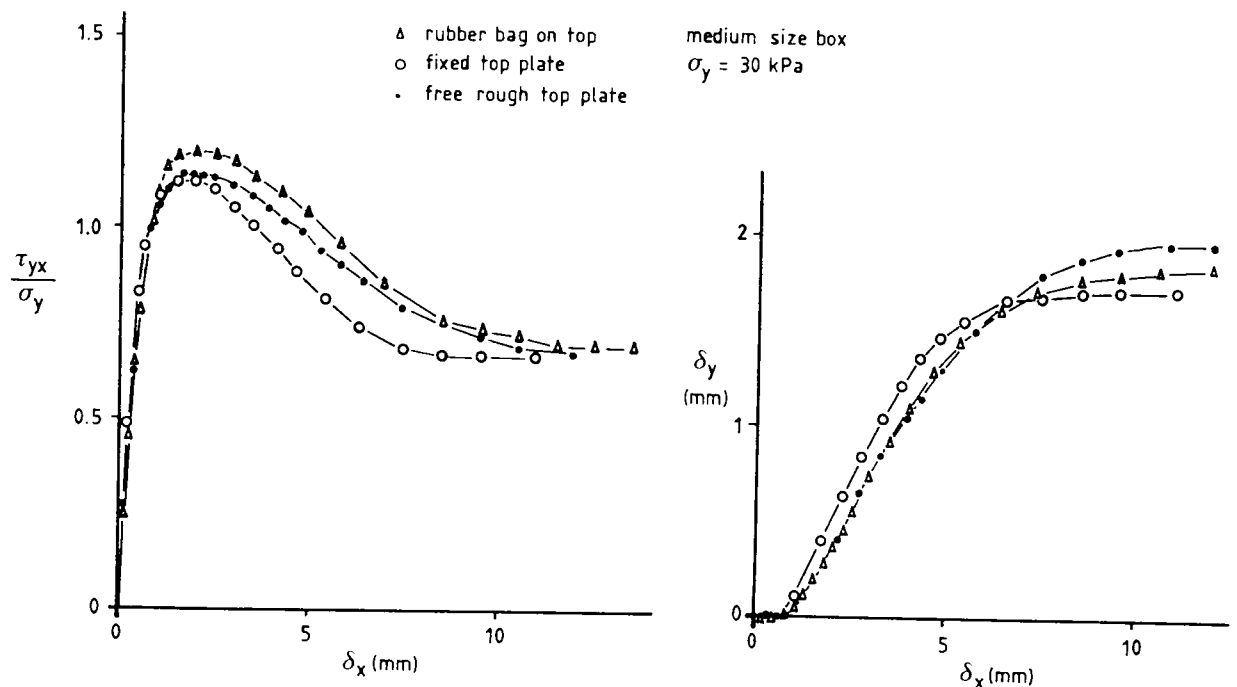


Figure 5.3 – Direct Shear Tests Results for Dense Leighton Buzzard Sand 14/25 Under Different Boundary Conditions on Top.

The same exercise was applied to a sample reinforced with grid 1. Tests with fixed, rigid and rough top plate (case 1) and with flexible boundary on top (case 3) were performed. The reinforcement was 143mm long and was placed along the vertical direction. Figure 5.4 shows the results obtained. In this case, a stiffer response response by the sample and an increase of 10% in strength was observed with the use of a flexible top boundary. This is believed to be due to non-uniformity of vertical stress distribution on top and bottom of the sample in case 1.

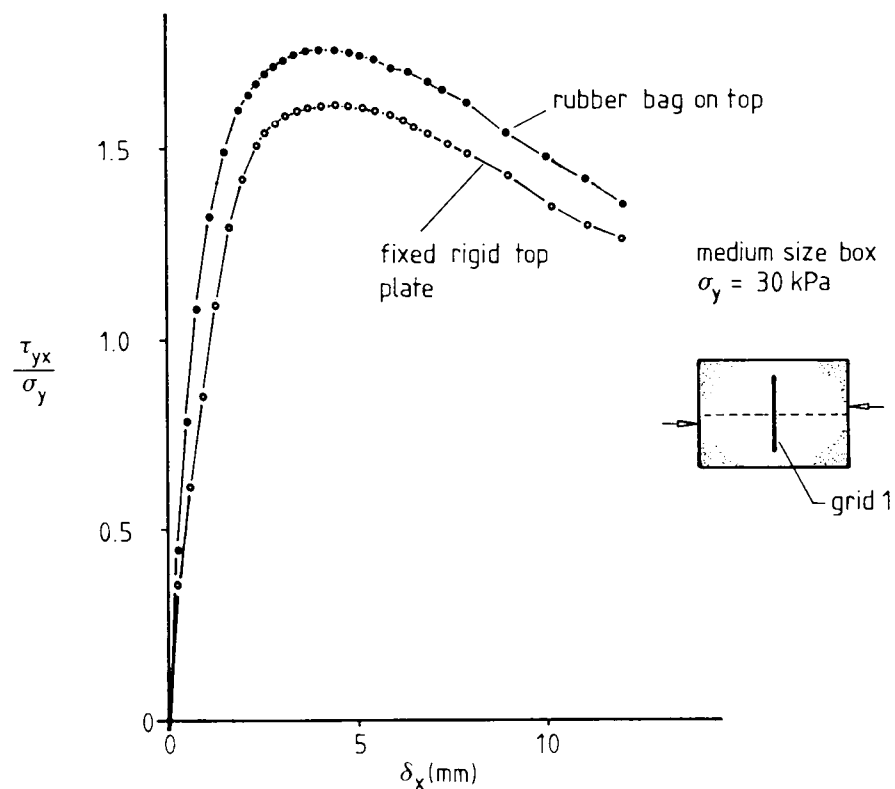


Figure 5.4 – Influence of the Top Boundary Condition on Reinforced Tests in the Medium Size Box.

5.3 - Large Scale Direct Shear Tests on Unreinforced Sand:

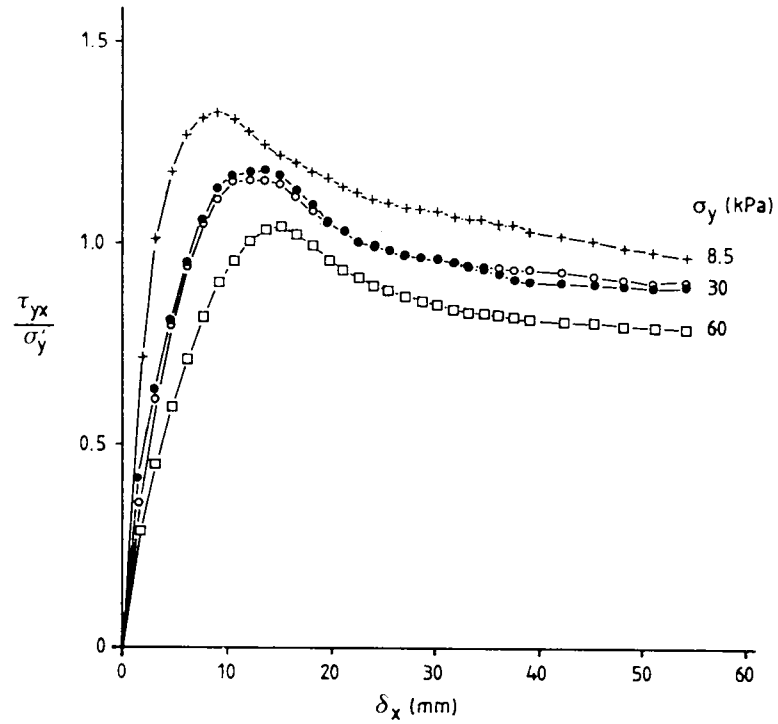
5.3.1 - Scale Effect:

Figure 5.5 shows the results of large scale direct shear tests on unreinforced Leighton Buzzard sand 14/25 at three different stress levels. Figure 5.5a shows the marked effect of stress level on the direct shear friction angle of sands. Also, in contrast to smaller scale tests, the stress ratio after peak decreases at a slower rate to the critical state friction angle ($\approx 35^{\circ}$) and, for these tests, much greater deformations would be necessary to reach that state. Figure 5.5b shows the development of mean vertical displacement at the top of the soil sample during the tests. It should be noted that the lower rate of decrease of the stress ratio after peak is associated with a still dilating behaviour of the sample, as shown in figure 5.5b.

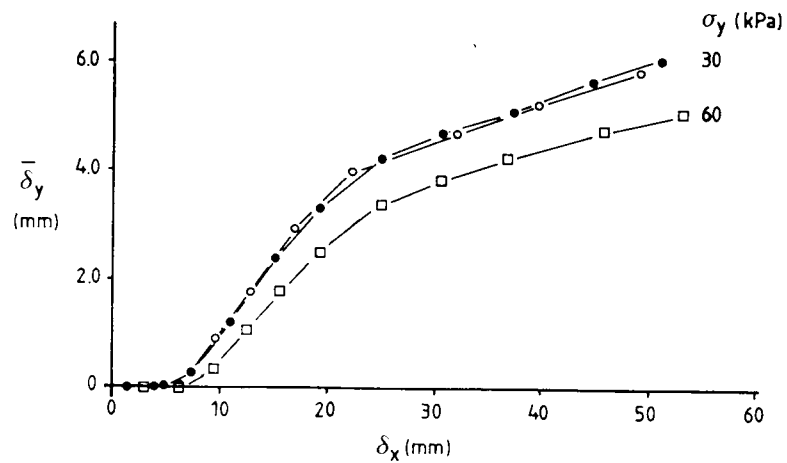
No volume variation measurements were taken in the test at 8.5 kPa vertical pressure because this test was performed as an index test to check if the lower rate of decrease on stress ratio could be caused by friction in the reaction frame. This test was performed without the reaction frame and the top bag, with vertical pressure due to the weight of sand only. This result has shown a similar trend which indicated that scale, not friction in the system, was responsible for that behaviour.

Figure 5.6 shows comparisons between test results at different scales, but the same boundary conditions (flexible top boundary). In this figure the shear displacement has been normalised by the shear zone thickness observed at the centre of each shear box so that comparisons can be made on the basis of a measure of mean shear strain. This made it

possible to bring all results within the same range of variation for the horizontal axis variable (mean shear strain). The shear zone thickness



(a)



(b)

Figure 5.5 - Large Scale Direct Shear Tests Results in Dense and Unreinforced Leighton Buzzard Sand 14/25.

was measured visually through the perspex wall of the large and medium size shear boxes. For the small shear box, tests were repeated with thin vertical wires inside the sample so that the shear zone thickness could be obtained from the deformed shape of the wires. The deformed shape of a metal strip reinforcement, after a test in the large shear box, confirmed the measurement of the shear zone at the boundary. Table 5.2 summarises the main results obtained in the tests shown in figure 5.6.

From figure 5.6 and Table 5.2 one can observe that scale seems to have little effect on the values of ϕ_{ds} and ψ obtained from boundary measurements. Post-peak behaviour is affected by the scale of the test. Mean vertical displacement non-dimensionalised by the shear zone thickness is also presented in that figure. Results from the small shear box and the medium size shear box compare closely. For the large box, even when to lines of markers close to the shear zone are used, the difference in behaviour is still evident for large deformations, where dilation continues in the large shear apparatus while in the smaller ones a state of zero volume variation has already been achieved. Table 5.2 shows that the mean shear zone thickness observed in the middle of the box depends strongly on the scale of the test.

Figure 5.7 shows the variation of peak stress ratio versus vertical pressure in the large shear box and in the small shear box (standard Casagrande shear box). The results show little difference in practical terms and can be accounted for by the differences in top boundary conditions.

From the previous paragraphs it can be concluded that the external observation of load versus displacement curves showed some differences

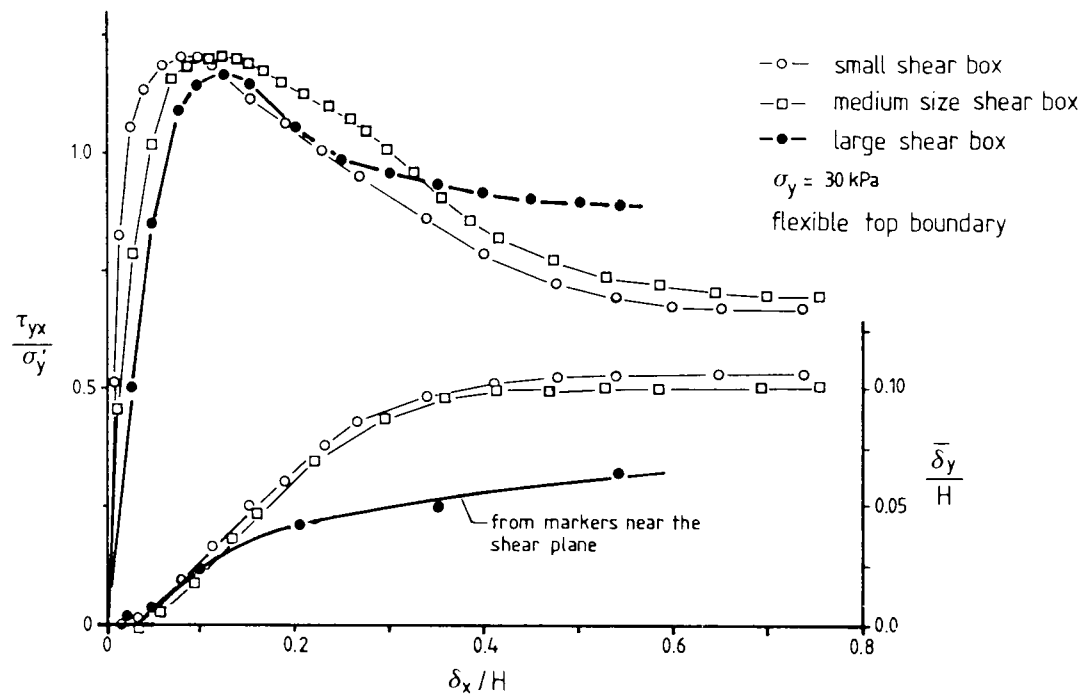
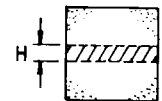


Figure 5.6 – Comparison Between Unreinforced Tests at Different Scales.

equipment	H (mm.)	ϕ_{ds} (°)	$\psi_{max.}$ (°)★
small shear box (60 × 60 × 32 mm)	9 ± 2	50.1	17.0
medium size shear box (250 × 150 × 150 mm)	18 ± 2	50.2	17.7
large shear box (1000 × 1000 × 1000)	100 ± 10	49.4	17.3



flexible top boundary
 $\sigma_y = 30 \text{ kPa}$

★ from top boundary measurements.

Table 5.2 – Summary of Results of Direct Shear Tests at Different Scales.

between the large shear box and the smaller ones. A more accurate way of comparing the results would be in terms of stress strain relations or flow rules, based on internal measurements. A limitation of the procedure used above for strain calculation, based on the shear zone thickness, is that this gives a mean value of strains, that are likely to vary throughout the thickness of the shear zone. Internal measurements obtained from

markers inside the shear zone overcome, to a certain extent, that limitation.

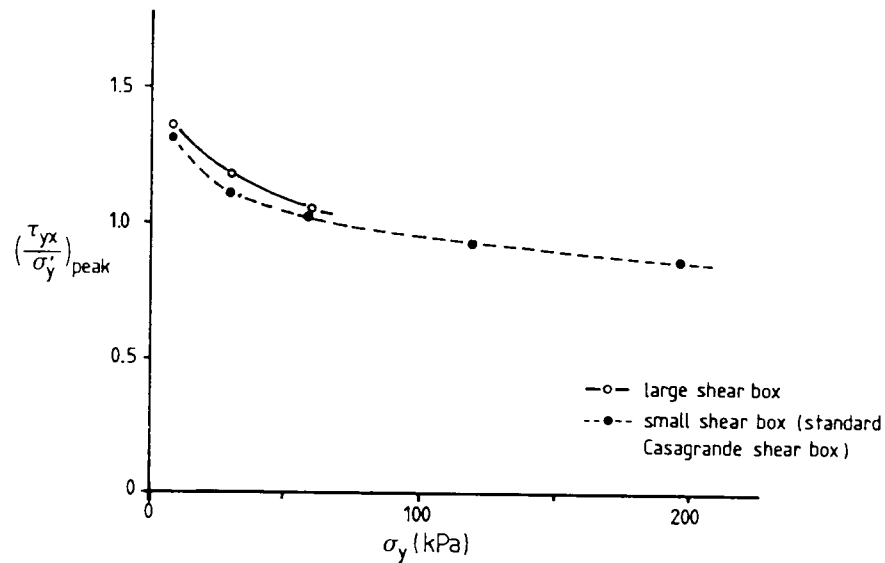
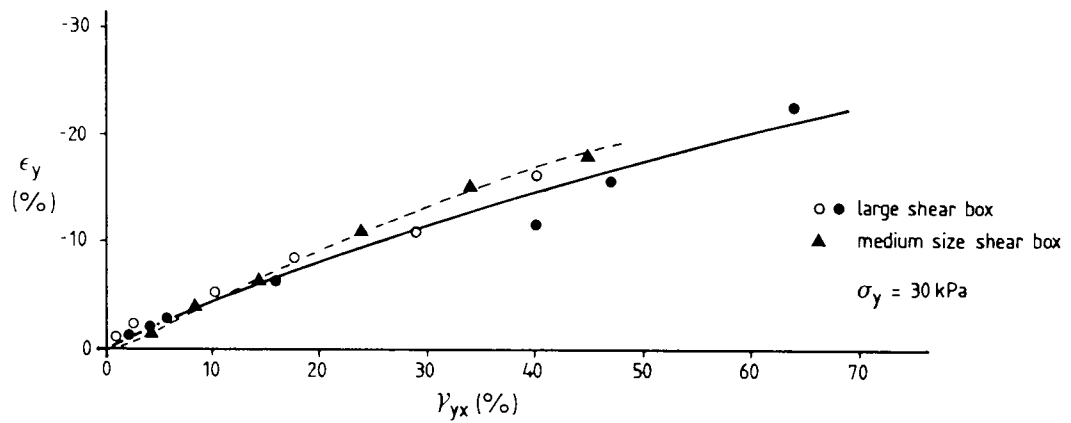


Figure 5.7 – Peak Stress Ratio versus Vertical Stress for Unreinforced Dense Leighton Buzzard Sand 14/25.

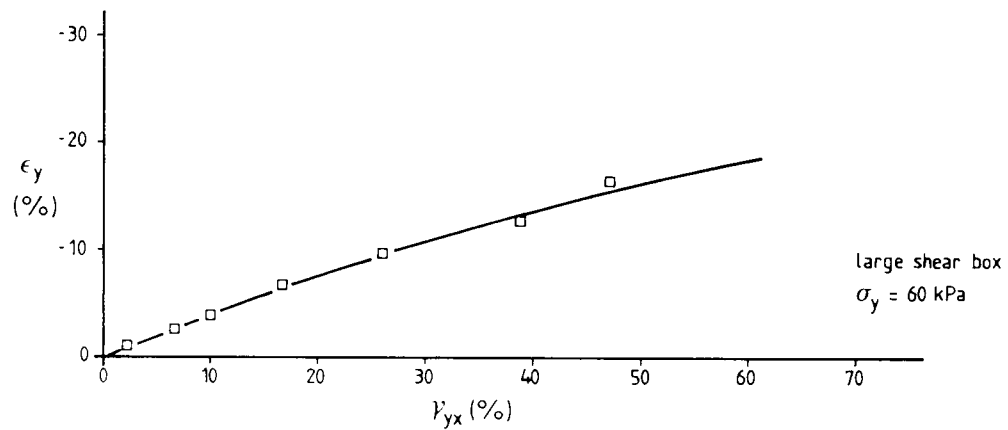
Figure 5.8 shows the variation of mean vertical strain versus mean shear strain in the middle of the sample obtained from markers in unreinforced tests in the large and medium size shear boxes. An interesting feature is that even for small shear strains the sample dilates, in contrast with what is observed by top measurements where a small contraction of a dense sample precedes the dilatant behaviour. This quick response to shear strain was also observed by internal measurements in the medium size shear box, as shown in the same figure.

The flow rule based on balance of energy (expression 5.6) can be employed using data from figures 5.5 and 5.8. The results are shown in figure 5.9. Also presented in this figure are findings by Stroud (1971) and Jewell (1980). The results from the large shear box compare well with

previous works and the differences shown can be accounted for by differences in the sand, boundary conditions or accuracy of strain measurements. It is important to note that the result from the medium size shear box compares very well with the trend shown by the large one and in both cases the energy relations is very close to the value of the tangent of the constant volume friction angle ($\phi_{cv} = 35^\circ$).



(a)



(b)

Figure 5.8 – Mean Vertical Strain versus Shear Strain in Unreinforced Tests.

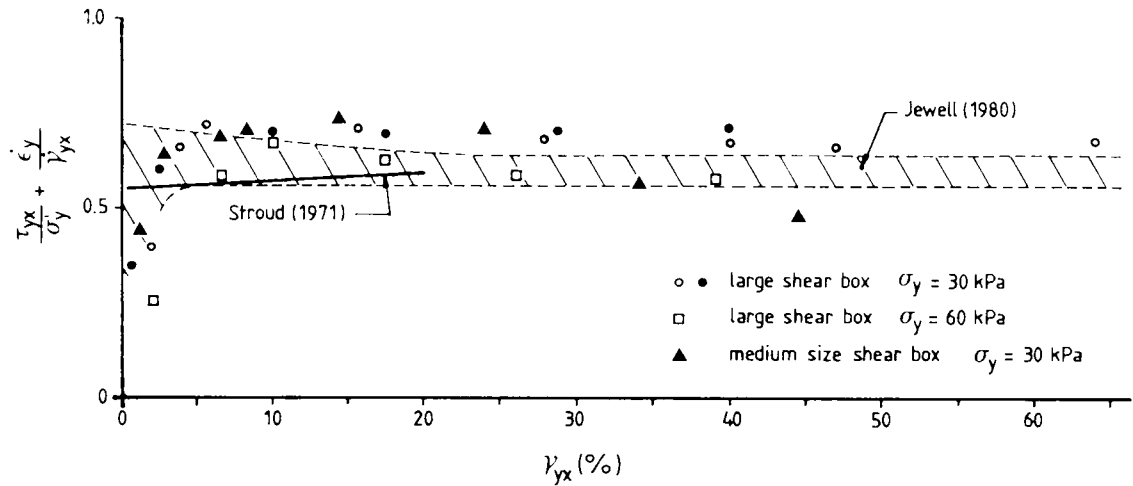


Figure 5.9 – Results Obtained by the Flow Rule Based on the Balance of Energy versus Shear Strain for Leighton Buzzard Sand 14/25.

5.3.2 – Stress and Strain Distributions in the Large Shear Box:

Figure 5.10 shows the stress distribution on the side of the large box for an unreinforced test with 30 kPa vertical pressure. Distributions of horizontal stress increments at the first reading ($\delta_x = 1.5\text{mm}$) and at peak stress ratio are presented non-dimensionalised by the shear stress at the central plane. Also presented in this figure are predictions using elastic solutions found in Poulos & Davis (1974). One of them is the

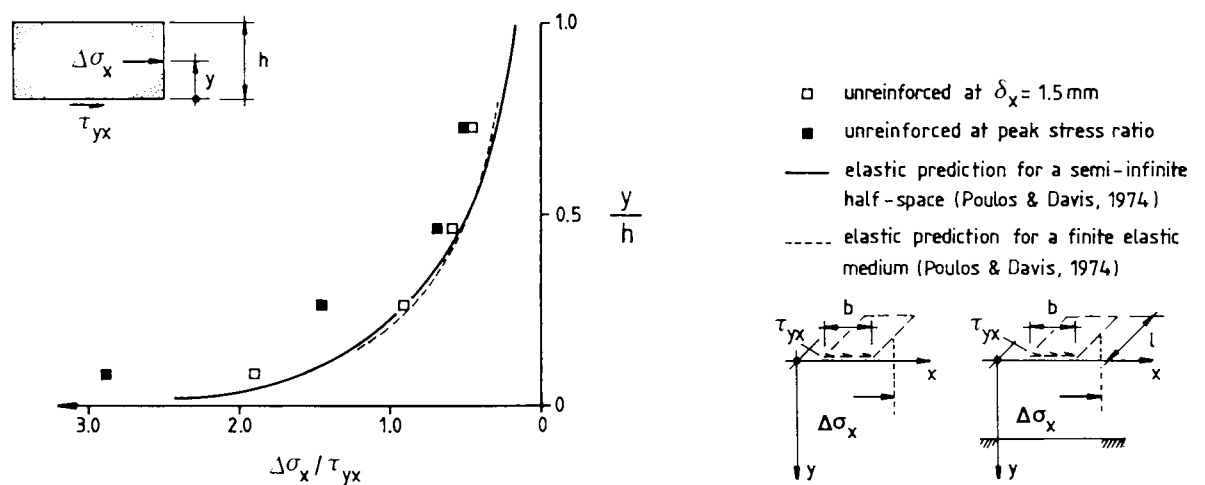


Figure 5.10 – Distribution of Horizontal Stress Increments on the Side Wall of the Box.

solution for the stress distribution in an infinite half space due to the shear stresses applied on the surface. The other is the elastic solution for stresses in a finite elastic layer overlying a rigid rough base due to shear stresses applied on the surface. Both led to close results due to the geometry of the problem and both predicted an infinite increment in horizontal stress at the central plane of the box (for $y/h = 0$ in fig. 5.10). This is not possible in the real problem due to yielding of the sand in that region. These predictions were made in order to assess the accuracy of the pressure cells, at least, in the elastic range (earlier stages of the test), since more realistic approaches were unavailable. The theoretical prediction and experimental values agree closely, which gives some confidence to the form and values of the pressure distribution obtained.

With the pressure distribution on the side of the box being known, the position of the resultant of forces on that side can be obtained and in conjunction with the other forces involved, the state of stress inside the box can be approached. The force distribution on the top half of the box is then shown in figure 5.11. The force acting on the side opposite to the one where the horizontal force is applied is considered to be negligible, because in that region an "active" state of stress occurs, which leads to very low horizontal pressures. This fact was confirmed by other pressure cells installed in that region of the bottom half of the box and by results presented in Dyer (1985). Equilibrium equations come from the condition that the sum of forces in the vertical and horizontal directions and their moments about point B in figure 5.11, must be zero.

The equilibrium of the top half of the box requires that the vertical stress distribution on the central plane cannot be uniform. This

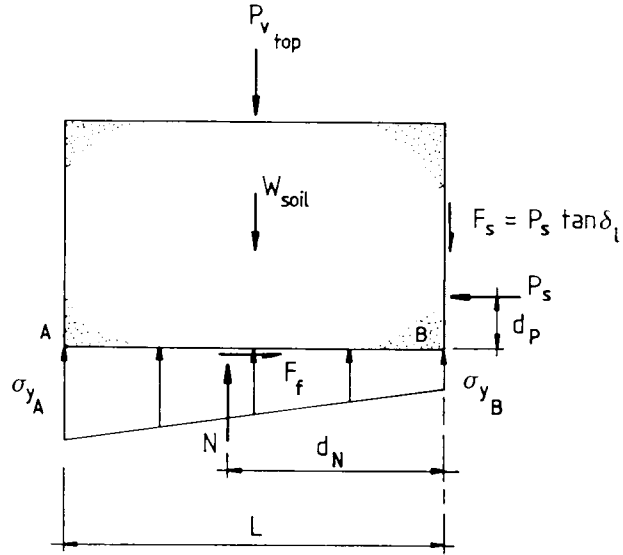


Figure 5.11 – Forces Acting on the Top Half of the Sample in the Large Shear Box.

is due to the moment caused by the force on the side of the box. In standard shear boxes this moment causes a rotation of the top half, which is minimised in the large shear box by the reaction frame. For the sake of simplicity in the present development the vertical stress distribution on the shear plane is considered to be trapezoidal. So, assuming the three conditions of equilibrium, the following expressions for the left and right corner of the trapezium can be derived (see fig. 5.11):

$$\frac{\sigma_{yA}}{\sigma_y} = 1 + 2(3d_p/L - \tan\delta_l) \frac{\tau_{yx}}{\sigma_y} \quad [5.7]$$

$$\frac{\sigma_{yB}}{\sigma_y} = 1 - 2(3d_p/L - 2\tan\delta_l) \frac{\tau_{yx}}{\sigma_y}$$

where δ_l is the angle of friction between soil and the internal wall of the box, τ_{yx} the shear stress on the central plane, σ_y the initial uniform vertical pressure on the central plane, d_p the distance between

the direction of the shear force and point B in figure 5.11 and L the length of the box. Substituting values in equation 5.7, leads to:

$$\frac{\sigma_{yA}}{\sigma_{yB}} \approx 2 \quad \text{and} \quad \frac{d_n}{L} \approx 0.57$$

Despite the rather crude approach to the shape of the vertical pressure distribution on the shear plane, the figures obtained above lead to the important conclusion that progressive failure is likely to occur in the central region of the box, due to the left extremity being under a stress level approximately double the one on the right side. Figure 5.12 shows the shear strain profile in the central region of the box for an unreinforced test ($\sigma_y = 30$ kPa), at peak stress ratio. The non-uniformity of the strain profile confirms the prediction of progressive failure based on the pressure distribution calculation presented above.

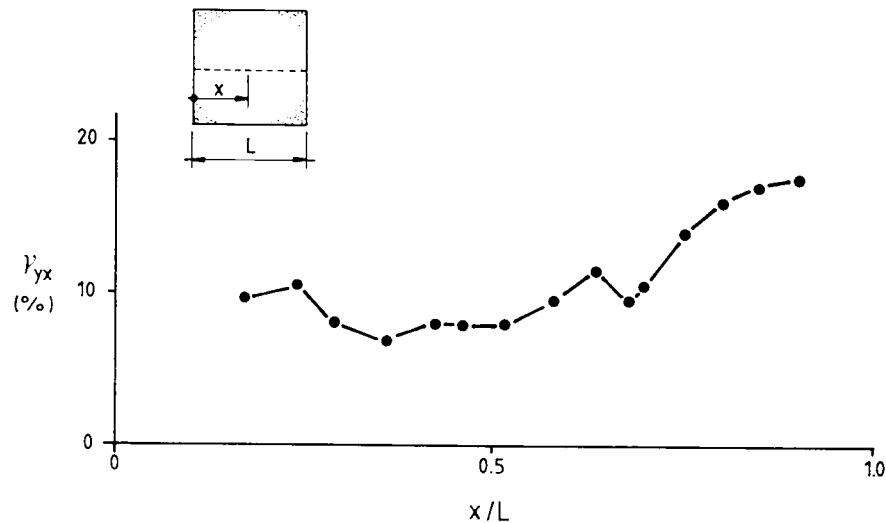


Figure 5.12 – Shear Strain Profile in the Central Region of the Sample.

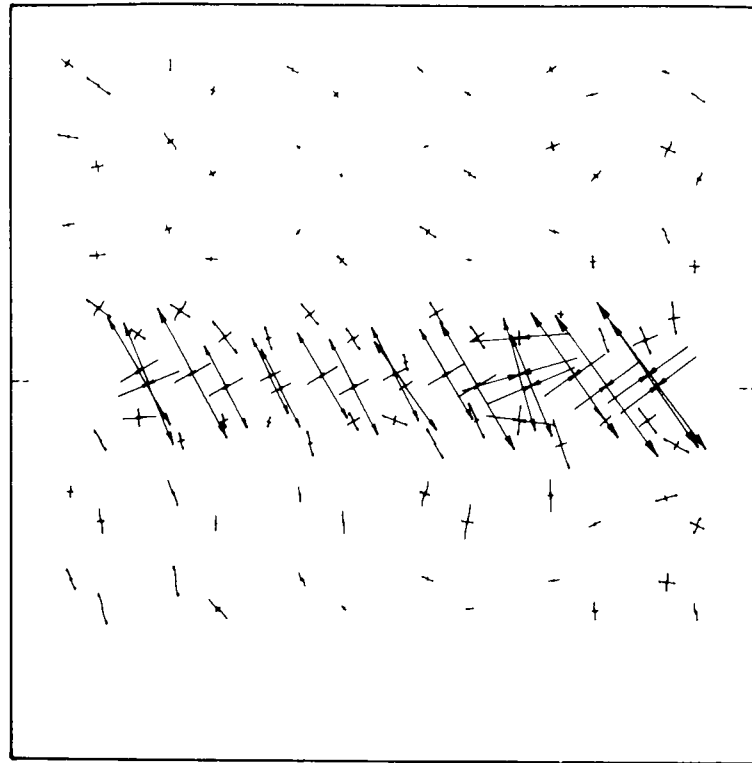
From what has been presented in the previous paragraphs a direct shear test starts with an initially uniform vertical pressure

distribution on the central plane (σ_y). As the shearing phase starts, the vertical pressure distribution changes to an approximately trapezoidal shape with a mean value (σ'_y) slightly above the initial one owing to the friction on the side of the sample.

The orientation of principal strains at peak stress ratio is shown in figure 5.13a for an unreinforced sand tested at $\sigma_y = 30$ kPa. It can be observed that the orientation of the minor principal tensile strain is inclined approximately 30° to the vertical direction. This agrees very well with values obtained by Jewell (1980) and Gray & Al-Refeai (1986) for dense sands. Figure 5.13b shows the orientation of zero extension lines in the large shear box. It can be observed that these lines coincide approximately with the horizontal direction in the region at the middle of the shear box.

For comparisons, the orientation of principal strains and zero extension lines for an unreinforced test at 30 kPa vertical stress in the medium size box are shown in figures 5.14 a and b. These results compare closely with the ones obtained in the large shear box.

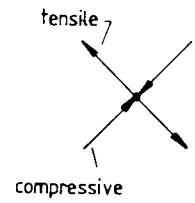
The mobilised friction angle on the horizontal plane of the large shear box (ϕ_{ds}) under a vertical pressure of 30 kPa was 49.4° , which agrees well with values obtained in other works using the same sand (Stroud - 1971, Arthur et al - 1977b). The angle of dilation at 30 kPa vertical pressure from internal measurements was 23.7° , which compares closely with the value 23° obtained by Stroud (1971). It should be pointed out that the value of the dilation angle obtained from boundary measurements was 17.3° (see Tab. 5.2), $\approx 6^\circ$ less than the one obtained by internal measurements. The friction angle obtained by expression 5.4,



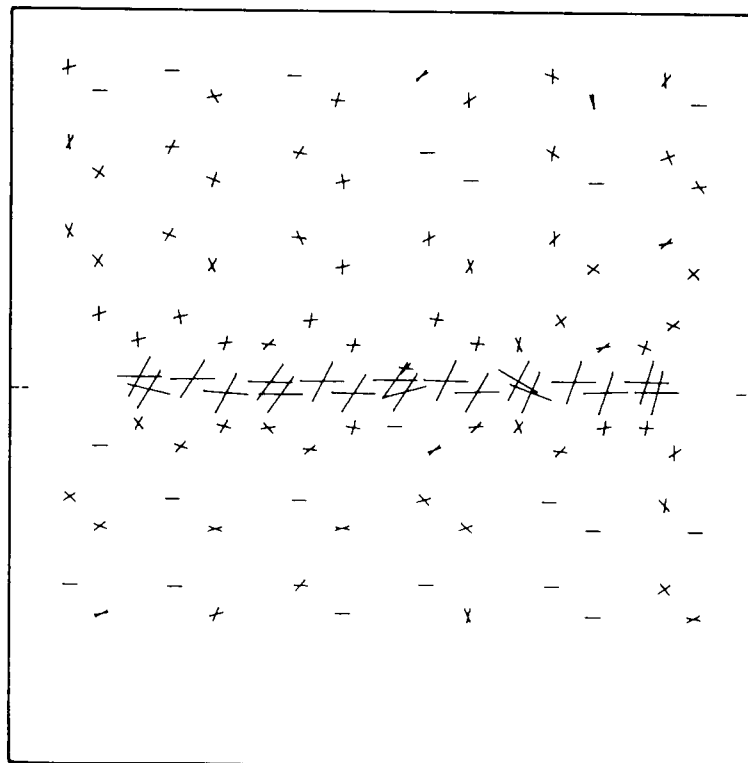
Scale:

5%
→

Convention for Strains:



(a) Principal Strain Orientation

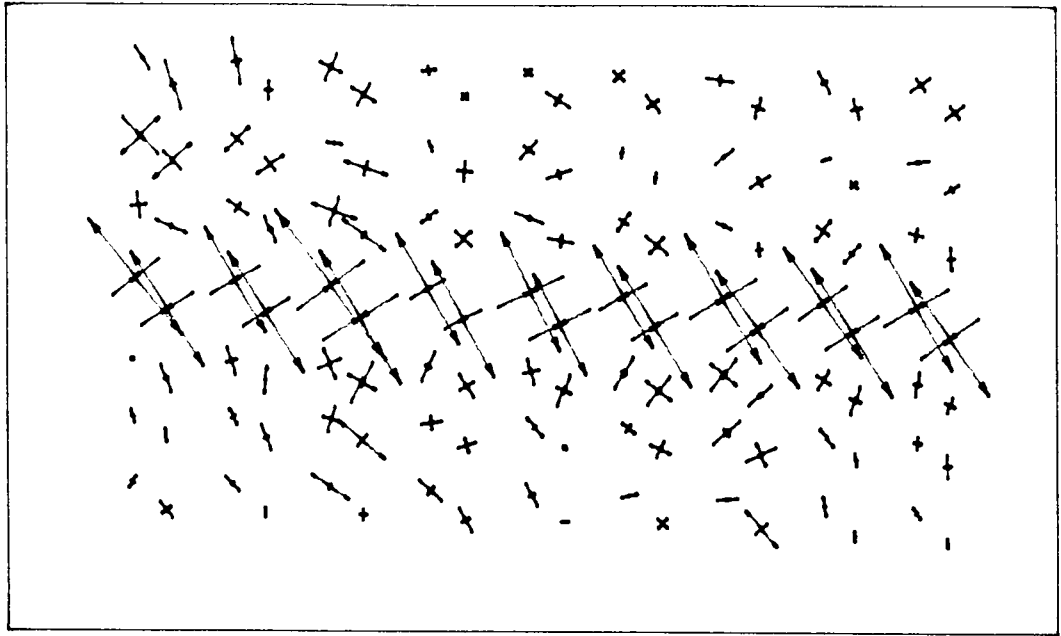


(b) Zero Extension Lines

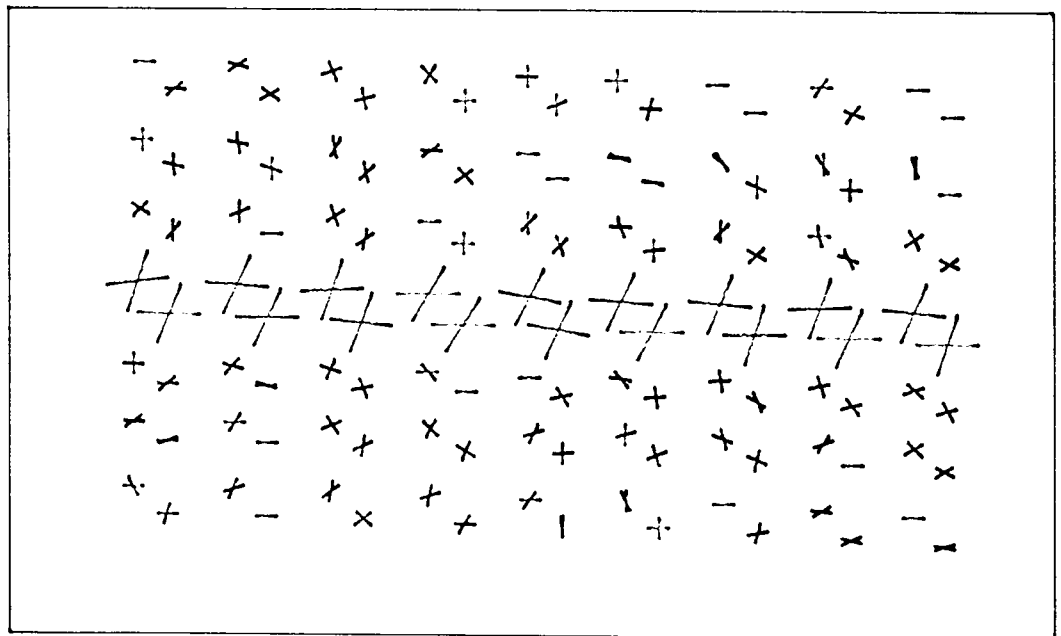
Figure 5.13 - Principal Strain and Zero Extension Lines Orientation in Unreinforced Tests with Leighton Buzzard Sand 14/25 at Peak Stress Ratio.

Scale: $\frac{5\%}{\rightarrow}$

Convention: same as in fig. 5.13



(a) Principal Strains



(b) Zero Extension Lines

Figure 5.14 - Principal Strain and Zero Extension Lines Orientation at Peak Stress Ratio in the Medium Size Shear Box - Flexible Top Boundary, $\sigma_y = 30$ kPa.

when coaxiality between stresses and strain increments is assumed, is 57.1° .

It is difficult to check if coincidence between stresses and strain increments directions occurred or not since the direction of principal stresses was not measured. Nonetheless, some comments can be made on that, based on the value of the horizontal stress (σ_x). From figure 5.1 one can easily obtain the following expressions for the horizontal stress at failure:

$$\text{Maximum Obliquity Concept: } \frac{\sigma_x}{\tau_{yx}} = 2 \frac{\tau_{yx}}{\sigma'_y} + \frac{\sigma'_y}{\tau_{yx}} \quad [5.8]$$

$$\text{Coaxiality Concept: } \frac{\sigma_x}{\tau_{yx}} = 2 \tan \psi + \frac{\sigma'_y}{\tau_{yx}} \quad [5.9]$$

Evaluating expressions 5.8 and 5.9 one obtains 3.2 and 1.7, respectively, for the ratio between horizontal stress and shear stress at failure. The value 3.2 is very close to the one obtained by the pressure cell on the side wall of the box near the shear plane, as show in figure 5.10. If that is so, a deviation between principal directions of about 10° would have occurred. The theoretical value obtained for the angle between principal directions of stress and strain increments from the Mohr circle (fig. 5.1), in the event of non-coincidence of axes, is equal to $(\phi_{ps} - \psi)/2$, which gives 12.9° . This value is a little higher than the one obtained above but the proximity between them reinforces the possibility of non-coaxiality in the present case. However, further investigation is required to check to what extent pressures measured at the boundaries can be extrapolated to the inner regions of the sand mass.

5.4 - Conclusions:

The following conclusions can be drawn from the tests with unreinforced sand:

1. Scale did not affect the values of peak friction angle or dilation angle measured at the top boundary for the size of apparatus used in the present work. The post peak behaviour and the thickness of the shear band in the centre of the box were scale dependent;
2. Test results are dependent on the boundary condition on the top of the sample. The utilization of a flexible top boundary led to an increase in the peak friction angle of approximately 2° ;
3. When the stress strain behaviour of the soil was investigated by means of internal measurements, results obtained in the medium size shear box and in the large shear box were very closely related;
4. Dilation angles obtained by monitoring the movements of the top boundary should be approached with caution in view of the evidence that they may be smaller than the value obtained from internal measurements in the central region of the box;
5. The stress distribution and boundary conditions in the shear box caused a non uniform development of strains along the region in the middle of the sample. The results obtained seem to suggest

that non-coincidence between principal directions of stress and strain increments is likely to have occurred in the present work.

Chapter 6: Large Direct Shear Tests on Reinforced Sand

Chapter 6: Large Direct Shear Tests on Reinforced Sand

6.1 - Introduction:

In this chapter the results of reinforced direct shear tests in the large shear box using Leighton Buzzard sand 14/25 are presented and discussed. Reference should be made to Chapter 3 and Appendix A3 for details of reinforcements. Additional data on test details are given in Appendix A4.

6.2 - Test Results in the Large Shear Box:

A total of 24 tests with reinforced samples were performed in the large shear box. A standard reinforcement length of 600mm was chosen as a compromise value to avoid boundary effects and for being a suitable length for reinforcement cutting, in view of the spacing between bearing members in the grids used. Therefore, all metal grids and geotextiles used in direct shear tests were 600mm long. Polymer grids were 560mm long. All reinforcements covered the whole width of the box ($W_r = 1000\text{mm}$) except the metal strip, which was 100mm wide. In all tests but two the vertical pressure applied on the central plane was 30 kPa.

The results of direct shear tests of reinforced samples are presented in figure 6.1. In this case the reinforcement was inclined at 30° to the vertical direction in order to coincide with the direction of minor principal strain in unreinforced tests where its efficiency reaches a maximum. From this figure the following observations can be made:

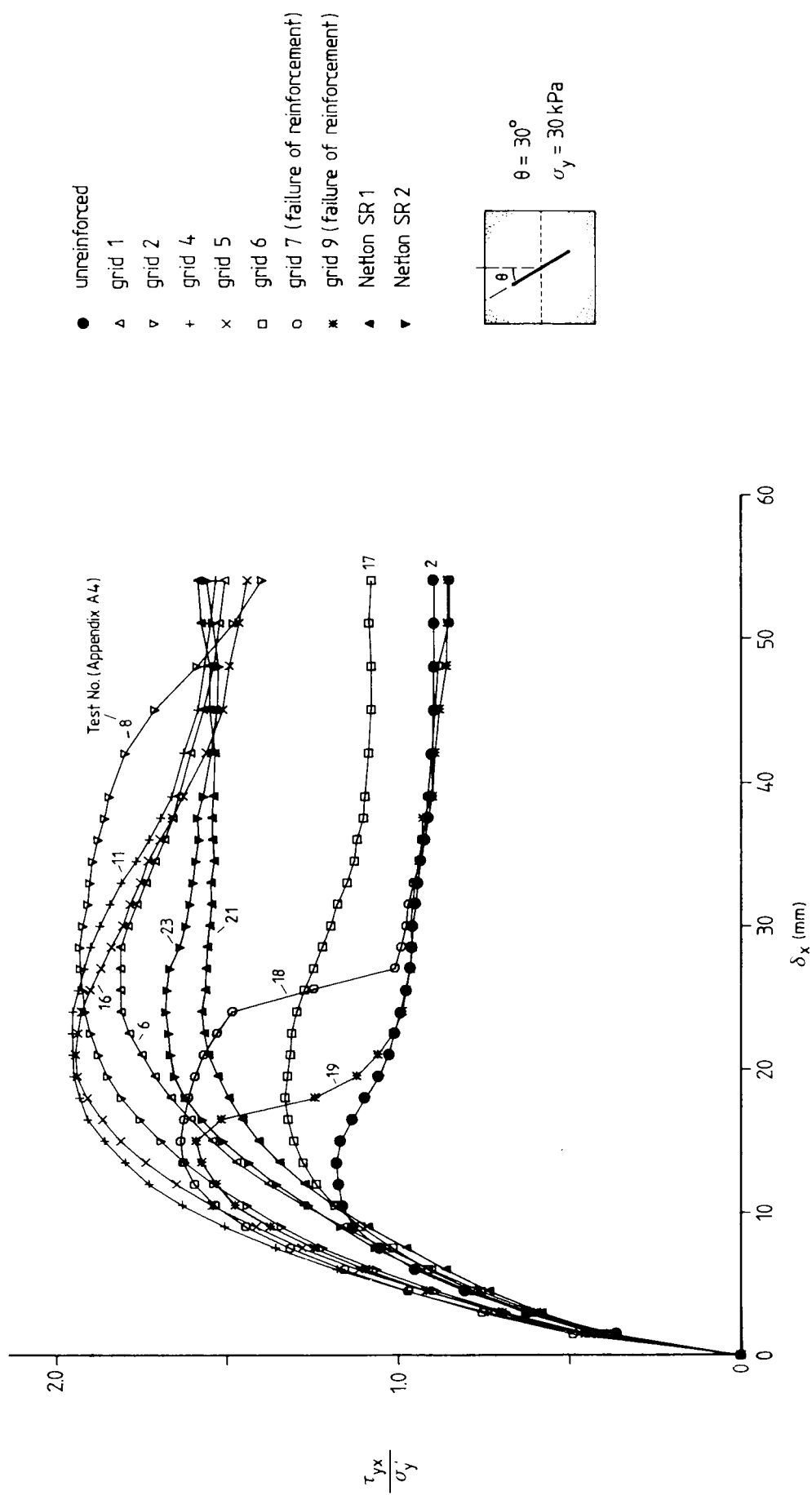


Figure 6.1 -- Reinforced Direct Shear Test Results -- $\theta = 30^\circ$.

1. In its best performance, reinforced sand was nearly twice as strong as unreinforced;
2. Despite differences in geometry and stiffness, metal grids 1, 2, 4, and 5 presented close values of peak stress ratio. The slightly smaller value obtained for grid 1 can be attributed to possible disturbances during sample preparation due to the small aperture size of that grid. Softening seemed to have occurred after peak stress ratio in tests with metal grids;
3. Grid 6 gave a poor performance in comparison with other metal grids due to its large spacing between bearing members;
4. Grids 7 and 9 failed by tension during the tests. The stress ratio dropped drastically to unreinforced soil levels after reinforcement failure;
5. Plastic grids Netlon SR1 and SR2 presented peak stress ratio about 20% smaller than metal grid reinforcement. As the test proceeded the stress ratio kept almost constant or slightly increased;
6. For large shear displacements, metal grids 1, 2, 4 and 5 and plastic reinforcement presented close values of stress ratio.

Figure 6.2 shows results of stress ratio versus shear displacement for samples reinforced with metal reinforcement placed along the vertical direction. The same observations made for the previous figure, regarding metal reinforcement, can be applied to the results in figure 6.2. It is interesting to notice the poor performance of a smooth metal strip (100mm wide) compared with results for grid reinforcements. It also should be noticed that all metal grids, but grid 2, showed approximately the same performance as the rough metal sheet.

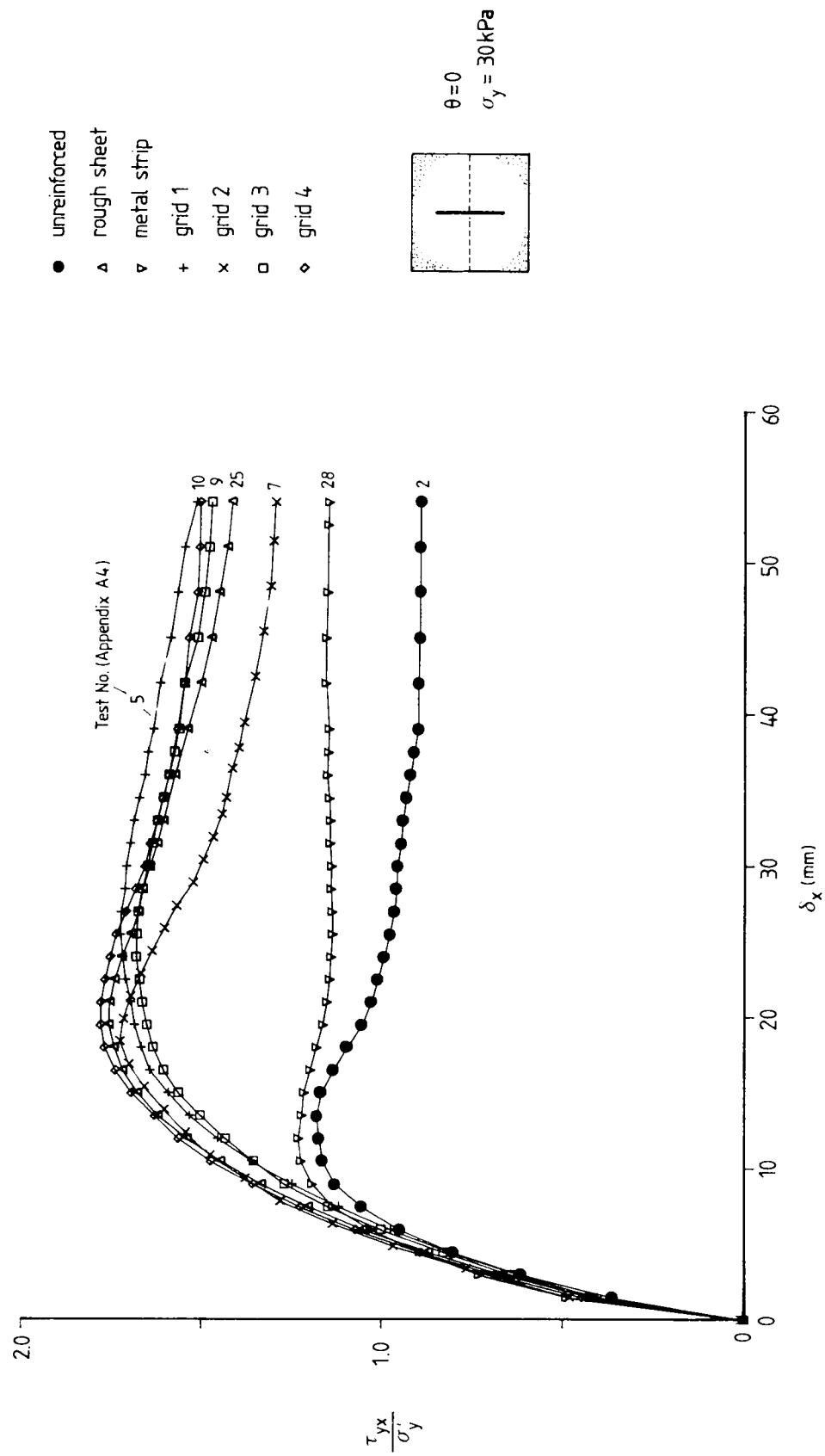


Figure 6.2 – Direct Shear Test Results for Samples Reinforced with Metal Reinforcement – $\theta = 0$.

In figure 6.3 the results obtained in tests with sand reinforced with plastic reinforcement, placed in the vertical direction, are shown. For comparison, the test result for the rough sheet is also presented. It can be observed that, despite differences in form and mechanical properties, the plastic reinforcements used strengthened the sand by approximately the same amount. Some particular features in this figure are the slightly lower strength shown by the sample reinforced with the more extensible geotextile (Geolon 70) and the continuous increase in strength, at large displacements, shown by the sample reinforced with polymer grid Netlon SR2.

The same pattern of results arises when tests are carried out under a higher vertical pressure. Figure 6.4 shows results of reinforced and unreinforced tests at 60 kPa vertical pressure. These results are consistent with the ones under 30 kPa vertical pressure. The stress ratio versus shear displacement curve for the test with the stiff metal grid follows the shape of the unreinforced curve after peak stress ratio, whereas the polymer grid, after a small drop following the peak, reveals a continuous increase in stress ratio at later stages of the test.

Comparisons between mean vertical displacement on top of the sample versus shear displacement are presented in figures 6.5 a and b. The mean vertical displacement was obtained by dividing the volume variation of the top rubber bag by the area of the sample. Figure 6.5a indicates that the vertical displacement on top for reinforcements placed in the vertical direction is influenced by stiffness and form of the reinforcement. However, when the reinforcement is aligned with the most efficient direction, the results for the polymer grid are very close to the ones obtained for stiffer grids, as shown in figure 6.5b.

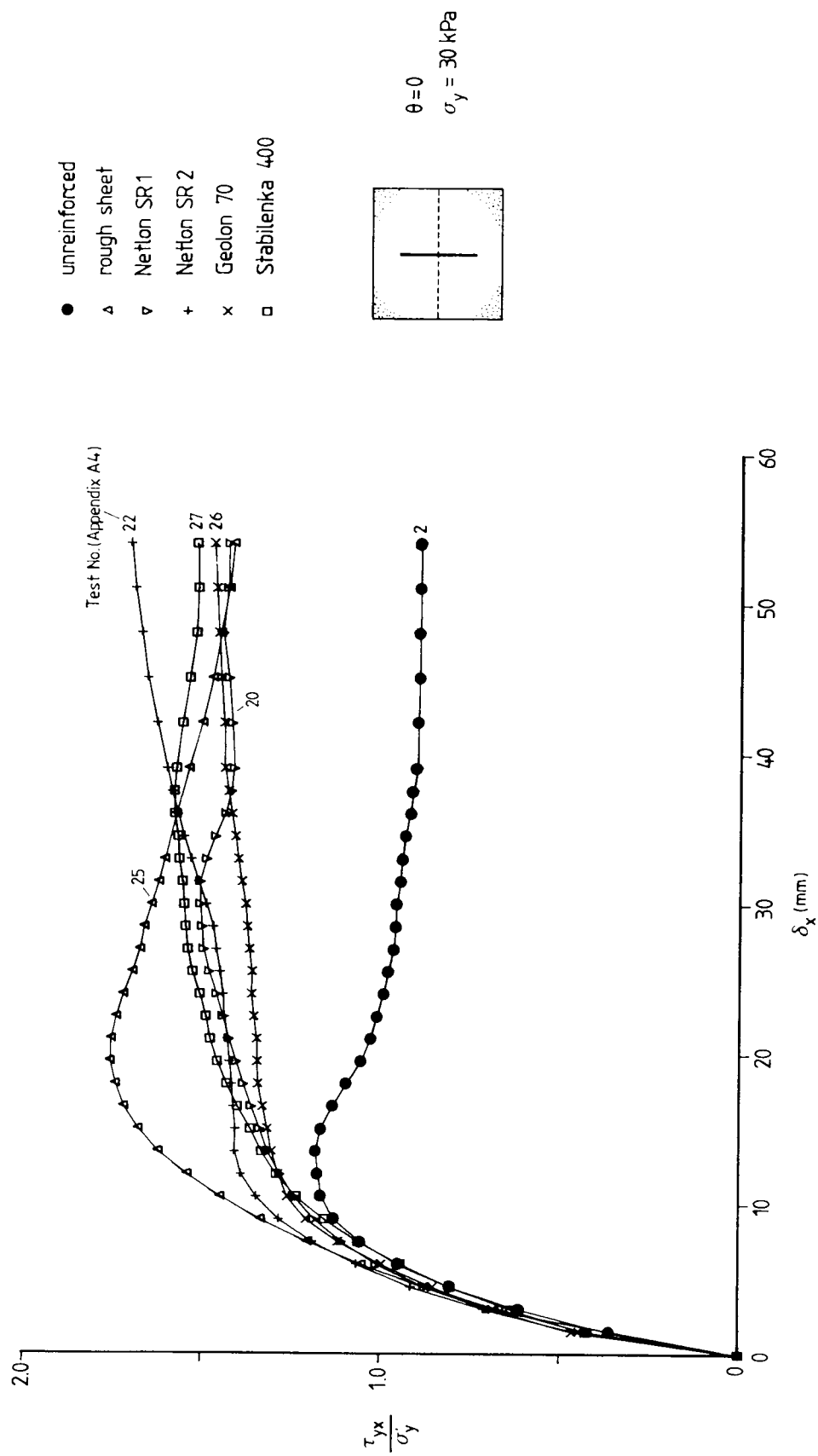


Figure 6.3 - Direct Shear Test Results for Samples Reinforced with Plastic Reinforcement - $\theta = 0$.

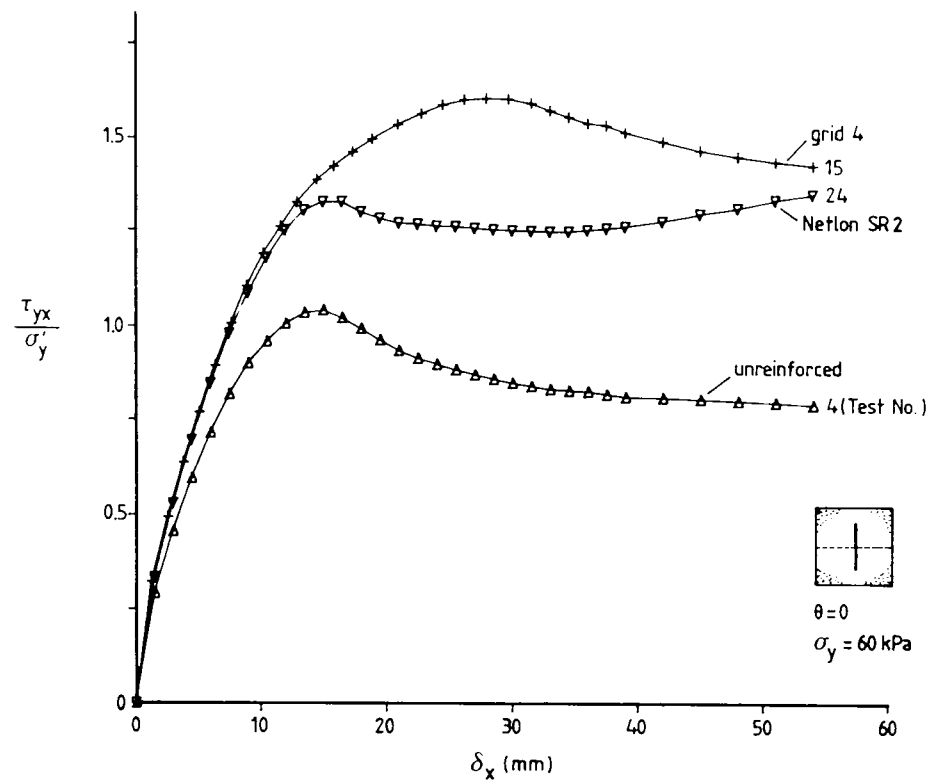


Figure 6.4 – Reinforced Direct Shear Test Results for $\sigma_y = 60$ kPa.

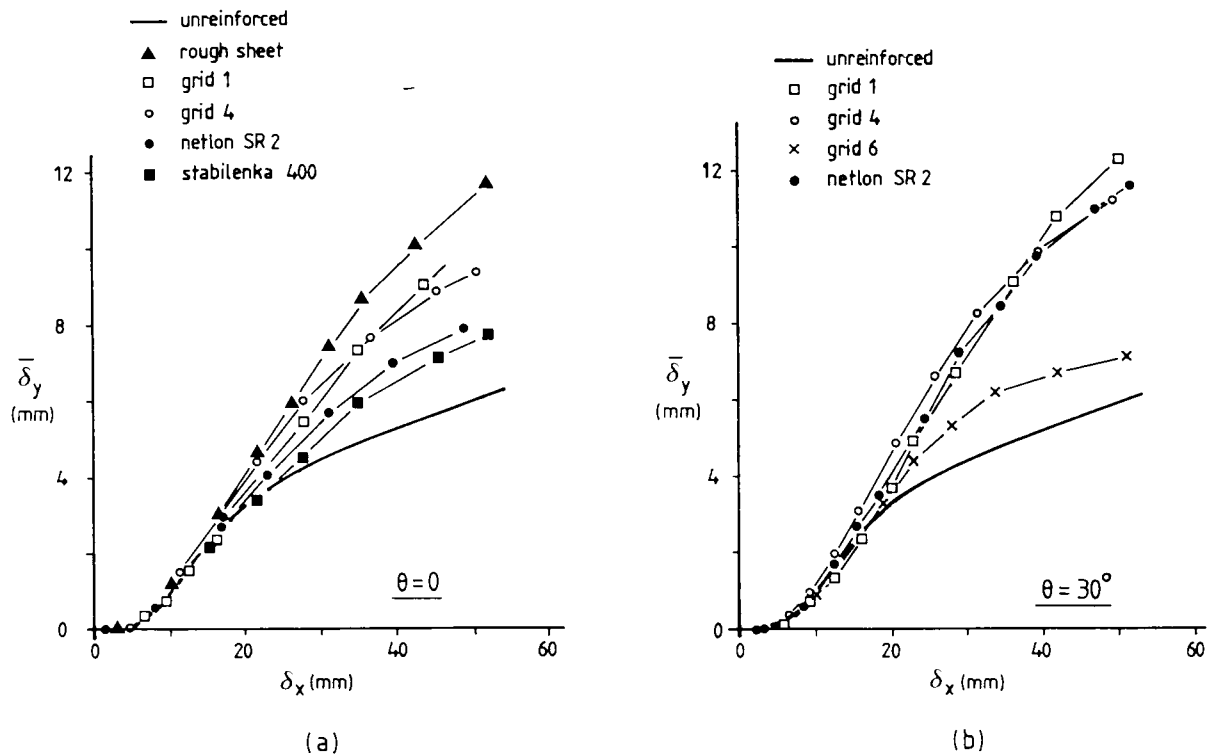


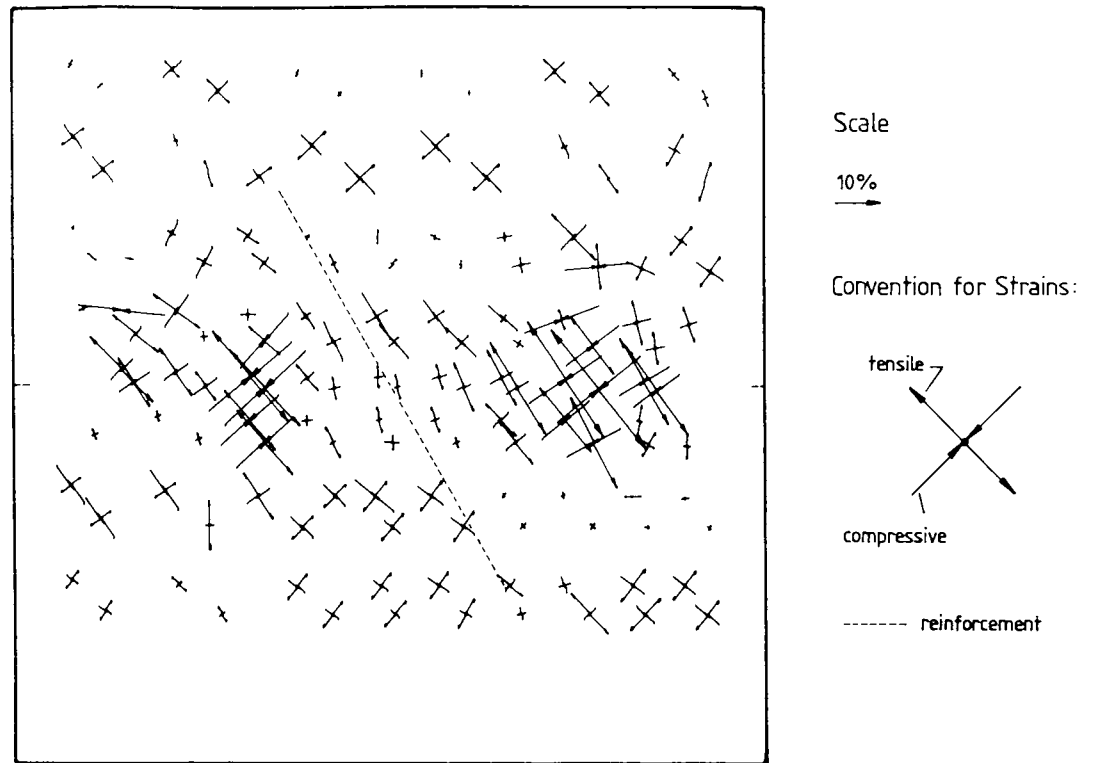
Figure 6.5 – Comparison Between Mean Vertical Displacement at the Top of Reinforced Sand Samples.

6.3 - Strain and Stress Distribution in Reinforced Sand Samples

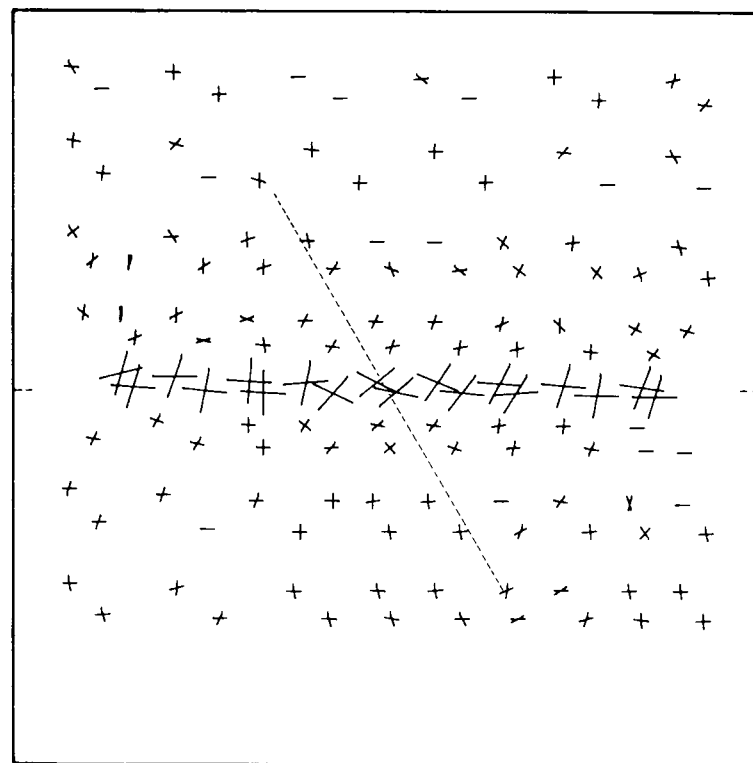
6.3.1 - Strain Distribution:

Figures 6.6 a and b show typical distributions of principal strains and zero extension lines in a sand sample reinforced with grid 4, inclined 30° to the vertical direction, at peak stress ratio. Principal strain magnitudes are severely reduced in the sand mass surrounding the reinforcement, in particular along the central plane of the sample. One of the zero extension lines is still predominantly aligned to the horizontal direction, as in the unreinforced tests (fig. 5.13). Figures 6.7 a and b show the distribution of principal strains at peak stress ratio for tests with the rough sheet and Netlon SR2 placed in the vertical direction. One can observe that in this case the sand mass was not as strained as in the case with inclined reinforcement.

In figures 6.8 a to c the shear strain profiles along the central plane, for reinforced and unreinforced samples at peak stress ratio, are presented. Figure 6.8a refers to tests where reinforcements were placed in the vertical direction and little difference between results for reinforced and unreinforced tests can be observed. However, one should note that these strain profiles are related to different overall shear displacements of the box. For the same shear displacement (equal to the shear displacement corresponding to peak stress ratio in reinforced tests) the shear strain magnitudes for the unreinforced sample are nearly two and a half times those for reinforced samples. Geotextile reinforcement showed a poor performance compared to grid reinforcement but, even so, shear strain development in the sample reinforced with geotextile was much smaller than in the unreinforced sample.

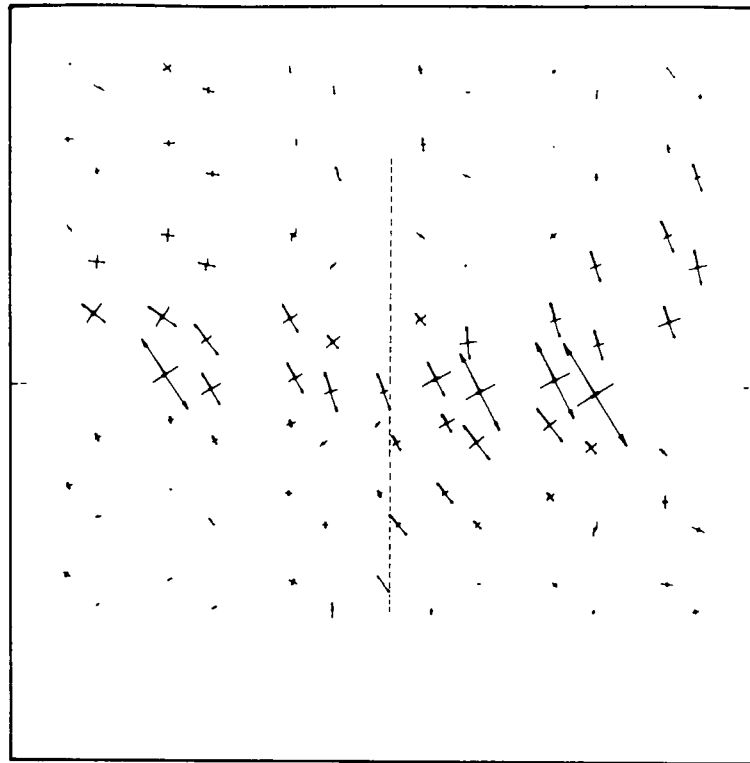


(a) Principal Strain Orientation

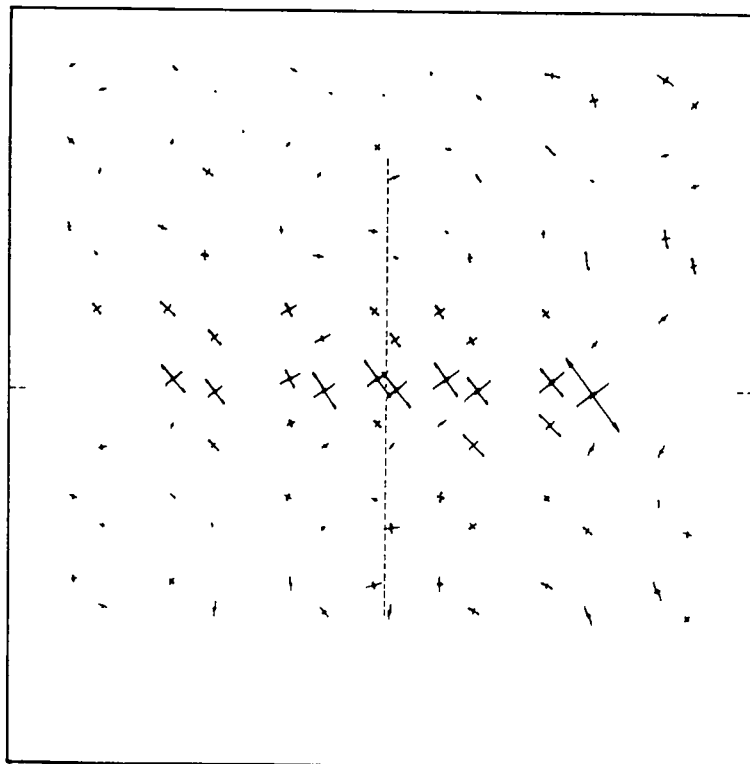


(b) Zero Extension Lines

Figure 6.6 - Principal Strains and Zero Extension Lines Orientation for a Reinforced Test with Grid 4 at Peak Stress Ratio - $\theta = 30^\circ$, $\sigma_y = 30$ kPa.



(a) Rough Sheet



(b) Netlon SR2

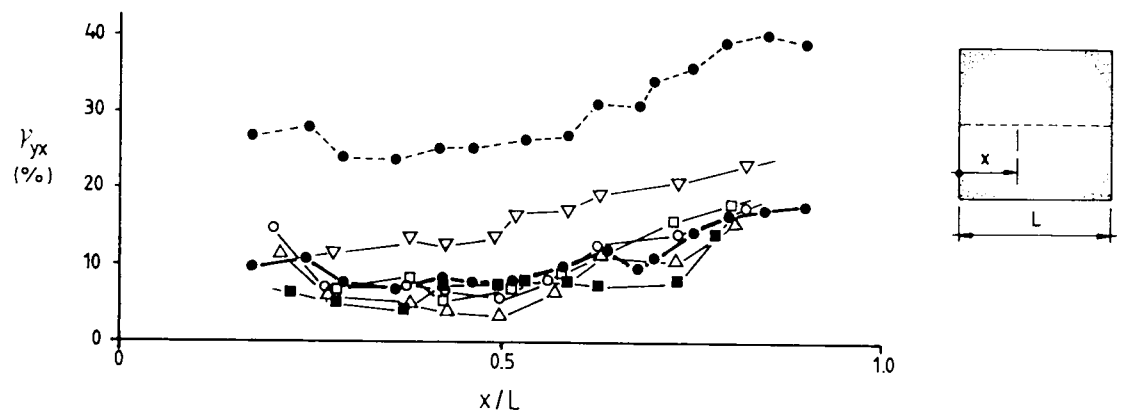
Figure 6.7 - Principal Strain Orientation at Peak for Samples Reinforced with a Rough Sheet and Netlon SR2 - $\theta = 0$, $\sigma_y = 30$ kPa.

Figure 6.8b shows shear strain profiles in the central region of the box, for tests with the reinforcement inclined 30° to the vertical direction, at peak stress ratio. In contrast to results in figure 6.8a, shear strains are significantly reduced in the central region of the box in comparison to the unreinforced case. This is believed to be caused by the action of the horizontal component of the reinforcement force, which is only significant for vertical reinforcements at large displacements due to the deformed shape of the reinforcement. One should pay attention to the result for grid 9, just before the tensile failure of the reinforcement, where the shear strain distribution is already very close to the one shown by the unreinforced test. Again, for the same shear displacement of the box, the unreinforced shear strain profile presents much higher values than the reinforced ones.

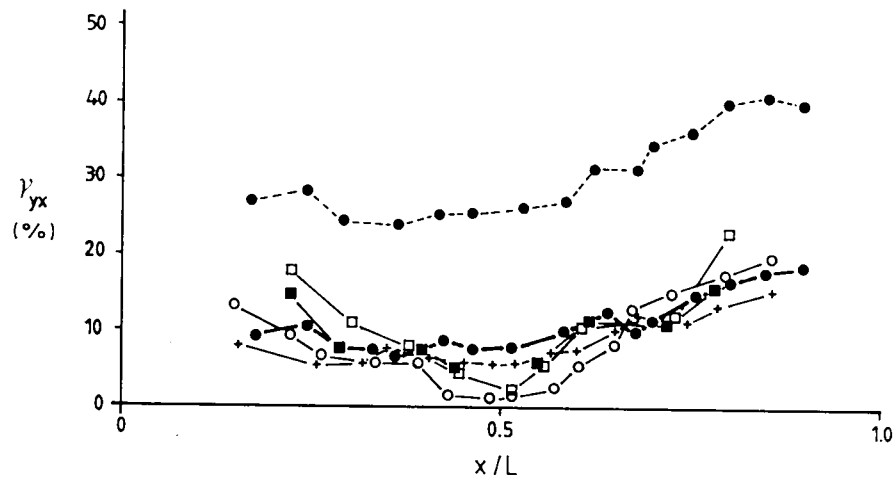
In figure 6.8c shear strain profiles at the end of the test, for samples with vertical reinforcements are presented. In contrast with results in figure 6.8a, at this stage the stiff reinforcement reduces strongly the development of shear strains in the central region of the sample. Note, however, that for the polymer grid the result is very close to the one obtained for the unreinforced sample, in contrast with the performance of the stiff geotextile, which shows significant reductions on the development of strains in the central region of the box.

6.3.2 - Stress Distributions:

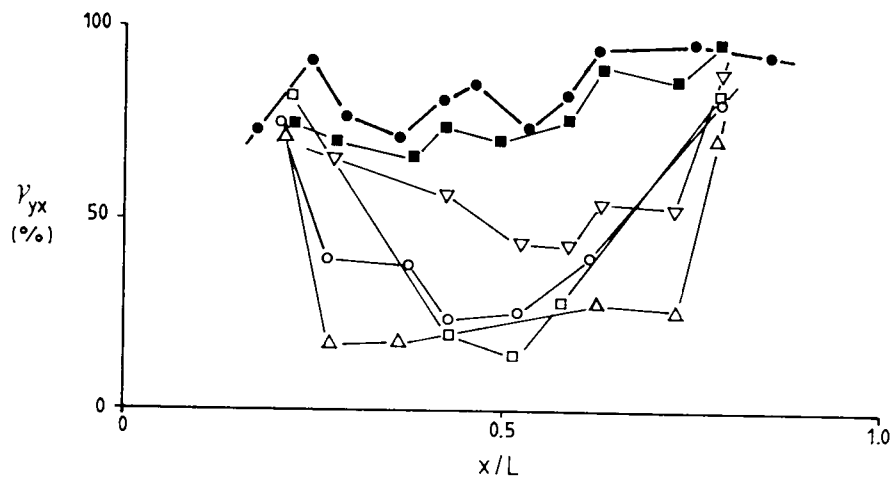
Figure 6.9 presents results of total pressure measurements on the side walls of the shear box in reinforced samples, at peak stress ratio. Increments of horizontal stress were non-dimensionalised by the shear



(a) Shear Strain Profiles at Peak Stress Ratio - $\theta = 0$



(b) Shear Strain Profiles at Peak Stress Ratio - $\theta = 30^\circ$



(c) Shear Strain Profiles at the End of Test - $\theta = 0$

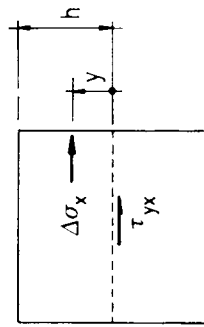
Symbols:

- | | |
|---|------------------------------|
| —●— unreinforced | —△— reinforced - rough sheet |
| ---●--- unreinforced at $\delta_x = 22.0$ mm; | —■— reinforced - Nefton SR 2 |
| —□— reinforced - grid 1 | —▽— reinforced - Stabilenka |
| —○— reinforced - grid 4 | |
| —+— reinforced - grid 9 (yielding of the reinforcement) | |

Figure 6.8 - Comparison Between Shear Strain Profiles in the Central Region of the Sample.

stress at peak and the position of the pressure cell was non-dimensionalised by the half height of the box. Figure 6.9a shows results for reinforcements inclined 30° to the vertical. There is a slightly greater scattering for the results of samples with vertical reinforcement. Nonetheless, the presence of the reinforcement or its characteristics seem not to have affected the development of horizontal stresses on the vertical boundaries, judged by the results for the unreinforced sample, also presented in this figure. This may be due to the distance from the reinforcement to the instrumented face of the box.

Pressure cells were also installed inside the reinforced soil mass in order to assess the normal stress distribution in specific regions. The type of pressure cell used has already been described in Chapter 2. Initially, cells placed on the central plane had their results very much affected by the shear distortion in that region. An attempt was then made to position the cells 70mm above the central plane in order to minimise the influence of shear distortions on the cells' measurements. Figure 6.10 shows results of vertical pressure distribution obtained in that case at peak stress ratio and at the end of the test, for two samples reinforced with grid 4 inclined 30° to the vertical direction. These tests were performed with two cells placed on the same position in both tests. This would give an assessment of the repeatability of the readings. The repeatability was encouraging and the form of stress distribution as might be anticipated. Note that the trapezoidal distribution assumed for an unreinforced sample is also presented in this figure. These results suggest a significant increase in vertical pressure due to the reinforcement. This figure also shows that, at the end of the test, the vertical pressure distribution is still about the same magnitude as at peak stress ratio. The pressure distribution obtained is consistent with



- unreinforced
- ▲ grid 1
- grid 2
- grid 4
- ▼ grid 5
- Netlon SR 1
- △ Netlon SR 2
- ◇ Stabilenka 400

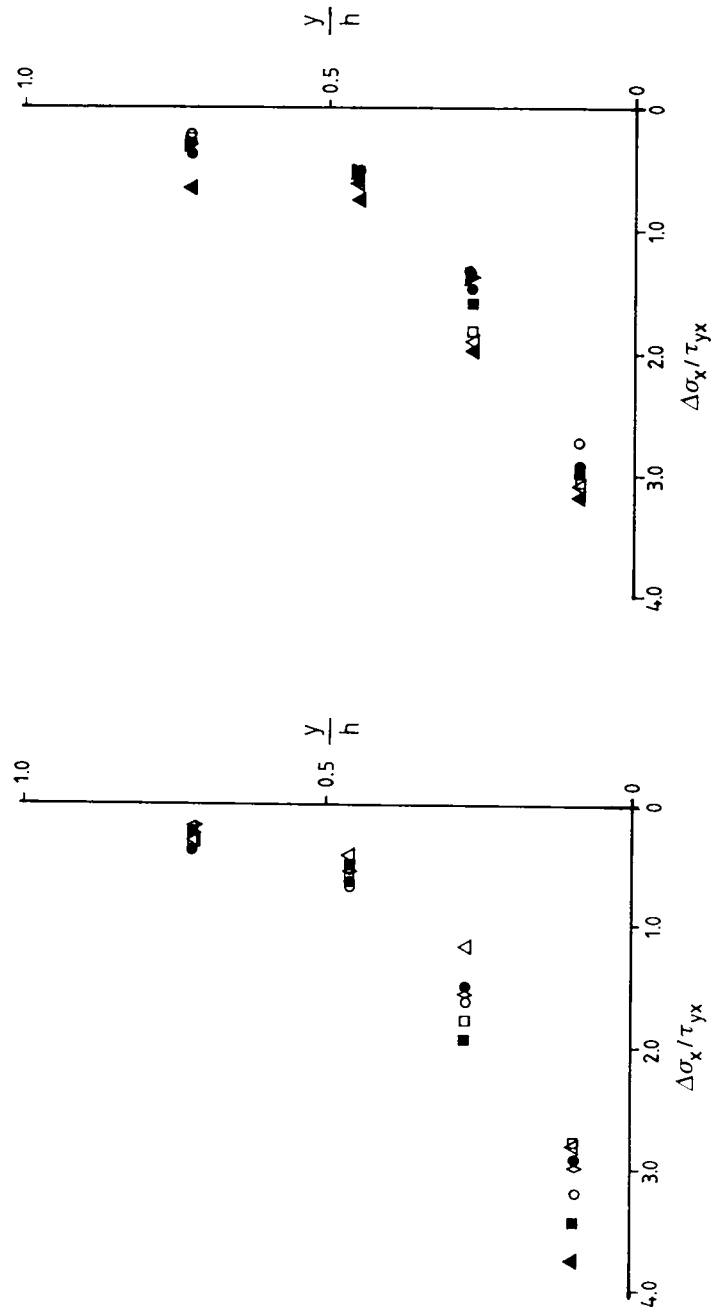


Figure 6.9 - Increments of Horizontal Stress on the Side of the Box in Reinforced Tests.

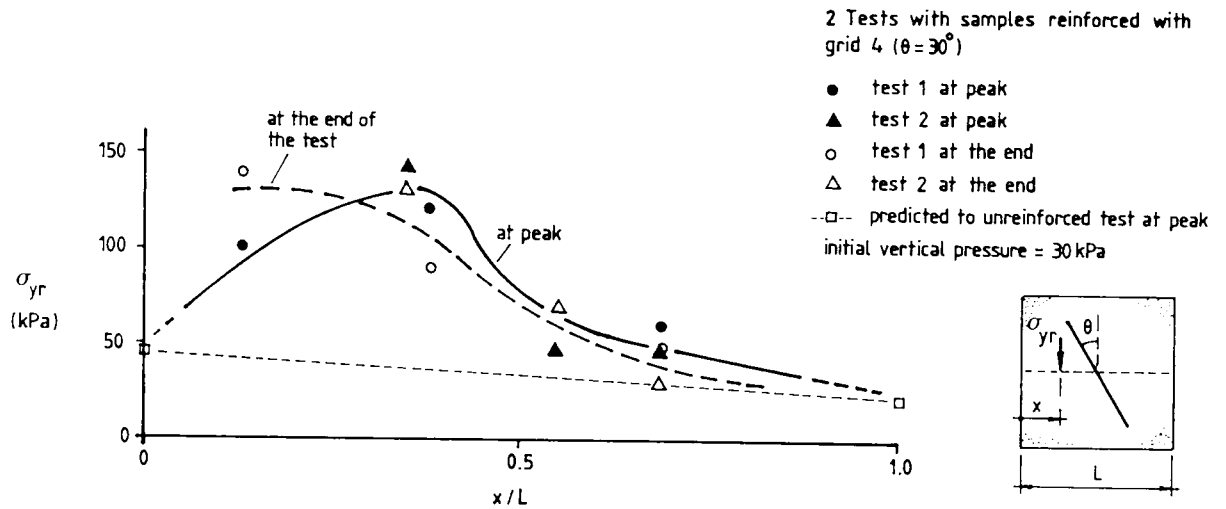


Figure 6.10 – Vertical Pressure Distribution on the Central Plane in a Test with Grid 4 – $\theta = 30^\circ$, $\sigma_y = 30$ kPa.

findings by Dyer (1985) who observed that, at the right side of the reinforcement in figure 6.10 ($0.6 < x/L < 1.0$), the vertical pressure should be controlled by the minor principal stress, since the direction of the major principal stress is close to the horizontal, at that distance from the middle plane. Despite these consistent patterns, the value of pressures obtained are likely to have still been affected to some extent by the level of distortion in the central region of the sample.

Figure 6.11 shows results obtained when pressure cells were placed on the rigid bottom face of the box in a sample reinforced with grid 1 in the vertical direction, at peak stress ratio. One can observe the drastic decrease in vertical stress close to the rigid boundary, due to the stress relief in the sand, caused by the tensile force in the reinforcement.

Normal stress distributions on the reinforcement were also obtained by placing three pressure cells at different points on the reinforcement

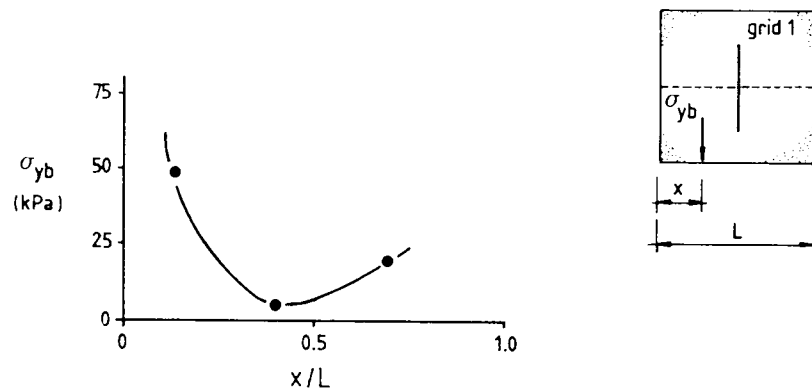


Figure 6.11 – Vertical Pressure Distribution on the Bottom Face of the Box in a Test with Grid 1 – $\theta = 0$, $\sigma_y = 30$ kPa.

plane. Figure 6.12 shows the results obtained in tests where these measurements were taken. Figure 6.12a shows the normal stress distribution on the reinforcement plane at peak stress ratio for tests with grid 4 and Stabilenka 400 geotextile placed in the vertical direction. Figure 6.12b shows these results for metal grids 4 and 5 inclined 30° to the vertical direction. As expected, the normal stress increases from the extremity of the reinforcement towards the central plane of the sample. These results may have been affected to some extent by the presence of the reinforcement or by the proximity to the central plane. However, the repeatability of results presented by the two tests with grid 4 was encouraging and the pressure distribution obtained was consistent with the results presented in the previous figures.

The important conclusion that arises from the results presented in figure 6.12 is that the mean normal pressure on the reinforcement plane is very high. So, for the geometry of reinforcement used in the tests, no bond failure can occur. Therefore, the force in the reinforcement is likely to increase continuously during the test and the strength of the reinforced sample will be dependent on how the reinforcement interacts with the surrounding soil. The balance of the combined effect of

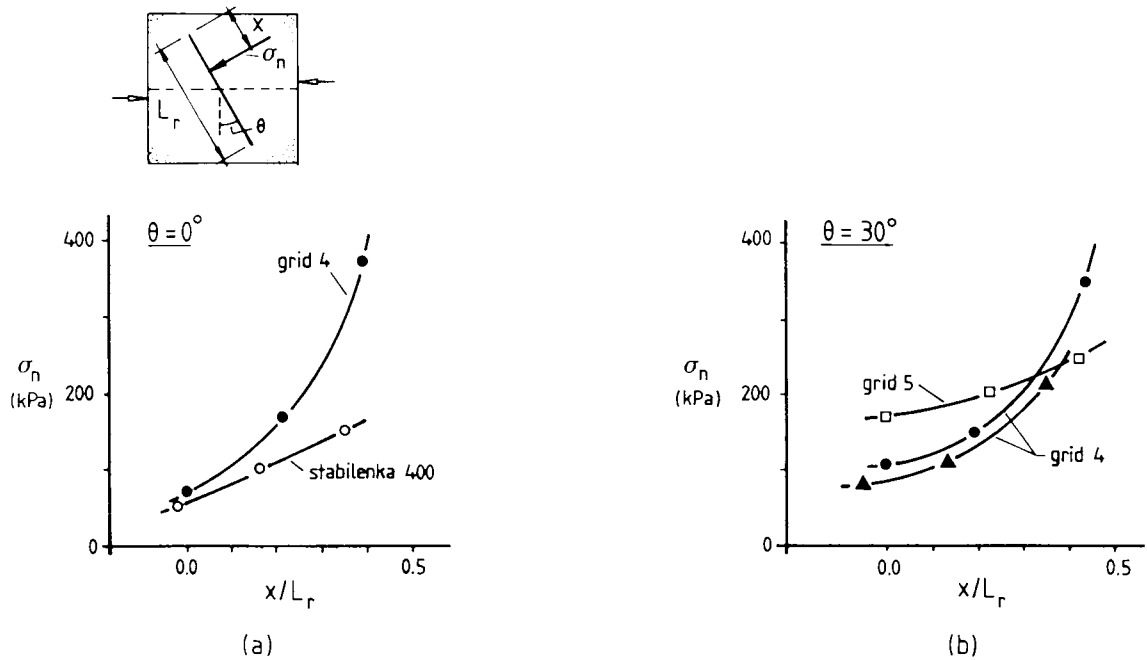


Figure 6.12 – Normal Stress Distribution on the Reinforcement Plane at Peak Stress Ratio.

reinforcement force increase and sand strength decrease during shear will determine the form of the curve of stress ratio versus shear displacement, for the reinforced sample. Not only the degree of interaction, but also the reinforcement stiffness, must play an important role in this process.

6.4 – Forces in the Reinforcement:

An estimate of forces acting in the reinforcement can be made by using limit equilibrium analysis. In figure 6.13 the forces acting on the top half of the box are shown. If equilibrium in the vertical and horizontal direction is analysed, one obtains the following expression for the force in the reinforcement, at peak:

$$\frac{P_r}{A_s \sigma'_y} = \frac{\bar{\tau}_{yx}/\sigma'_y - \tan\phi_{ds}}{\sin(\theta+\beta) + \cos(\theta+\beta)\tan\phi_{ds}} \quad [6.1]$$

and for the mean vertical pressure on the central plane, at peak stress ratio:

$$\frac{\bar{\sigma}_{yr}}{\sigma'_y} = \frac{\tan(\theta+\beta) + \bar{\tau}_{yx}/\sigma'_y}{\tan(\theta+\beta) + \tan\phi_{ds}} \quad [6.2]$$

where: P_r is the force in the reinforcement, A_s the sample area, θ initial reinforcement orientation, β increment in θ due to distortion of the reinforcement during the test, ϕ_{ds} friction angle mobilised on the central plane of the sample, $\bar{\tau}_{yx}$ mean shear stress on the central plane in a reinforced test, $\bar{\sigma}_{yr}$ mean vertical stress on the central plane in a reinforced test and σ'_y pressure on the central plane due to the pressure on top plus the sample weight and friction on the side of the box. Note that $\bar{\sigma}_{yr}$ is greater than σ'_y since it takes into account the contribution due to the vertical component of the reinforcement force.

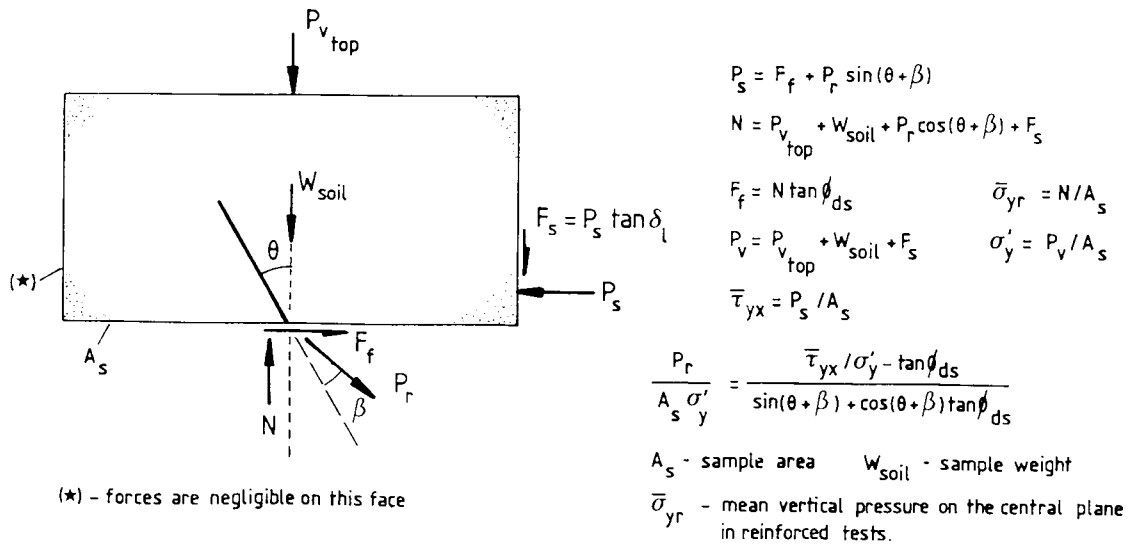


Figure 6.13 – Forces Acting on the Top Half of the Sample in a Reinforced Test.

Figure 5.7 showed that the peak friction angle is a function of the stress level. So, an iterative procedure is required to obtain P_r from expression 6.1. This procedure consists in attributing values to ϕ_{ds} in expression 6.2 and checking if ϕ_{ds} and σ_{yr} satisfy the variation of peak friction angle with vertical stress presented in figure 5.7. If so, this value of friction angle is used in equation 6.1 to obtain the force in the reinforcement. When the friction angle correspondent to the vertical pressure used in the test (30 kPa) is adopted, the force in the reinforcement will be underestimated by about 10%.

From reinforced tests where the force in the reinforcement was obtained, comparisons can be made between the prediction by equation 6.1 and the measurements. In five reinforced tests the force in the reinforcement was known at peak stress ratio: 3 tests with plastic grids where strains were measured by means of markers placed on the reinforcement and 2 tests with metal grids that failed through tension during the experiment (grids 7 and 9). Because of the movement of the reinforcement during the test, sand grains covered the markers completely in two reinforced tests with plastic grids. Only in two out of five tests the maximum strain could be obtained during the entire test. From the strain measurement and the time elapsed, the force acting in Tensar grids can be obtained using data from McGown (1982) or figure 1.2.

For the metal grids that failed through tension during the test it was assumed that the soil reached its maximum peak stress ratio approximately at the same time as the grid material broke. This hypothesis was confirmed by the profile of shear strains in the central region of the sample at peak stress ratio. As can be seen in figure 6.8b the shear strain profile for the reinforced sample, during yielding of

the reinforcement, is very close to the unreinforced sand shear strain profile. The maximum tensile stress for grids 7 and 9 was obtained by means of tensile tests. This value was 366 N/mm^2 which compares well with data from Dyer (1985) in similar tests with the same material (375 N/mm^2).

Figure 6.14 shows maximum tensile strains measured at the mid length of plastic grids versus shear displacement of the box. With these values, the force in Netlon SR2 polymer grids can be estimated at any stage of the test using data from figure 1.2. For Netlon grids SR1, data presented by McGown (1982) was used to obtain forces in the reinforcement. Figure 1.2 can still be used in this case, but the force obtained for Netlon SR1 must be reduced by about 16% to allow for the difference between the index stress strain curves of the two materials.

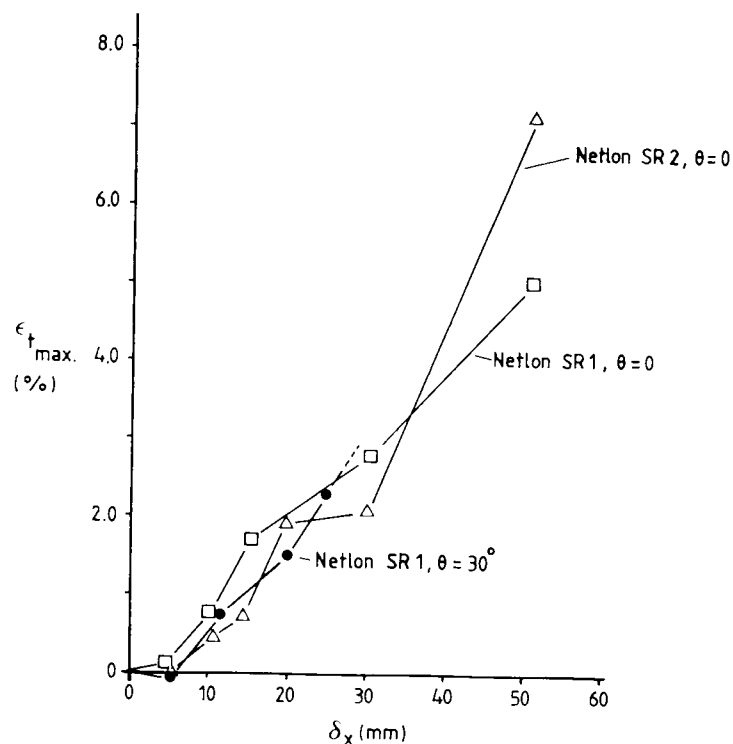


Figure 6.14 - Variation of Maximum Tensile Strain in a Plastic Reinforcement During the Test.

The change in reinforcement orientation during the test (β) must also be known in order to use equation 6.1 and 6.2. As will be seen later, this value will be significant for flexible materials only at large shear displacements. Nonetheless, β was obtained from markers placed on the reinforcement. Figure 6.15 shows profiles of reinforcements at peak stress ratio for reinforcements placed in the vertical direction and inclined 30° to the vertical. This figure also presents the deformed shape of an initially vertical line in an unreinforced test. Horizontal displacements of the reinforcement are normalised by the overall shear displacement of the box. Note that, only away from the central plane is the horizontal displacement of the reinforcement equal to the displacement of the top half of the box. The stiffness and form of the reinforcement affect the profile of the reinforcement when placed in the vertical direction. Flexible reinforcements tend to follow the movement of an initially vertical line in an unreinforced test, while stiffer metal reinforcements present less deformed profile. For inclined reinforcements the difference of behaviour between a stiff and a flexible reinforcement was negligible.

From data from figure 6.15 the value of β can be obtained. These values, for peak stress ratio and at the end of the test, are presented in Table 6.1 for some of the tests performed. Note that β assumes significant values only at the end of the test. At that stage this angle for a stiff reinforcement is still much smaller than the one for a flexible reinforcement. This suggests that limit equilibrium methods for stability analysis of reinforced soil structures considering the deformed shape of the reinforcement, like the one proposed by Leshchinsky & Reinschmidt (1985), should be used with due care regarding the choice of

values for β . It seems unwise to use large values for that angle in those methods when conditions at peak are being analysed.

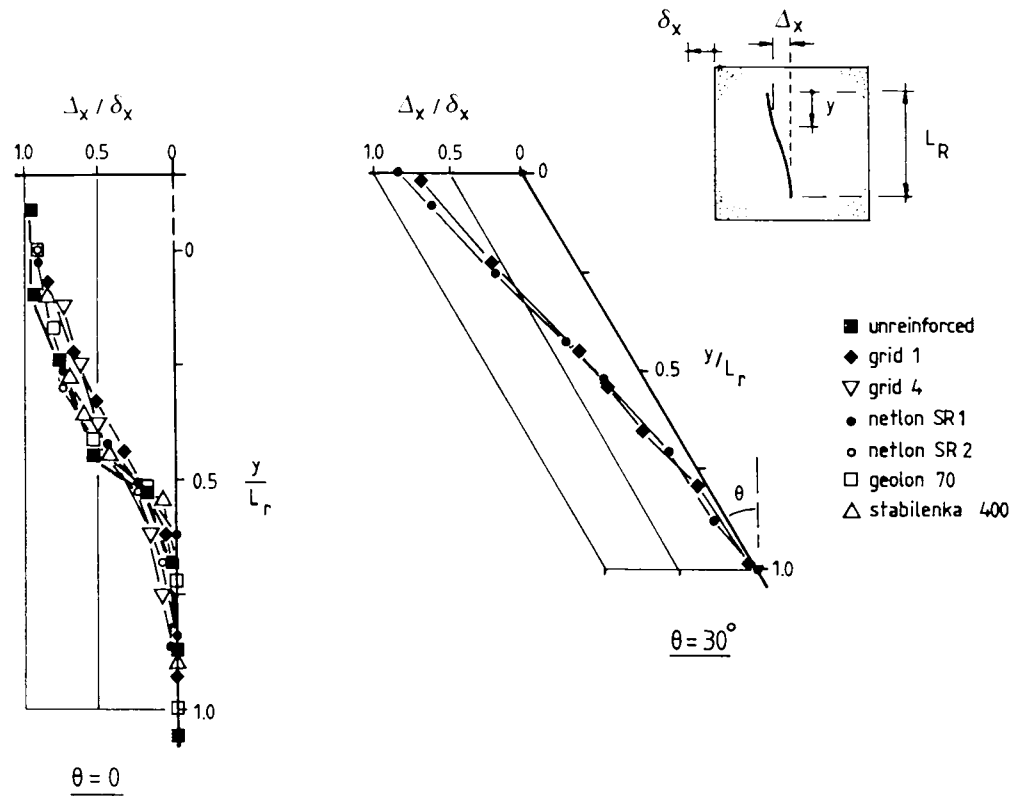


Figure 6.15 – Profiles of Reinforcements at Peak Stress Ratio.

Reinforcement	$\beta(^{\circ})$	
	Peak	End of Test
Netlon SR1 ($\theta=0$)	5.4	22.4
Netlon SR1 ($\theta=30^{\circ}$)	1.3	-
Netlon SR2 ($\theta=0$)	4.0	20.3
Grid 1 ($\theta=30^{\circ}$)	0.9	1.4
Grid 4 ($\theta=0$)	2.7	8.7
Grid 7 ($\theta=30$)	1.4	-
Grid 9 ($\theta=30$)	1.2	-

Table 6.1 – Values of β Obtained in Reinforced Tests at Peak.

Using the value of β and data from figures 6.1 to 6.3 in equations 6.1 and 6.2 the force in the reinforcement can be estimated. Comparisons

between predictions from those equations and values measured or obtained from strain measurements at peak stress ratio are presented in Table 6.2. In general terms, the reinforcement forces predicted by limit equilibrium analysis are remarkably close to values obtained by strain or maximum tensile load measurements. Similar good agreement between predictions and measured values were reported by Jewell (1980). For polymer grid Netlon SR1 ($\theta = 30^\circ$) a greater difference between predicted and measured forces occurred. This may have been caused by lack of accuracy on reinforcement strain measurements in this test, since after maximum stress ratio has been reached all strain measurements were lost due to the sand having covered the markers on the reinforcement.

Reinforcement	P_r (kN/m)		$\bar{\sigma}_{yr}$ (kPa)
	Predicted	Measured	
Netlon SR1 ($\theta=0$)	11.8	11.7	44.9
Netlon SR2 ($\theta=0$)	9.9	10.0	42.9
Netlon SR1 ($\theta=30^\circ$)	11.3	9.8	42.7
Grid 7 ($\theta=30^\circ$)	12.9	11.5	44.2
Grid 9 ($\theta=30^\circ$)	11.9	11.5	43.0

Table 6.2 – Comparison Between Predictions and Measurements of Reinforcement Forces at Peak Stress Ratio.

Strictly speaking, expression 6.1 can only be used if the stress ratio in the sand is known. This happens at failure when that value is equal to the tangent of the mobilised friction angle. However, at any other stage of the test the stress ratio in the sand should be known accurately in order to estimate the force in the reinforcement. To a certain extent, that can be accomplished by relating stress ratio to

shear strain for unreinforced sand. In doing so, a mean shear strain in the reinforced sand could be used to obtain the stress ratio at any stage of the test. This technique has, however, to be approached with caution since, as shown in figure 6.8, the shear strain profile is very non-uniform in the central region of the box. Nevertheless, some interesting conclusions may arise from this exercise.

In figure 6.16 stress ratio versus shear strain (obtained by markers) for unreinforced sand is presented. At later stages of the test the shear strain profile in the sample reinforced with a vertical polymer grid is very close to the unreinforced one (fig. 6.8) and a typical value of mean shear strain for a metal reinforced sample would be about 60%.

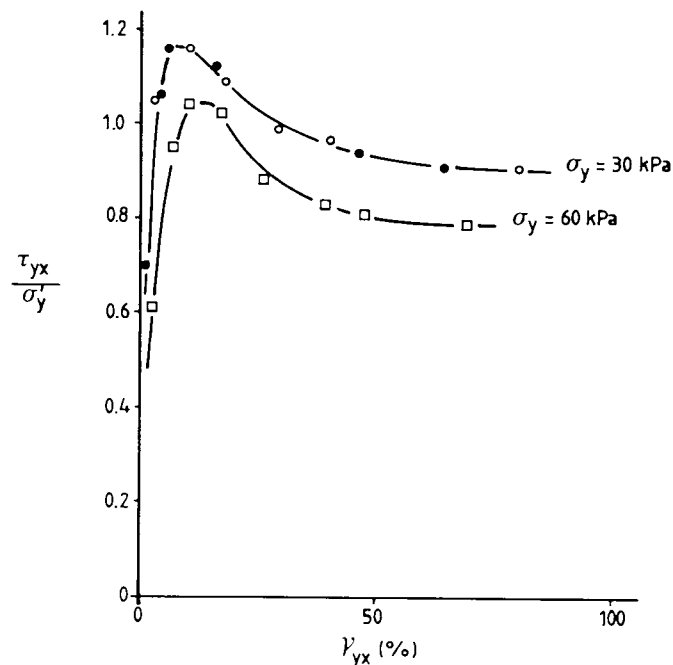


Figure 6.16 – "Stress-Strain" Relation for Unreinforced Sand.

From figure 6.16 the stress ratio in the sand, at that stage, for the polymer grid reinforced sample would be between 0.79 and 0.90 and between 0.80 and 0.92 for the sample reinforced with grid 4, depending on the

current vertical stress on the central plane. These limits are very close due to the form of the stress ratio versus shear strain curves. Using equations 6.1 and 6.2 one obtains the results presented in Table 6.3. One should note that the force measured is close to the predicted value corresponding to a stress ratio in the sand given by the test under 60 kPa vertical pressure. Also, the predicted vertical pressure is still about twice its initial value, before shearing has started. This result is consistent with the data from figure 6.12 where even at later stages of the test the magnitudes of pressures on the central plane were close to the values measured at peak stress ratio.

Reinforcement	" $\tan\phi_{ds}$ "	P_r (kN/m)		$\bar{\sigma}_{yr}$ (kPa)
		Predicted	Measured	
Netlon SR1 ($\theta=0$)	0.79	19.9	21.0	51.4
	0.90	15.2		47.1
Netlon SR2 ($\theta=0$)	0.79	28.8	32.0	60.0
	0.90	23.3		54.8
Grid 4 ($\theta=0$)	0.80	27.3	—	59.3
	0.92	19.9		52.7

Table 6.3 – Comparison Between Predictions and Measurements of Reinforcement Forces at the End of the Test.

With the results of strain measurements in polymer grids, the maximum force in the reinforcement can be obtained at several stages of the test. Figure 6.17 shows plots of forces in the reinforcement versus shear displacement. Also presented in this figure are predictions of forces in grid 4 at peak and at the end of the test, by limit equilibrium analysis. It is interesting to note that for the polymer grids the force

continuously increased, more or less at the same rate during the tests, whereas for the metal grid the rate of force increase would be greater than the one for polymer grids before peak and lower after it. This may be explained by the fact that stiffer reinforcements will respond more quickly to shear displacements of the box, leading to higher forces in the reinforcement and a greater degree of shear strain inhibition in the sand along the central region. The rate of reinforcement force increase will depend on parameters relevant to the mechanism of interaction between soil and reinforcement (stiffness, shape and form of reinforcement, dimensions and spacing of bearing members, etc.) as well as how this interaction affects the rate of softening of the sand mass. Because in the large shear box the strain softening is not so severe, the deformation in the polymer grid is likely to mobilise magnitudes of reinforcement force sufficient to make up for the fall in soil strength due to softening.

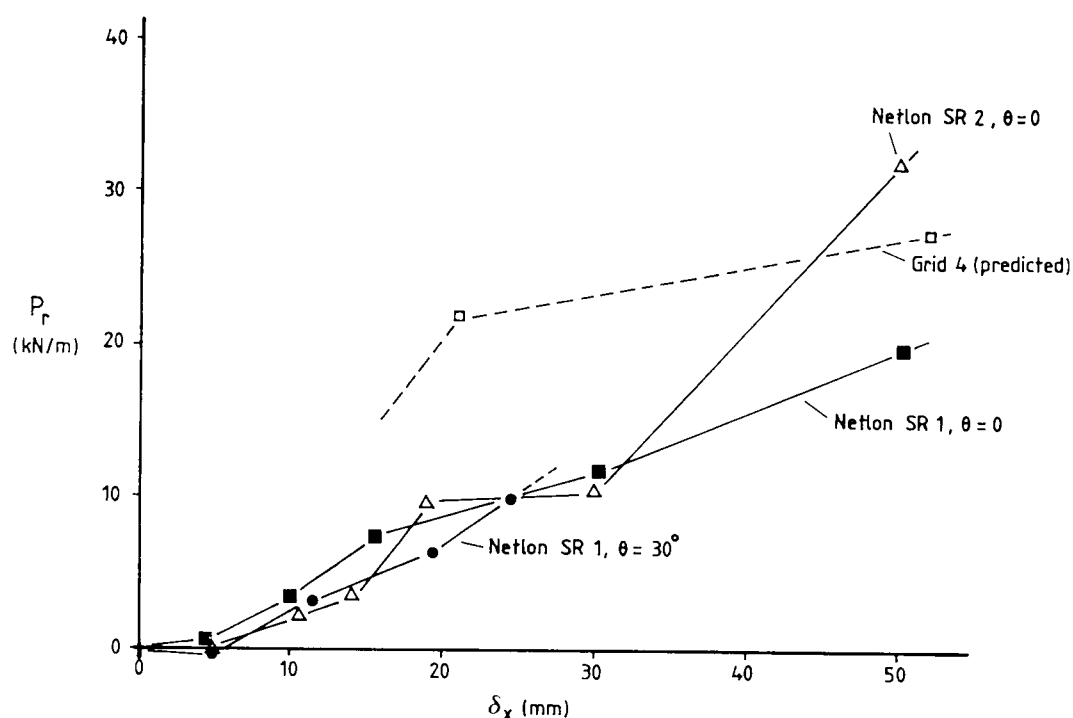


Figure 6.17 - Maximum Force in the Reinforcement During the Test.

6.5 - Conclusions:

This chapter has presented the results obtained from large direct shear tests in reinforced samples of dense Leighton Buzzard sand 14/25. The main conclusions can be summarised, as follows:

1. The presence of the reinforcement in the sand caused a remarkable increase in shear strength. For metal grids the strength of the sand was nearly doubled;
2. Grids 1 to 5 all gave similar peak stress ratio values, independent of the grid characteristics. This was due to the fact that, because the normal pressures on the reinforcement plane are very high, the reinforcement is still far away from experiencing bond failure with the surrounding soil. Therefore, in terms of pull-out behaviour, the mobilisation of pull-out force is still small and does not allow one to distinguish differences in sample behaviour caused by different reinforcements with approximately the same longitudinal stiffness and bearing member diameter to spacing ratios;
3. The reinforcement action caused a reduction by a factor of 2 in the development of strains in the central region of the sample. Inclined reinforcements are more efficient for this because of the contribution from the horizontal component of the reinforcement force;

4. The horizontal pressure distribution on the side wall of the box was not affected by the presence of the reinforcement. In mean terms, the vertical stress on the central plane of the box is doubled in reinforced tests with metal grids. This stress is still nearly twice the initial value in that region at the end of the test. Pressures on the reinforcement are very high, which prevents bond failure. The pressure distribution on the rigid bottom of the box was strongly affected by the tensile force in the reinforcement which caused a stress relief on that boundary and a consequent non-linearity of the stress distribution;
5. Limit equilibrium analysis provides a powerful tool for the estimate of reinforcement forces. Comparison between predicted and measured reinforcement forces showed a difference smaller than 10% in most of the cases. The deformed shape of the reinforcement has little effect on the force calculation up to peak stress ratio, which means that for the range of values tested, bending stiffness had negligible effect. However, for large shear displacements the deformed shape causes an increase on the horizontal component of the reinforcement force. This favours plastic reinforcements since they are more deformable than metal ones. As an example: for an initially vertical polymer grid, the horizontal component of the reinforcement force was increased from zero to about 38% of the total force at the end of the test, while the vertical component was reduced by only 7.5%, due to the deformed shape of the reinforcement; for metal grid 4 these figures were 15% and 1.2%, respectively. So, because of the strong anchorage provided by high normal pressures on the reinforcement plane a combination of low bending stiffness and

high longitudinal stiffness of a vertical reinforcement can be beneficial to the strengthening of the sample after peak stress ratio;

6. In terms of strength, the direct shear test of reinforced samples resembled unreinforced tests under a higher vertical pressure. The presence of the reinforcement causes an increase in the vertical stress and a decrease in shear stress transferred to the sand mass. Shear strains are reduced in the central region of the box due to the action of the reinforcement. The shear load-shear displacement curve obtained in a reinforced test will be determined by the balance between the ability of the reinforcement to strengthen the soil and the softening characteristics of the latter, under higher vertical stresses induced by the reinforcement;
7. Regarding the performance of instruments, some alterations would be suggested in order to improve the results obtained from them. The procedure used to measure reinforcement strains is not very efficient because in half of the tests performed with this intent, the markers were covered with sand grains during the test. A technique using wires fixed to the reinforcement bearing members, as was employed for the pull-out tests, is likely to be more successful. The pressure cells that were used buried in the sand would probably have their performance improved if they were a little smaller than their actual size;
8. Due to the complexity of stress and strain fields presented in direct shear tests of reinforced samples, the interpretation of

some important aspects of the reinforcement characteristics, relevant to interaction with the surrounding soil, such as reinforcement geometry and interference between bearing members, is very difficult to approach. The investigation of these points is simpler in pull-out tests. So, in the following chapters the results of pull-out tests are presented and discussed.

Part II - Pull-out Tests

Chapter 7: Pull-out Test Apparatus

Chapter 7: Pull-out Test Apparatus

7.1 - Introduction:

This chapter deals with the presentation of the pull-out test apparatus used in the present work. Most of the relevant information has already been presented in Chapter 2 and reference should be made to that chapter for additional details.

Two sizes of pull-out box were used in this part of the work. They were adapted for pull-out tests from the medium size and large shear boxes. In order to be consistent with the previous chapters, the names medium and large will remain unchanged as a reference to the size of the box used in pull-out tests. No pull-out test was performed in a box smaller than the medium size one.

7.2 - Description of Equipments and Instrumentation:

7.2.1 - Medium Size Pull-out Box:

The medium size box was used for the study of scale and boundary effects and for tests with grids containing few bearing members. The alterations made in the medium size box to perform pull-out tests were to fix both halves of the box together with a 3mm gap in the front face, at the mid height of the box, and to provide a clamping system for the reinforcement fixed to the deflector bar (see Chapter 2 and Jewell, 1980). Apart from tests where the effect of the top boundary was studied, all the other tests were performed with a rubber bag filled with water on top of the sample to apply the vertical pressure and a rigid smooth

bottom boundary. Additional details of this box can be found in Chapter 2 of the present work or in Jewell (1980) and Dyer (1985).

7.2.2 - Large Pull-out Box:

The same sort of alterations presented above were made in the large box in order to perform pull-out tests. The two halves of the box were held together by means of 12mm bolts distributed along the available perimeter of the box. A 10mm gap to allow for the inclusion of the reinforcement layer through the front face of the box was provided by an appropriate arrangement of the internal plates. In all tests the internal wall was lubricated using the technique presented in Chapter 4 to minimise the effect of friction on that boundary. The clamping structure consisted of a stiff metal frame resting on rollers on the ground and fixed to the load cell and jack, as shown in figure 7.1. The clamping of the reinforcement was achieved by special clamps held by the pull-out frame by means of eight 19mm dia. bolts (see fig.7.1). To clamp the reinforcement effectively, a low melting point alloy (Cerrobend, 70°C melting point) was used to fill the free space left by the reinforcement inside the clamps. The molten alloy was poured through 9mm holes distributed along the length of the top clamp and through its sides, when geotextiles were tested. Figure 7.2 shows a general view of the equipment during a test. Figure 7.3 shows the clamping system in detail.

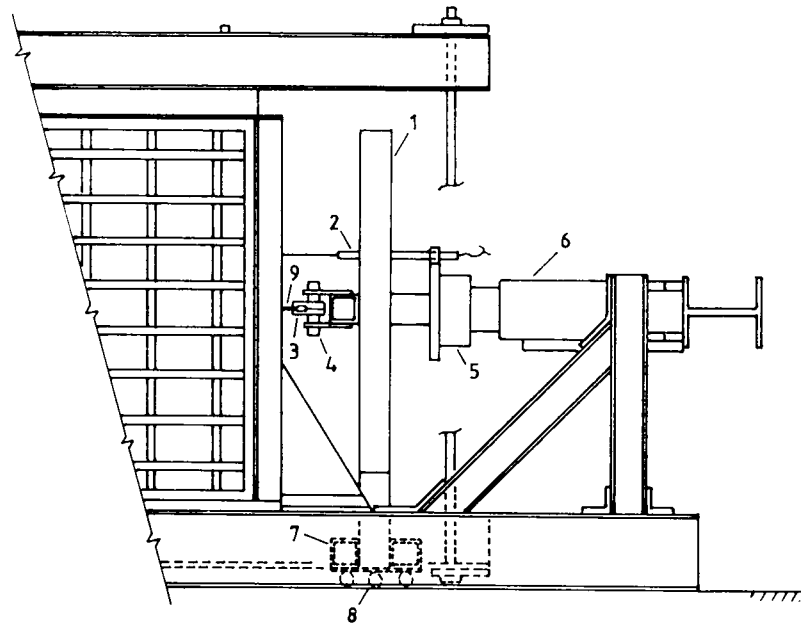
Split plates are available to be distributed on the front face of the box to allow for the performance of pull-out tests with two layers of reinforcement and varying spacing between them. This arrangement was

Elevation

Scale: 1/200

- 1 Pull-out frame
- 2 L.V.D.T.
- 3 Clamps
- 4 Bolts
- 5 Load Cell
- 6 Jack
- 7 Pull-out Frame Footing
- 8 Rollers
- 9 Reinforcement

Dimensions and additional details are given in figures 2.2, 7.2 and 7.3



Plan

Notes: same as above.

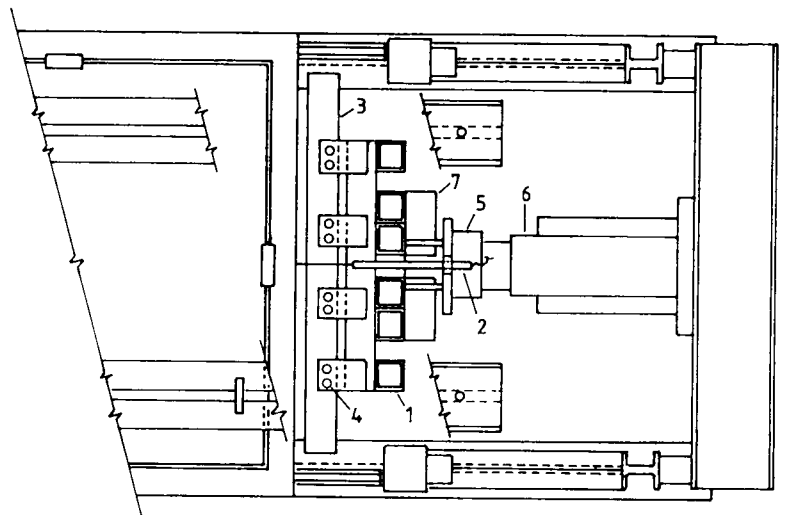


Figure 7.1 - Large Pull-out Box.

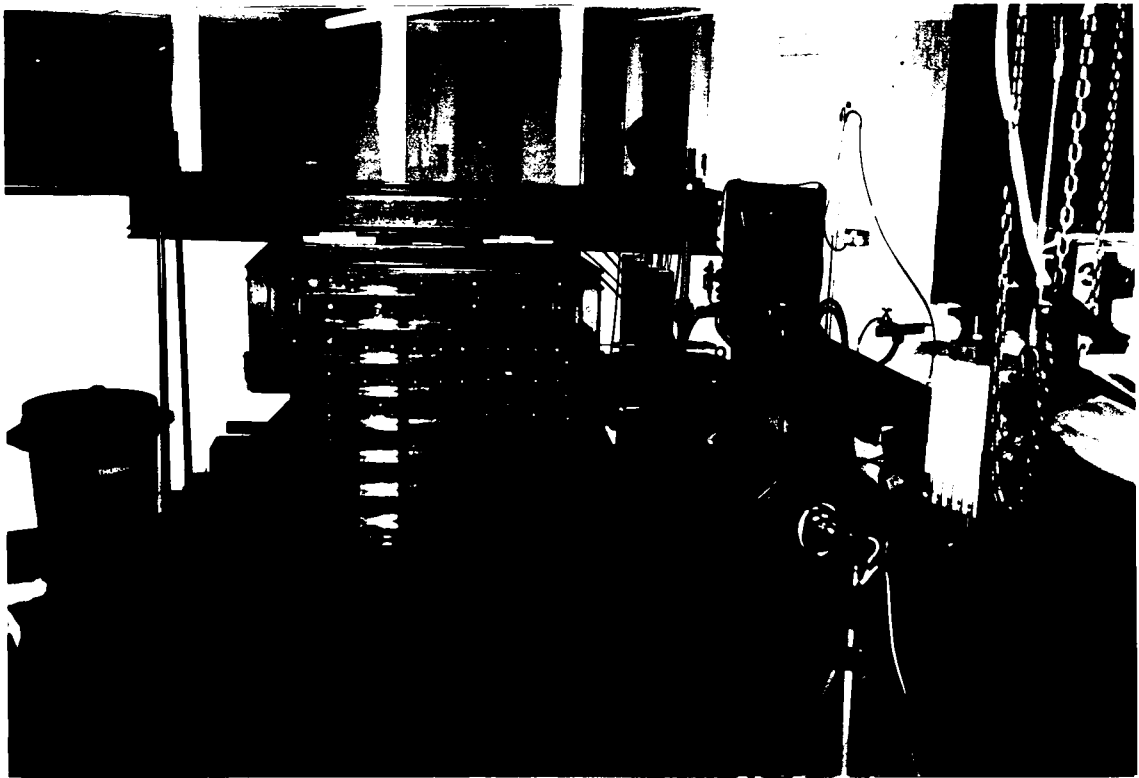


Figure 7.2 - General View of the Large Pull-out Box During a Test.

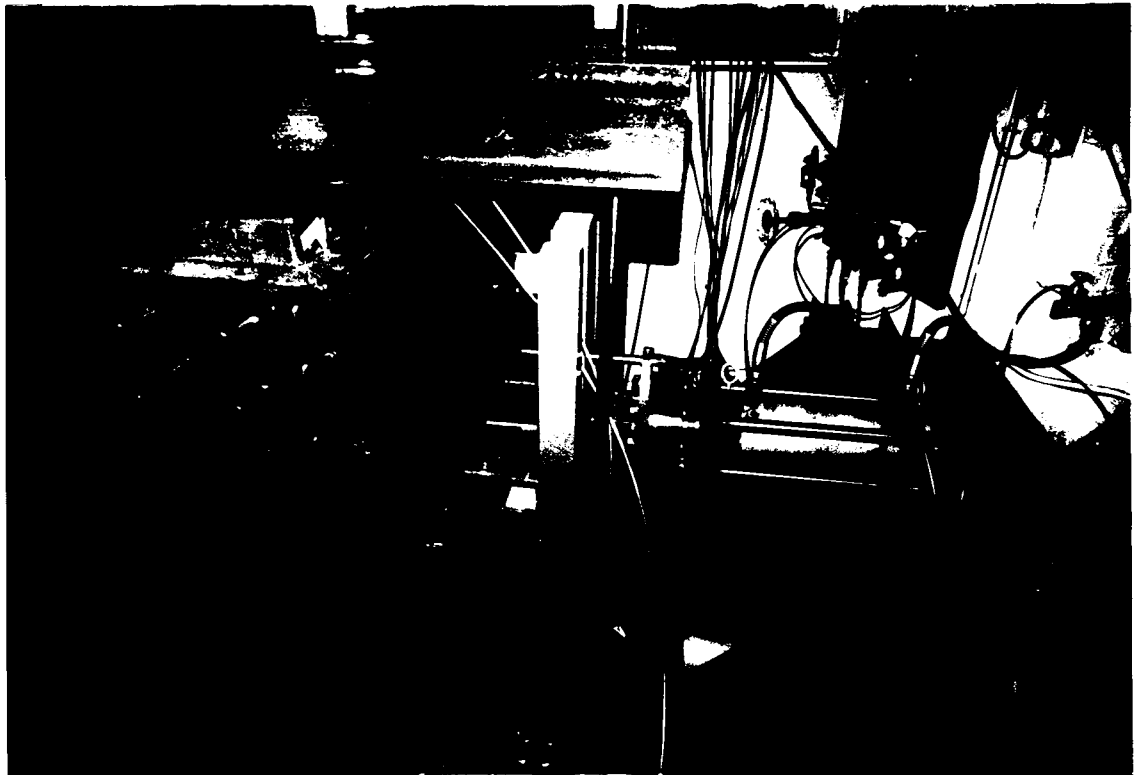


Figure 7.3 - Detail of the Clamping System.

employed in the tests to study the interference between layers of reinforcement under pull-out conditions. Figure 7.4 shows the arrangement for tests with two layers of reinforcement.



Figure 7.4 - Arrangement for Tests with Two Reinforcement Layers.

The same photographic technique described in Chapter 2, to monitor marker displacements, was used in the series of pull-out tests. The eight pressure cells, already presented in Chapter 2, were distributed along the height of the front wall of the box in order to assess the horizontal stress distribution on that boundary. Vertical stress on the sample was applied using the water filled rubber bag, in the same way as in the direct shear tests.

Tensile strains in polymer grids were measured by means of 3mm dia. cables fixed to the grid bearing members, as shown in figure 7.5. To

accommodate one of the cable extremities, holes of about the same diameter were made in the bearing members of the grid. Before each cable was placed in position, its extremity was deformed into an L shape, coated with Araldite and driven through the member thickness. The other extremity of the cables reached the outside of the tank through a gap between plates opposite to the reinforcement layer and rested on an

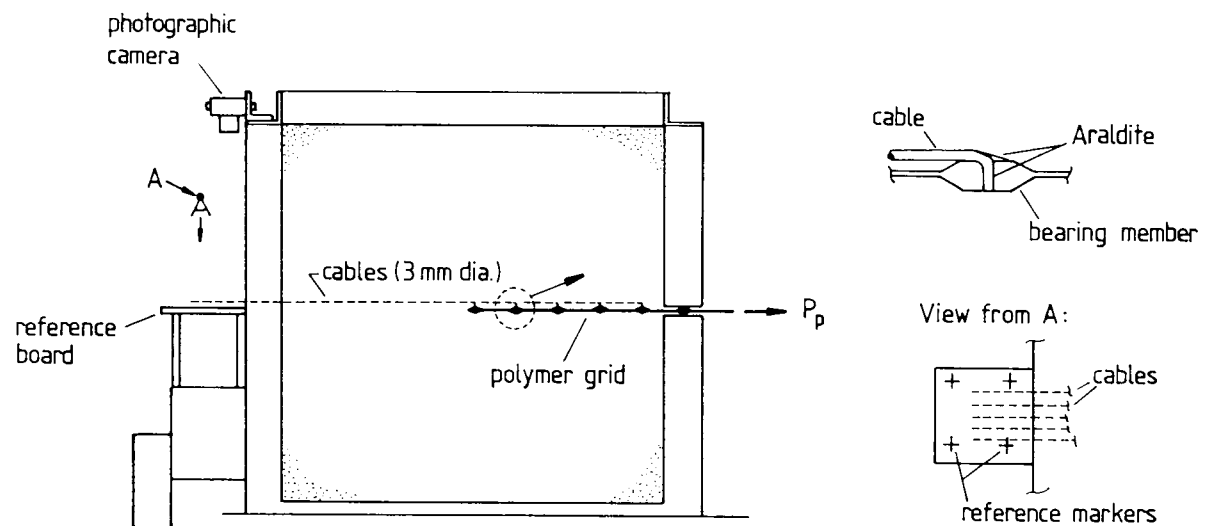


Figure 7.5 – Technique Used to Measure Strains in Polymeric Grids.

horizontal board containing reference markers. An Olympus OM1n photographic camera, loaded with a 400ASA slide film, was used to take shots of the cable extremities during the test. The movements of markers on the cables were then related to the reference markers and relative displacements between bearing members were obtained using the enlarger Varicon Devere 203, as described in Chapter 2. This technique was successfully used with polymer grids but led to disappointing results when tried with geotextiles. As was initially anticipated, the localised deformation of the geotextile around the cable (1mm dia. in this case) affected the accuracy of the measurements.

Chapter 8: Soils and Reinforcements Used in Pull-out Tests

Chapte 8: Soils and Reinforcements Used in Pull-out Tests

8.1 - Introduction:

In this chapter the soils and reinforcements used in pull-out tests are presented. Most of the data has already been presented in Chapter 3 and reference should be made to that chapter for additional information.

8.2 - Soils Used in the Pull-out Tests:

Three uniform sands were used in the pull-out test series. They were Leighton Buzzard sands 7/14, 14/25 and 25/52. The reason for the use of more than one sand was to study the influence of the soil particle size on the performance of grid reinforcement. All three sand types were used in tests with the medium size box but only Leighton Buzzard sand 14/25 was used in the tests with the large pull-out box.

The general properties of the sands used are presented in Table 8.1. Data in this table refer to a dense state of the sand. Friction angle values presented were obtained by direct shear tests under 25 kPa vertical pressure, which was the value used in most of the pull-out tests. Figure 8.1 presents an enlarged photographic view of the sand particles. All sands have a predominantly angular shape but the 25/52 sand seems to present a smoother surface, which may in part account for the smaller friction angle.

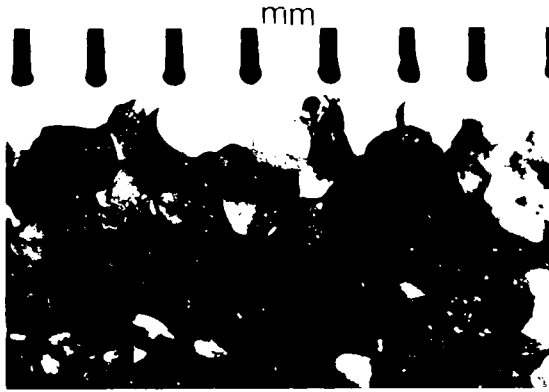
8.3 - Reinforcement Characteristics:

Data on reinforcement characteristics has already been presented in Chapter 3. Reference should be made to that chapter and, in particular, Table 3.1 for information on the reinforcements used in the pull-out tests. Additional information is provided in Appendix 3. As in the direct shear tests, not all reinforcements listed in Table 3.1 were used in the series of pull-out tests. In all pull-out tests performed, either in the medium size or in the large pull-out box, the reinforcement layer covered the whole width of the box.

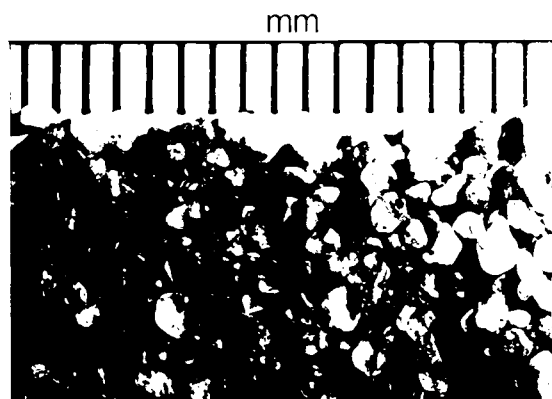
Sand	Range of Particle Sizes (mm.)	D_{50} (mm.)	G_s	e (± 0.005)	I_D (%)	CU	ϕ_{ds} ($^\circ$)
Leighton Buzzard 25/52	0.2 — 0.6	0.4	2.66	0.52	87	1.5	38.3
Leighton Buzzard 14/25	0.6 — 1.18	0.8	2.66	0.53	87	1.3	51.3
Leighton Buzzard 7/14	1.18 — 2.0	1.6	2.66	0.55	86	1.4	48.2

D_{50} = mean particle dia.; G_s = soil particle density; e = void ratio; I_D = relative density; CU = coefficient of uniformity; ϕ_{ds} = direct shear friction angle at 25 kPa vertical pressure.

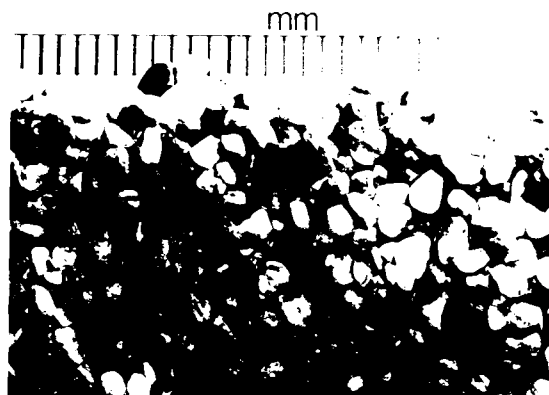
Table 8.1 - Properties of Sands Used in the Pull-out Tests.



(a) Leighton Buzzard Sand 25/52.



(b) Leighton Buzzard Sand 14/25.



(c) Leighton Buzzard Sand 7/14.

Figure 8.1 - Photographic Enlargement of the Sands Used In Pull-out Tests.

Chapter 9: Sample Preparation and Test Procedure in Pull-out Tests

Chapter 9: Sample Preparation and Test Procedure Used in Pull-out Tests

9.1 - Introduction:

This chapter describes the sample preparation and test procedure used in the pull-out tests. As mentioned in the previous chapters, most of the information presented in Chapter 4 is valid for the present chapter.

9.2 - Tests with the Large Pull-out Box:

Basically, the sample preparation for pull-out tests followed the same procedure as for direct shear tests. The only difference was with respect to the reinforcement installation. The sand was poured from the hopper and the markers placed on the boundary following the same technique described in Chapter 4. The procedure used to install geotextiles or small aperture size grids (grids 1, 2 and polymer grids) was as follows: when the sand reached the middle height of the box its surface was levelled to the horizontal by carefully pouring small amounts of sand manually from a small hopper; the reinforcement was laid on the sand surface and measurements of reinforcement length taken to an accuracy of one millimeter; when polymer grids or geotextiles were used, the cables for tensile strain measurements were positioned and initial distances measured; the extremity of the reinforcement was then clamped using the clamps and the low melting point alloy; The bolts that hold the clamps to the frame were positioned and tightened and the sand pouring continued. For grids with large aperture size, the reinforcement was held horizontally by weak strings hanging from support bars fixed to the internal walls of the box, normal to the direction of the pull-out load.

After a layer of sand, thick enough to bury the reinforcement, had been poured, the strings were cut and the support bars removed.

The testing procedure was essentially the same as described in Chapter 4. The only difference was that the hydraulic pump that pressurises the jack was operated in order to reverse the jack ram movement, applying tensile loads in the reinforcement. During the test, photographs of the extremities of cables used to assess tensile strains in polymer grids were taken and the time elapsed from the beginning of the test recorded.

After the test had finished, the reinforcement was cut near the clamps and the alloy casting removed. This material was then melted to be used in the next test. Emptying of the box followed the procedure described in Chapter 4.

9.3 - Tests with The Medium Size Pull-out Box:

The sample preparation technique was basically the same as used for direct shear tests. Reinforcement was installed in a way similar to that used in the large box.

9.4 - Post-Test Procedure:

After the end of each test, the procedures followed for emptying the boxes and preparing for the next test were the same as described in Chapter 4.

Chapter 10: Pull-out Test Results

Chapter 10: Pull-out Tests Results

10.1 - Introduction:

This chapter presents results of pull-out tests performed in the medium size pull-out box and in the large pull-out box. Influence of scale and boundary conditions are also presented and discussed.

10.2 - Effect of Boundary Conditions on Pull-out Tests Results:

10.2.1 - Influence of the Top Boundary:

As part of the present work, a series of pull-out tests using grid 1 was performed in the medium size box, under different boundary conditions. The aim was to investigate to what extent boundaries can affect the result of the test and which measures can be taken to minimise these effects. Due to the limitation of space in the present dissertation, a more detailed description of these experiments is given elsewhere (Palmeira & Milligan, 1987) and only the main conclusions are presented here.

Basically, the two limiting conditions of a pull-out box top boundary are the free, rigid and rough top plate and the flexible, fluid filled pressure bag. Therefore, tests in the medium size box, using each of these boundaries were performed on a piece of grid 1, 75mm long, under 25 kPa vertical pressure. The ratio between reinforcement length and depth was equal to 1. The soil used was Leighton Buzzard sand 14/25. Figure 10.1 shows the results obtained. The use of a flexible top boundary decreased the peak pull-out load by about 10%. It should be

pointed out that despite the small difference between pull-out loads observed, the "friction angle" between soil and reinforcement obtained is well above the soil friction angle in both cases. This fact will be discussed later in this work. It will also be seen that the stiff and smooth bottom face of the box affects the stress distribution on the front wall and the movement of markers. Nevertheless, due to the localised failure mechanism close to the reinforcement layer, the effect of that boundary on the value of the pull-out load, for the geometry and arrangement used, must be small.

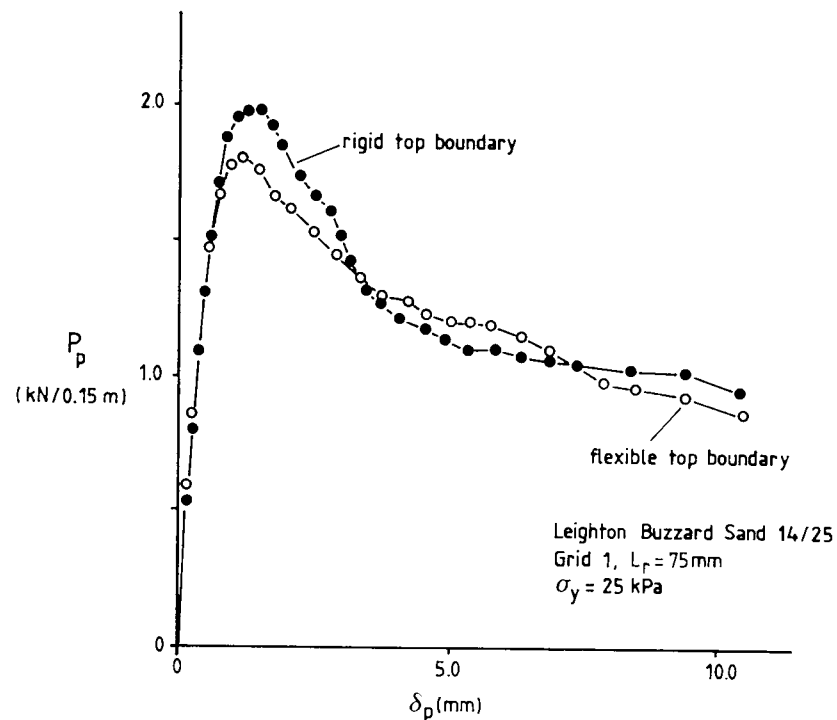


Figure 10.1 – Influence of the Top Boundary on the Results of Pull-out Tests in the Medium Size Box.

10.2.2 – Influence of the Roughness of the Front Wall:

If the reinforcement is away from the top and bottom boundaries, the front wall is the only box boundary left to influence significantly the

test result. A series of tests was conducted with different frictional characteristics being used on the internal front wall of the medium size box. The wall condition varied from the "smooth case", where the lubricating system described in Chapter 4 was employed, to the "rough case" where particles of the same sand used in the test were glued to the wall. Intermediate states were achieved by using the original smooth metal surface and sand paper glued to the wall. More details on these arrangements can be found in Palmeira & Milligan (1987).

Grid 1 (75mm long), Leighton Buzzard sand 14/25 and a vertical pressure of 25 kPa were used in these tests. Figure 10.2 shows the variation of the tangent of the "friction angle" (τ_b/σ_y) between soil and reinforcement versus angle of friction between soil and front wall (δ). The bond stress between soil and reinforcement (τ_b) was defined as the maximum pull-out force divided by the total area of the reinforcement ($2W_r L_r$). Figure 10.2 shows a marked effect of the front wall roughness on the test result due to the increase in vertical stress on the reinforcement plane caused by the friction force on the wall.

From these results it would clearly be wise to lubricate the box front wall to minimise the influence of side friction. Also, the remaining increase in vertical stress due to the frictional force on the wall should be added to the initial vertical pressure on the reinforcement plane when calculating friction coefficients between soil and reinforcement. However, this last measure can be applied on a very approximated basis, because one does not know exactly on what percentage of the reinforcement length the increment of vertical stress caused by side friction is distributed.

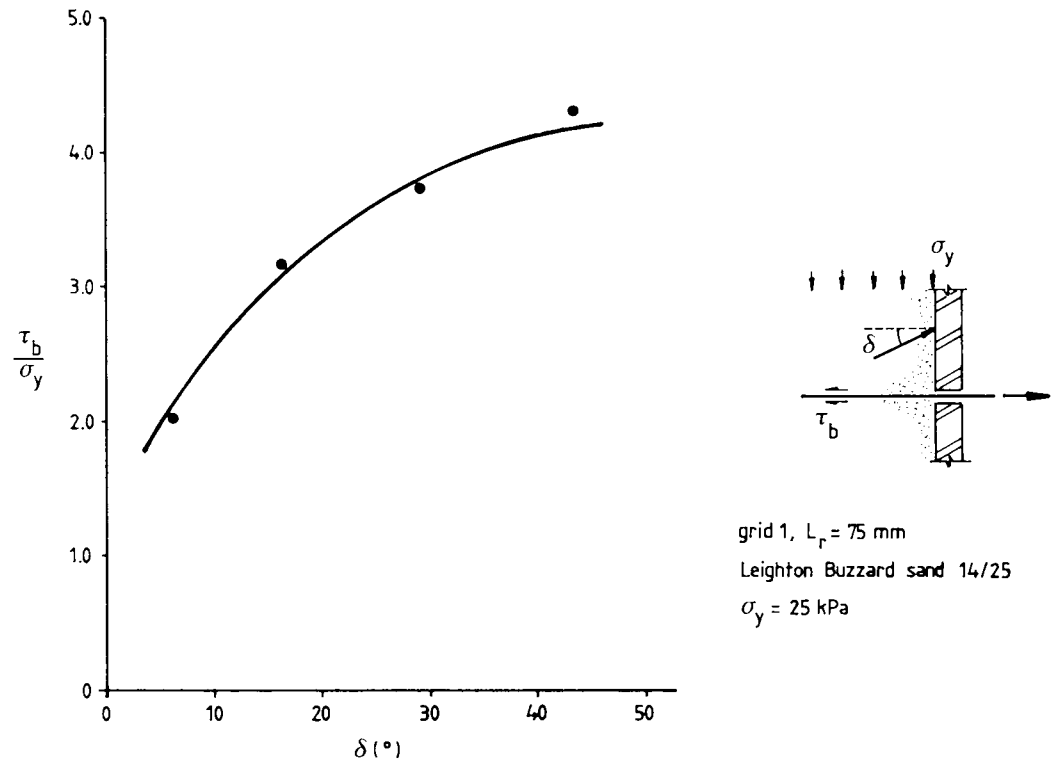


Figure 10.2 – Influence of the Roughness of the Front Wall on the Result of Pull-out Tests.

Tests with single bearing members buried in Leighton Buzzard sand 14/25 suggest that the friction on the front wall (smooth metal surface) only begins to affect the test result when the distance between the member and the wall is smaller than 15 member diameters (Palmeira & Milligan, 1987). This favours large scale tests where grids with large values of S/B can be tested. Also, because longer grid reinforcements can be used in a large scale apparatus, the influence of the wall friction may be relevant only to a small percentage of the reinforcement length and may have little significance on the total pull-out load obtained.

The alternative of having the reinforcement away from the front wall may look attractive. However, depending on the scale of the test and on the box and reinforcement geometries, a failure pattern in which failure

mechanisms develop from the reinforcement extremities towards the sample surface can occur, increasing the difficulty of analysing the test result (Hueckel & Kwasniewski - 1961 and Palmeira & Milligan - 1987). Nevertheless, grid 4 was used in two tests to check the influence of the proximity of the front wall in the large pull-out box. In the first test, a 500mm long piece of grid 4 ($S/B = 15.9$) was tested in the standard way, close to a lubricated front wall. In the second test the same length of reinforcement was tested 300mm (≈ 63 bearing members dia.) away from the lubricated front wall. The results are presented in figure 10.3 where it is shown that the proximity of the front wall had little effect on the maximum pull-out load observed. The pull-out load for the test with the reinforcement away from the boundary continuously increases with the pull-out displacement due to the fact that "fresh sand" is being failed, ahead of the grid bearing members, as the test proceeds. In these tests there was no evidence of a failure pattern coming from the reinforcement towards the sample surface, probably due to the scale of the test and the geometric characteristics of the box and reinforcement used. These results seem to confirm that the friction on a lubricated wall, in a large scale box, would affect very little the pull-out test result for grids with large S/B values.

10.3 - Influence of Soil Particle Size to Member Diameter Ratio:

The ratio between the soil particle size, here represented by the "diameter" corresponding to 50% passing (D_{50}), and the bearing member diameter (B) is likely to affect the results of pull-out test of grids. To investigate this possibility a series of pull-out tests was carried out in the medium size pull-out box, with single isolated bearing members, far away from the lubricated front wall (Palmeira & Milligan,

1987). In all tests the depth to member diameter ratio used was greater than 9 to force a deep failure mechanism. Leighton Buzzard sands 7/14, 14/25 and 25/52 were used in the tests. Figure 10.4 shows typical results of normalised bearing stress (σ_b/σ_y) versus normalised pull-out displacement (δ_p/B) for tests with Leighton Buzzard sand 14/25 and different member diameters. The bearing stress was defined as the pull-out load divided by the member bearing area (BW_r). It can be observed that σ_b/σ_y and δ_p/B at failure increase when B/D_{50} decreases.

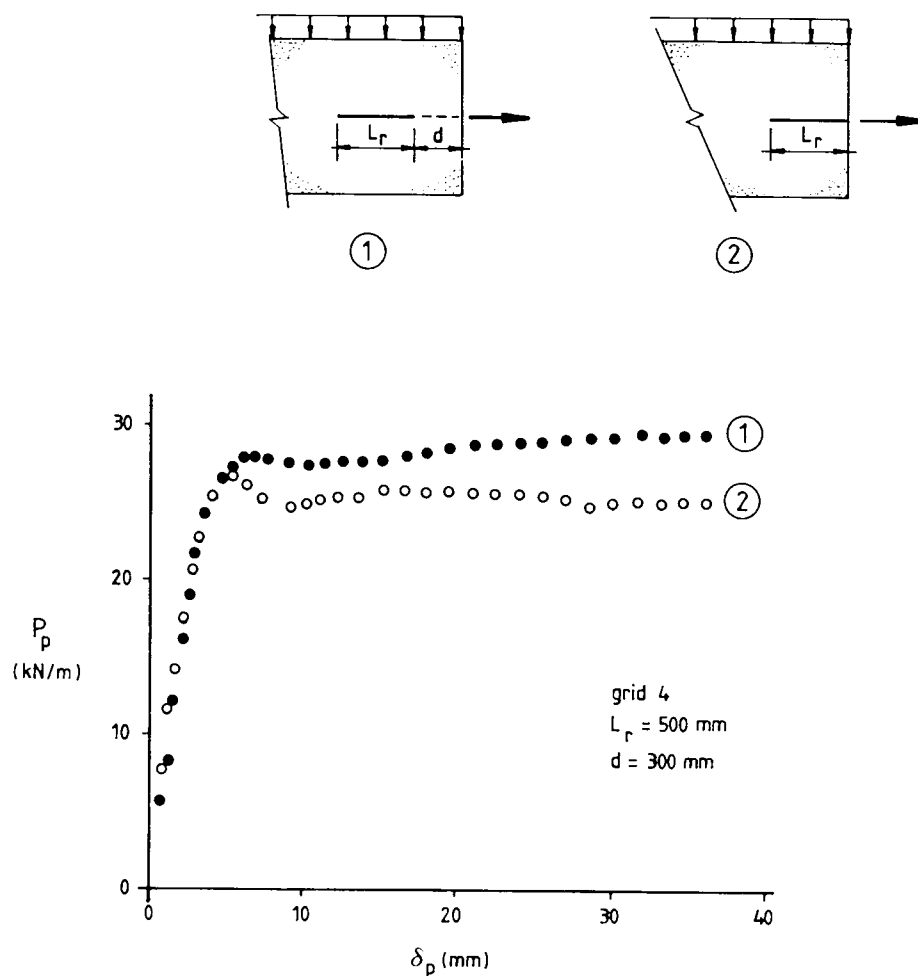


Figure 10.3 – Influence of the Proximity of the Front Wall in Pull-out Tests in the Large Pull-out Box.

Figure 10.5 shows the influence of B/D_{50} on the results of all pull-out tests with single and isolated bearing members. In this figure the ratio σ_b/σ_y was divided by the tangent of the soil friction angle because ϕ must be one of the conditioning factors influencing the test results and also because this procedure brought the results for Leighton Buzzard sands into a narrow band of variation in tests with round bars. Obviously this may not be a unique pattern for all sands since particle shape and surface characteristics must influence the pull-out resistance. That figure shows the strong effect of B/D_{50} on the value of $\sigma_b/\sigma_y \tan \phi$. The latter seems to be constant only for B/D_{50} values above 15, which agrees well with the finding by Kerisel (1972) from a similar study regarding tests with footings on photoelastic disks. It should be pointed out that the tests presented in figure 10.5 with $B/D_{50} = 24$ in Leighton Buzzard sand 14/25

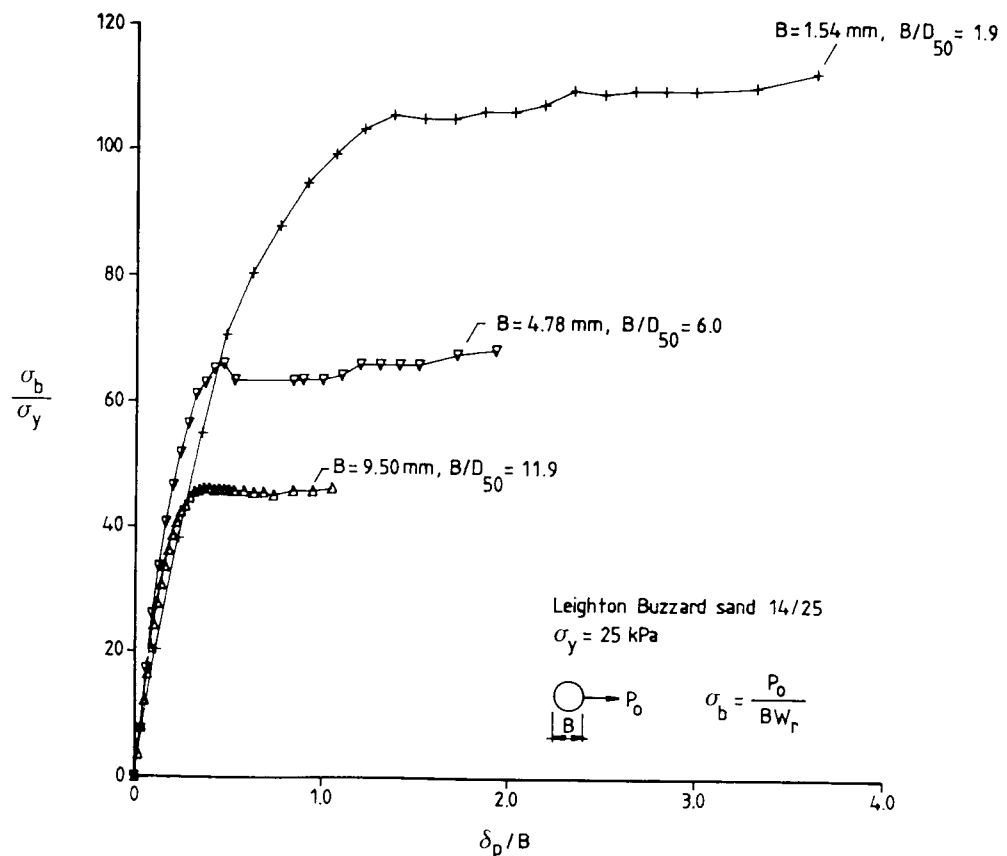


Figure 10.4 - Typical Results for Pull-out Tests of Single Isolated Bearing Members in the Medium Size Pull-out Box.

were performed in the large pull-out box, to avoid the influence of the boundaries. Figure 10.5 also shows that the use of square sections increased the pull-out resistance, although for B/D_{50} values below 5 the difference between the results obtained for round or square bearing members was very small.

Figure 10.6 shows σ_b/σ_y versus soil friction angle for the test results obtained in the present work and for data collected in the literature. The large scattering of test results shows the difficulty of trying to correlate σ_b/σ_y with ϕ only. In that figure are also presented the lower and upper limits for σ_b/σ_y suggested by Jewell et al (1984) based on the analogy to bearing capacity problems. It shows that the

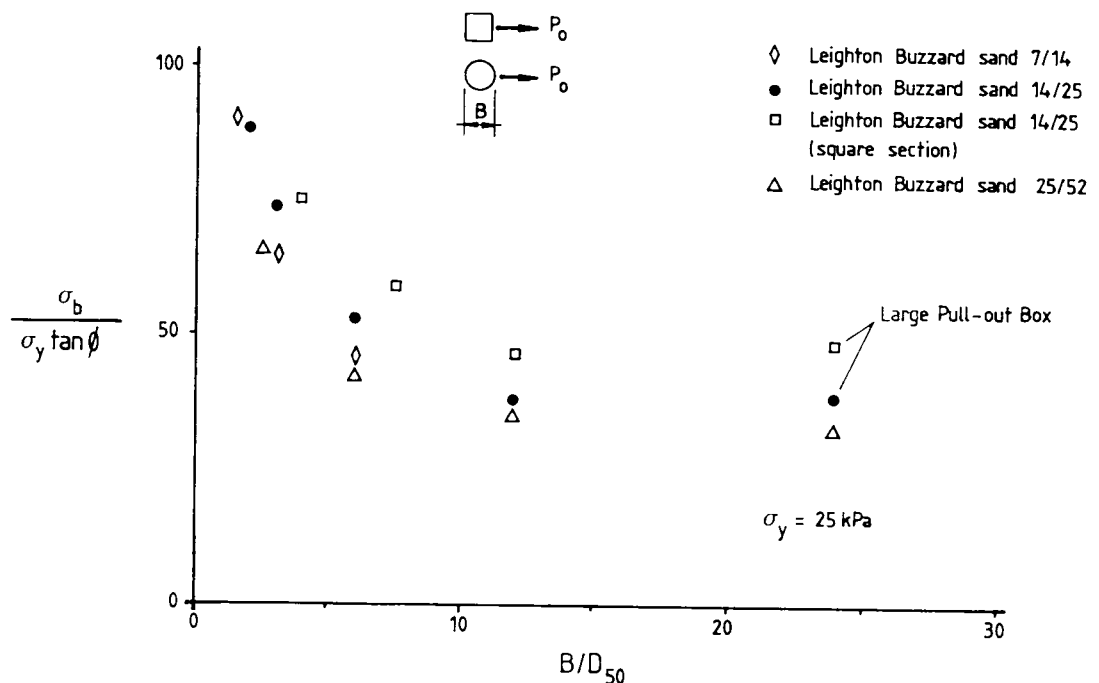


Figure 10.5 – Influence of B/D_{50} on the Result of Pull-out Tests of Single Isolated Bearing Members.

lower limit seems to be a safe estimate for σ_b/σ_y in the absence of an accurately determined value.

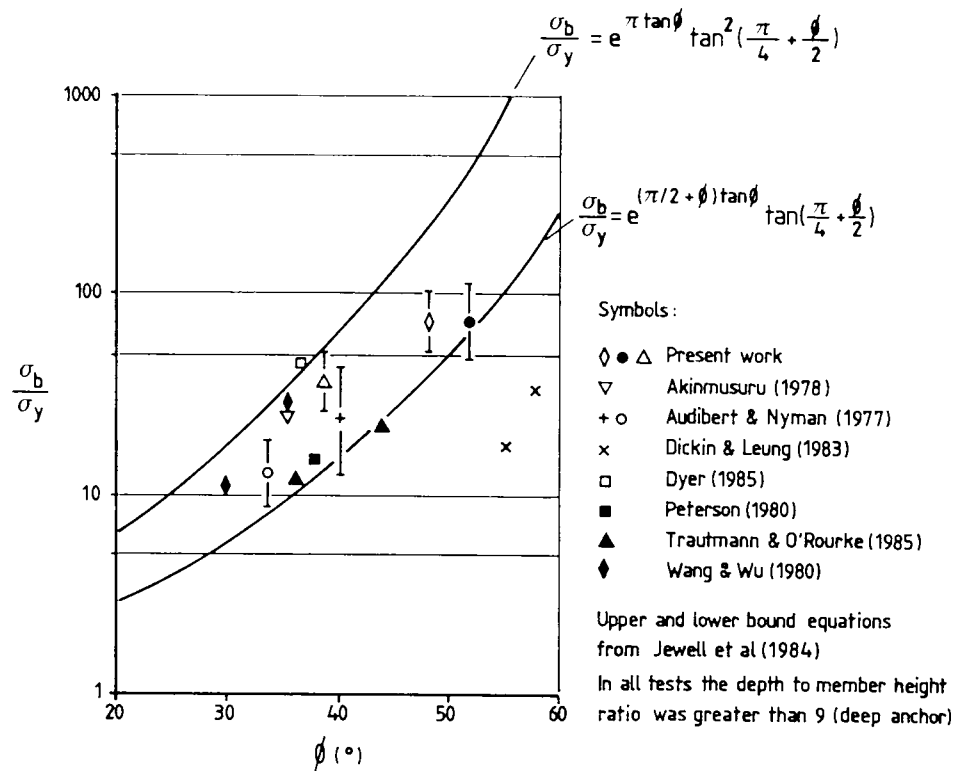


Figure 10.6 – Bearing Stress Ratio versus Soil Friction Angle.

10.4 – Interference Between Grid Bearing Members in Pull-out Tests:

The proximity of one bearing member to another affects the behaviour of the group due to interference between them. As a result, the total pull-out force for a grid with n bearing members will always be smaller than or equal to n times the force that each bearing member would develop if tested in isolation. Figure 10.7 emphasises this point by showing the results of pull-out tests with two bearing members, buried in Leighton Buzzard sand 14/25, with varying spacing between them. As the spacing between the two members increases the overall pull-out load also increases, owing to the decreasing degree of interference between members. This is due to the fact that each bearing member loosens the sand mass behind it and increases the stress in front, affecting the

behaviour of neighbouring members. Additional test results are presented in Appendix A4.

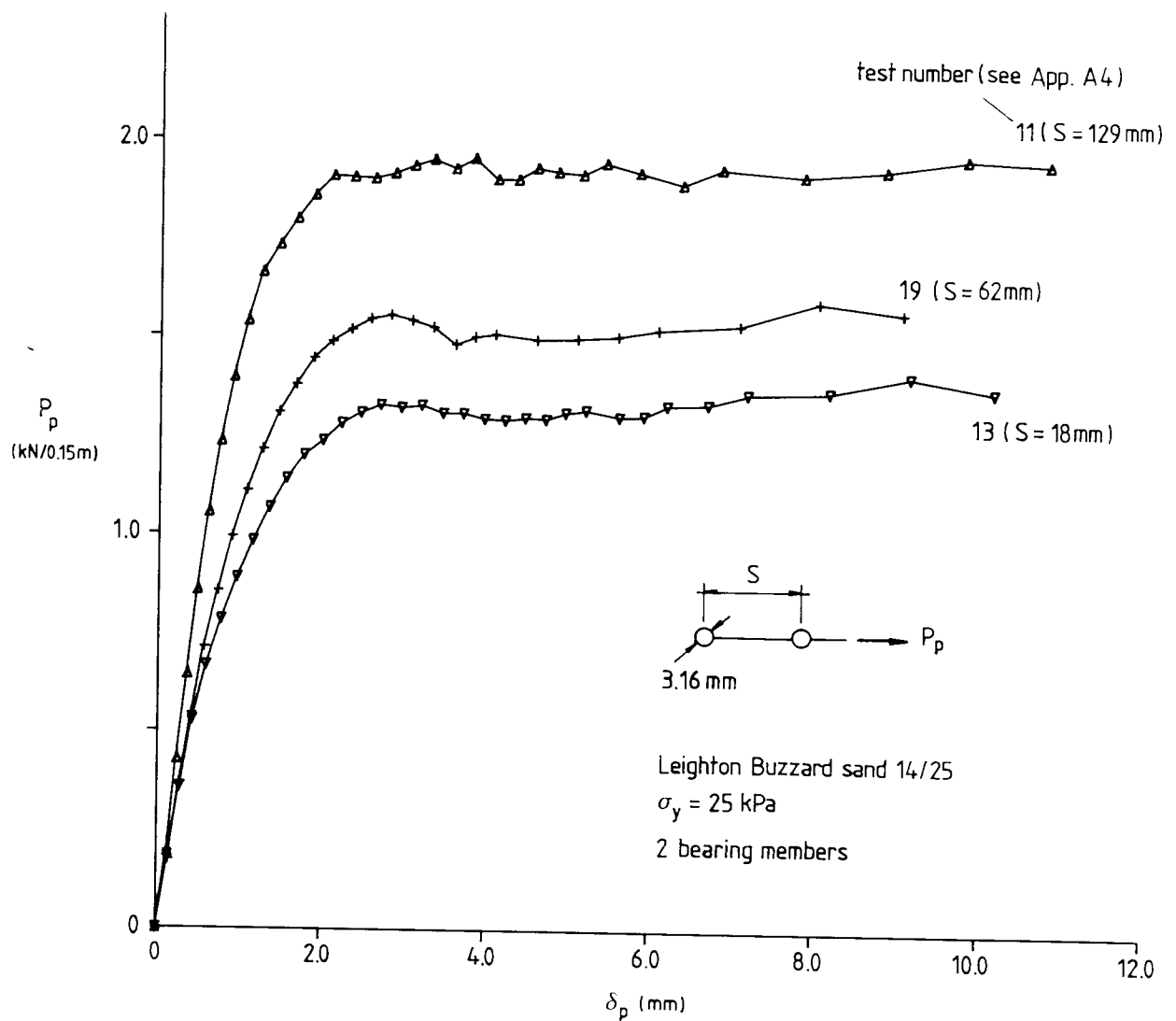


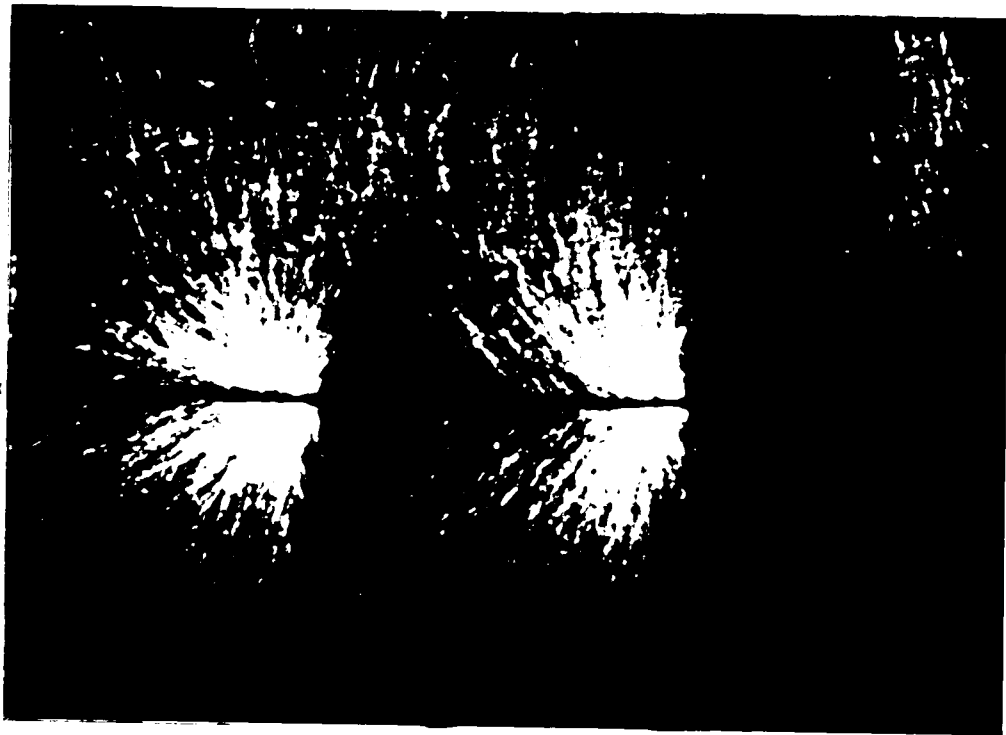
Figure 10.7 – Influence of Interference Between Two Bearing Members in Pull-out Tests in the Medium Pull-out Box.

Photoelastic studies conducted by Dyer (1985), at Oxford, have already shown the effect of interference between bearing members. In figures 10.8 and 10.9 some of his findings are presented. The light stripes in these figures can be considered as approximately the trajectories of maximum principal compressive stress and their brightness

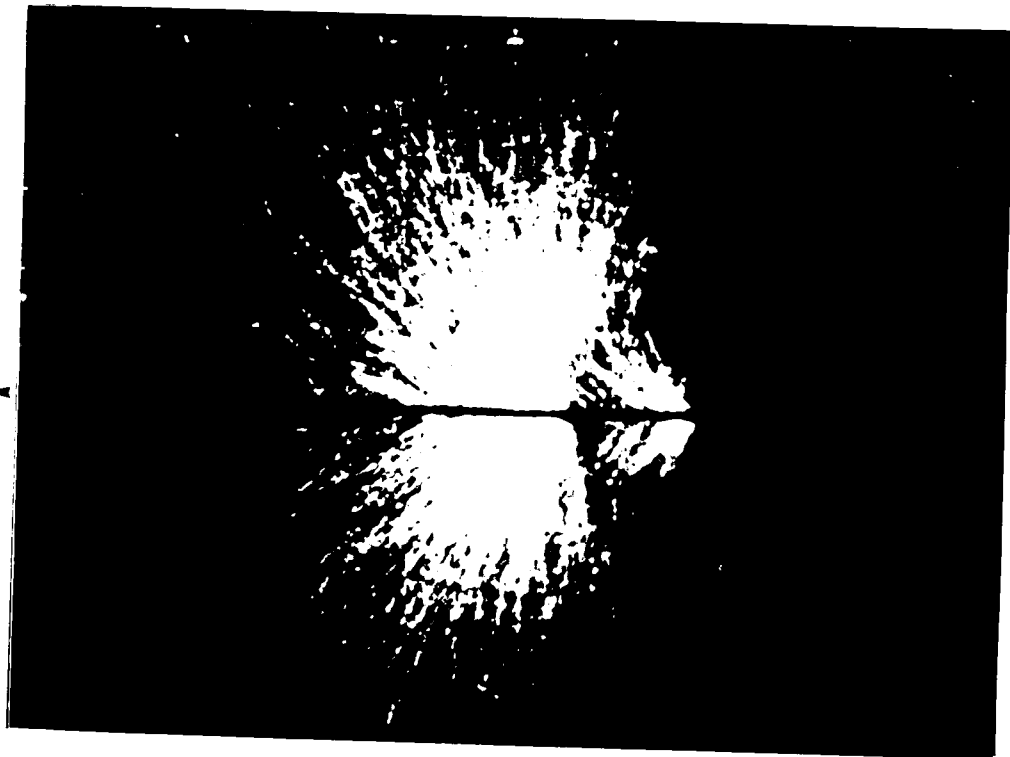
is a function of the stress magnitude. Figure 10.8a shows the stress field for two bearing members widely spaced in a pull-out test, at maximum load. Because of the large spacing between them, they behave as two isolated members, each one carrying approximately one half of the total pull-out load. As the spacing decreases there is a visible imbalance of load carried by each bearing member with the second member contributing less to the total pull-out force, as indicated in figure 10.8b. Figure 10.9 shows the stress field for a longer grid. In this case it is easy to see how the dark fields behind each bearing member (low stress regions) increase in size towards the last member. These zones of loose material between bearing members cause the angle between the light stripes and the grid layer also to increase towards the last member, because the chains of particles available to provide reaction against the load in the member must avoid the expanding zones of low stresses. This is summarised schematically in figure 10.10.

Figures 10.8 to 10.10 show that the equilibrium condition for each bearing member is very unstable. When the force on the bearing member reaches the maximum value borne by the surrounding chain of particles, the failure process that follows is catastrophic due to a new condition where only the loose mass of soil, ahead of the bearing member, is left to react against the bearing pressure. As this process continues, there is a decrease in overall pull-out force, leading to the usual peaky shape of the pull-out force versus pull-out displacement curve obtained in pull-out tests of grids with low values of S/B in dense sands.

To study the interference between bearing members in a grid and how it affects the maximum pull-out load observed, a series of tests was conducted in the medium size and in the large boxes. A total of 56 tests



(a) $B = 1.63 \text{ mm.}$, $S/B = 30.7$



(b) $B = 1.63 \text{ mm.}$, $S/B = 7.7$

Figure 10.8 - Photoelastic Results for Pull-out Tests with 2 Bearing Members (After Dyer, 1985).

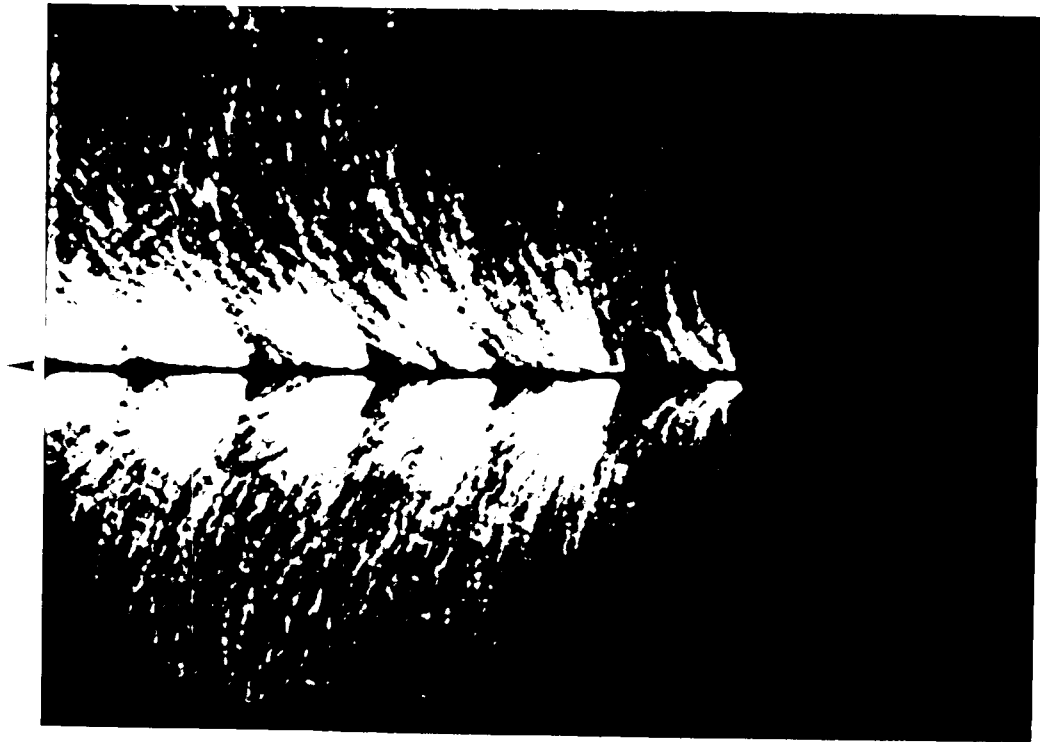


Figure 10.9 – Photoelastic Result for a Pull-out Test with Grid 1 (After Dyer, 1985).

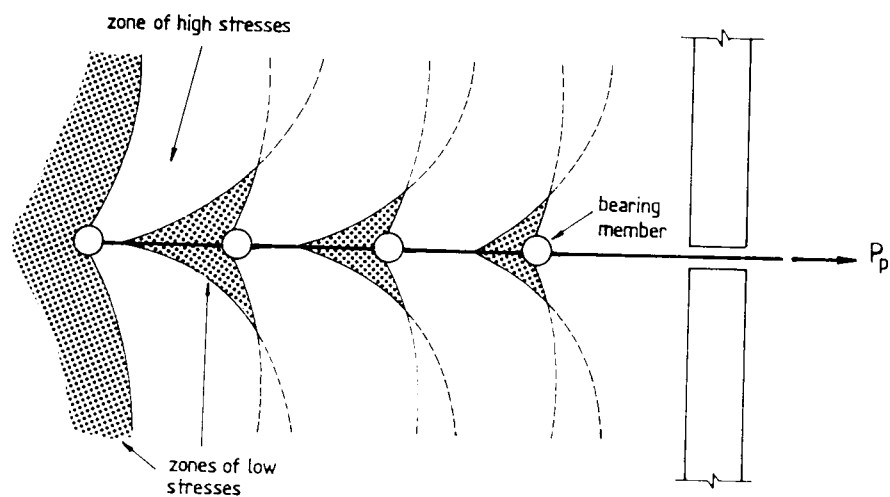


Figure 10.10 – Effect of Interference Between Bearing Members in Pull-out Tests of Grids.

were performed in the medium size box, using different Leighton Buzzard sands (see Chapter 8) and grids with few bearing members to minimise

boundary effects. The large pull-out box was used for tests with Leighton Buzzard 14/25 and grids with greater number of bearing members. A vertical pressure of 25 kPa was used in all tests. Figure 10.7 presented some typical results obtained with the medium size box. Additional tests results are presented in Appendix A4. More details of these results can be found in Palmeira & Milligan (1987).

Figure 10.11 shows pull-out load versus pull-out displacement for tests with grids buried in Leighton Buzzard sand 14/25 performed in the large pull-out box. One can observe the peaky behaviour presented by grids with low S/B values (grid 1) and how the softening decreases as S/B increases. For the grid geometries used, a value of S/B of about 16 seems to be the boundary between a brittle and a ductile behaviour. However, this value may not be only a function of S/B, but also a function of the reinforcement length. This behaviour simply demonstrates the mechanism of interference and failure in grids described in figure 10.10. Note that for grid 2, which is shorter and as a consequence has fewer bearing members, a continuous drop in pull-out load is observed. This drop is accentuated when δ_p approaches S ($\approx 19\text{mm}$) because then each bearing member is surrounded by loose sand.

A simple way to try to quantify the intensity of interference between bearing members in a grid would be to compare the pull-out load for an ordinary grid to the load that would be presented by its equivalent ideal grid. The equivalent ideal grid would have the same geometry as the ordinary one but would not be affected by interference between members. The pull-out load for the ideal grid would be the number of bearing members in the grid times the pull-out load developed by one

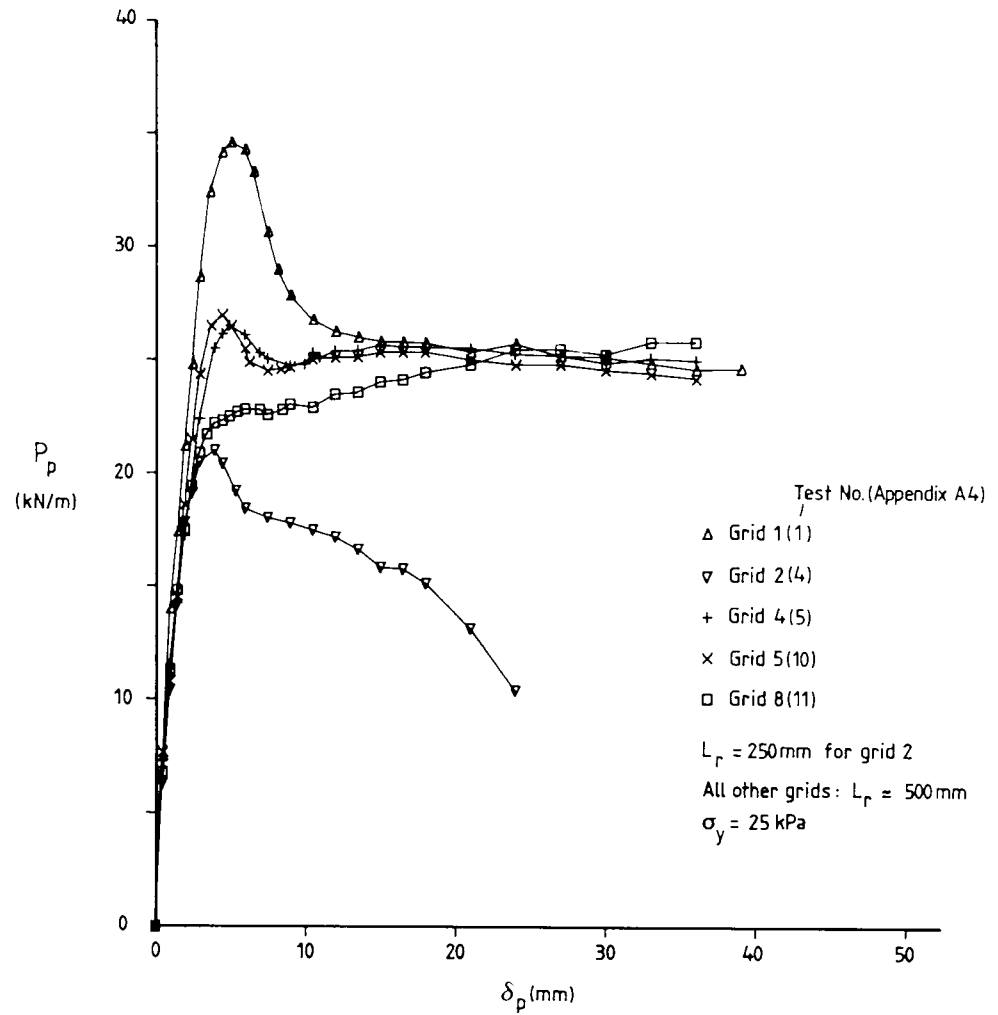


Figure 10.11 – Pull-out Test Results for Metal Grids in the Large Pull-out Box.

bearing member, under the same circumstances, when tested in isolation. Therefore a Degree of Interference could be defined as:

$$DI = 1 - \frac{P_p}{nP_o} \quad [10.1]$$

where:

DI – Degree of Interference;

- P_p - Maximum pull-out load obtained for a grid with n bearing members;
- P_o - Maximum pull-out load for a single isolated member of the grid;
- n - Number of bearing members.

Data from figures 10.4, 10.7, 10.11 and the data in Appendix A4 can be used in expression 10.1 to obtain the results presented in figure 10.12. In this figure the variation of DI with S/B is shown. Two important conclusions can be taken from this figure. First, it seems that interference between bearing members is negligible only for values of S/B above 50. Second, the degree of interference is dependent not only on S/B but also on the number of bearing members in the grid (n). For the same sand or sands with similar characteristics, the interference must increase with B and n and decrease with S . Therefore,

$$DI = f\left(\frac{nB}{S}\right) \quad \text{or} \quad DI = f\left(\frac{L_r B}{S^2}\right) \quad [10.2]$$

If the test data is then plotted in terms of DI versus $L_r B/S^2$, the result is shown in figure 10.13. Data collected from the literature is also presented in this figure. A very definite trend is observed if one takes into account the range of grids, sands and test conditions displayed in figure 10.13. Note that even the tests with varying boundary conditions using grid 1, despite the larger scatter, obey the general trend. This is encouraging in the sense that expression 10.2 seems to provide a simple but powerful way to unify pull-out test of grids into a single pattern of variation.

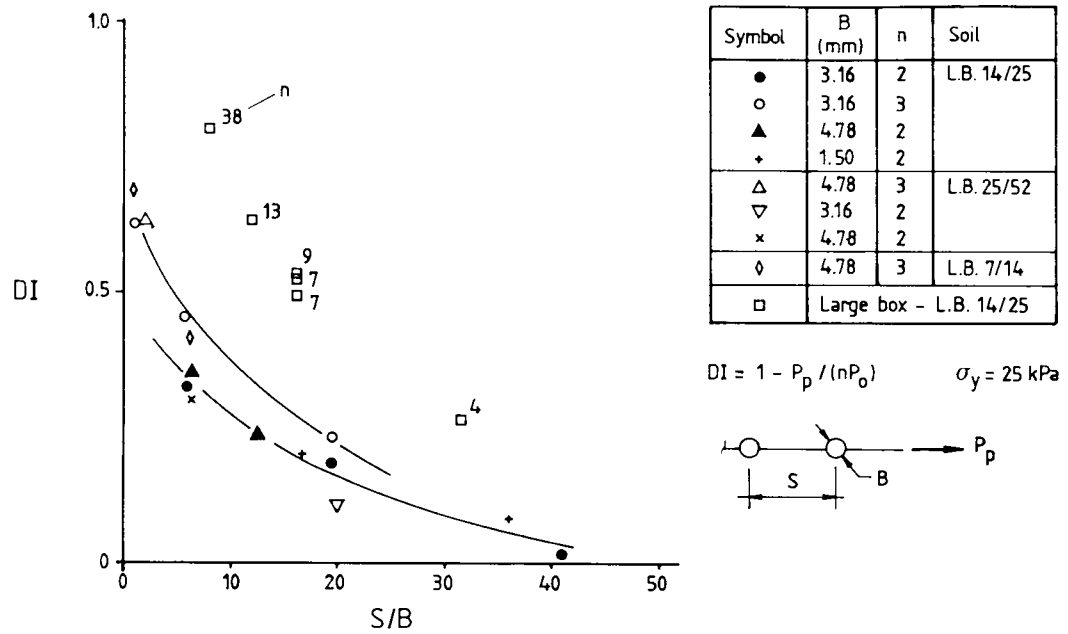


Figure 10.12 – Degree of Interference versus S/B.

Note that expression 10.2 does not take into account B/D_{50} , which must influence DI either when smaller than one or when very large. It should also be noted that the results from Jewell (1980) and Dyer (1985) presented in figure 10.13 refer to tests with B/D_{50} equal or smaller than one and some deviations from the main trend may be noticed. At the other extreme, Basset (1978) reported tests with underreamed anchors (disks) in London clay where interference between underreams was small only for S/B values greater than 4.

Deviations from the trend shown in figure 10.13 must also occur when S/B tends towards 1. In this case tangency between bearing members will take place and a more frictional mechanism will prevail, making the definition of DI by expression 10.1 not appropriate. The same comment applies to extensible reinforcements or long ones where a small length of the reinforcement, close to the leading end, may be the only part of the reinforcement length affected by the pull-out load.

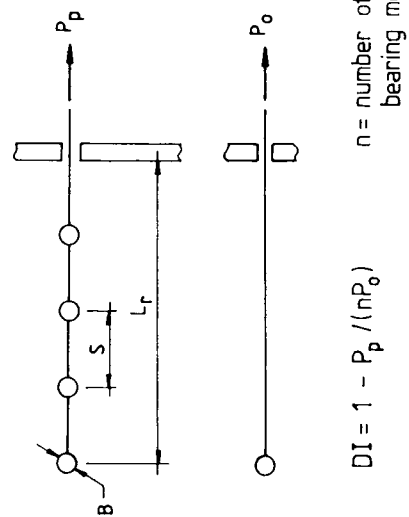
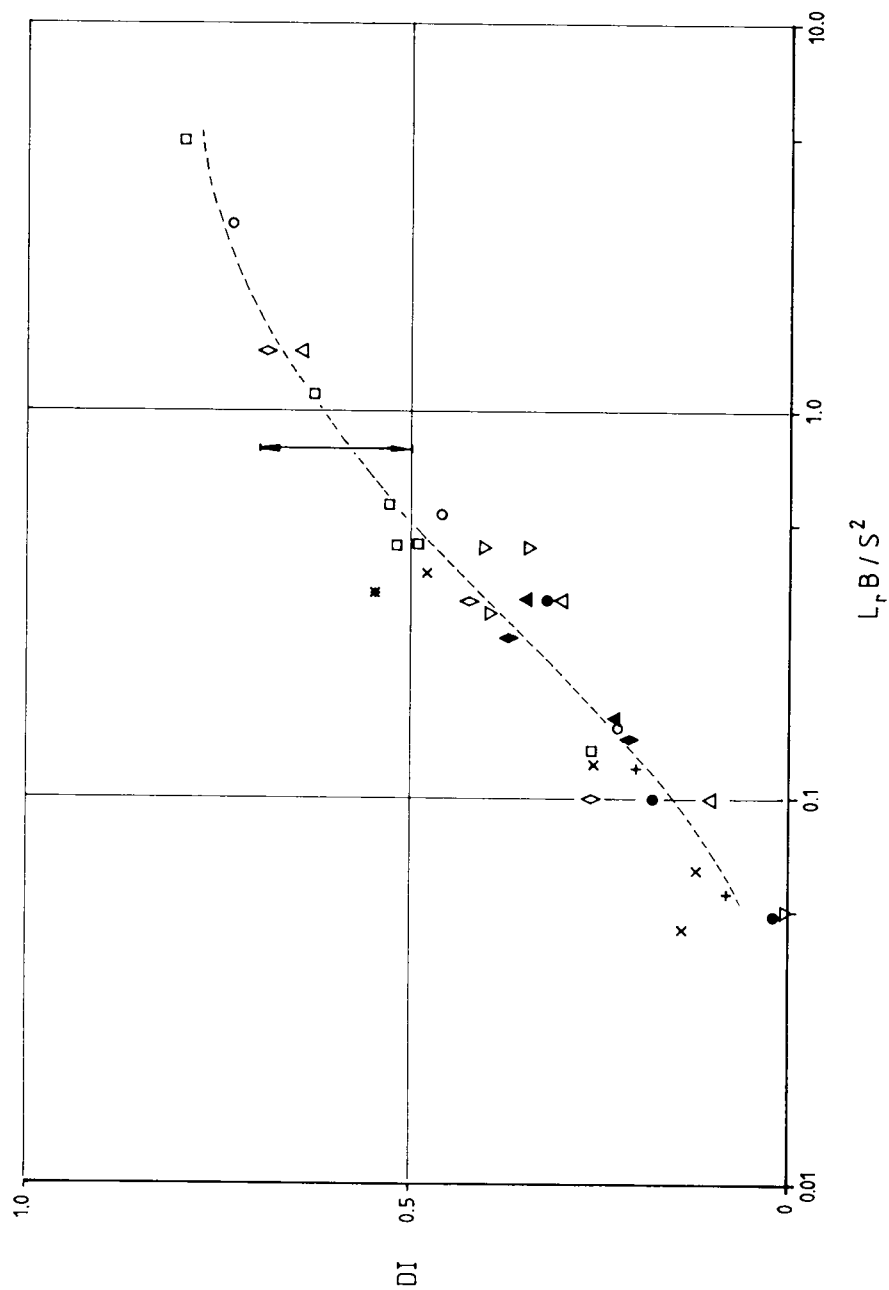


Figure 10.13 – Degree of Interference as a Function of the Grid Geometry.

Bearing in mind the obvious limitations of the theory of Elasticity to the present problem, it is interesting to note that the same pattern of variation shown in figure 10.13 can be obtained for the elastic analysis of underreamed anchors. From data presented in Rowe & Booker (1980) one can obtain the result presented in figure 10.14. In this figure, the elastic variation of DI versus $L_r B/S^2$ is presented for a series of deep underreamed square anchors. Because in this case it is an elastic analysis, DI was calculated comparing force values that would cause the same elastic displacement for a single anchor (P_o) and for a series of anchors (P_p). It is interesting to note that the values are obviously different but the trend of variation is very much the same, despite the limitations of the analysis and the shape of the anchors. Also, if the elastic curve in figure 10.14 were to be translated to the region of data points in figure 10.3 one would observe that it would fit the experimental data remarkably well.

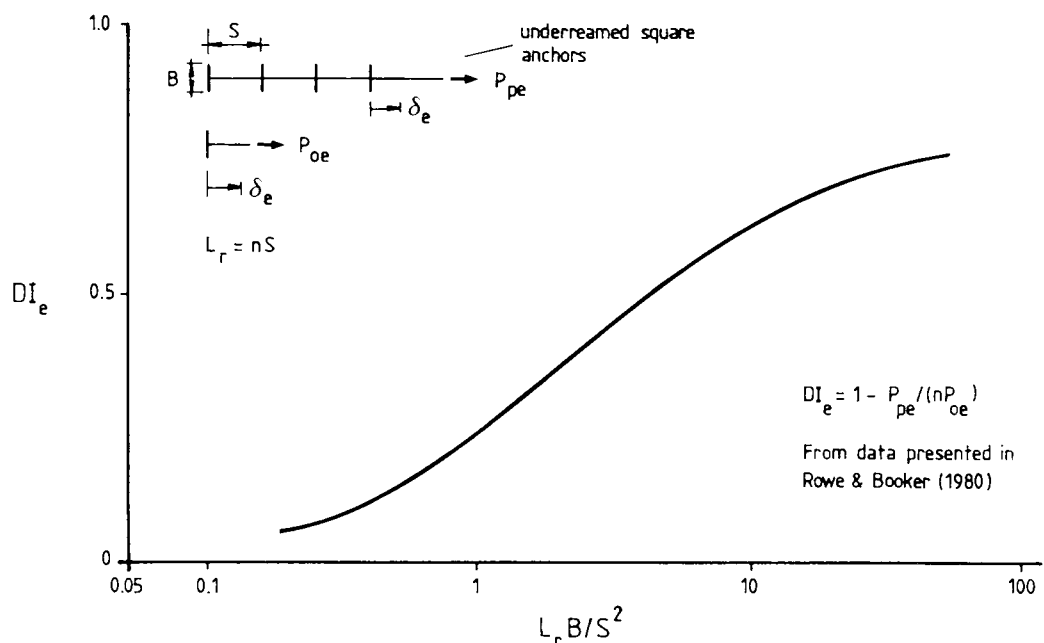


Figure 10.14 - Elastic Results for Underreamed Square Anchors (After Rowe & Booker, 1980).

From the above discussion it can easily be demonstrated that the bond coefficient f_b between soil and reinforcement, taking into account interference between grid members, is given by the following expression:

$$f_b = \frac{\tan \delta}{\tan \phi} = \frac{(1 - DI)}{2} \frac{B}{S} \frac{\sigma_b}{\sigma_y \tan \phi} \quad [10.3]$$

where:

- f_b - Bond coefficient between grid and soil;
- δ - Equivalent friction angle between grid and soil ($\tan^{-1} \tau_b / \sigma_y$);
- ϕ - Soil friction angle;
- DI - Degree of interference for the soil and grid used;
- B, S - Bearing member diameter and spacing between bearing members;
- σ_b - Maximum bearing stress for a single isolated bearing member of the grid buried in the same soil, under the same vertical pressure;
- σ_y - vertical pressure.

10.5 - Comparison Between Performances of Different Reinforcements Under Pull-out Conditions:

Figure 10.15 presents normalised bond stress (or bond coefficient, f_b) versus pull-out displacement (δ_p) for tests in the large pull-out box with different reinforcements buried in Leighton Buzzard sand 14/25. The result for the "perfectly rough sheet" is presented for comparison. All

tests were performed under 25 kPa vertical pressure and the following conclusions can be drawn:

1. The stiffer the reinforcement the stiffer the response to the pull-out load is and the smaller is the pull-out displacement required to achieve maximum bond;
2. The bond coefficient and the form of its variation with δ_p for grids is a function of their geometry and degree of interference between bearing members, as discussed in the previous item;
3. For the stress level used there was no significant difference, in terms of stiffness, between the Stabilenka geotextile and Netlon SR2. However, the more extensible geotextile Geolon 70 required a much greater pull-out displacement to mobilise its full bond strength. The similar behaviour, in terms of stiffness, between Netlon SR2 and Stabilenka 400 may have been coincidental due to the different mechanism of interaction in each case (frictional for the geotextile and a mixture of friction and bearing for the polymer grid);
4. The Stabilenka 400 geotextile presented a fairly constant maximum bond coefficient but for the stress level used in these tests the bond coefficient for the polymer grid was considerably greater;
5. The fact that the rough sheet (same sand glued to a metal sheet) presented bond coefficient slightly greater than one can be attributed to the difficulty in making a uniform flat rough surface of such dimensions. Note that the $f_b \times \delta_p$ curve for grid 1 ($S/B = 7.7$) is very similar to the one for the rough sheet; this confirms that the mechanism of interaction is essentially frictional for small S/B values. The similarity in the

performances of grids 4 and 5 is likely to be due to both having the same length and similar values of S/B and B/D_{50} ;

6. For extensible reinforcements a process of progressive failure was probably developed along the reinforcement length due to different degrees of mobilisation of bond stresses between soil and reinforcement, as discussed in Milligan & Palmeira (1987).

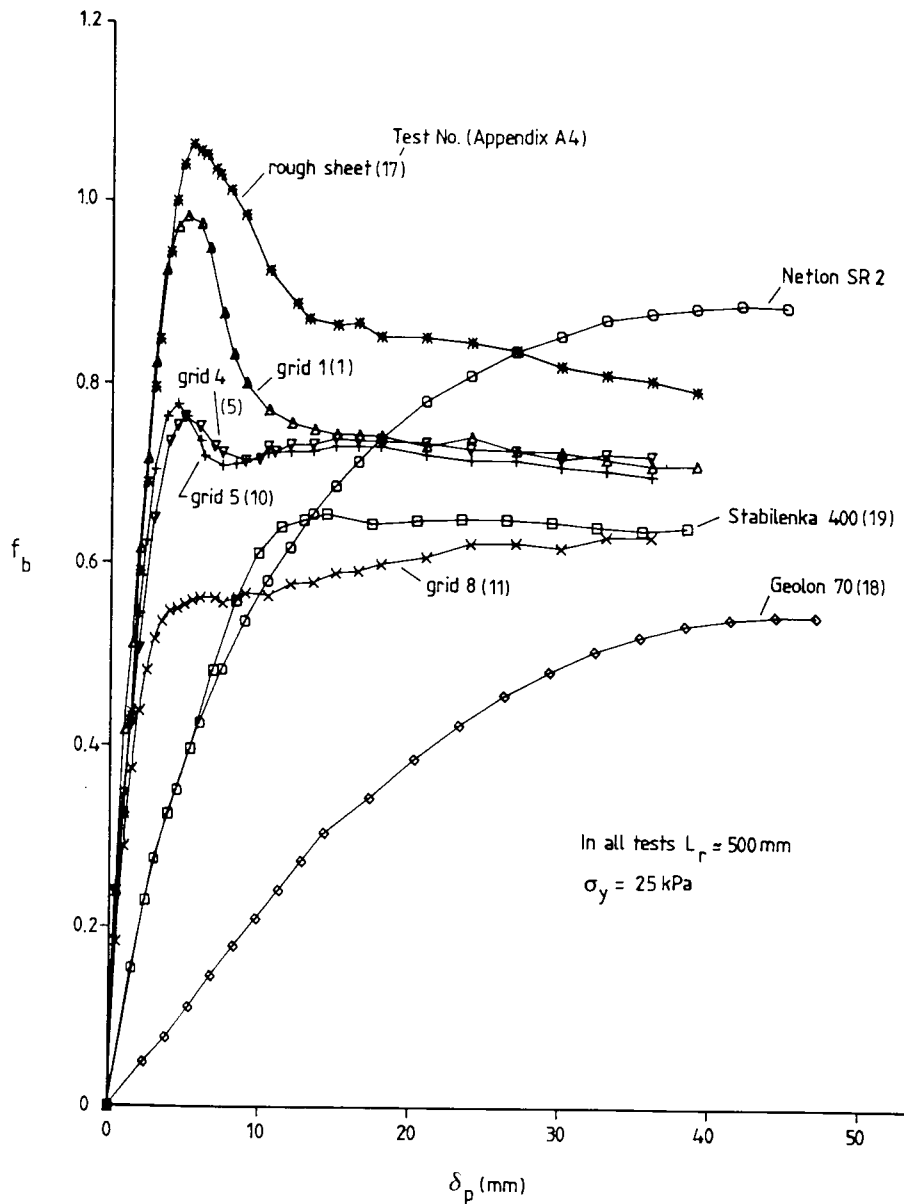
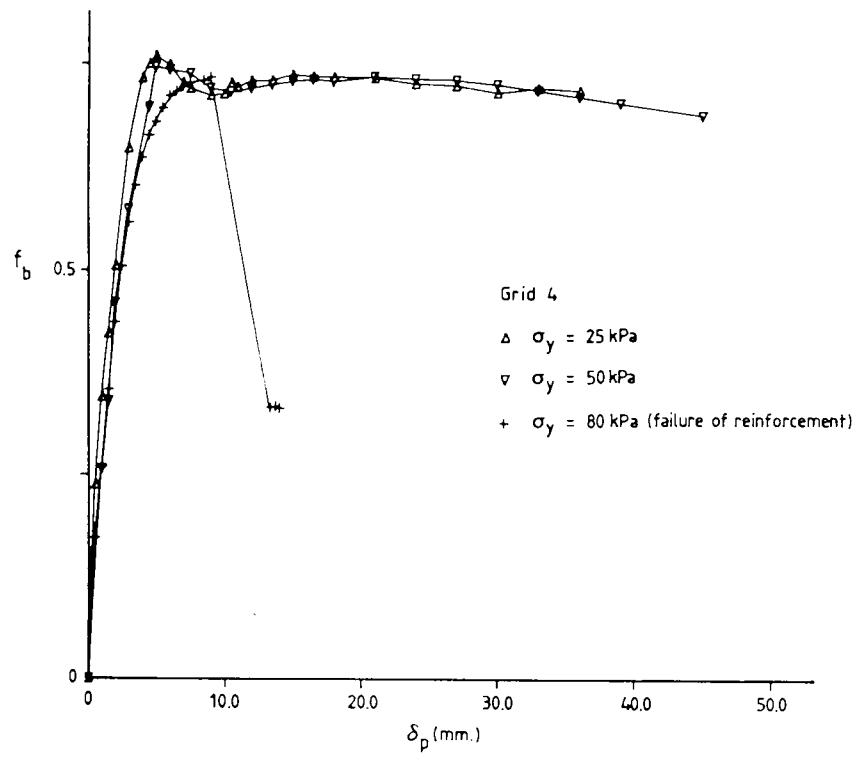


Figure 10.15 – Pull-out Test Results for Different Reinforcements in the Large Pull-out Box.

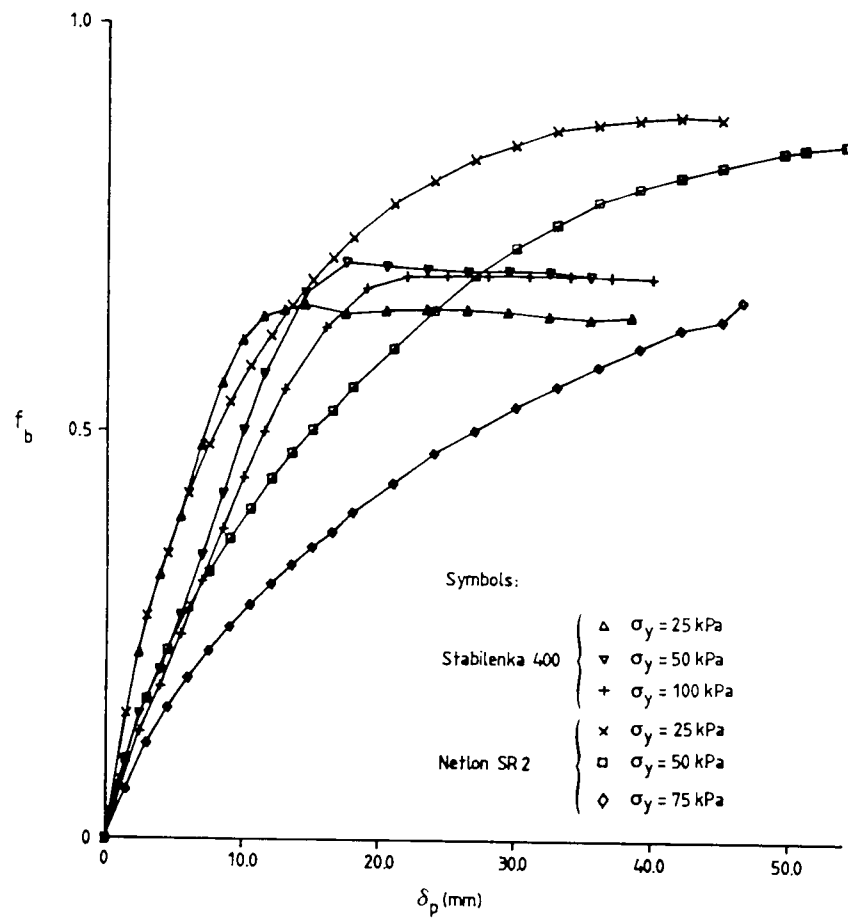
It should be pointed out that the results of tests with geotextiles presented in this work were corrected for the initial "stretching phase" of the reinforcement, which would result in a "S shape" load x displacement curve because of the negligible pull-out forces recorded during this stretching phase. In these cases, the new origin for δ_p was obtained by prolonging the almost linear part of the load versus displacement curve, in the "elastic phase" of the test, until it reached the axis of pull-out displacements.

Figure 10.16 a and b shows the variation of bond coefficient versus pull-out displacement obtained in tests in the large pull-out box for a wider range of vertical pressures. Since a constant reinforcement length was adopted the maximum vertical pressure used was limited by the tensile strength of the reinforcement material. Figure 10.16a shows that the result for metal grid 4, in terms of bond strength and stiffness, was little affected by the varying stress level. The same applies to the stiff Stabilenka 400 geotextile in figure 10.16b. However, the polymer grid Netlon SR2 showed increasing extensibility as the stress level increased. For the length of reinforcement used (522mm) and vertical stresses above 75 kPa the tensile failure of the polymer grid would occur before bond failure with the surrounding soil.

In the pull-out tests with reinforcements that have a purely frictional mechanism of interaction with the sand mass, such as the geotextiles and rough sheet tested, a band of loose sand was observed, about 10mm thick, above and below the reinforcement layer at the end of the test. This was also observed in the tests with grid 1.



(a) Metal Grid 4.



(b) Plastic Reinforcements.

Figure 10.16 - Influence of Stress Level on the Bond Coefficient.

Standard interface tests were also carried out using the small shear box (see Chapter 2) with Leighton Buzzard sand 14/25 and Stabilenka and Geolon 70 geotextiles. These tests were performed following the usual procedure of having the sand on the top half of the box with the reinforcement fixed to the lower part and lying on a rigid plate. The results of bond coefficient obtained (f_b) at 25 kPa vertical pressure were 0.62 and 0.67 for Geolon 70 and Stabilenka 400, respectively. In the large pull-out box these results were 0.56 and 0.69, respectively. The results for Stabilenka compare very well but the result obtained for Geolon in the large pull-out box was slightly smaller. This is believed to have been caused by the greater influence of stiffness and progressive failure in tests with longer lengths of that reinforcement in the large pull-out box.

10.6 - Stress, Strains and Displacements Distributions in Pull-out Tests:

10.6.1 - Stresses on the Front Wall of the Large Pull-out Box:

Figures 10.17 to 10.19 show typical results for the variation of horizontal stress increments on the side wall of the box normalised by the bond stress versus pull-out displacement, during tests under 25 kPa vertical pressure. The normalised bond stress or bond coefficient versus pull-out displacement curve are also presented in these figures. It is interesting to note that in all of the cases shown in these figures, the maximum increment of horizontal stress occurred well before the maximum pull-out load had been reached.

Figure 10.17 shows the results of $\Delta\sigma_x$ versus δ_p for the test with grid 4. The behaviour of the pressure cells closest to the reinforcement

layer (cells 1 and 3) should be noted. They reached a peak value at about 1.5 mm pull-out displacement and then $\Delta\sigma_x$ began to drop. Meanwhile the cells immediately above and below (cells 2 and 6) had their results continuously increasing during the test. Cells far from the reinforcement layer were very little affected by it. This behaviour is believed to be caused by the interaction between the first bearing members of the grid and the box wall. As failure occurs for the first bearing member, this is immediately felt by the cells close to the reinforcement and the horizontal pressure on them must obviously decrease. A continuous redistribution of load to other bearing members takes place and the cells away from the reinforcement begin to experience increments of stress caused by the other bearing members of the grid, which are being overstressed and are approaching the box wall as the test proceeds. The same sort of behaviour was noted in the other tests with grid reinforcement.

Figure 10.18 shows $\Delta\sigma_x$ versus δ_p for the test with the polymer grid Netlon SR2. The same comments made in the previous paragraph apply to this case since a similar process of progressive failure, throughout the reinforcement length starting from the leading end, also takes place in this case.

Figure 10.19 presents $\Delta\sigma_x$ versus δ_p for the test with Stabilenka 400 geotextile. Again the pressure cells closest to the reinforcement have their peak value reached at the early stages of the test, which also indicates a mechanism of progressive failure along the reinforcement layer. It is interesting to note that when the maximum pull-out load was reached the readings from the cells were approximately constant thereafter, in agreement with the fairly constant overall pull-out load.

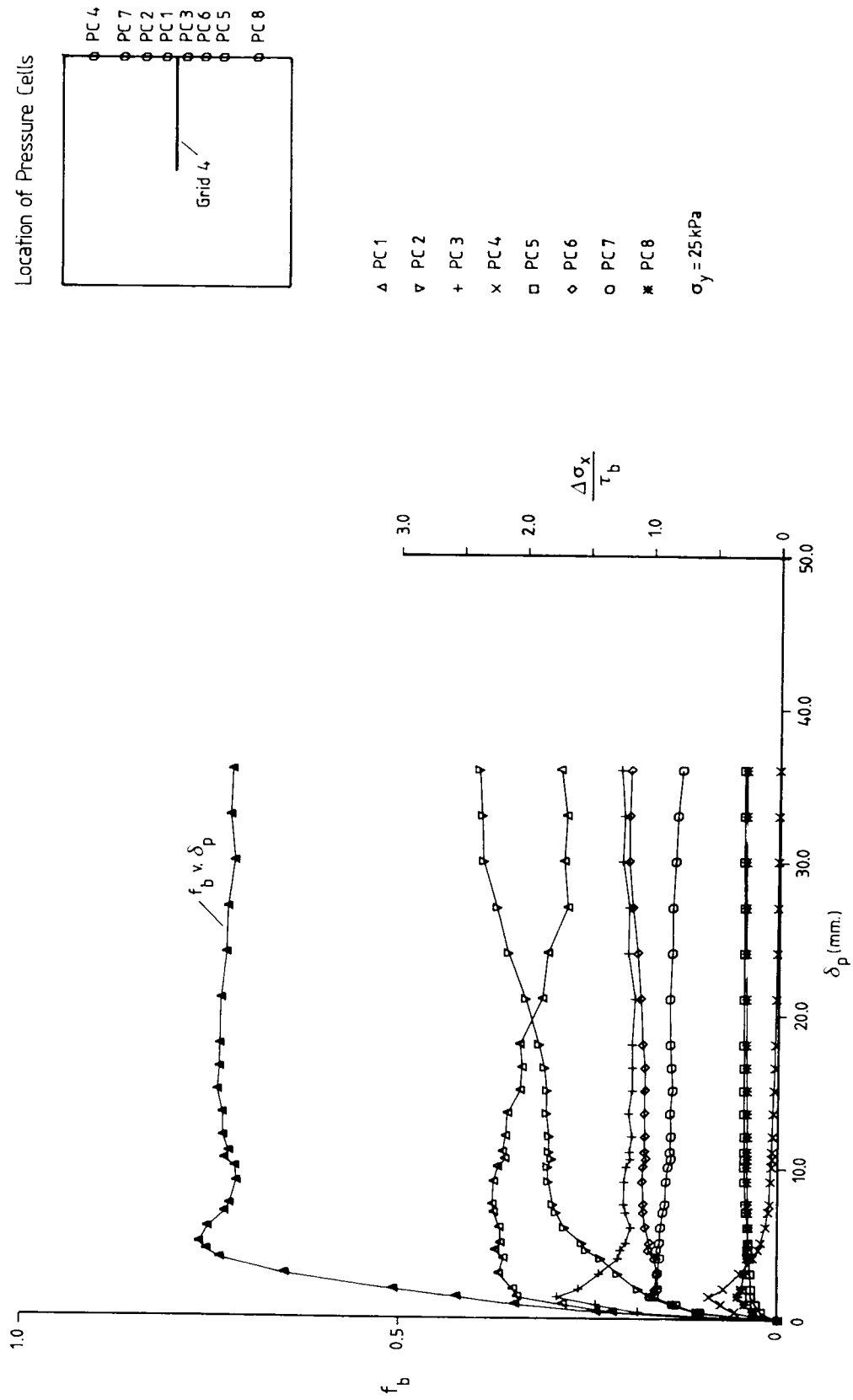


Figure 10.17 - Normalised Increments of Horizontal Stress on the Front Wall During the Test - Grid 4.

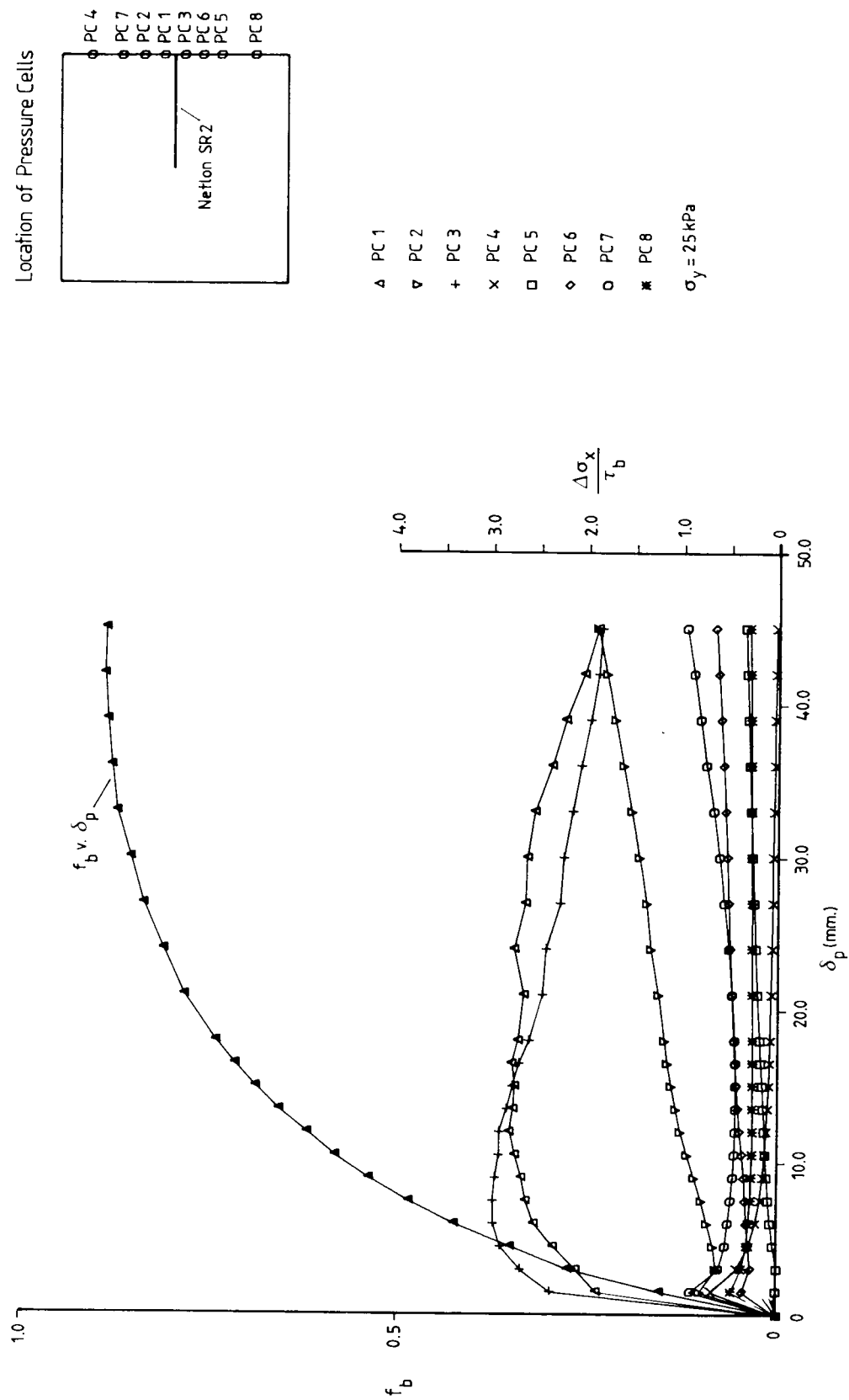


Figure 10.18 - Normalised Increments of Horizontal Stress on the Front Wall During the Test - Netlon SR2.

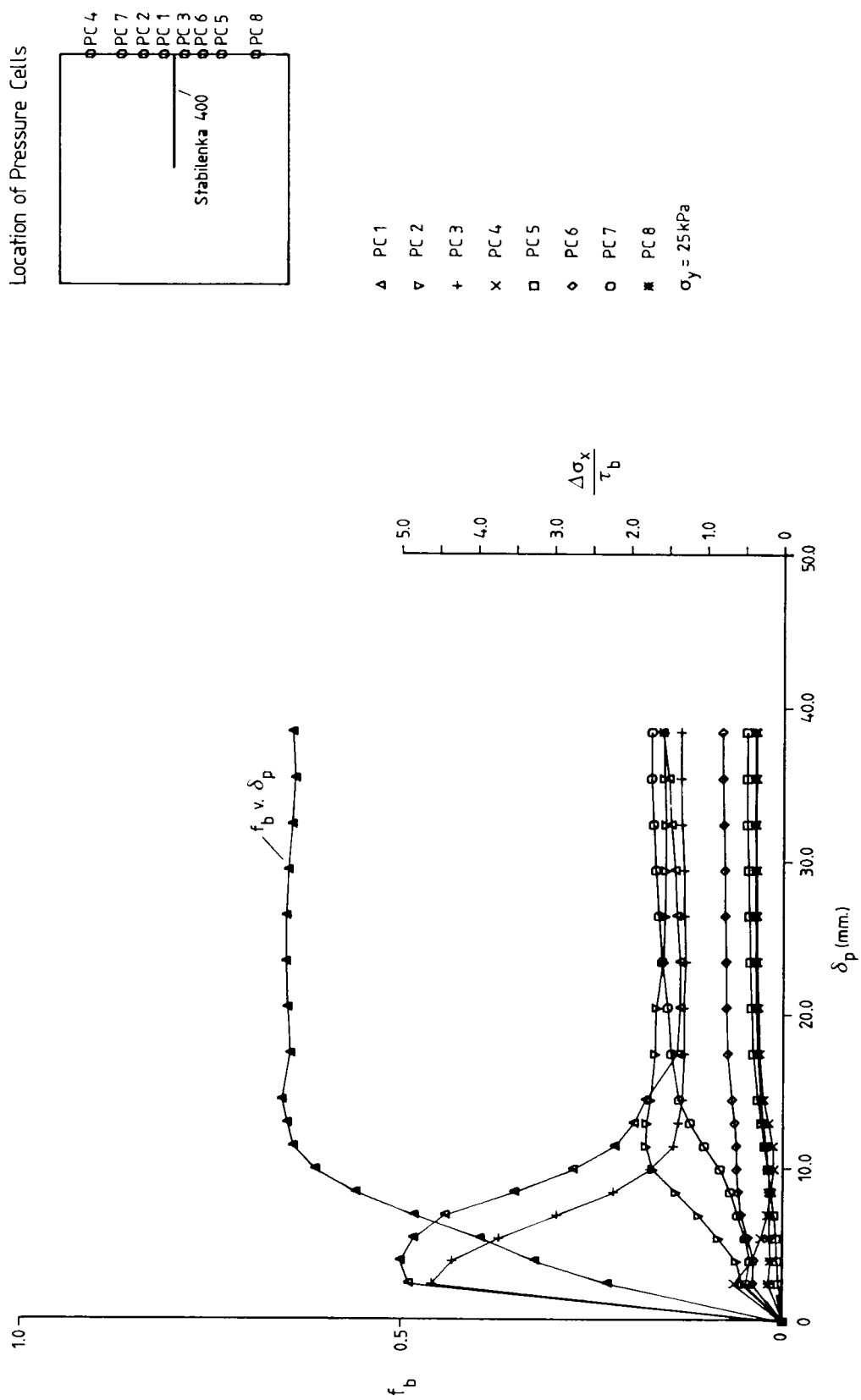
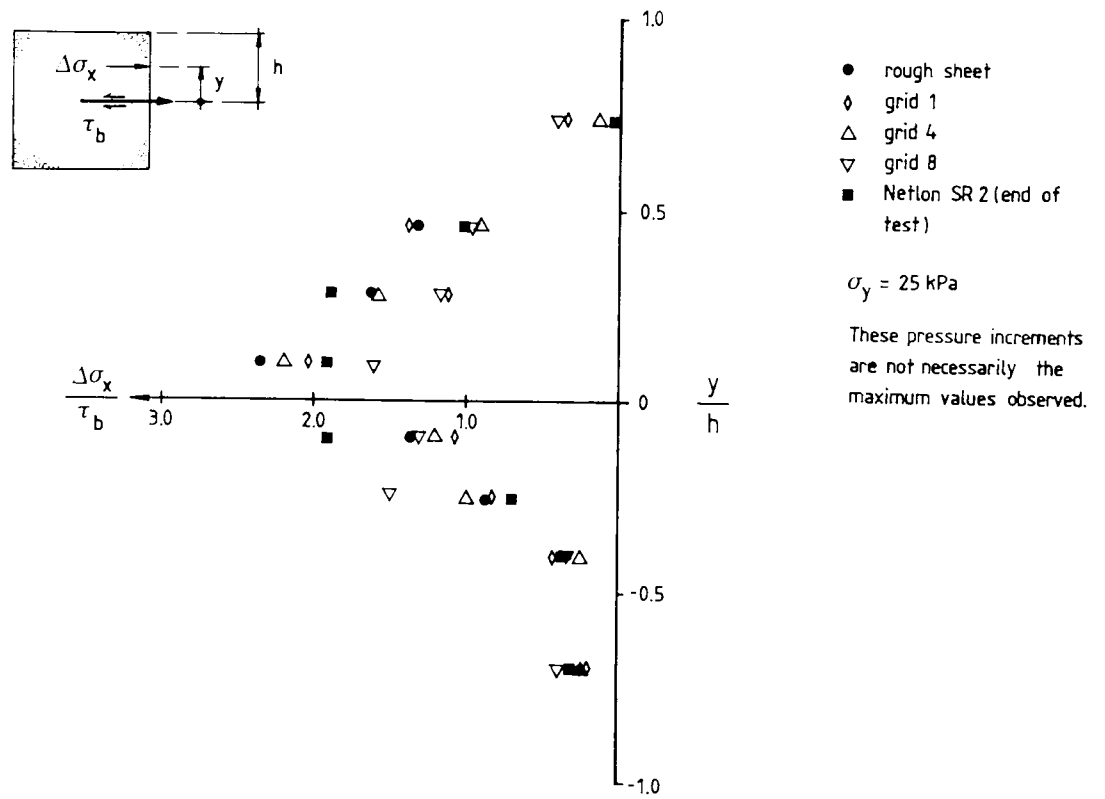


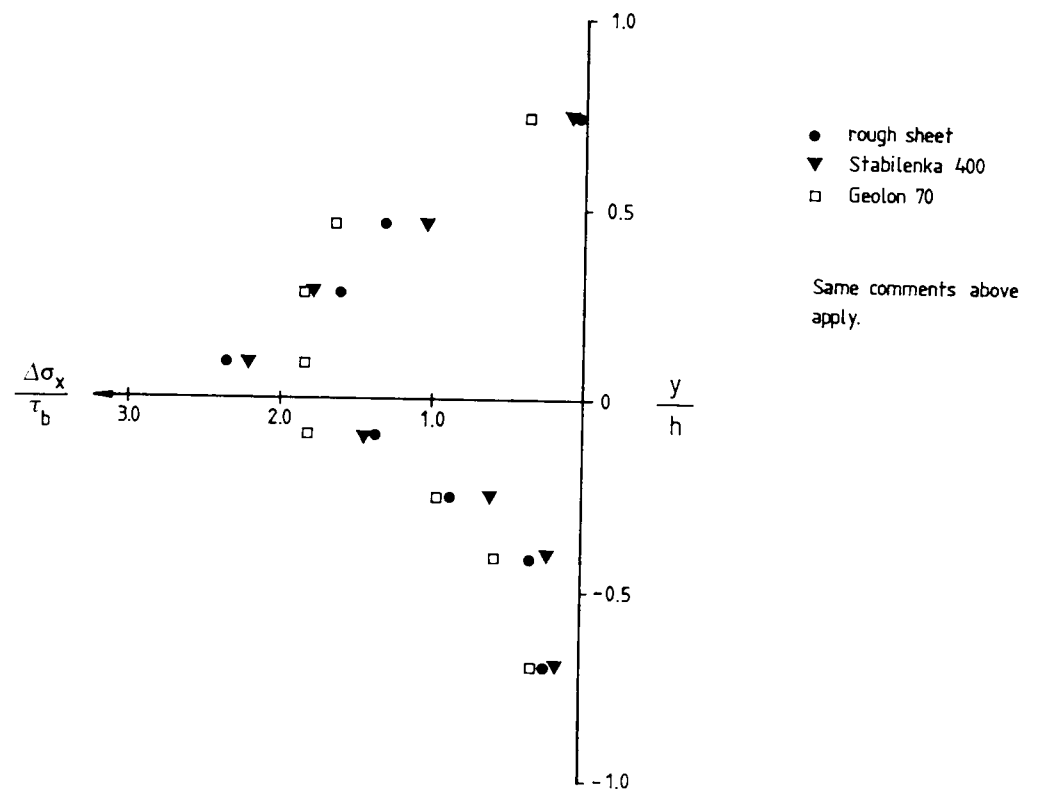
Figure 10.19 – Normalised Increments of Horizontal Stress on the Front Wall During the Test – Stabilenka 400.

The same sort of behaviour was observed in the tests with the Geolon 70 geotextile.

Figures 10.20 a and b present profiles of horizontal stress increments on the front wall normalised by the bond stress, at maximum pull-out load. The results in this figure are not necessarily the maximum pressure readings recorded by the cells, because of the progressive failure effect reported in the previous paragraphs. Figure 10.20a shows profiles of $\Delta\sigma_x$ for grid reinforcements. The results for the rough sheet are also presented for comparison. It can be seen that the grid geometry affects the profile of stress increments on the front wall. It is also interesting to note the difference between the increment distributions above and below the reinforcement layer. Schlosser & Elias (1978) reported photoelastic tests in model reinforced walls in which different states of stress on top and bottom faces of the reinforcement were observed. This difference was not obtained in the photoelastic study conducted by Dyer (1985), but it is clear that the bottom face of the front wall is less stressed than the top one, as can be seen in figure 10.9. So, the difference in horizontal stress increment distributions is likely to be due to the differences in top and bottom boundary conditions in the large pull-out box. Figure 10.20b shows the same sort of results for the purely frictional reinforcements. The same comments made above still apply but the scatter between results for different reinforcements is smaller in this case. This is likely to be due to the fact that the normalisation of horizontal stress increment by the bond stress is not an appropriate choice for grid reinforcements with large S/B values.



(a) Grid reinforcements



(b) Frictional reinforcements

Figure 10.20 – Horizontal Stress Increment Profiles on the Front Wall of the Large Pull-out Box.

10.6.2 - Strains and Displacements in the Sand Mass in Pull-out Tests in the Large Pull-out Box:

In contrast with what was observed in direct shear tests, the strains developed in the sand in pull-out tests were very small, making the procedure available for strain measurements not sufficiently accurate. This can be visualised in figure 10.21 where the principal strain distribution for the test with the rough sheet at peak pull-out load is presented. The increase in strain magnitude around the reinforcement layer can be seen but the general pattern of variation is far from clear. This fact, to a certain extent, was anticipated in particular for tests with grid reinforcements where high strain levels are concentrated around the reinforcement bearing members and for lower strain levels, away from the reinforcement, the technique used is not accurate enough.

Despite the disappointing results from the strain measurements commented above, the data from the markers can still be used to plot the field of displacements in the sand mass surrounding the reinforcement layer. Figures 10.22 a and b show contours of vertical and horizontal displacements in the sand for tests with the "perfectly rough" sheet and grid 4, at peak pull-out load. These are typical results for frictional and bearing mechanisms of soil-reinforcement interaction. As expected, the sand mass above the reinforcement layer is more affected by its presence. The size of the region affected by the reinforcement is a function of the degree of interaction between soil and reinforcement. Very small volume variations were observed in the rubber bag filled with water at the top of the sample due to the deep embedment of the

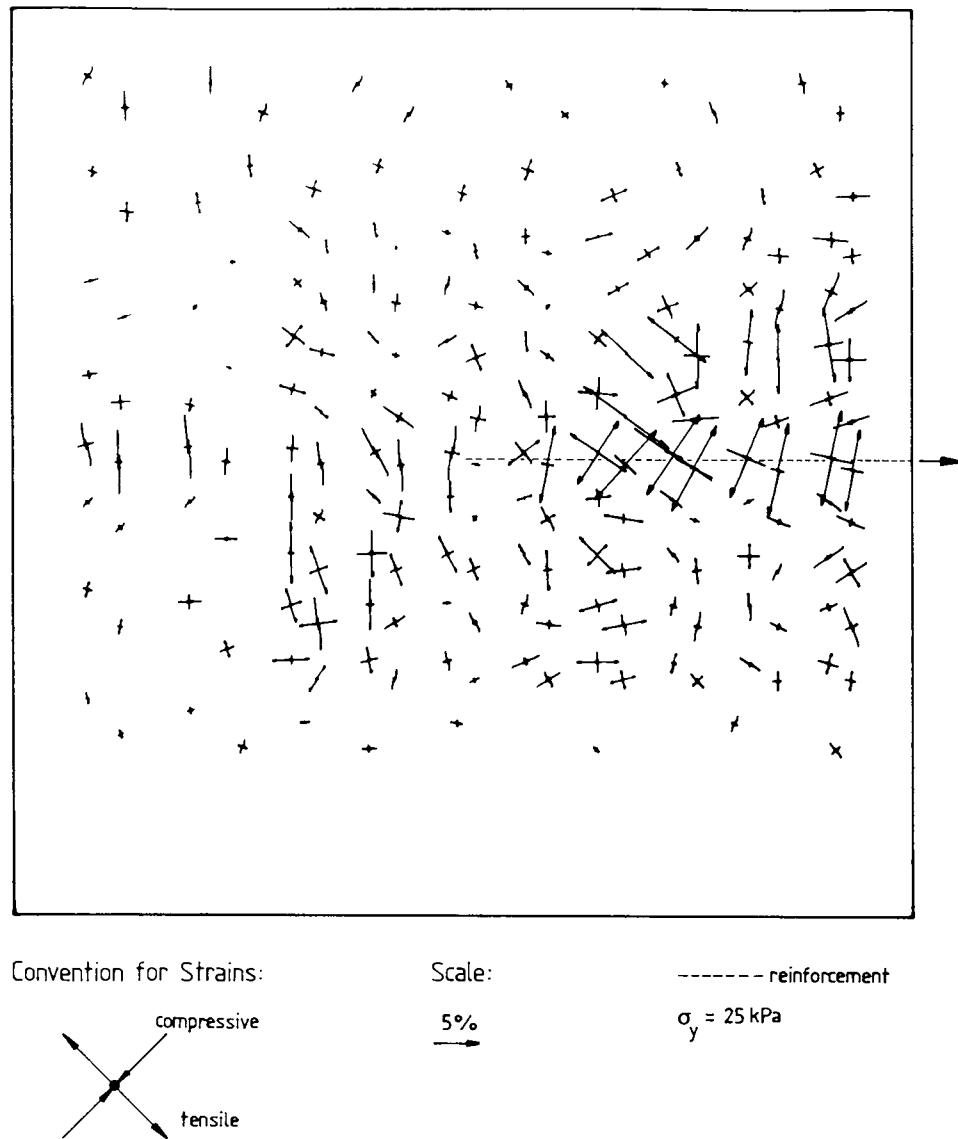
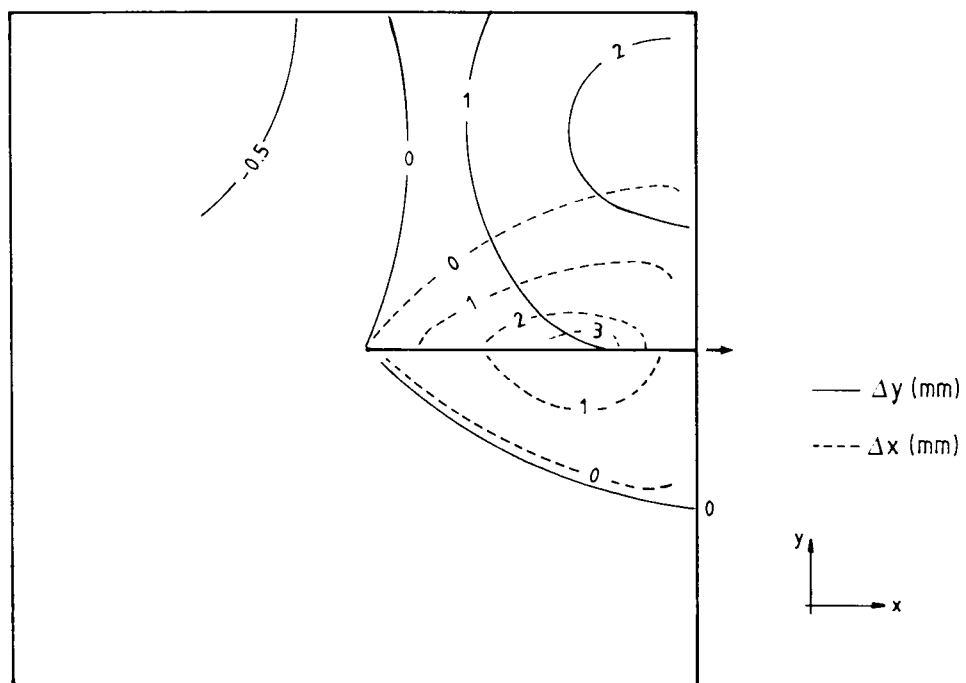
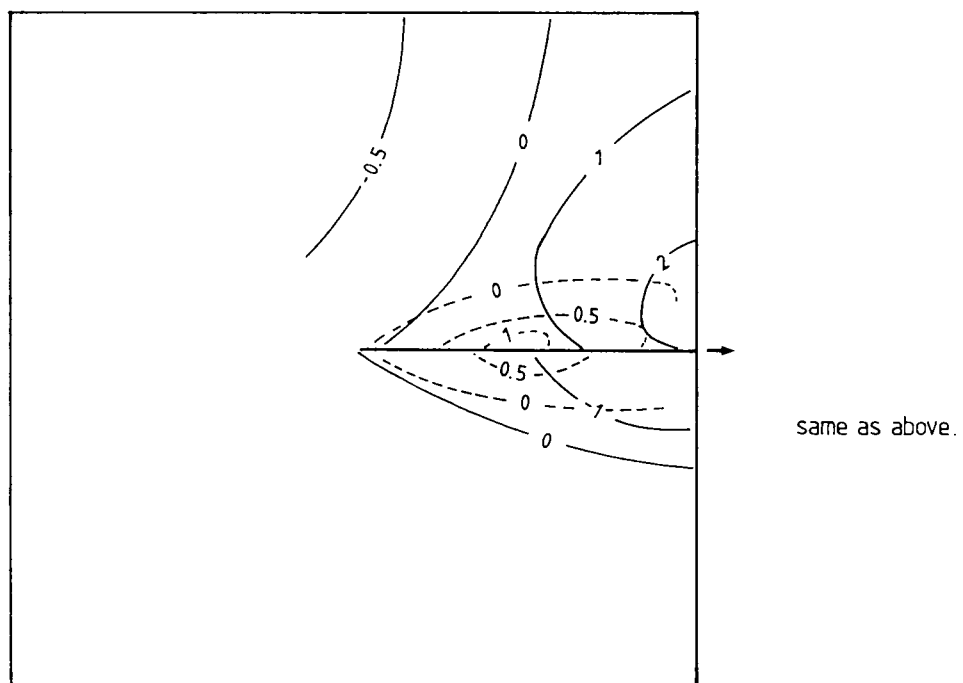


Figure 10.21 – Principal Strain Orientation in a Pull-out Test with the Rough Sheet at Peak Pull-out Load.

reinforcements. The horizontal displacements were concentrated over a fairly narrow region around the reinforcement layer. The smooth and rigid bottom of the box restrained the propagation of movements in the lower region of the box. The same pattern of displacement isocurves was observed for other sheet or grid reinforcements with lower degree of interaction with the soil. However, as the degree of interaction decreased, so did the size of the region influenced by the reinforcement



(a) rough sheet



(b) grid 4

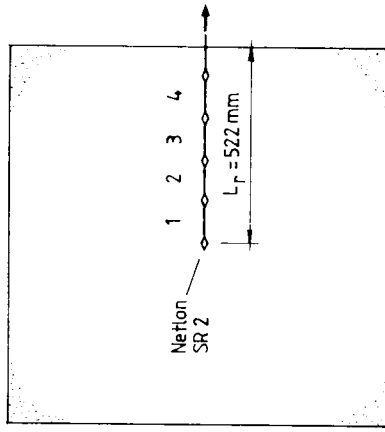
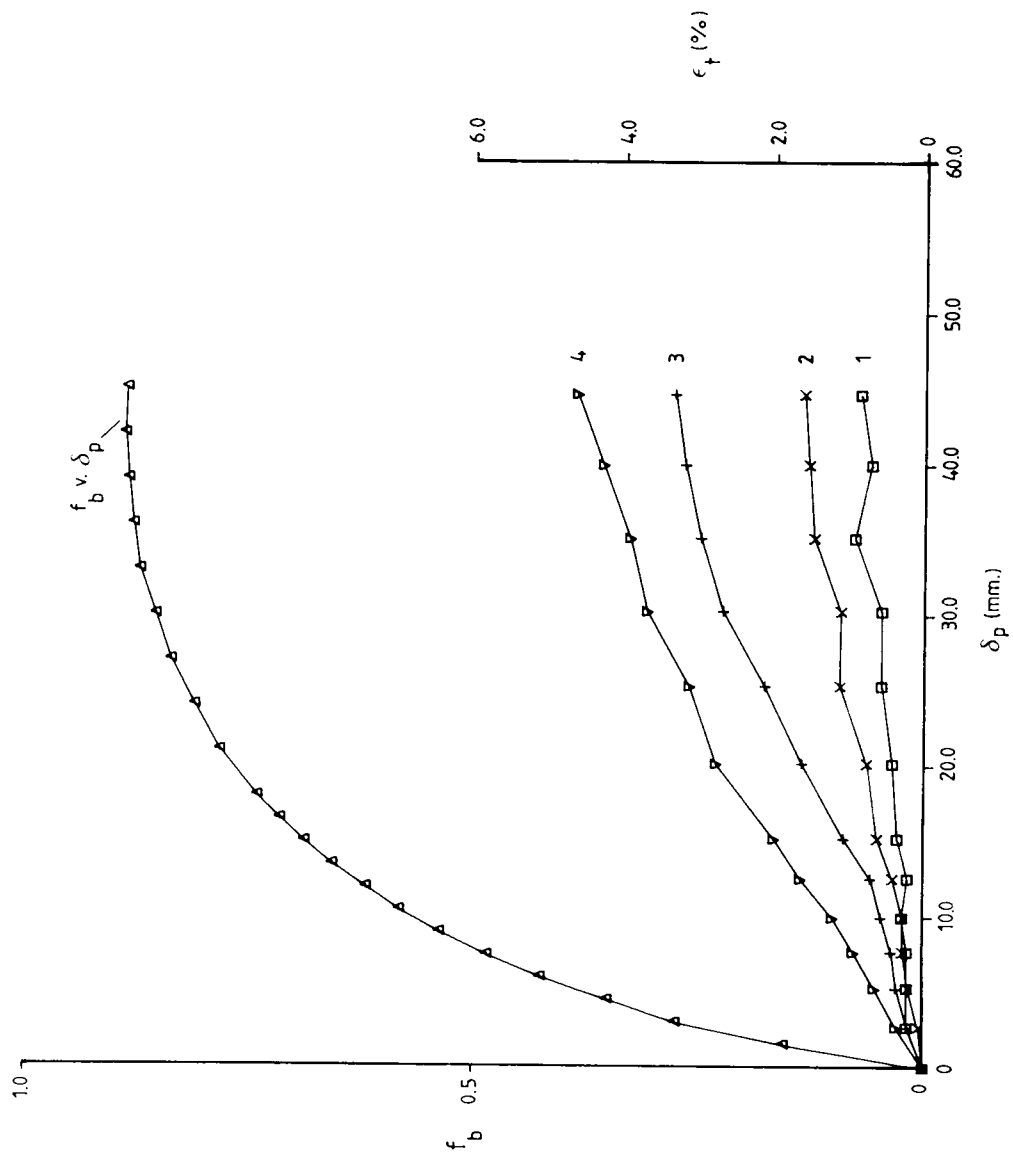
Figure 10.22 - Contours of Vertical and Horizontal Displacements.

and the magnitude of displacements observed, whose accuracy was therefore doubtful.

10.6.3 - Strain and Force Distributions in the Reinforcement:

Figures 10.23 to 10.25 show the development of strains between bearing members of the polymer grid Netlon SR2, during tests with different vertical stresses. The variation of normalised bond stress versus pull-out displacement is also presented in these figures. The technique used to measure strains in extensible reinforcements in pull-out tests was described in Chapter 7. Figure 10.23 shows the results for the test under 25 kPa vertical pressure. It can be observed that away from the leading end of the reinforcement the mobilisation of strain is much smaller than close to it. This effect is magnified as the vertical pressure increases, as shown in figures 10.24 and 10.25. Broken lines in these figures represent the strain path of the instrumented segments on the reinforcement after the pull-out load has been completely removed. It can be observed that the segments away from the box front wall tend to maintain their level of strain, due to the constraint imposed by the soil mass surrounding the bearing members.

From data presented in figures 10.23 to 10.25 the profile of tensile strains along the reinforcement length can be plotted at different stages of the test. Figures 10.26 a to c show strain profiles in the tests with Netlon SR2 at the beginning, middle and end of each test. These figures demonstrate that at the beginning of the test only a small portion of the reinforcement length, close to the point of application of the load, is significantly deformed. As the test proceeds other segments of the reinforcement layer begin to have their strain level increased. This



- strain in segment 1
- × strain in segment 2
- + strain in segment 3
- ▽ strain in segment 4

ϵ_t - tensile strain on the reinforcement

$\sigma_y = 25$ kPa

Figure 10.23 - Strains in the Polymer Grid During a Pull-out Test in the Large Box - $\sigma_y = 25$ kPa.

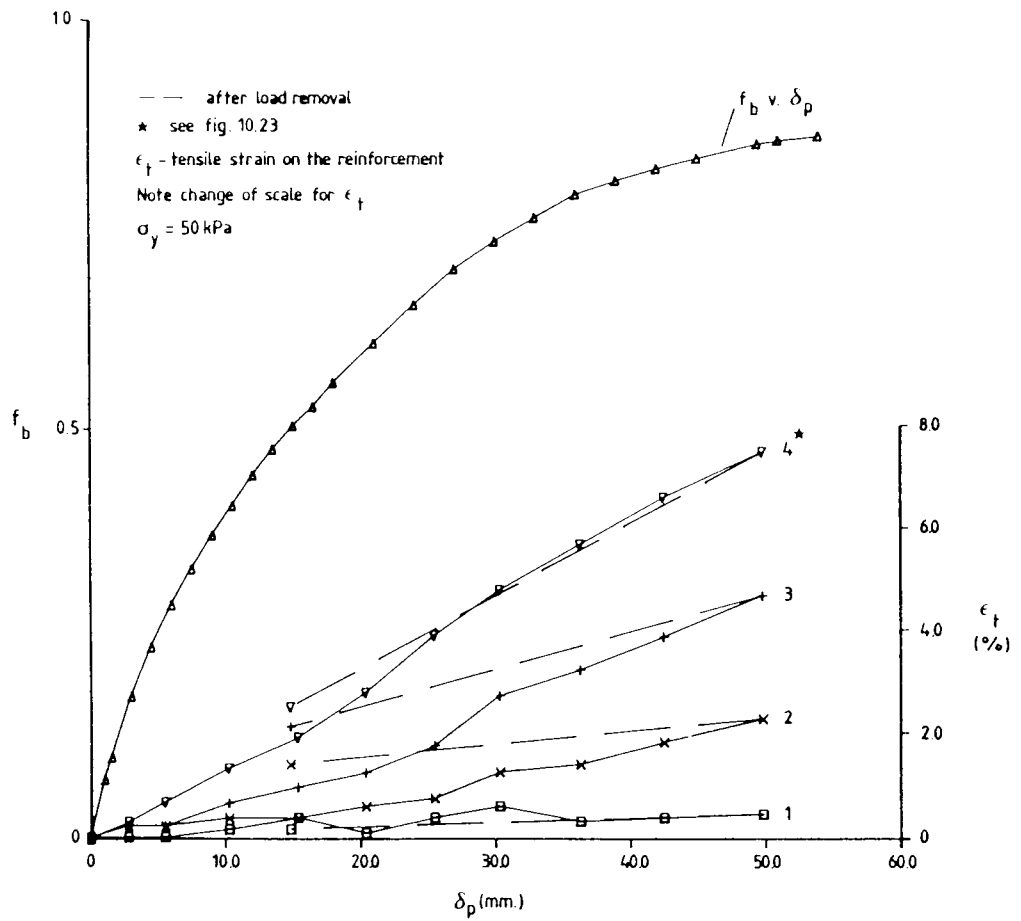


Figure 10.24 - Strains in Netlon SR2 During the Test - $\sigma_y = 50 \text{ kPa}$.

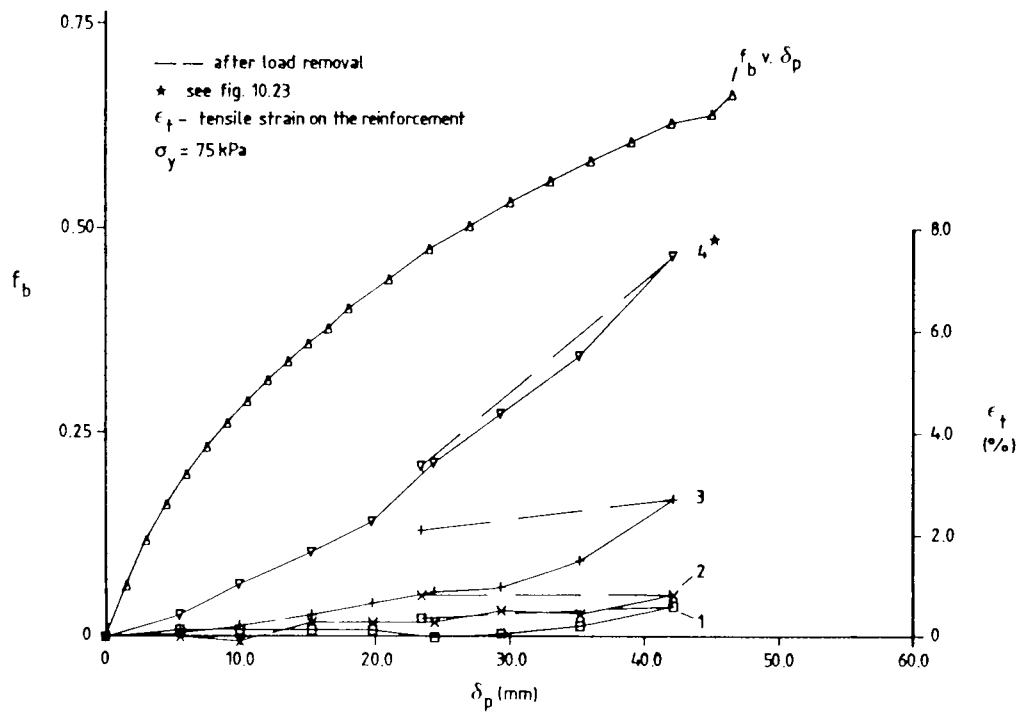


Figure 10.25 - Strains in Netlon SR2 During the Test - $\sigma_y = 75 \text{ kPa}$.

process is affected by the value of the vertical pressure on the reinforcement. This can be seen by the results in figure 10.26c, where even at the end of the test only one half of the reinforcement length presented significant strain values. These results raise two important points when testing extensible reinforcements:

1. In a pull-out test one must be able to verify whether bond resistance between soil and reinforcement is being tested or a simple tensile test of the reinforcement is being performed. In the latter case all that one obtains from the test is a lower bound for the bond resistance. For tests with polymer grids in the present work, only the one under 25 kPa vertical pressure presented bond failure and the test under 50 kPa was probably close to it.
2. The non-uniformity of the reinforcement strain distribution is another evidence of a process of progressive failure in the soil elements surrounding the reinforcement layer, which produces different strength mobilisations depending on the position of the element along the reinforcement length.

The latter comment presented above has some practical importance in the sense that it becomes difficult to choose soil strength parameters for design of reinforced soil structures under these circumstances . A conservative approach when using extensible reinforcement would be to choose critical state parameters for design (Milligan & Palmeira, 1987).

Figure 10.27 presents tensile load profiles along the reinforcement layer at the end of the tests with Netlon SR2 grids. These profiles were

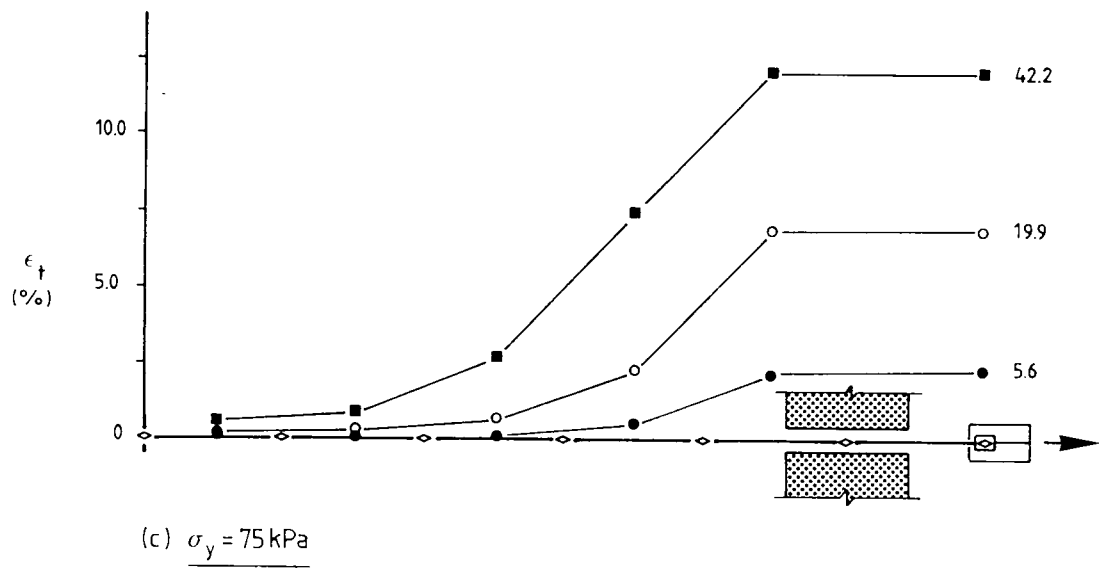
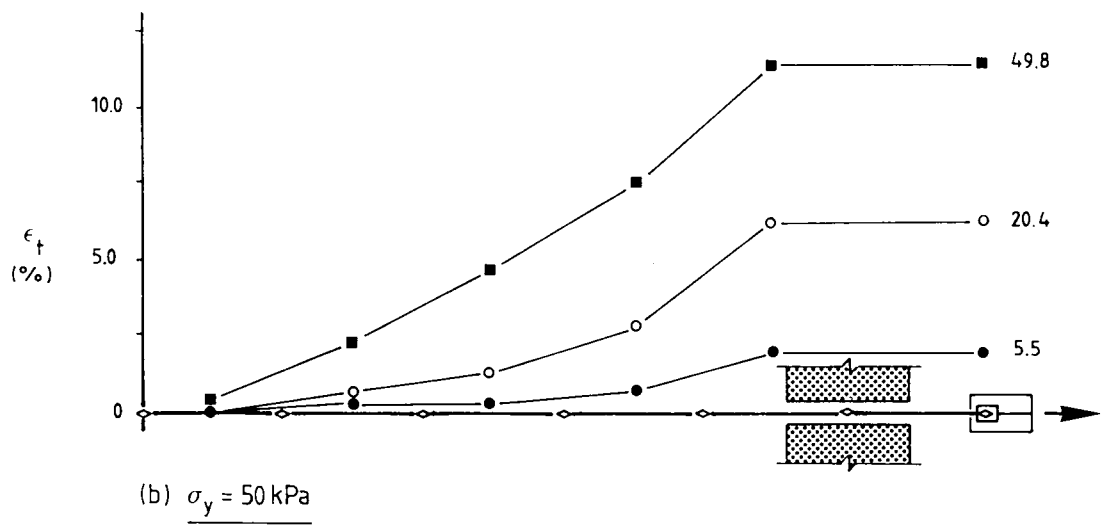
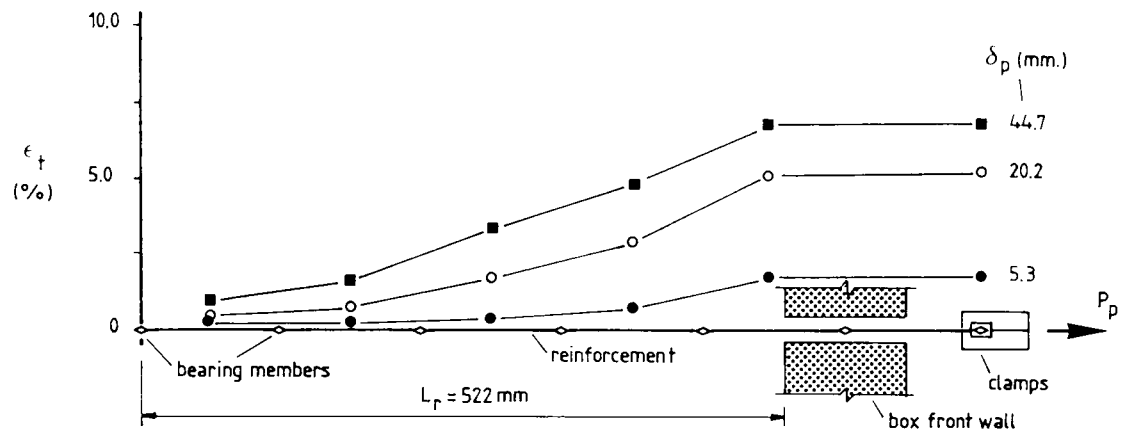


Figure 10.26 – Profiles of Tensile Strains in Netlon SR2 at Different Stages of the Test.

obtained from the strain distributions and stress-strain data from McGown (1982). These results only emphasise what has already been discussed regarding the strain distributions. However, the very good agreement observed between the pull-out load measured at the leading end of the reinforcement by the load cell and the value obtained from the strain distribution should be noted.

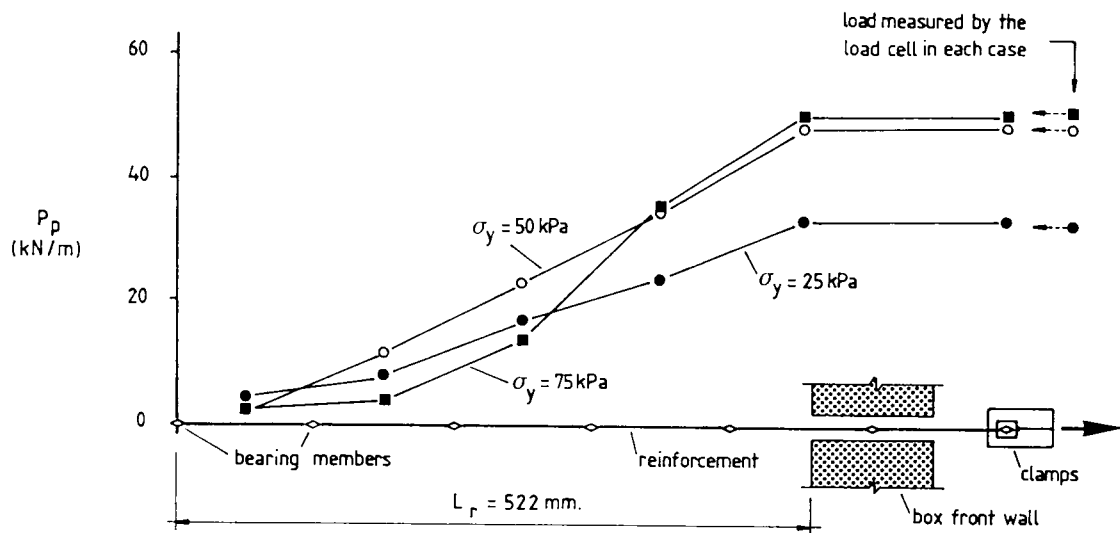


Figure 10.27 - Load Distribution in Netlon SR2 at the End of the Test.

The form and geometry of the polymer grids used in the present work, despite being beneficial in comparison with sheet reinforcements, increase the complexity of the study of interaction between soil and reinforcement. For Netlon grids about 50% of the plan area is solid. So, a mixed mechanism of friction and bearing is responsible for the bond strength. Individual measurements of bond coefficient for each individual mechanism (bearing and friction) when superimposed may not necessarily represent accurately the real situation, since the existence of one mechanism may affect the development of the other. Nevertheless, at the present stage of knowledge, there does not seem to be a better choice. Based on a skin friction coefficient of 0.6 reported in the literature

for Netlon grids (Jewell et al, 1984) it can be estimated that, in the test results reported in the present work, about 25% of the total pull-out load was likely to be caused by friction.

The same technique for strain measurement adopted for polymer grids was tried with geotextiles. Similar profiles of strains on the reinforcement were obtained but the magnitude of the strains were well above (2 to 3 times greater) what could be expected by predictions using the value of the pull-out load and data on the stiffness of the reinforcement. This was certainly due to the local deformations in regions where the wires were fixed to the reinforcement, despite precautions employed to minimise it. For this reason, the measurement of strains on geotextiles was very doubtful and the results abandoned.

10.7 - Interference Between Two Layers of Reinforcement Under Pull-out Condition:

Figure 10.28 presents results of pull-out load versus pull-out displacement for tests with two layers of reinforcement performed in the large pull-out box. A typical test arrangement can be seen in figure 7.4. Metal grids 1 ($S/B = 7.7$) and 4 ($S/B = 15.9$) were used in these tests with 160mm spacing between grid layers. The vertical pressure applied to the sample of Leighton Buzzard sand 14/25 was 25 kPa. The results of tests with single reinforcement layers, multiplied by 2, are also presented in figure 10.28. The results in this figure show that there was very little difference between the result for the test with two reinforcement layers and twice the value of the result for the equivalent test with a single reinforcement layer. The post-peak behaviour was affected by interference but for the better since the pull-out load for

double reinforcement layer arrangements was systematically greater than twice the value for a single layer of the same reinforcement. Only for large pull-out displacements was the difference between results negligible. The pull-out displacement at peak was slightly greater for the test with two reinforcements.

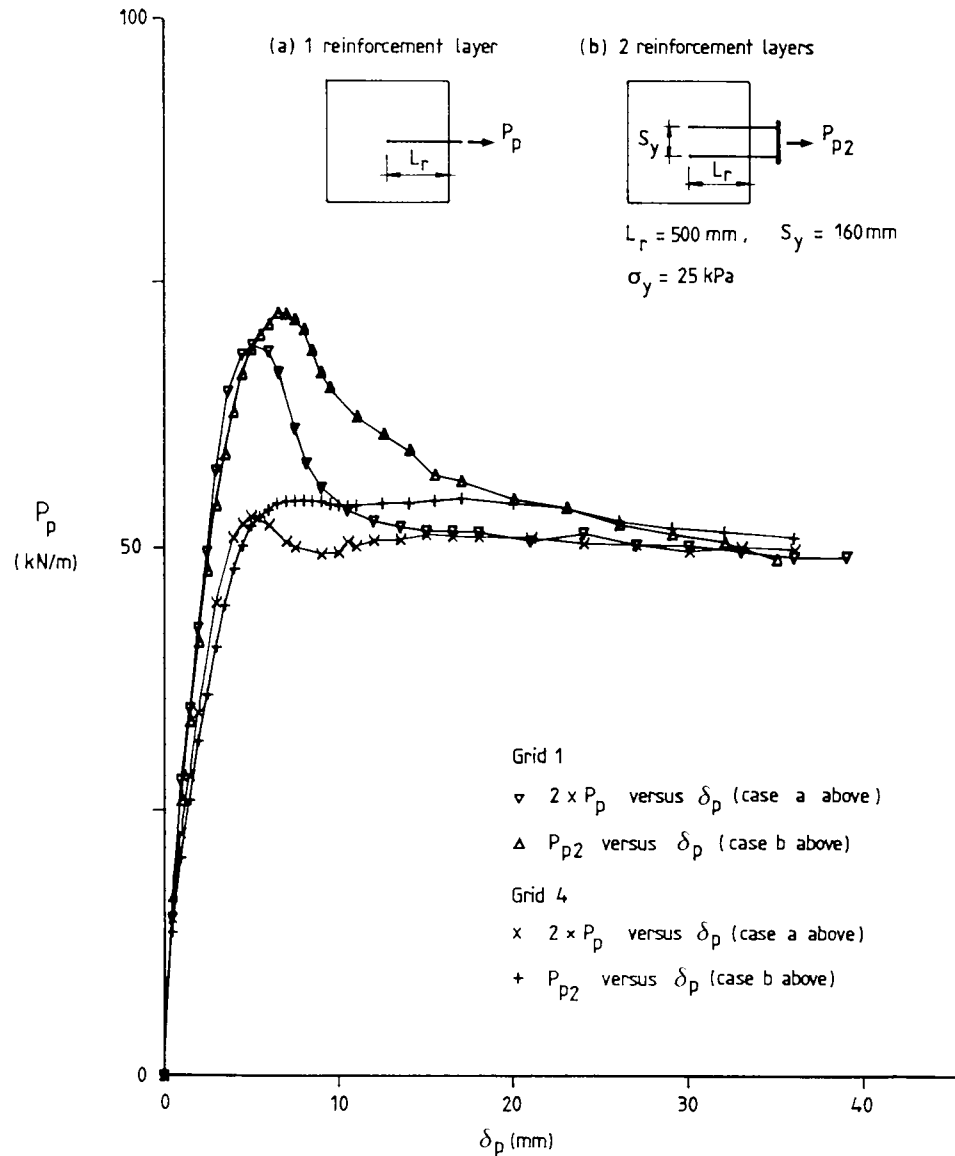


Figure 10.28 - Interference Between Two Layers of Reinforcement in Pull-out Tests.

The difference in post-peak behaviour for tests with two layers of reinforcement is believed to be due to the fact that the effect of the regions of low stresses, behind bearing members (see fig. 10.9), is minimised by the stress increments in that region caused by the neighbouring reinforcement. The slight increase in the maximum pull-out force and the increase in the pull-out displacement required to reach it can also be attributed to the same reason.

10.8 Conclusions:

The main conclusions regarding the series of pull-out tests are summarised as follows:

1. Pull-out test results can be significantly affected by boundary conditions, in particular by the roughness of the front wall of the apparatus. Measures such as lubrication of front wall and increase in the scale of the test should be taken to minimise that effect. Tests with a grid reinforcement away from the front wall showed no practical difference from the test close to a lubricated wall in terms of maximum pull-out load;
2. The maximum bearing pressure in a grid bearing member is not a constant for a given soil. It depends on the ratio between the member diameter and the soil particle "diameter". It also depends on the member shape. Tests with uniform Leighton Buzzard sands suggest that the bearing pressure assumes constant values only for B/D_{50} values above 15;

3. Interference between bearing members of a grid is a major factor determining the maximum pull-out load value. A semi-empirical approach to try to quantify the degree of interference between bearing members was developed and it fitted experimental data and data from the literature well for pull-out tests with stiff grids. These results showed that the expression for the bond coefficient (f_b) for a grid should take into account the interference between grid members. An additional expression to obtain f_b is suggested (expression 10.3);
4. Data on pull-out test results from the present work and from the literature suggest that, in the absence of better information, the bearing pressure obtained by the lower bound solution proposed by Jewell et al (1984) gives a conservative estimate. The large scatter of σ_b/σ_y values observed may be, in part, due to tests with different B/D_{50} ratios;
5. The value of the bond coefficient is a function of the reinforcement type and form. For a stiff grid reinforcement the bond coefficient is controlled by the interference between bearing members and for typical values of S/B there is no physical analogy between the interaction mechanism of a grid and an ideally rough material. Due to this fundamental difference in interaction mechanisms, predictions of bond coefficients assuming for those grids a similar behaviour to a rough sheet are bound to be inconsistent. Nevertheless, the ideally rough sheet can be used as a proper reference for interaction mechanisms based on friction, such as in the case of geotextiles and plain metal surfaces. Values of f_b of about 0.7 were obtained for stiff

geotextiles whereas values for stiff grids varied between 0.5 and 1.0, depending on the grid geometry;

6. Reinforcement longitudinal stiffness is of major importance to the value of pull-out displacement at maximum pull-out load. In tests with extensible reinforcements progressive failure is likely to occur due to the different mobilisation of strain and strength levels in the soil mass along the reinforcement length. Interference between bearing members of a stiff grid caused non-uniformity of bearing stress distribution along the grid length at maximum pull-out load;
7. The stress distribution on the side wall of the box depends on the type and form of the reinforcement tested. The behaviour of pressure cells on the front wall close to the reinforcement layer indicated the occurrence of progressive failure along the reinforcement length;
8. The strain measurement technique was not accurate enough to detect strains in the sand mass. This was due to the strains being concentrated in a small region around the bearing members in grids and in a narrow band ($\approx 10\text{mm}$ thick) surrounding frictional reinforcements. Negligible displacements were observed at the top boundary of the sample, which confirms the initial assumption of a deep failure mechanism;
9. The strain distribution along the reinforcement length is a function of the reinforcement stiffness. Vertical pressure influences strongly the percentage of reinforcement length that

will be significantly strained by the pull-out force. One should be able to distinguish between pull-out displacements of the leading end caused by bond yielding and by reinforcement yielding. This can be accomplished by measuring the strains on the reinforcement and with a comprehensive knowledge of the stress-strain-time behaviour of the reinforcement material. As in the direct shear tests, the data from McGown (1982) proved to be a very useful tool to obtain force distribution in Netlon grids;

10. Tests with two grid reinforcement layers were performed to check the effect of interference between them. For the length of reinforcement to spacing between layers ratio tested ($L_r/S_y = 3.1$) there was no significant effect of interference in the test result. A beneficial effect was observed in the post-peak behaviour.

Chapter 11: Summary, Main Conclusions and Suggestion for Future Work

Chapter 11: Summary, Main Conclusions and Suggestions for Future Work

The present work investigated the interaction between soil and reinforcement making use of different scales of test apparatus. Two types of tests were performed for this end: direct shear and pull-out. A 1 m³ direct shear and pull-out box was designed by the author in order to perform tests using large scale equipment. Tests with smaller equipment available at the Oxford University soil mechanics laboratory were also carried out. Each piece of equipment was used for appropriate tests to take the greater advantage of the benefit of each.

The work concentrated on tests with grid and sheet reinforcements of different types and forms in order to cover a wide range of reinforcement materials available. The tests were performed with dry Leighton Buzzard sands (no. 14/25 in most of the cases). About 116 tests were performed (50 in the large box, 48 in the medium size box and 18 in the small box). In these tests loads, displacements, stresses and strains relevant to the study were recorded. After the presentation of results and analyses shown in the previous chapters, the main conclusions are summarised as follows:

On Direct Shear Tests:

.The use of a flexible boundary on top of the box caused an increase of 2° in the friction angle observed in unreinforced sand tests, in comparison with the value obtained with a rigid top boundary. Scale did not affect the value of the friction angle obtained under similar boundary conditions but affected strongly the post-peak behaviour and the thickness of the shear zone in the central region of the sample;

- .The soil dilation angle obtained from internal measurements can be significantly greater than the value obtained from measurements at the top of the soil sample;
- .Progressive failure and non-uniformity of the strain distribution were observed in unreinforced direct shear tests;
- .The presence of the reinforcement can cause an increase in shear strength of about 100%. The reinforcement can also limit severely the shear strains in the central region, in particular when the reinforcement orientation coincides with the direction of the minor principal strain;
- .The use of limit equilibrium analysis predicted the force in the reinforcement within a narrow band of variation ($\pm 10\%$). Data on stress-strain-time-temperature dependence for polymer grids (McGown - 1982 and 1983) was very useful in these calculations;
- .For the geometry and type of reinforcement used in this work there was no bond failure between soil and reinforcement in tests with reinforced sand. This was due to the large normal pressures on the reinforcement plane. Failure occurred along the central region of the box first, when a critical combination between the shear stresses applied to the sample and vertical stresses caused by the reinforcement was reached. Therefore, under these circumstances there is no possibility of obtaining bond coefficients between soil and reinforcement;

.Stiff reinforcements caused a stiffer response by the reinforced sample, although softening occurred after maximum shear stress had been reached. On the other hand, plastic reinforcement continuously strengthened the soil sample throughout the test. The change in reinforcement orientation due to its deformed shape at peak stress ratio had little effect on the sample strength. Nonetheless, at large displacements such distortion was beneficial in the case of plastic reinforcement;

.The test results obtained in the large shear box confirmed observations made in smaller apparatus (Jewell, 1980) that the reinforcement bending stiffness has little relevance to the sample behaviour for the typical reinforcement types and geometries available.

On Pull-out Tests:

.Pull-out test results can be severely affected by the friction on the front wall of the box. One should try to minimise this effect by lubricating this boundary and trying to include its effect on the calculations for the test. The increase of the scale of the test is beneficial in the sense that the reinforcement can be placed away from boundaries and tested with greater length;

.The bearing pressure on a grid bearing member is a function of the ratio between its diameter and the soil particle size. In the absence of a better value the lower bound suggested by Jewell et al (1984) provides a safe estimate to the bearing pressure for a grid bearing member in isolation;

- .Interference between grid bearing members is the factor controlling the amount of bond with the surrounding soil. A Degree of Interference between bearing members was defined and an expression for the bond coefficient between soil and a stiff grid was suggested based on that concept;
- .The bond coefficient between soil and reinforcement is a function of the reinforcement type and form. Typical values of f_b were obtained in this work for woven geotextiles. The comparison between the "perfectly rough" sheet to a geotextile in terms of related efficiency seems to be appropriate since both develop the same sort of mechanism of interaction with the soil mass. Regarding a grid reinforcement, these mechanisms are different and are likely to be close only for low values of S/B ($S/B < 7$);
- .The polymer grid provided a higher bond coefficient than the other plastic reinforcement tested. This was due to the contribution from the bearing mechanism;
- .Longitudinal stiffness is of major importance for the pull-out displacement necessary to develop full bond. In this sense the metal grid and the stiff geotextile tested showed no appreciable difference of behaviour for tests with vertical pressures varying from 25 to 100 kPa. The polymer grid response was affected by the vertical pressure. Because of the increase in bond strength, tensile failure of the grid material would be reached before bond failure;
- .The results from the pressure cells on the side wall of the box suggested a progressive failure mechanism along the reinforcement

length throughout the test. This fact was marked in tests with plastic reinforcements;

.Results of pull-out tests with two layers of grid reinforcement suggested that the interference between these layers was of minor importance to the amount of bond between soil and reinforcement. A beneficial aspect of this interference was observed in the post-peak behaviour of the test with two layers of grid reinforcement.

On Suggestions for Future Work:

.Pull-out and direct shear tests with round bars with special regard to problems in soil nailed structures;

.Fundamental work on the behaviour of granular material taking advantage of the scale provided by the large shear box;

.Pull-out tests with single isolated bearing members buried in soil with different grading characteristics. Pull-out tests of single isolated bearing members under different initial stress states. Behaviour of a single bearing member under varying lateral pressure (active state of stresses);

.Fundamental investigation of the interaction mechanism of an isolated bearing member with the surrounding granular mass using photoelasticity or numerical discrete-particle modelling;

.Large scale direct shear and pull-out tests with poor quality soil materials. Large scale direct shear tests with randomly orientated mesh and fibre reinforced samples;

.Numerical modelling of the direct shear and pull-out tests results.

On Improvements for Equipments and Techniques:

.Strain measurements in polymer grid reinforcement in direct shear tests by means of wires fixed to the reinforcement in a similar manner to the one used in pull-out tests. The wires could reach the exterior of the box by means of holes at the bottom of the direct shear box. Measurements of strains in the soil mass internally by means of instruments buried in the soil;

.Use of smaller pressure cells buried in the soil to try to measure pressure distribution inside the shear zone developed at the mid height of the sample;

.Measurement of strains in metal grid reinforcement by means of strain gauges.

References

References:

- Akinmusuru J.O. (1978) - Horizontally Loaded Vertical Plate Anchors in Sand - J. of the Geotech. Engng. Div. Am. Soc. Civ. Engrs, vol. 104, No. GT2 - pp 283-286;
- Al-Hussaini M. & Perry E.B. (1978) - Field Experiment of Reinforced Earth Wall - Proc. Symp. on Earth Reinforcement - ASCE, Pittsburgh, USA, pp 127-156;
- Allersma H.G.B. (1982) - Photo-Elastic Stress Analysis and Strains in Simple Shear - IUTAM Conf. Def. Fail. Gran. Mat., Delft, pp 345-353;
- Arthur J.R.F., Dunstan T. Al-Ani Q.A.J.L. & Assadi A. (1977a) - Plastic Deformation and Failure in Granular Media - Geotechnique 27, No. 1, pp 53-74;
- Arthur J.R.F., Chua K.F. & Dunstan T. (1977b) - Induced Anisotropy in a Sand - Geotechnique 27, No. 1, pp 13-30;
- Audibert J.M.E. & Nyman K.J. (1977) - Soil Restraint Against Horizontal Motion of Pipes - J. Geotech. Engng. Div. Am. Soc. Civ. Engrs., vol. 103, No. GT10, pp 1119-1142;
- Basset R.H. (1967) - The Behaviour of Granular Materials in the Simple Shear Apparatus - Ph.D. Thesis, University of Cambridge;
- Basset R.H. (1978) - Underreamed Ground Anchors - Revue Francaise de Geotechnique, No. 3, pp 11-17
- Blivet J.C. & Gestin F. (1979) - Etude de l'Adherence Entre le Phosphogypse et Deux Geotextiles - Proc. Int. Conf. on Soil Reinforcement, Paris, vol. 2, pp 403-408
- Bolton M.D., Choudhury S.P. & Pang P.L.R. (1978) - Reinforced Earth Walls: A Centrifugal Model Study - Proc. Symp. on Earth Reinforcement - Am. Soc. Civ. Engrs., Pittsburgh, USA, pp 252-281;

- Bolton M.D. (1986)** – The Strength and Dilatancy of Sands – Geotechnique 36, No 1, pp 65-78;
- Brown I.E.W. & Rochester T.A. (1979)** – Reinforced Earth – Technical Guidance Provided by the Department of Transport, England – Proc. Int. Conf. on Soil Reinforcement, Paris, vol. 2, pp 423-430;
- Chang J.C., Hannon J.B. & Forsyth R.A. (1977)** – Pull Resistance and Interaction of Earthwork Reinforcement and Soil – Transport Research Record No. 640, Washington D.C., USA;
- Cole E.R. (1967)** – The Behaviour of Soils in the Simple Shear Apparatus – PhD Thesis – University of Cambridge;
- Dantu P. (1957)** – Contribution a l'Etude Mecanique et Geometrique des Milieux Pulverulents – Proc. 4th Int. Conf. Soil Mech. Fdn. Engng., London, vol. 1, pp 144-148;
- Dash U. (1978)** – Design and Field Testing of a Reinforced Earth Wall – Proc. Symp. on Earth Reinforcement – Am. Soc. Civ. Engrs., Pittsburgh, USA, pp 334-357;
- Degoutte G. & Mathieu G. (1986)** – Etude Experimentale du Frottement Sol-Membranes et Sol- Geotextiles a l'Aide d'une Boite de Casagrande de 30x30 cm² – Proc. 3rd Int. Conf. on Geotextiles, Vienna, vol. 3, pp 791-796;
- de Josselin de Jong G. (1958)** – The Undeiniteness in Kinematics for Friction Materials – Proc. Conf. on Earth Pressure Problems 1, Brussels, pp 55-70;
- de Josselin de Jong G. (1959)** – Static and Kinematics in the Failure Zone of a Granular Material – Delft Uitgeverig Waltman;
- de Josselin de Jong G. (1971)** – The Double Sliding Free Rotating Mode for Granular Assemblies – Geotechnique 21, No. 1, pp 155-163;
- de Josselin de Jong G. (1976)** – Rowe's Stress-Dilatancy Relation Based on Friction – Geotechnique 26, No. 3, pp 527-534;

- Delmas P., Gourc J.P. & Giroud J.P. (1979) - Analyse Experimental de l'Interaction Mecanique Sol-Geotextile - Proc. Int. Conf. on Soil Reinforcement, Paris, vol. 1, pp 29-34;
- Dickin E.A. & Leung C.F. (1983) - Centrifugal Model Tests on Vertical Anchor Plates - J. of Geotech. Engng. Am. Soc. Civ. Engrs., vol. 109, No. 12;
- Drescher A. (1976) - An Experimental Investigation of Flow Rules for Granular Materials Using Optically Sensitive Glass Particles - Geotechnique 26, No. 4, pp 591-601;
- Drescher A. & De Josselin de Jong G. (1972) - Photoelastic Verification of a Mechanical Model for the Flow of a Granular Material - J. Mech. Phys. Solids 20, pp 337-351;
- Dyer M.R. (1985) - Observation of the Stress Distribution in Crushed Glass with Applications to Soil Reinforcement - DPhil. Thesis - University of Oxford;
- Elias V. (1979) - Friction in Reinforced Earth Utilizing Fine Grained Backfills - Proc. Int. Conf. on Soil Reinforcement, Paris, Vol. 2, pp 435-438;
- Gardner N.J. & Morgado H.M. (1984) - Steel Mesh Reinforcement for Soil Structures - Proc. Int. Conf. of In Situ Soil and Rock Reinforcement, Paris, pp 263-268;
- Gray D.H. & Al-Refeai T. (1986) - Behaviour of Fabric versus Fiber-Reinforced Sand - J. of Geotech. Engng. Am. Soc. Civ. Engrs., vol. 112, No. 8, pp 804-820;
- Guilloux A., Schlosser F. & Long N.T. (1979) - Etude du Frottement Sable-Armature en Laboratoire - Proc. Int. Conf. on Soil Reinforcement, Paris, vol. 1, pp 35-40;
- Hueckel S.M. & Kwasniewski J. (1961) - Essais Sur Modele Reduit de la Capacite d'Ancrage d'Elements Rigides Horizontaux Enfouis dans le Sable -

- Proc. of the 4th Int. Conf. Soil Mech. Fdn. Engng., vol. 1, Paris, pp 431-434;
- Ingold T.S. & Templeman J.E. (1979)** - The Comparative Performance of Polymer Net Reinforcement - Proc. Int. Conf. on Soil Reinforcement, Paris, vol. 1, pp 65-70;
- Ingold T.S. (1982)** - Reinforced Earth - Thomas Telford Ltd., London;
- Jewell R.A. (1980)** - Some Effects of Reinforcement on Soils - PhD Thesis, University of Cambridge;
- Jewell R.A., Milligan G.W.E., Sarsby R.W. & Dubois D. (1984)** - Interaction Between Soil and Geogrids - Proc. Symp. on Polymer Grid Reinforcement, ICE, London, paper 1.3;
- Jewell R.A. (1985)** - Material Properties for The Design of Geotextile Reinforced Slopes - Geotextiles and Geomembranes, vol. 2, No. 2, pp 83-109;
- Jewell R.A. & Wroth C.P. (1987)** - Direct Shear Tests on Reinforced Soil - Geotechnique 37, No. 1, pp 53-68;
- Juran I., Schlosser F., Long N.T. & Legeay G. (1979)** - Experimentation en Vraie Grandeur Sur un Mur en Terre Armee Soumis a des Surcharges en Tete - Proc. Int. Conf. on Soil Reinforcement, Paris, vol. 3, pp 557-562;
- Kerisel J. (1972)** - The Language of Models in Soil mechanics - Proc. of the 5th Europ. Conf. Soil Mech. Fdn. Engng., Madrid, Spain;
- Koivumaki O. (1983)** - Friction Between Sand and Metal - Proc. of the 8th Europ. Conf. Soil Mech. Fdn. Engng., Improvement of Ground, Helsinki, vol. 2, pp 517-520;
- Leshchinsky D. & Reinschmidt A.J. (1985)** - Stability of Membrane Reinforced Slopes - J. of Geotech. Engng. Am. Soc. Civ. Engrs., vol. 111, No. 11, pp 1285-1300;
- Matsuoka H., Iwata Y. & Sakakibara K. (1986)** - A Constitutive Model of Sands and Clays for Evaluating the Influence of Rotation of the Principal

- Stress Axes - Proc. of the 2nd Conf. on Numerical Models in Geomechanics, Gent, Belgium;
- McGown A., Andrawes K.Z. and Al-Hasani M.M. (1978)** - Effect of Inclusion Properties on the Behaviour of Sand - Geotechnique 28, No. 3, pp 327-346;
- McGown A., Andrawes K.Z., Mashhour M.M. and Myles B. (1981)** - Strain Behaviour of Soil-Fabric Model Embankment - Proc. of the 10th Int. Conf. Soil Mech. Fdn. Engng., Stockholm, vol. 3, pp 739-744;
- McGown A. (1982)** - Progress Report to Tensar Steering Committee at Oxford University 5th May 1982 - Strathclyde University;
- McGown A. (1983)** - Report to Tensar Steering Committee at Leeds University on 29th March 1983 - Strathclyde University;
- McGown A., Andrawes K.Z. & Yeo K.C. (1984)** - The Load-Strain-Time Behaviour of Tensar Geogrids - Proc. Symp. on Polymer Grid Reinforcement, ICE, London, paper 1.2
- Milligan G.W.E. & Bransby P.L. (1976)** - Combined Active and Passive Rotational Failure of a Retaining Wall in Sand - Geotechnique 26, No. 3, pp 473-494;
- Milligan G.W.E. (1986)** - Personal Communication;
- Milligan G.W.E. & Palmeira E.M. (1987)** - Prediction of Bond Between Soil and Reinforcement - Proc. Int. Symp. on Prediction and Performance in Geotech. Engng., Calgary, Alberta, Canada;
- Miyamori T., Iwai S. & Makiuchi K. (1986)** - Frictional Characteristics of Non-Woven Fabrics - Proc. 3rd Int. Conf. on Geotextiles, Vienna, vol.3, pp 701-706;
- Murray R.T. & Bolden J.B. (1979)** - Reinforced Earth Wall Constructed with Cohesive Fill - Proc. Int. Conf. on Soil Reinforcement, Paris, vol. 2, pp 569-577;

- Oda M. & Konishi J. (1974) - Rotation of Principal Stresses in Granular Material in Simple Shear - Soils and Foundations, Vol. 14, No. 4, pp 39-53;
- Palmeira E.M. (1981) - Utilization of Geotextile Reinforcement as a Reinforcement for Access Roads on Soft Ground - MSc Thesis - Coppe/Federal University of Rio de Janeiro, Brazil, (in portuguese);
- Palmeira E.M. (1984) - First Year Report, University of Oxford;
- Palmeira E.M. (1987) - Guide-lines for the Use of the Large Direct Shear and Pull-out Boxes - University of Oxford;
- Palmeira E.M. & Milligan G.W.E. (1987) - Scale and Other Factors Affecting the Results of Pull-out Tests of Grids Buried in Sand - Report OUEL 1678/87, University of Oxford;
- Perrier H., Blivet J.C. & Khay M. (1986) - Stabilisation de Talus par Reinforcement tout Textile: Ouvrage Experimental et Reel - Proc. 3rd Int. Conf. on Geotextiles, Vienna, vol. 2, pp 313-318;
- Peterson L.M. (1980) - Pull-out Resistance of Welded Wire Mesh Embedded in Soil - MSc Thesis, Utah State University, USA;
- Potts D.M., Dounias G.T. & Vaughan P.R. (1987) - Finite Element Analysis of the Direct Shear Box Test - Geotechnique 37, No. 1, pp 11-24;
- Poulos H.G. & Davis E.H. (1974) - Elastic Solutions for Soil and Rock Mechanics - John Wiley & Sons;
- Ramalho-Ortigao J.A. & Palmeira E.M. (1982) - Geotextile Performance at an Access Road on Soft Ground Near Rio de Janeiro - Proc. 2nd Int. Conf. on Geotextiles, Las Vegas, USA, Vol. 2, pp 353-358;
- Richards D.A. & Scott J.D. (1985) - Soil Geotextile Frictional Properties - Proc. 2nd Can. Symp. on Geotextiles and Geomembranes, Edmonton, Canada, pp 13-24;
- Rowe P.W. (1962) - The Stress-Dilatancy Relation for Static Equilibrium of an Assembly of Particles in Contact - Proc. of the Royal Soc. 269, pp 500-527;

- Rowe R.K. & Booker J.R. (1980) - The Elastic Response of Multiple Underream Anchors - Int. J. for Num. and Anal. Meth. in Geomechanics, vol. 4, No. 4, pp 313-332;
- Rowe R.K., Ho S.K. & Fisher D.G. (1985) - Determination of Soil-Geotextile Interface Strength Properties - Proc. 2nd Can. Symp. on Geotextiles and Geomembranes, Edmonton, Canada, pp 25-34;
- Sarsby R.W. & Marshall (1983) - A Method for Determining the Interactive Behaviour of Polymer Grids and Granular Soils - Report No. BCS/G1/2A, Bolton Institute of Higher Education;
- Scarpelli G.S. & Wood D.M. (1982) - Experimental Observation of Shear Band Patterns in Direct Shear Tests - Proc. IUTAM Conf. on Def. and Failure of Granular Materials, Delf, pp 473-484;
- Schlosser F. & Elias V. (1978) - Friction in Reinforced Earth - Proc. Symp. on Earth Reinforcement - Am. Soc. Civ. Engrs., Pittsburgh, USA, pp 735-763;
- Shen C.K., Mitchell J.F., De Natale J.S. & Romstad K.M. (1979) - Laboratory Testing and Model Studies of Friction in Reinforced Earth - Proc. Int. Conf. on Soil Reinforcement, Paris, vol. 1, pp 169-174;
- Sims F.A. & Jones C.J. (1979) - The Use of Soil Reinforcement in Highway Schemes - Proc. Int. Conf. on Soil Reinforcement, Paris, vol. 2, pp 361-366;
- Smith A.K.C. & Wroth C.P. (1978) - The Failure of Model Reinforced Earth Walls - Proc. Symp. on Earth Reinforcement - Am. Soc. Civ. Engrs., Pittsburgh, USA, pp 794-855;
- Spencer A.J.M. (1964) - A Theory of Kinematics of Ideal Soils Under Plane Strain Conditions - J. Mech. Phys. Solids, No. 12, pp 337-351;
- Stroud M.A. (1971) - The Behaviour of Sand at Low Stress Levels in the Simple Shear Apparatus - PhD Thesis - University of Cambridge;

- Symes M.J., Hight D.W. & Gens A. (1982) - Investigating Anisotropy and the Effects of Principal Stress Rotation and of the Intermediate Principal Stress Using a Hollow Cylinder Apparatus - IUTAM Conf. Def. Fail. Gran. Mat., Delft, pp 441-449;
- Taylor D.W. (1948) - Fundamentals of Soil Mechanics - John Wiley & Sons;
- Trautmann C.H. & O'Rourke T.D. (1985) - Lateral Force-Displacement Response of Buried Pipe - J. of Geotech. Engng. Am. Soc. Civ. Engrs., vol. 111, No.9, pp 1077-1094;
- Wang M.C. & Wu A.H. (1980) - Yielding Load of Anchor in Sand - Proc. of the Symp. on Limit Equil., Plasticity and Generalised Stress Strain Appl. in Geotech. Engng. - Am. Soc. Civ. Engrs., Florida, USA - pp 291-307;
- Weiler Jr. W.A. & Kulhawy F.H. (1982) - Factors Affecting Stress Cell Measurements in Soil - J. of Geotech. Engng. Am. Soc. Civ. Engrs., vol. 108, GT12, pp 1529-1548;
- Wernick E. (1978) - Stresses and Strains on the Surface of Anchors - Revue Francaise de Geotechnique, No. 3, pp 113-119;
- Wong R.K.S. & Arthur J.R.F. (1985) - Induced and Inherent Anisotropy in Sand - Geotechnique 35, No. 4, pp 471-481;
- Wroth C.P. (1958) - The Behaviour of Soils and Other Granular Media when Subjected to Shear - PhD Thesis - University of Cambridge.

List of Symbols

List of Symbols:

A_s	- Plan area of the soil sample;
b	- Width of a surcharge on the surface on an elastic medium;
B	- Bearing member diameter;
C.U.	- Coefficient of Uniformity;
d	- Distance between a reinforcement layer and the box front wall;
d_N	- distance between the point of application of N and the right extremity of the central plane;
d_p	- distance between the point of application of P_s and the right hand extremity of the central plane;
DI	- Degree of Interference between bearing members of a grid reinforcement;
DI_e	- Degree of Interference for a group of underreamed square anchors buried in an elastic medium;
D_{50}	- Soil particle diameter corresponding to 50% passing;
e	- soil void ratio;
E	- Young modulus;
\dot{E}	- Increment of energy per unit volume, normal stress and shear strain;
E_L	- Equivalent longitudinal stiffness of a reinforcement layer;
f	- Aperture size in a photographic camera;
f_b	- Bond coefficient between soil and reinforcement ($= \tan\delta/\tan\phi$);
F_f	- Resultant shear force acting on the central plane;
g.s	- Galvanised steel;
G_s	- Specific Gravity of soil particles;

h	- Half height of the shear or pull-out box;
I	- Second moment of area;
I_D	- Relative Density Index;
K	- Reinforcement bending stiffness;
l	- Length of the surcharge on the surface of an elastic medium;
L	- Length of the shear or pull-out box;
L_r	- Reinforcement length buried in the soil mass;
m.s.	- Mild steel;
n	- Number of bearing members in a grid reinforcement;
N	- Normal force acting on the central plane of the soil sample;
PC	- Pressure cell;
P_o	- Maximum pull-out load for a single isolated bearing member;
P_{oe}	- Pull-out load applied to a single square underream buried in an elastic medium that causes a displacement equal to δ_e ;
P_p	- Pull-out load applied to a reinforcement layer;
P_{pe}	- Pull-out load of a group of underreamed square anchors in an elastic medium that causes a pull-out displacement equal to δ_e at the 1st underream;
P_r	- Force in the reinforcement in a direct shear test;
P_s	- Shear force applied to the top half of the shear box;
P_{p2}	- Pull-out load applied to an arrangement with two reinforcement layers;
$P_{v_{top}}$	- Total vertical load applied on the top half of the shear box
s	- $= (\sigma_1 + \sigma_3)/2$;
S	- Spacing between bearing members in a grid reinforcement;

- S_l - Spacing between longitudinal members in a grid reinforcement;
 S_y - Vertical spacing between two layers of reinforcement;
 t - $= (\sigma_1 - \sigma_3)/2$;
 W_r - Reinforcement width;
 W_{soil} - Weight of the top half of the soil sample;
 x - Cartesian axis (horizontal);
 y - Cartesian axis (vertical);

Greek Characters:

- α_B - Percentage of a grid total bearing area which is available for bearing;
 α_S - percentage of a grid total plan area which is solid;
 β - Increment in θ due to the deformation of the reinforcement;
 γ - Soil unit weight;
 $\dot{\gamma}, \dot{\gamma}_{yx}$ - Shear strain increment;
 δ - Friction angle between soil and reinforcement (interface friction angle). Friction angle between soil and a smooth metal surface;
 δ_e - Elastic pull-out displacement of the 1st underream in a group of n underreamed square anchors buried in a elastic medium;
 δ_l - Friction between soil and a lubricated metal surface;
 δ_p - pull-out displacement at the leading end of the reinforcement;
 δ_x - Relative displacement between top and bottom halves of a direct shear box (shear displacement);

- $\bar{\delta}_y$ - Mean vertical displacement at the top of the soil sample;
- Δx - Increment in x;
- Δy - Increment in y;
- $\Delta \sigma_x$ - Increment in σ_x ;
- ε - Tensile Strain;
- $\varepsilon_1, \varepsilon_3$ - Major and minor principal strains;
- $\dot{\varepsilon}_1, \dot{\varepsilon}_3$ - Major and minor principal strain increments;
- ε_t - Tensile Strain in a reinforcement;
- $\varepsilon_{t_{\max}}$ - Maximum tensile strain in a reinforcement layer;
- $\dot{\varepsilon}_{\text{vol}}$ - Volumetric strain increment;
- $\dot{\varepsilon}_x, \dot{\varepsilon}_y$ - Strain increments on the x and y directions;
- θ - Angle between the reinforcement orientation and the normal to the shear plane;
- σ_b - Bearing stress on a grid bearing member;
- σ_x - Stress on the x direction (horizontal stress);
- σ_y - Stress on the y direction (vertical stress). Initial vertical stress on the central plane of the box;
- σ_y' - Mean vertical pressure on the central plane including the contribution due to friction on the side wall of the box;
- $\sigma_{y_A}, \sigma_{y_B}$ - Vertical stresses at the corner of a trapezoidal stress distribution;
- σ_{y_b} - Vertical pressure on the bottom face of the box in a reinforced test;
- σ_{y_r} - Vertical pressure on the central plane in a reinforced test;

- $\bar{\sigma}_{yr}$ - Mean vertical pressure on the central plane in a reinforced test;
- σ_1, σ_3 - Major and minor principal stresses;
- τ_b - Shear stress between soil and reinforcement (bond stress);
- τ_{yx} - Shear stress on the plane which has the y direction as normal and is parallel to the x direction;
- $\bar{\tau}_{yx}$ - Mean shear stress on the central plane;
- ϕ - soil friction angle;
- ϕ_{crit} - constant volume or critical state soil friction angle;
- ϕ_{cv} - Constant volume friction angle;
- ϕ_{ds} - Soil friction angle obtained in direct shear tests;
- ϕ_f - Equivalent soil friction angle ($\phi_\mu < \phi_f < \phi_{cv}$);
- ϕ_{max} - Maximum (plane strain) soil friction angle;
- ϕ_{ps} - Plane strain friction angle;
- ϕ_μ - Interparticle friction angle;
- ψ - Soil dilation angle;
- ψ_{max} - Maximum soil dilation angle;

List of Figures

List of Figures and Tables:

<u>Chapter 1: Soil Reinforcement Technique</u>	<u>Page</u>
Fig. 1.1 - Typical Examples of Soil Reinforcement Application;	1.2
Fig. 1.2 - Long Term Behaviour of Polymer Reinforcement (After McGown, 1984);	1.6
Fig. 1.3 - Failure Mechanisms in a Reinforced Soil Retaining Wall	1.10
Fig. 1.4 - Direct Shear and Pull-out Tests Results Collected from Literature;	1.13
Fig. 1.5 - Friction Angle Dependence on Stress Level (After Bolton, 1986);	1.15
Fig. 1.6 - Histogram of Direct Shear and Pull-out Test Results;	1.17
Tab. 1.1 - Common Types of Reinforcement;	1.7
Tab. 1.2 - Some Plane Strain Testing Configurations for the Study of Soil-Reinforcement Interaction;	1.9
 <u>Chapter 2: Direct Shear Apparatus</u>	
Fig. 2.1 - Schematic View of the Large Shear Box;	2.4
Fig. 2.2 - Detailed View of the Large Shear Box;	2.5
Fig. 2.3 - The Large Shear Box During a Test;	2.6
Fig. 2.4 - Total Pressure Cells Used in the Large Shear Box;	2.9
Fig. 2.5 - General View of the Total Pressure Cells;	2.10
Fig. 2.6 - Photographic Technique to Monitor Marker Movements;	2.11
Fig. 2.7 - Medium Size Shear Box (After Jewell, 1980);	2.13
 <u>Chapter 3: Soil and Reinforcement Characteristics</u>	
Fig. 3.1 - Photographic View of Leighton Buzzard Sand 14/25;	3.2
Fig. 3.2 - Geometry of the Metal Grids Used in the Present Work;	3.5
Fig. 3.3 - Photographic View of the Frictional Reinforcements Used in the Present Work;	3.6
Fig. 3.4 - Geometry of the Polymer Grids Used in the Present Work;	3.7
Tab. 3.1 - Characteristics of Reinforcements Used in the Present Study;	3.3
 <u>Chapter 4: Sample Preparation and Test Procedure</u>	
Fig. 4.1 - Friction on the Sides of the Large Shear Box;	4.2
Fig. 4.2 - Sample Preparation in the Large Shear Box;	4.4
Fig. 4.3 - Emptying Procedure in the Large Shear Box;	4.9
Fig. 4.4 - Repeatability of Test Results in the Large Shear Box;	4.13
Fig. 4.5 - Comparison Between Mean Vertical Displacements at the Top of the Large Shear Box;	4.14
 <u>Chapter 5: Direct Shear Tests on Unreinforced Sand</u>	
Fig. 5.1 - Definition of Parameters in Direct Shear Tests;	5.2
Fig. 5.2 - Theoretical Relation Between ϕ_{ps} and ϕ_{ds} based on Coaxiality Between Stress and Strain Increments Directions;	5.5
Fig. 5.3 - Direct Shear Test Results for Dense Leighton Buzzard Sand 14/25 Under Different Boundary Conditions on Top;	5.10
Fig. 5.4 - Influence of the Top Boundary Condition on Reinforced Tests in the Medium Size Box;	5.11

Fig. 5.5 - Large Direct Shear Test Results in Dense Unreinforced Leighton Buzzard Sand 14/25;	5.13
Fig. 5.6 - Comparison Between Unreinforced Tests at Different Scales;	5.15
Fig. 5.7 - Peak Stress Ratio versus Vertical Stress for Unreinforced Dense Leighton Buzzard Sand 14/25;	5.16
Fig. 5.8 - Mean Vertical Strain versus Shear Strain in Unreinforced Tests;	5.17
Fig. 5.9 - Results Obtained by the Flow Rule Based on the Balance of Energy versus Shear Strain for Leighton Buzzard Sand 14/25;	5.18
Fig. 5.10 - Distribution of Horizontal Stress Increments on the Side Wall of the Box;	5.18
Fig. 5.11 - Forces Acting on the Top Half of the Sample in the Large Shear Box;	5.20
Fig. 5.12 - Shear Strain Profile in the Central Region of the Sample;	5.21
Fig. 5.13 - Principal Strain and Zero Extension Lines Orientation in Unreinforced Tests with Leighton Buzzard Sand 14/25 at Peak Stress Ratio in the Large Shear Box;	5.23
Fig. 5.14 - Principal Strain and Zero Extension Lines Orientation at Peak Stress Ratio in the Medium Size Shear Box - Flexible Top Boundary, $\sigma_y = 30$ kPa;	5.24
Tab. 5.1 - Works in the Literature Where the Orientation of Principal Axes of Stress and Strain Increments Were Measured;	5.6
Tab. 5.2 - Summary of Results of Direct Shear Tests at Different Scales;	5.15

Chapter 6: Large Direct Shear Tests on Reinforced Sand

Fig. 6.1 - Reinforced Direct Shear Test Results - $\theta = 30^\circ$;	6.2
Fig. 6.2 - Direct Shear Test Results of Samples Reinforced with Metal Reinforcement - $\theta = 0$;	6.4
Fig. 6.3 - Direct Shear Test Results of Samples Reinforced with Plastic Reinforcement - $\theta = 0$;	6.6
Fig. 6.4 - Reinforced Direct Shear Test Results for $\sigma_y = 60$ kPa;	6.7
Fig. 6.5 - Comparison Between Mean Vertical Displacement at the Top of Reinforced Sand Samples;	6.7
Fig. 6.6 - Principal Strains and Zero Extension Lines Orientation for a Reinforced Test with Grid 4 at Peak Stress Ratio - $\theta = 30^\circ$, $\sigma_y = 30$ kPa;	6.9
Fig. 6.7 - Principal Strain Orientation at Peak for Samples Reinforced with a Rough Sheet and Netlon SR2 - $\theta = 0$, $\sigma_y = 30$ kPa;	6.10
Fig. 6.8 - Comparison Between Shear Strain Profiles in the Central Region of the Sample;	6.12
Fig. 6.9 - Increments of Horizontal Stress on the Side of the Box in Reinforced Tests;	6.14
Fig. 6.10 - Vertical Pressure Distribution on the Central Plane in a Test with Grid 4 - $\theta = 30^\circ$, $\sigma_y = 30$ kPa;	6.15
Fig. 6.11 - Vertical Pressure Distribution on the Bottom Face of the Box in a Test with Grid 1 - $\theta = 0$, $\sigma_y = 30$ kPa;	6.16

Fig. 6.12 - Normal Stress Distribution on the Reinforcement Plane at Peak Stress Ratio;	6.17
Fig. 6.13 - Forces Acting on the Top Half of the Sample in a Reinforced Test;	6.18
Fig. 6.14 - Variation of Maximum Tensile Strain in a Plastic Reinforcement During the Test;	6.20
Fig. 6.15 - Profiles of Reinforcements at Peak Stress Ratio;	6.22
Fig. 6.16 - "Stress-Strain" Relation for Unreinforced Sand;	6.24
Fig. 6.17 - Maximum Force in the Reinforcement During the Test;	6.26
Tab. 6.1 - Values of β Obtained in Reinforced Tests at Peak;	6.22
Tab. 6.2 - Comparison Between Predictions and Measurements of Reinforcement Forces at Peak Stress Ratio;	6.23
Tab. 6.3 - Comparison Between Predictions and Measurements of Reinforcement Forces at the End of the Test;	6.25

Chapter 7: Pull-out Test Apparatus

Fig. 7.1 - Large Pull-out Box;	7.3
Fig. 7.2 - General View of the Large Pull-out Box During a Test;	7.4
Fig. 7.3 - Detail of the Clamping System;	7.4
Fig. 7.4 - Arrangement for Tests with Two Reinforcement Layers;	7.5
Fig. 7.5 - Technique Used to Measure Strains in Polymeric Grids;	7.6

Chapter 8: Soils and Reinforcements Used in Pull-out Tests

Fig. 8.1 - Photographic Enlargement of the Sands Used in Pull-out Tests;	8.3
Tab. 8.1 - Properties of Sands Used in the Pull-out Tests;	8.2

Chapter 9: Sample Preparation and Test Procedure in Pull-out Tests (None)

Chapter 10: Pull-out Test Results

Fig. 10.1 - Influence of the Top Boundary on the Results of Pull-out Tests in the Medium Size Box;	10.2
Fig. 10.2 - Influence of the Roughness of the Front Wall on the Results of Pull-out Tests;	10.4
Fig. 10.3 - Influence of the Proximity of the Front Wall in Pull-out Tests in the Large Pull-out Box;	10.6
Fig. 10.4 - Typical Results for Pull-out Tests of Single Isolated Bearing Members in the Medium Size Pull-out Box;	10.7
Fig. 10.5 - Influence of B/D_{50} on the Result of Pull-out Tests of Single Isolated Bearing Members;	10.8
Fig. 10.6 - Bearing Stress Ratio versus Soil Friction Angle;	10.9
Fig. 10.7 - Influence of Interference Between Two Bearing Members in Pull-out Tests in the Medium Size Pull-out Box;	10.10
Fig. 10.8 - Photoelastic Results for Pull-out Tests with 2 Bearing Members (After Dyer, 1985);	10.12
Fig. 10.9 - Photoelastic Result for a Pull-out Test with Grid 1 (After Dyer, 1985);	10.13
Fig. 10.10 - Effect of Interference Between Bearing Members in Pull-out Tests of Grids;	10.13
Fig. 10.11 - Pull-out Tests Results for Metal Grids in the Large Pull-out Box;	10.15
Fig. 10.12 - Degree of Interference versus S/B ;	10.17
Fig. 10.13 - Degree of Interference as a Function of the Grid	

	Geometry;	10.18
Fig. 10.14	- Elastic Results for Underreamed Square Anchors (After Rowe & Booker, 1980);	10.19
Fig. 10.15	- Pull-out Test Results for Different Reinforcements in the Large Pull-out Box;	10.22
Fig. 10.16	- Influence of Stress Level on the Bond Coefficient;	10.24
Fig. 10.17	- Normalised Increment of Horizontal Stress on the Front Wall During the Test - Grid 4;	10.27
Fig. 10.18	- Normalised Increment of Horizontal Stress on the Front Wall During the Test - Netlon SR2;	10.28
Fig. 10.19	- Normalised Increment of Horizontal Stress on the Front Wall During the Test - Stabilenka 400;	10.29
Fig. 10.20	- Horizontal Stress Increment Profiles on the Front Wall of the Large Pull-out Box;	10.31
Fig. 10.21	- Principal Strain Orientation in a Pull-out Test with the Rough Sheet at Peak Pull-out Load;	10.33
Fig. 10.22	- Contours of Vertical and Horizontal Displacements;	10.34
Fig. 10.23	- Strains in the Polymer Grid During a Pull-out Test in the Large Box - $\sigma_y = 25$ kPa;	10.36
Fig. 10.24	- Strains in Netlon SR2 During the Test - $\sigma_y = 50$ kPa;	10.37
Fig. 10.25	- Strains in Netlon SR2 During the Test - $\sigma_y = 75$ kPa;	10.37
Fig. 10.26	- Profiles of Tensile Strains in Netlon SR2 at Different Stages of the Test;	10.39
Fig. 10.27	- Load Distribution in Netlon SR2 at the End of the Test;	10.40
Fig. 10.28	- Interference Between Two Layers of Reinforcement in Pull-out Tests;	10.42

Appendices

Appendix A1: Data on the Instrumentation of the Large Direct Shear and
Pull-out Boxes

A1.1 - Data on the Load Cell:

General Information:

- . Manufacturer: Tokyo Sokki Kenkyujo Co., Ltd. - 8 Ban 2 - GO Minami
OH1, 6 Chome, Shinagawa, KU, Tokyo, Japan;
- . Type: TCLM - 20A;
- . Capacity: 196.1 kN (20 tf);
- . Last Calibration: February/1986;
- . Calibration Coefficient: $3139.74 \text{ kN/V/V}_{\text{input}}$;

A1.2 - L.V.D.T.:

General Information:

- . Manufacturer: RDP;
- . Type: DC;
- . Maximum Stroke: 150mm;
- . Last Calibration: February/1986;
- . Calibration Coefficient: $6.125054 \text{ mm/V/V}_{\text{input}}$.

A1.3 - Pressure Cells:

General Information:

- . Design by E.M. Palmeira;
- . Manufactured at the Oxford University workshops under the
supervision of Mr. R. Earl and Mr. R. Stone;
- . Reccomended Voltage Input: 5V;

. Last Calibration: February/1986

Calibration Coefficient:

Pressure Cells on The Side Wall (see fig. 2.6):

Cell No.	Cal. Coeff. (kPa/V/V _{input})	Coeff. of Correlation	Max. Pressure (kPa)
1	21829.0	0.9999	800
2	20992.0	0.9981	800
3	21089.0	0.9991	800
4	8092.8	0.9994	100
5	7745.2	0.9992	100
6	8440.4	0.9996	100
7	8032.0	0.9996	100
8	6211.8	0.9999	100

Pressure Cells Buried in the Sand (see fig. 2.6):

Calibration with cells buried in dense Leighton Buzzard Sand 14/25

Cell No.	Cal. Coeff. (kPa/V/V _{input})	Coeff. of Correlation	Max. Pressure (kPa)
1	54216.0	0.9980	450
2	34880.0	0.9951	450
3	54878.0	0.9973	450

A1.4 - Power Supply:

General Information:

- . Designed and Manufactured by E.M. Palmeira at the Oxford University workshops;
- . Voltage: 5V DC;
- . 15 Channels.

Appendix A2: Software for the Large Direct Shear and Pull-out Boxes

Software Name	Language	Aim
BB.BAS	Basic	Data logging of instruments in the large direct shear and pull-out boxes;
BIT.FOR	Fortran	Calculates displacements and strains from markers at the boundary of the box;
PLOT1.FOR	Fortran	Plots principal strain and zero extension lines. Input data file is created by program BIT.FOR;
PLOT2.FOR	Fortran	Plots load (or stress) versus displac.;
PLOT3.FOR	Fortran	Plots increments of horizontal stress on a plot already containing load x displac. curve;
PLOT4.FOR	Fortran	Plots additional load (or stress incr.) x displac. curves at the user's choice;
PLOT5.FOR	Fortran	Plots strains in the reinf. x displac. in a plot already containing a load x displac. curve;
PLOT7.FOR	Fortran	Plots a series of load (or stress incr.) x displac. curves at once.

Appendix A3: Additional Data on Reinforcement Materials

Data from manufacturers' catalogues or from published works in addition to what was presented in Table 3.1.

Metal Grids:

Grids 1, 2, 3, 7 and 9 (Galvanised steel)

- Yielding stress: 366 N/mm^2 ;
- Young Modulus (raw material): 51 kN/mm^2 ;

Grids 4, 5, 6 and 8 (mild steel):

- Yielding stress: 430 N/mm^2 ;
- Young Modulus (raw material): 200 kN/mm^2 ;

Rough Sheet:

Aluminium sheet (0.8mm thick) with Leighton Buzzard sand 14/25 ($D_{50} = 0.8\text{mm}$) glued (Araldite) to both sides.

- Yielding Stress: 320 N/mm^2 ;
- Young Modulus: 70 kN/mm^2 ;

Plain Metal Strip:

Made from an aluminium sheet of 1.68mm thick. Smooth. Interface friction angle for dense Leighton Buzzard Sand 14/25 $\approx 16^\circ$. Yielding stress and Young modulus are the same as for the rough sheet.

Polymer Grids: Netlon Tensar SR1 and SR2

- Manufacturer: Netlon
- Raw Material: Co-polymer grade high density polyethylene;
- Mass per Area: 0.94 kg/m^2 (SR2) and 0.87 kg/m^2 (SR1);
- Colour: Black;
- Quality Control Longitudinal Strength (kN/m): 57.5 (SR1)*
68.8 (SR2)
- Approximate Peak Strain: 18 % (SR1 and SR2)
- Data on Time-Temperature Behaviour: see McGown (1982, 1983)
and McGown et al (1984);
- * From McGown (1982).

Woven Geotextiles:

Geolon 70:

- Manufacturer: Nicolon;
- Raw Material: Polyester;
- Mass per Area: 220 gr/m^2 ;
- Colour: White;
- Tensile Strength: 70 kN/m (warp and weft direction)
- Elongation at Failure: 11% (warp dir.) and 14% (weft dir.).

Stabilenka 400:

- Manufacturer: Enka;
- Raw Material: Polyester;

- Colour: White;
- Mass per Area: 900 gr/m^2 ;
- Tensile Strength: 400 kN/m ;
- Elongation at Failure: $\approx 10\%$

Appendix A4: Summary of Test Results

Table A4.1 - Direct Shear Tests in the Large Shear Box

Test No.	Reinf.	θ (°)	σ_y (kPa)	L_r (mm)	$P_{s_{max}}$ (kN/m)	Comments:
1	---	---	8.5	---	12.80	unreinforced.
2	---	---	30	---	37.68	unreinforced.
3	---	---	30	---	38.20	unreinforced.
4	---	---	60	---	64.51	unreinforced.
5	Grid 1	0	30	599	58.30	press. cells on the box bottom face.
6	Grid 1	30	30	599	61.39	
7	Grid 2	0	30	593	58.32	
8	Grid 2	30	30	597	65.30	
9	Grid 3	0	30	602	56.81	
10	Grid 4	0	30	604	60.32	press. cells on the reinf. plane.
11	Grid 4	30	30	603	66.03	press. cells on the central plane.
12	Grid 4	30	30	604	65.10	press. cells on the central plane.
13	Grid 4	30	30	605	67.26	press. cells on the reinf. plane.
14	Grid 4	30	30	604	65.84	press. cells on the reinf. plane.
15	Grid 4	0	60	604	102.01	
16	Grid 5	30	30	605	65.71	press. cells on the reinf. plane.
17	Grid 6	30	30	599	44.46	
18	Grid 7	30	30	600	55.08	failed during test.

19	Grid 9	30	30	601	53.24	failed during test.
20	Netlon SR1	0	30	560	50.63	
21	Netlon SR1	30	30	560	51.92	
22	Netlon SR2	0	30	660	57.24	
23	Netlon SR2	30	30	565	56.44	
24	Netlon SR2	0	60	660	85.82	
25	Rough Sheet	0	30	600	59.38	
26	Geolon 70	0	30	600	49.40	
27	Stabilenka 400	0	30	600	53.10	Press. cells on the reinf. plane.
28	Metal Strip	0	30	600	41.12	$W_r = 100$ mm.

Table A4.2 - Pull-out Tests in the Large Pull-out Box

Test No.	Reinf.	σ_y (kPa)	n	L_r (mm)	$P_{p_{max}}$ (kN/m)	Comments:
1	Grid 1	25	38	500	34.60	
2	Grid 1	50	38	500	57.95	failure of reinf.
3	Grid 1	25	38	500	72.19	2 reinf. layers.
4	Grid 2	25	13	250	21.00	
5	Grid 4	25	7	500	25.66	
6	Grid 4	50	7	500	56.80	
7	Grid 4	80	7	500	63.30	failure of reinf.
8	Grid 4	25	8	500	29.17 [*]	reinf. away from the boundary.
9	Grid 4	25	7	500	54.40	2 reinf. layers
10	Grid 5	25	9	500	27.00	
11	Grid 8	25	4	500	25.80 [*]	
12	Netlon SR2	25	5	522	32.41	

13	Netlon SR2	50	5	522	48.26	
14	Netlon SR2	75	5	522	53.48	
15	1 bearing member	25	1	---	23.28	round steel bar B = 19.1mm
16	1 bearing member	25	1	---	29.25	square section B = 19.1mm
17	Rough Sheet	25	-	475	35.55	
18	Geolon 70	25	-	500	18.60	
19	Stabilenka 400	25	-	500	21.87	
20	Stabilenka 400	50	-	500	39.87	
21	Stabilenka 400	100	-	500	67.45	

* Value of pull-out load at the end of the test.

Test No.	n	B (mm)	S (mm)	Sand	Comments	Test No.	n	B (mm)	S (mm)	Sand	Comments
1	1	9.50	---	14/25		32	6	1.63	12.5	14/25	grid 1, Lr = 75 mm, sand glued on the front wall.
2	1	4.78	---	14/25		33	3	3.16	3.16	14/25	
3	1	1.54	---	14/25		34	1	4.78	---	14/25	to investigate wall proximity, d = 92.5 mm.
4	1	2.40	---	14/25		35	1	4.78	---	14/25	same as above, d=47.5mm.
5	1	6.00	---	14/25	square section	36	1	4.78	---	14/25	same as above, d=25.0mm.
6	1	9.50	---	14/25	square section	37	1	4.78	---	14/25	same as above, d=12.0mm.
7	1	3.16	---	14/25	grid 1, Lr=75mm, close to a smooth metal wall.	38	1	4.78	---	25/52	
8	6	1.63	12.50	14/25	same as above, away from the wall.	39	1	1.00	---	25/52	
9	7	1.63	12.50	14/25	grid 1, Lr = 75mm, rigid rough top plate.	40	1	2.40	---	25/52	
10	6	1.63	12.50	14/25	lost, repeated in test no. 19	41	2	4.78	30.0	25/52	
11	2	3.16	129.0	14/25	plastic bearing member, not relevant to the present work.	42	3	3.16	3.16	25/52	
12	2	3.16	62.0	14/25	same as above.	43	2	3.16	62.0	25/52	
13	2	3.16	18.0	14/25	lost, repeated in test no. 18	44	1	4.78	---	7/14	
14	1	4.40	---	14/25		45	1	2.40	---	7/14	
15	1	4.40	---	14/25		46	1	9.50	---	7/14	
16	3	3.16	62.0	14/25		47	2	4.78	30.0	7/14	
17	3	3.16	18.0	14/25		48	3	3.16	3.16	7/14	
18	3	3.16	62.0	14/25	repeat of test 16.	49	2	3.16	60.0	7/14	
19	2	3.16	62.0	14/25	repeat of test 12.	50	6	1.63	12.5	14/25	grid 1, Lr = 75mm, not relevant to this work.
20	2	4.78	93.7	14/25	lost, repeated in test no. 21.	51	3	4.78	9.50	7/14	
21	2	4.78	93.7	14/25	repeat of test 20.	52	3	4.78	9.50	25/52	
22	2	4.78	30.0	14/25		53	6	1.63	12.5	7/14	grid 1, Lr = 75 mm, influence of reinforcement length.
23	2	4.78	60.0	14/25	three lubricated longtd. bars (3.16mm dia., 188mm. long, Sl = 40mm), for friction correction.	54	12	1.63	12.5	7/14	same as above, Lr = 150mm.
24	2	1.50	53.5	14/25	grid 1, Lr = 75mm., lubricated front wall.	55	3	1.63	12.5	7/14	same as above, Lr=37.5mm.
25	2	1.50	25.0	14/25	same as above.	56	1	9.50	---	25/52	
26	-	----	---	14/25	grid 1, not relevant to the present work.						
27	6	1.63	12.5	14/25	grid 1, Lr = 75mm, sand paper on the front wall.						
28	6	1.63	12.5	14/25	repeat of test 30.						
29	6	1.63	12.5	14/25							
30	6	1.63	12.5	14/25							
31	6	1.63	12.5	14/25							

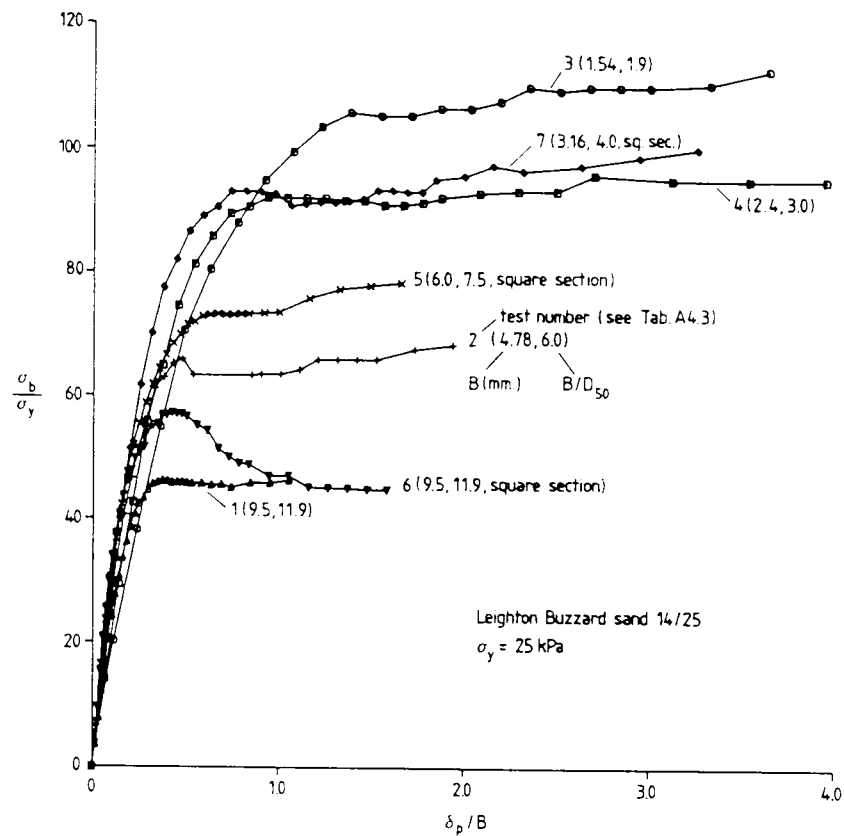
Notes:

1. Tests were performed using round mild steel bars, unless stated otherwise;
2. Tests performed using flexible top boundary and lubricated front wall unless stated otherwise;
3. Tests with single isolated members were performed with a minimum distance to the front wall of 40 member diameters in most of the cases and never less than 20.

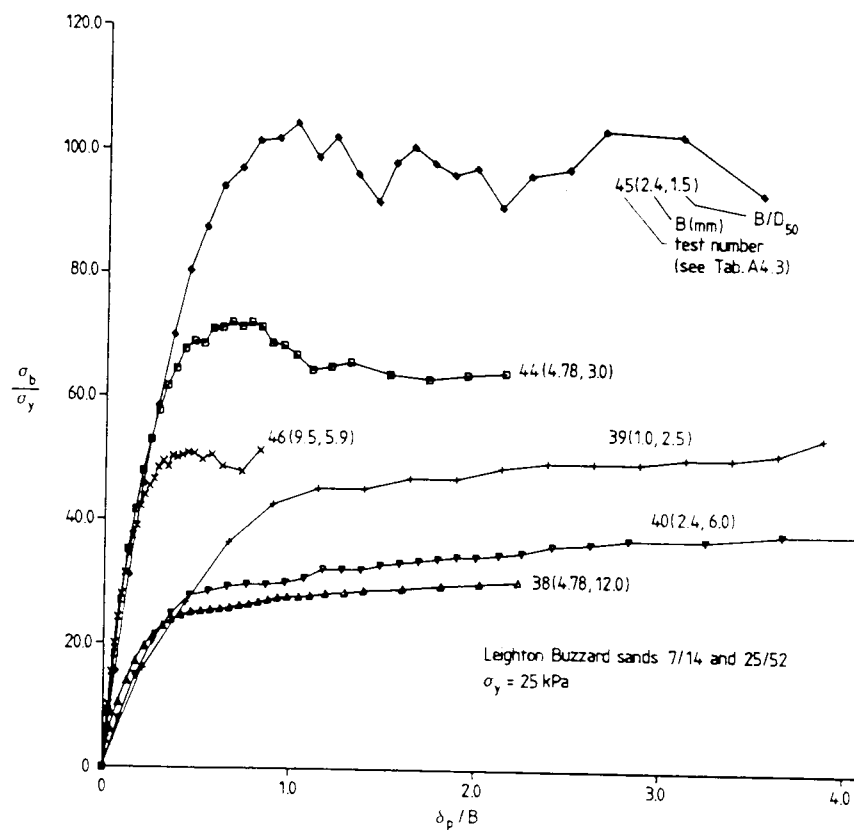
Table A4.3 - Data on Pull-out Tests Performed in the Medium Size Pull-out Box.

Sand	n	B (mm)	S (mm)	Test No. in Tab. A4.3
7/14	1	2.40	---	45
7/14	1	4.78	---	44
7/14	1	9.50	---	46
14/25	1	1.54	---	3
14/25	1	2.40	---	4
14/25	1	4.78	---	2
14/25	1	9.50	---	1
14/25	1	3.16	---	7 (sq. section)
14/25	1	6.00	---	5 (sq. section)
14/25	1	9.50	---	6 (sq. section)
25/52	1	1.00	---	39
25/52	1	2.40	---	40
25/52	1	4.78	---	38
25/52	1	9.50	---	56
7/14	2	3.16	60.0	49
7/14	2	4.78	30.0	47
14/25	2	1.50	25.0	25
14/25	2	1.50	53.5	24
14/25	2	3.16	18.0	13
14/25	2	3.16	62.0	19
14/25	2	3.16	129.0	11
14/25	2	4.78	30.0	22
14/25	2	4.78	60.0	23
14/25	2	4.78	93.7	21
25/52	2	3.16	62.0	43
25/52	2	4.78	30.0	41
7/14	3	3.16	3.16	48
7/14	3	4.78	9.50	51
14/25	3	3.16	3.16	33
14/25	3	3.16	18.0	17
14/25	3	3.16	62.0	18
25/52	3	3.16	3.16	42
25/52	3	4.78	9.50	52

Table A4.4 - Pull-out Tests Relevant to the Study of Interference Between Bearing Members - Medium Size Pull-out Box.

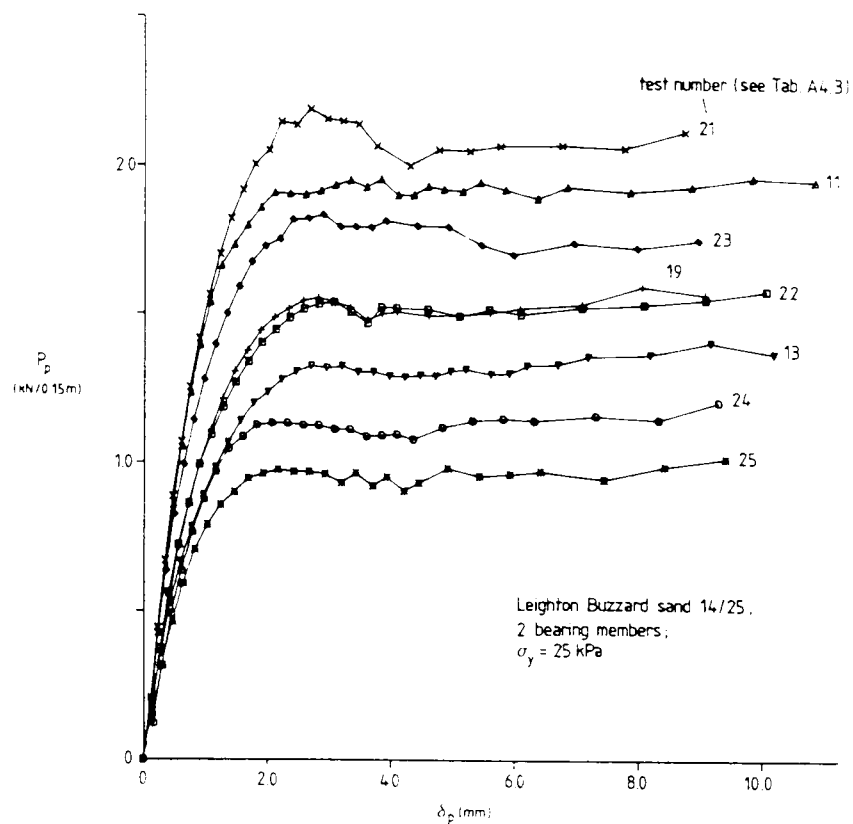


(a) Leighton Buzzard Sand 14/25.

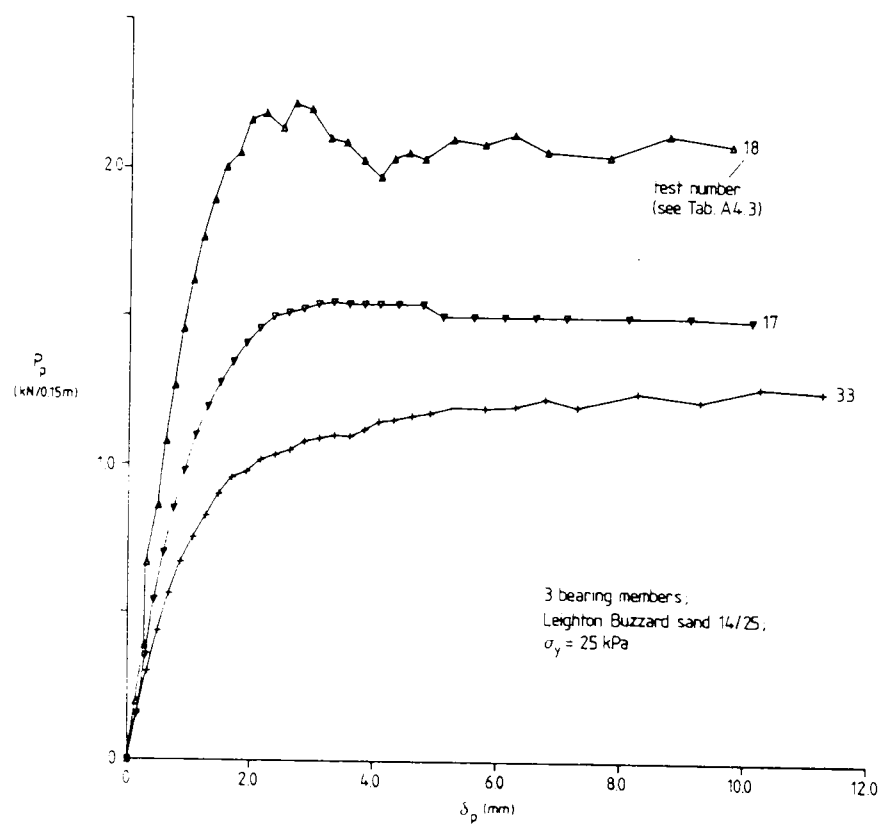


(b) Leighton Buzzard Sands 7/14 and 25/52.

Figure A4.1 – Results of Tests with Single Isolated Bearing Members in the Medium Size Pull-out Box.



(a) Two Bearing Members.



(b) Three Bearing Members.

Figure A4.2 - Results of Tests with Grids with Two and Three Bearing Members in the Medium Size Pull-out Box - Leighton Buzzard Sand 14/25.

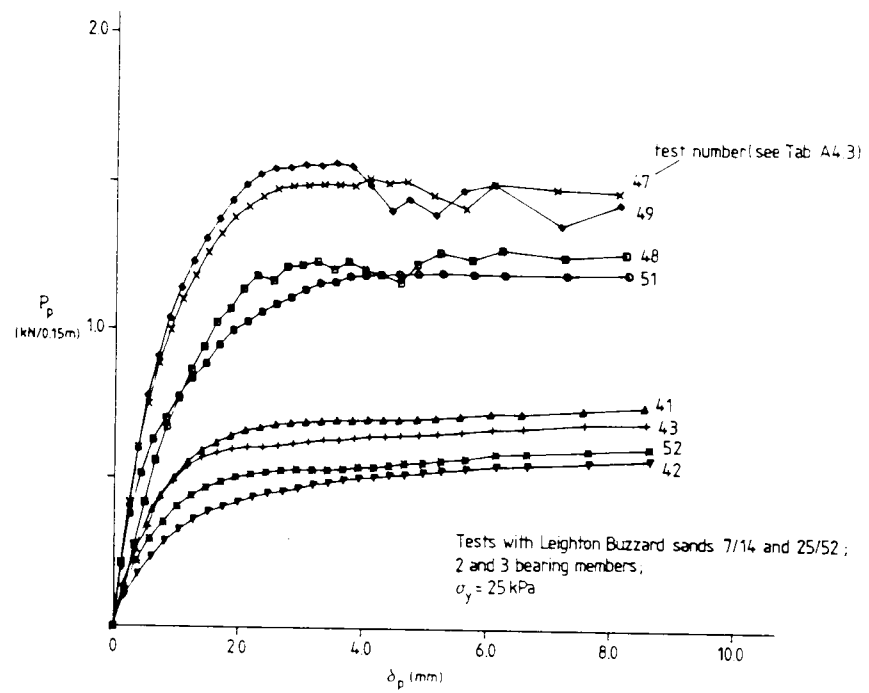


Figure A4.3 – Result of Tests with Grids with Two and Three Bearing Members in the Medium Size Pull-out Box – Leighton Buzzard Sands 7/14 and 25/52.